

**DESIGN OF A THERMORESPONSIVE HYDROGEL FOR ENHANCED  
INTRATUMORAL PERMEATION OF A CHEMOTHERAPEUTIC AGENT IN ORAL  
SQUAMOUS CELL CARCINOMA**

**SANDRINE TANGA**

A thesis submitted in fulfilment of the requirements for the degree of

Master of Science in Pharmaceutical Sciences

Faculty of Natural Sciences, School of Pharmacy, University of the Western Cape, Bellville,  
South Africa



Supervisor: Prof. Marique Aucamp

School of Pharmacy, Faculty of Natural Sciences, University of the Western Cape, Cape Town,  
South Africa

Co-Supervisor: Dr Poornima Ramburrun

Wits Advanced Drug Delivery Platform, Department of Pharmacy and Pharmacology, School of  
Therapeutic Sciences, Faculty of Health Sciences, University of the Witwatersrand,  
Johannesburg, South Africa

March 2023

## ABSTRACT

**Introduction:** Oral squamous cell carcinoma is the most common and aggressive cancer occurring in the oral cavity. Intravenous chemotherapy remains a pivotal part of treatment for the disease; however, these drugs cause debilitating systemic side effects and are unable to permeate into the deep compact layers of tumorous tissue cells. Herein, the intratumoral delivery of doxorubicin using a novel hydrogel blend, of chitosan/*k*-carrageenan and Pluronic™ F127, for a rapid solution-to-gel thermoresponsive transition at 37 °C is proposed to achieve tumour-specific delivery and controlled drug release. For enhanced permeation, a novel monoterpene – limonene with high lipophilicity and anti-cancer effect is combined with the hydrogel system.

**Methods:** Pluronic™ F127, chitosan, *k*-carrageenan and limonene were prepared via cold mixing to form a thermosensitive hydrogel. Physicochemical characterisation was performed to investigate the crosslinking and thermal behaviour of the polymer blend. The most optimal hydrogel systems were investigated through compression, rheological, swelling and erosion studies. Drug release from the hydrogel system was evaluated through drug diffusion studies. Finally, the parallel artificial membrane permeability assay (PAMPA) was utilised to assess the *in vitro* drug permeation delivered through the thermoresponsive hydrogel system.

**Results:** The polymers were able to crosslink via polyelectrolyte complexation as suggested by FTIR data. The addition of chitosan/*k*-carrageenan increased the mechanical strength and allowed for slow degradation of the hydrogel system over 5 weeks. The blend also enabled rapid gelation at ambient temperature and a sustained release of doxorubicin. The thermosensitive hydrogel resulted in excellent DOX incorporation. Limonene showed a concentration-dependent increase in the permeation rate of DOX when in the hydrogel formulation.

**Conclusion:** The thermosensitive hydrogel demonstrates good solution-gel behaviour with extended drug release and improved permeability. Therefore, the system is a potential candidate for locally injectable gel-depot systems and could improve treatment outcomes in OSCC.

## ACKNOWLEDGEMENTS

First and foremost, I would like to express my sincere gratitude to God, without whom I would be nothing. I feel blessed and grateful for all the challenges I encountered throughout my studies. A great spiritual mentor of mine once said, “When God blesses you, he makes you forget the pain and hardships of the past.” – today, the struggles I have faced are no longer a memory I hold onto; rather, I am excited and hopeful for the blessings that await the next chapter of my life. I want to thank my family, whom I love so much – my dad, Pius Tanga; my mother, Magdalene Tanga; and my sisters, Nissi and Chantal Tanga. Thank you for your prayers, encouraging words and unwavering support throughout my studies. Special recognition goes to my supervisors, Prof Aucamp and Dr Ramburrun, for their mentorship throughout this project, for sharing their knowledge and for guiding and provoking my thoughts. Every victory and milestone would not have been possible without the wisdom of these inspiring women. Thank you to my laboratory colleagues Candidah, Geoffrey, Bola, Vennesa, Nnamdi, Yves, and especially my dear friend Yusuf for being my confidant, motivator and jokester in difficult and good times alike. Thank you to Prof Samsodien for her kindness toward me, her intriguing life lessons, and for bringing fun to the academic environment.



UNIVERSITY *of the*  
WESTERN CAPE

## DEDICATION

I dedicate this thesis to my Lord and saviour, Jesus Christ.



## RESEARCH OUTPUT

### Conference proceedings

1. Tanga S, Aucamp M, and Ramburrun P. Design of a thermoresponsive hydrogel for enhanced permeation of a model drug in oral squamous cell carcinoma, Young Scientists Competition, The 42<sup>nd</sup> Academy of Pharmaceutical Sciences South Africa (APSSA) Conference 2022, Rhodes University, Makhanda, 21-23/08/2022. **(Podium)**. **(Competition winner)**. (Appendix A1).
2. Tanga S, Aucamp M, and Ramburrun P. Design of a thermoresponsive hydrogel for enhanced permeation of a model drug in oral squamous cell carcinoma, University of the Western Cape, School of Pharmacy 7<sup>th</sup> Annual Symposium, Bellville, Cape Town, 05/08/2022. **(Podium)**. (Appendix A2).
3. Tanga S, Aucamp M, and Ramburrun P. Design of a thermoresponsive hydrogel for enhanced permeation of a chemotherapeutic agent in oral squamous cell carcinoma, Africans in STEM symposium, Maxwell Centre, Cambridge, UK, 29/04/2022. **(Poster)**. (Appendix A3).


### Research publications

1. Tanga S, Ramburrun P and Aucamp M. Injectable thermosensitive hydrogels for cancer therapy: challenges and prospects. (Review article submitted to *Gels* for peer review). (Appendix A4)
2. Tanga S, Aucamp M, and Ramburrun P. Design and characterisation of a Pluronic-F127-based thermoresponsive intratumoral hydrogel. 2023. *South African Pharmaceutical Journal*, 90(1), pp.41-44. (Research article) (Appendix A5)

## DECLARATION

I declare that this thesis, “Design of a thermoresponsive hydrogel for enhanced intratumoral permeation of a chemotherapeutic agent in oral squamous cell carcinoma”, is my own work. It has not been submitted before for any degree or examination at this or any other university, and all sources used have been indicated by citation within the text and acknowledged in the reference section.

Sandrine Tanga, March 2023

 .....

Signed: University of the Western Cape, Bellville



# TABLE OF CONTENTS

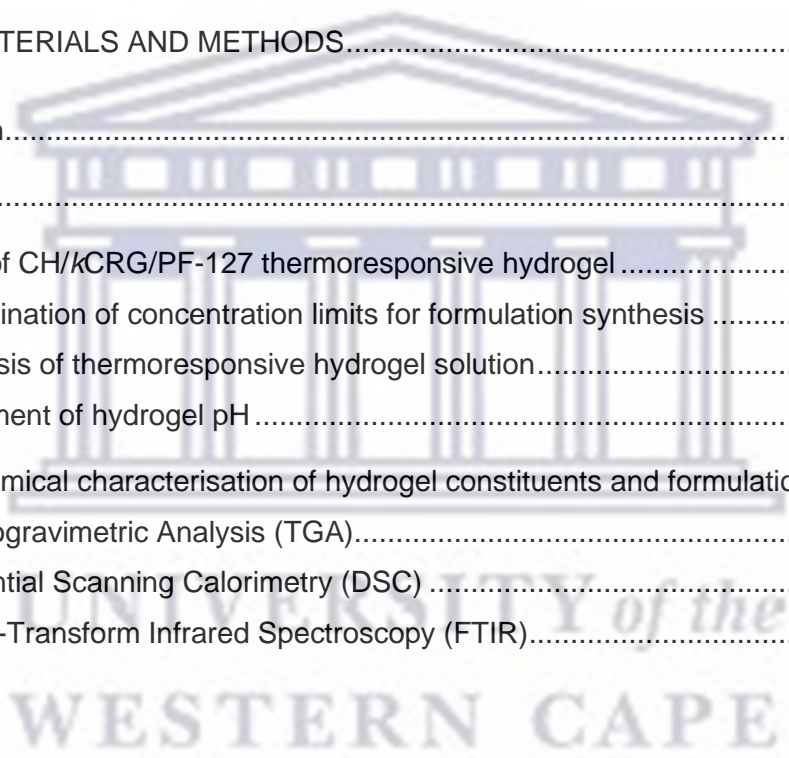
|  |     |
|--|-----|
| ABSTRACT.....                          | i   |
| ACKNOWLEDGEMENTS .....                 | ii  |
| DEDICATION.....                        | iii |
| RESEARCH OUTPUT .....                  | iv  |
| DECLARATION .....                      | v   |
| TABLE OF CONTENTS .....                | vi  |
| LIST OF ABBREVIATIONS.....             | xi  |
| LIST OF FIGURES .....                  | xii |
| LIST OF TABLES.....                    | xv  |
| LIST OF EQUATIONS .....                | xvi |
| CHAPTER 1: BACKGROUND OF RESEARCH..... | 1   |



|   |       |
|---|-------|
| 1.1 Background of research.....   | 1     |
| 1.2 Rationale and motivation .....  | 2     |
| 1.3 Novelty of study.....   | 3     |
| 1.4 Potential therapeutic applications of the drug delivery system (DDS): ..... | 4     |
| 1.5 Aim .....   | 4     |
| 1.6 Objectives.....   | 4     |
| 1.7 Conclusion.....   | 5     |
| 1.8 References .....  | 6     |
| <br>CHAPTER 2: LITERATURE REVIEW .....  | <br>9 |
| 2.1 Introduction.....   | 9     |
| 2.2 Current treatment challenges in OSCC.....                                   | 10    |
| 2.2.1 Anatomy of OSCC.....  | 10    |
| 2.2.1.1 Tumour vasculature and hypoxia.....                                     | 12    |
| 2.2.1.2 Tumour pH.....  | 13    |
| 2.2.1.3 Depth of invasion and tumour thickness.....                             | 14    |
| 2.2.1.4 Histopathological differentiation.....                                  | 15    |
| 2.3 Clinical interventions: the challenges .....                                | 16    |
| 2.3.1 Side-effects .....  | 16    |
| 2.3.1.1 Surgery .....   | 17    |
| 2.3.1.2 Radiation.....  | 17    |
| 2.3.1.3 Chemotherapy.....   | 18    |
| 2.3.2 Permeation of chemotherapeutics.....                                      | 20    |
| 2.3.3 Inaccessibility of treatment.....   | 22    |
| 2.4 Requirements for an ideal DDS .....   | 22    |
| 2.5 Drug delivery systems .....   | 23    |
| 2.5.1 Nanoparticles .....   | 23    |
| 2.5.2 Liposomes.....  | 24    |
| 2.5.3 Hydrogels.....  | 25    |
| 2.5.3.1 Stimuli-responsive hydrogels.....                                       | 25    |

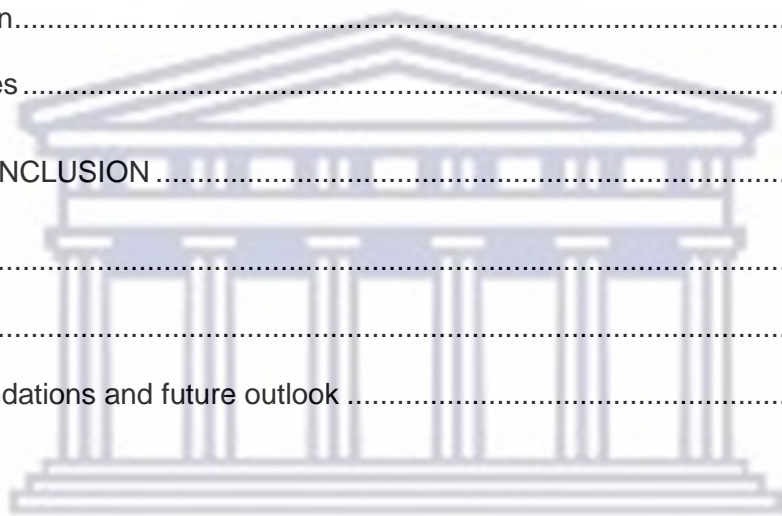


|   |    |
|---|----|
| 2.5.3.1.1 pH-responsive hydrogels.....  | 26 |
| 2.5.3.1.2 Photosensitive hydrogels.....   | 26 |
| 2.5.3.1.3 Magnetic-sensitive hydrogels .....  | 26 |
| 2.5.3.1.4 Thermoresponsive hydrogels .....  | 27 |
| 2.5.3.2 Multicomponent systems.....   | 32 |
| 2.6 Strategies for enhancing drug permeation .....                                  | 33 |
| 2.7 Conclusion.....   | 35 |
| 2.8 References .....  | 37 |
| <br>  |    |
| CHAPTER 3: MATERIALS AND METHODS.....   | 57 |
| <br>  |    |
| 3.1 Introduction.....   | 57 |
| 3.2 Materials.....  | 58 |
| 3.3 Synthesis of CH/kCRG/PF-127 thermoresponsive hydrogel .....                     | 59 |
| 3.3.1 Determination of concentration limits for formulation synthesis .....         | 59 |
| 3.3.2 Synthesis of thermoresponsive hydrogel solution.....                          | 61 |
| 3.3.3 Adjustment of hydrogel pH.....  | 64 |
| 3.4 Physicochemical characterisation of hydrogel constituents and formulation ..... | 64 |
| 3.4.1 Thermogravimetric Analysis (TGA).....   | 64 |
| 3.4.2 Differential Scanning Calorimetry (DSC) .....                                 | 65 |
| 3.4.3 Fourier-Transform Infrared Spectroscopy (FTIR).....                           | 65 |



|  |        |
|--|--------|
| 3.5 Gelation time .....  | 65     |
| 3.6 Rheological analysis of the thermoresponsive hydrogels.....                  | 66     |
| 3.7 Determining the compressive strength of the thermoresponsive hydrogel .....  | 66     |
| 3.8 Swelling of thermoresponsive hydrogel samples .....                          | 67     |
| 3.9 Erosion of thermoresponsive hydrogel samples.....                            | 67     |
| 3.10 Evaluation of DOX loading.....  | 67     |
| 3.11 Drug diffusion studies .....  | 68     |
| 3.12 Permeability studies.....   | 69     |
| 3.13 References .....  | 71     |
| <br>CHAPTER 4: THERMORESPONSIVE HYDROGEL SYNTHESIS AND CHARACTERISATION<br>..... | <br>73 |
| 4.1 Introduction.....  | 73     |
| 4.2 Hydrogel synthesis .....   | 74     |
| 4.2.1 Preliminary trial formulations for hydrogel synthesis.....                 | 74     |
| 4.2.2 Outcome of hydrogel synthesis .....  | 77     |
| 4.2.3 pH of hydrogel formulations .....  | 77     |
| 4.3 Fourier-transform infrared spectroscopy (FTIR).....                          | 79     |
| 4.4 Thermal analysis .....   | 82     |
| 4.4.1 Thermogravimetric analysis (TGA).....                                      | 82     |
| 4.4.2 Differential scanning calorimetry (DSC).....                               | 87     |

|  |     |
|--|-----|
| 4.5 Gelation time .....                                | 90  |
| 4.6 Rheological analysis of the hydrogel samples ..... | 91  |
| 4.7 Compression strength.....                          | 97  |
| 4.8 Swelling and erosion .....                         | 101 |
| 4.9 Evaluation of drug loading efficiency.....         | 107 |
| 4.10 Drug diffusional release studies.....             | 110 |
| 4.11 Permeability.....                                 | 113 |
| 4.12 Conclusion.....                                   | 116 |
| 4.13 References .....                                  | 117 |
| CHAPTER 5: CONCLUSION .....                            | 122 |
| 5.1 Summary.....                                       | 122 |
| 5.2 Limitations .....                                  | 123 |
| 5.3 Recommendations and future outlook .....           | 124 |



UNIVERSITY *of the*  
WESTERN CAPE

## LIST OF ABBREVIATIONS

BN: Batch number

BCS: Biopharmaceutics classification system

CH: Chitosan

DDS: Drug delivery system

DSC: Differential scanning calorimetry

EPR: Enhanced permeation and retention

FTIR: Fourier transform infrared spectroscopy

HPLC: High-performance liquid chromatogram

*k*CRG: *k*-Carrageenan

LIM: Limonene

MW: Molecular weight

OSCC: Oral squamous cell carcinoma

PAMPA: Parallel Artificial Permeability Assay

PBS: Phosphate buffer solution

PF-127: Pluronic™ F127

PNIPAM: Poly (N-isopropyl acrylamide)

TGA: Thermogravimetric analysis



## LIST OF FIGURES

|  |    |
|--|----|
| Figure 2.1: Structural representation of oral squamous cell carcinoma. ....  | 11 |
| Figure 2.2: Representation of the anatomical locations of OSCC occurrence.....   | 11 |
| Figure 2.3: Oral squamous tumour showing necrotic and hypoxic areas. ....  | 13 |
| Figure 2.4: Schematic depicting the measurement of depth of invasion and tumour thickness..  | 15 |
| Figure 2.5: Degree of differentiation of OSCC cells across varying clinical stages (a-d) well-differentiated, (d-f) moderately differentiated, (g-l) poorly differentiated (Zhang <i>et al.</i> , 2020). Reproduced with permission from Springer Nature © 2020..... | 16 |
| Figure 2.6: Drug permeation through passive targeting. Chemotherapeutic drugs penetrate through leaky vessels in the tumour. ....  | 20 |
| Figure 2.7: Representation of intravenous delivery and intratumoral delivery. A. Intravenous delivery: the drug is systemically circulated throughout the body. B. Intratumoral delivery: the drug remains localised within the tumour. ....                         | 28 |
| Figure 2.8: Sol-to-gel transition of thermosensitive hydrogel at low and high temperatures.....  | 29 |
| Figure 3.1: Schematic representing the synthesis of thermoresponsive PF-127/CH/kCRG hydrogel with DOX-LIM. ....  | 63 |
| Figure 3.2: Tube-inversion method from (A) flowable hydrogel to (B) non-flowable hydrogel, where $T = 23 \pm 2 \text{ }^\circ\text{C} / 37 \pm 2 \text{ }^\circ\text{C}$ . ....  | 66 |
| Figure 4.1: Spontaneous separation of LIM from the hydrogel formulation.....   | 75 |
| Figure 4.2: The molecular structures of CH and kCRG, with a depiction of the protonation of the $\text{NH}_2$ -group on the CH molecule, rendering it in the protonated state. ....  | 76 |
| Figure 4.3: (A) Depiction of mesh formation after slow mixing (600 rpm) of CH/kCRG, (B) depiction of the mesh formation upon vigorous stirring (1400 rpm) of CH/kCRG.....  | 76 |

|  |    |
|--|----|
| Figure 4.4: Sol-gel transition of hydrogel samples. A: flowable liquid. B: immovable gel. ....   | 77 |
| Figure 4.5: Photographic evidence depicting the instability of the prepared hydrogel with increasing pH. ....  | 78 |
| Figure 4.6: FTIR spectra of individual hydrogel constituents – A: CH, B: PF-127, C: <i>k</i> CRG, D: LIM, and E: DOX. ....   | 80 |
| Figure 4.7 FTIR spectra of the 9 hydrogel formulations indicating peak similarities to CH, <i>k</i> CRG, PF-127, and LIM. ....   | 81 |
| Figure 4.8: Thermogravimetric thermograms obtained with CH, <i>k</i> CRG, PF-127, LIM and DOX during heating from ambient temperature to 600 °C. ....  | 84 |
| Figure 4.9a: TGA thermograms of hydrogel formulations 1-6 from a temperature of 20 °C to 600 °C. ....  | 85 |
| Figure 4.9b: TGA thermograms of hydrogel formulations 7-9 from a temperature of 20 °C to 600 °C. ....  | 86 |
| Figure 4.10: DSC thermograms of CH, <i>k</i> CRG, PF-127 and DOX from a temperature of 25 °C to 300 °C. ....   | 88 |
| Figure 4.11: DSC thermograms of thermosensitive hydrogel formulations (sample 1-3) from a temperature of 25 °C to 300 °C. ....   | 89 |
| Figure 4.12 (a): Shear storage ( $G'$ ) and shear loss ( $G''$ ) modulus as a function of temperature (4-40 °C) for hydrogel samples 1-3 Sample 1: 01%LIM;0.1%CH;0.1% <i>k</i> CRG, sample 2: 01%LIM;0.3%CH;0.1% <i>k</i> CRG, sample 3: 0.1%LIM;0.3%CH;0.3% <i>k</i> CRG. ....        | 92 |
| Figure 4.12 (c): Shear storage ( $G'$ ) and shear loss ( $G''$ ) modulus as a function of temperature (4-40 °C) for hydrogel samples 7-9. Sample 7: 0.5%LIM;0.1%CH;0.1% <i>k</i> CRG, sample 8: 0.5%LIM;0.3%CH;0.1% <i>k</i> CRG, sample 9: 0.5%LIM;0.3%CH;0.3% <i>k</i> CRG. ....     | 94 |
| Figure 4.13 (a) Compression results indicating the peak and Young's modulus ( $E$ ) of the hydrogel samples at 37 °C, over a force of 20 N and a displacement of 5 mm for samples 1-6. Sample 1: 01%LIM;0.1%CH;0.1% <i>k</i> CRG, sample 2: 01%LIM;0.3%CH;0.1% <i>k</i> CRG, sample 3: |    |

|   |   |
|---|---|
| 0.1%LIM;0.3%CH;0.3% <i>k</i> CRG, sample 4: | 0.3%LIM;0.1%CH;0.1% <i>k</i> CRG, sample 4: |
| 0.3%LIM;0.1%CH;0.1% <i>k</i> CRG, sample 5: | 0.3%LIM;0.3%CH;0.1% <i>k</i> CRG, sample 6: |
| 0.3%LIM;0.3%CH;0.3% <i>k</i> CRG.....       | 98  |

Figure 4.13 (b): Compression results indicating the peak and Young’s modulus (E) of the hydrogel samples at 37 °C, over a force of 20 N and a displacement of 5 mm for samples 7-9. Sample 7: 0.5%LIM;0.1%CH;0.1%*k*CRG, sample 8: 0.5%LIM;0.3%CH;0.1%*k*CRG, sample 9: 0.5%LIM;0.3%CH;0.3%*k*CRG.....

99

Figure 4.14: Hydrogel samples 1, 4 and 7 immersed in PBS after 1 week of erosion studies. Hydrogel destructured: no difference between PBS and gel. Samples 2 and 5: hydrogel structure still intact with visible difference between PBS and hydrogel.....

105

Figure 4.15: Hydrogel samples 3, 6, 8 and 9 after 2 and 5 weeks, respectively, after erosion. 108

Figure 4.16: DOX regression line obtained from HPLC data. ....

109

Figure 4.18: DOX release profile of samples 3 and 8, at 37 °C, over 7 days. ....

110

Figure 4.19: Schematic of drug release from hydrogel matrix. Sample 3 – 1 CH: 1 *k*CRG, with higher drug entrapment capacity and less drug release. Sample 8 – 3 CH: 1 *k*CRG, with lower drug entrapment capacity and more drug released. ....

112



## LIST OF TABLES

|  |     |
|--|-----|
| Table 2.1: Solubility of chemotherapeutic agents and their smart drug delivery systems.....  | 19  |
| Table 2.2: LCST of commonly used polymers in water.....  | 30  |
| Table 2.3: Thermosensitive hydrogels that have undergone clinical trials for cancer treatment.   | 32  |
| Table 3.1: Composition and observations of preliminary trial formulations .....  | 60  |
| Table 3.2: Concentration of ingredients for hydrogel formulations .....  | 61  |
| Table 4.1: pH of the formulated hydrogel samples at $4 \pm 2$ °C and $37 \pm 2$ °C .....   | 79  |
| Table 4.2: Selected FTIR data for CH, <i>k</i> CRG, LIM and DOX .....  | 79  |
| Table 4.3: Gelation time of hydrogels 1-9 at $23 \pm 2$ °C and $37 \pm 2$ °C after 1 hr observation .....                              | 91  |
| Table 4.4: Tan- $\delta$ values for hydrogel formulations at 4 °C, 23 °C and 37 °C .....   | 97  |
| Table 4.5: Swelling of hydrogels 1-9 after 72 hrs at $37 \pm 2$ °C.....  | 102 |
| Table 4.6: Erosion of hydrogel samples 1-9 for 5 weeks at 37 °C .....  | 104 |
| Table 4.7: Concentration of DOX in hydrogel .....  | 108 |
| Table 4.8: Thermosensitive hydrogel volume required with 5 mg/mL DOX.....  | 109 |
| Table 5.1: A summary of the effect of CH, <i>k</i> CRG and LIM on the physicochemical properties of the thermosensitive hydrogel ..... | 123 |



## LIST OF EQUATIONS

|   |    |
|---|----|
| Equation 3.1: Swelling % of hydrogel .....          | 67 |
| Equation 3.2: Erosion % of hydrogel .....           | 67 |
| Equation 3.3: Initial amount of drug released ..... | 69 |
| Equation 3.4: Final amount of drug released .....   | 69 |
| Equation 3.5: Drug release rate .....               | 69 |
| Equation 3.6: Permeation rate .....                 | 70 |



UNIVERSITY *of the*  
WESTERN CAPE

## CHAPTER 1: BACKGROUND OF RESEARCH

*Chapter 1 provides an introduction and background to the study, including the rationale, aim, objectives, novelty, and potential beneficial applications of the proposed system.*

### 1.1 Background of research

Oral cancer is the sixth most common cancer worldwide, and squamous cell carcinoma accounts for more than 90% of all oral cancers (Omura *et al.*, 2014). Oral squamous cell carcinoma (OSCC) is caused by a combination of host genetics and environmental factors, including cigarette and alcohol use, betel quid chewing, and human papillomavirus infection (Scully and Bagan., 2009). The disease can cause pain and general discomfort, limiting chewing, swallowing, speaking, or causing difficulty opening the mouth. If the gums are affected, teeth can become loose, or dentures may no longer fit properly. Also, it can sometimes spread into the lymph nodes, causing a lump to appear in the neck (Scully and Bagan, 2009).

The primary goal of the treatment for OSCC is to eradicate the cancer, prevent reoccurrence, and insofar as is possible, to restore the form and function of the affected parts. Intravenous chemotherapeutic agents such as doxorubicin, paclitaxel and cisplatin have proven very effective in killing cancer cells; however, these drugs also affect normal cells, causing side effects such as nephrotoxicity, infertility, myelosuppression, anaphylaxis, and alopecia (Schirmacher, 2019). Chemotherapeutic agents also lack localised delivery, foster the development of complications such as oral mucositis, and do not prevent the reoccurrence of the disease (Haung *et al.*, 2020). Importantly, cancer therapies face the challenge of accessing targets deep within the tumour tissue due to the compactness of the neoplasm, which forms a barrier, restricting drug diffusion and convection (Haung *et al.*, 2020). Systemically delivered therapeutics encounter countless obstacles leading to a very small fraction of the drug reaching the tumour and unwanted distribution to healthy tissues.

Although many studies have investigated the improvement of chemotherapeutic accumulation and permeation in many types of cancers (Al Sabbagh *et al.*, 2020; Li *et al.*, 2018, 2020), to date of this research, there has been no approved hydrogel system for treatment in OSCC. Recently, Wang *et al.*, 2021 designed a bio-inspired tumour-responsive theranostic nano vehicle system loaded with melittin propeptide, theranostic probe of photochlor and gemcitabine prodrug, which increased the permeation in tumour mass. Although the study showed acceptable cytotoxic results in non-cancer cells, the present study aims to improve such results

and increase safety by using mostly natural ingredients such as polysaccharide polymers to assist the drug delivery process. Also, Wang and his colleagues did not make modifications targeted for the oral cavity in their delivery design, an aspect that this study explored.

Doxorubicin (DOX) is a highly potent topoisomerase II inhibitor derived from natural products such as plants (Renu *et al.*, 2018). Despite its potency in OSCC, its effectiveness remains restricted due to high toxicity and poor permeation into tumour cells (Li *et al.*, 2019; Mu *et al.*, 2019). This study, therefore, aimed to develop a formulation that exhibits enhanced permeability to the tumour cells, remains localised within the tumour, maintains a controlled release of the drug, and possesses increased cytotoxicity to cancer cells. To achieve these effects, a thermoresponsive hydrogel formulation was prepared consisting of limonene (LIM). LIM is a cyclic monoterpene with chemopreventive and chemotherapeutic activities in cancers such as lung, breast, gastric, and prostate cancer (Ren *et al.*, 2020). It is recognised as safe since it is used as a flavouring agent in the food industry. Its high lipophilicity contributes to favourable cellular absorption, leading to acceptable bioavailability in systemic circulation (Ren *et al.*, 2020).

To retain the toxic DOX at the targeted area, intratumoral drug delivery is a more appropriate technique that will be utilised. Pluronic™ F127 (PF-127) is a well-known synthetic thermoresponsive polymer, but factors such as poor mechanical strength and poor biocompatibility limit its individual use (Chatterjee *et al.*, 2018). To that extent, chitosan (CH) will remain a primary polymer in this study. CH is a cationic polymer which can form polyelectrolyte complex (PEC) gels with anionic polymers such as *k*-carrageenan (*k*CRG). A fundamental part of this study was to evaluate CH and *k*-CRG for their crosslinking ability and thermosensitivity in combination with PF-127.

## 1.2 Rationale and motivation

In the last 30 years, the 5-year survival rate of patients with OSCC has failed to increase despite advances in diagnostic techniques and treatment modalities (Almangush *et al.*, 2020). In 2020 alone, the World Health Organization International Agency for Research on Cancer, reported 377 713 new oral cancer cases, of which 1933 were from South Africa (Sung *et al.*, 2021). The global number of oral cancer deaths was 177 757, in which South Africa boasted 814 deaths (Sung *et al.*, 2021). These statistics prove that oral cancer is of great global and national concern. With squamous cell carcinoma being the most common oral cancer, one can only conclude that a large portion of these figures is credited to OSCC. Indeed, the incidence and

prevalence of OSCC is increasing, particularly in younger persons. In a country such as South Africa where youth engage in high-risk activities such as smoking and excessive alcohol intake (Reddy et al., 2015), improved treatment for OSCC is of high relevance.

Also, due to the adverse effects caused by traditional anti-cancer therapies, poor compliance in cancer therapies including OSCC, is heightening. Ultimately, this may negatively influence patients' clinical outcomes and, in turn, cause an increase in costs, number of hospitalisations and time spent in the hospital, thus increasing the burden on the already strained healthcare system in South Africa. Furthermore, oral cancer treatment may include surgery that involves removing large areas of facial features. Altered facial appearance can cause social isolation and psychological distress in patients (Valdez and Brennan, 2018). These facts reflect the urgent need for innovative drug delivery systems, such as that explored in this study, to transform oral cancer treatment in South Africa and the world at large.

### 1.3 Novelty of study

The novelty of this study stems from the incorporation of LIM within a thermoresponsive hydrogel system to enhance permeation in intratumoral delivery. This improvement is expected to grant superiority compared to other available OSCC treatments since cancer cells will be better targeted. LIM has provided enhanced flux and permeation when used in a cellulose hydrogel for the delivery of flurbiprofen to the stratum corneum (Fang *et al.*, 2003). It has also shown decreased thermal stability of curcumin and gellan gum hydrogel as well as a decrease in swelling capacity when designed as a film for wound dressing (Jaafar and Thatchinamoorthi, 2018). These studies have therefore proven the compatibility of LIM for hydrogel incorporation. Although the poor thermal stability and swelling results, as identified by Jaafar and Thatchinamoorthi (2018), are unfavourable, the use of the different polymers and concentrations suggested herein may be beneficial in achieving better results. The novelty in the proposed study, therefore, lies in the further investigation of whether the LIM-hydrogel compatibility applies in the context of CH-*k*CRG and PF-127, a novel crosslinking polymer blend, for the desired permeation effect and the production, if at all, of their thermoresponsive ability at normal body temperature.

Furthermore, the present knowledge of LIM as a permeability enhancer for oral tumours is still in its infancy. In contrast to the skin, the oral cavity is covered by a stratified epithelium and three different types of oral mucosa. These reflect the functional demands put upon different regions of the oral cavity, making permeation in this area challenging. It is, therefore, sensible to

investigate and modify LIM-hydrogel formulations for cancer, in order to realise its full potential in intratumoral permeation.

#### 1.4 Potential therapeutic applications of the drug delivery system (DDS):

- Potential use for intratumoral delivery of DOX in OSCC.
- DDS could be used for intratumoral delivery in various types of cancers.
- DDS could be used as a carrier for other drugs to target tumours.
- DDS could be employed for veterinary use in site specific diseases.
- Potential for use as transdermal therapy for various diseases.
- Could serve as a replacement for wound care in oral cancer since polysaccharide polymers possess proven tissue-healing properties.

#### 1.5 Aim

The aim of this study was to investigate the potential for crosslinking and thermal gelation of PF-127, kCRG and CH polymers, as well as to enhance the permeation of DOX, using LIM.

#### 1.6 Objectives

- I. To synthesise DOX-LIM, CH/kCRG/PF-127 hydrogel solution.
- II. To evaluate the pH of the hydrogel solution.
- III. To assess molecular transitions and crosslinking of the hydrogels using Fourier-transform infrared spectroscopy (FTIR).
- IV. To assess the thermal profile of the hydrogels using differential scanning calorimetry (DSC) and thermogravimetric analysis (TGA).
- V. To determine the viscoelastic behaviour of the hydrogel system using rheological analysis.
- VI. To assess the compression strength of the thermoresponsive gel at  $37 \pm 2$  °C, using a mechanical analyser.
- VII. To determine swelling and erosion kinetics of the thermoresponsive hydrogel.
- VIII. To determine the loading capacity of DOX in the thermosensitive hydrogel system using high-performance liquid chromatography (HPLC).
- IX. To perform *in vitro* drug release studies of the hydrogel formulations by determining DOX diffusion at  $37 \pm 0.5$  °C.
- X. To investigate the permeation of DOX by employing the Parallel Artificial Permeability Assay (PAMPA) kit.

## 1.7 Conclusion

This chapter provided a brief overview of OSCC and the treatment limitations associated with the disease, particularly for the chemotherapeutic drug DOX. A delivery strategy using thermoresponsive hydrogels and a permeation enhancer was highlighted as a potential resolution. In addition, the rationale, aim, objectives, and novelty of the current study were discussed.



## 1.8 References

- Al Sabbagh, C., Seguin, J., Agapova, E., Kramerich, D., Boudy, V. and Mignet, N. 2020. Thermosensitive hydrogels for local delivery of 5-fluorouracil as neoadjuvant or adjuvant therapy in colorectal cancer. *European Journal of Pharmaceutics and Biopharmaceutics*, 157, pp.154-164.
- Almangush, A., Mäkitie, A.A., Triantafyllou, A., de Bree, R., Strojan, P., Rinaldo, A., Hernandez-Prera, J.C., Suárez, C., Kowalski, L.P., Ferlito, A. and Leivo, I. 2020. Staging and grading of oral squamous cell carcinoma: An update. *Oral Oncology*, 107, Article ID: 104799.
- Alopaeus, J.F., Hellfritsch, M., Gutowski, T., Scherließ, R., Almeida, A., Sarmento, B., Škalko-Basnet, N. and Tho, I. 2020. Mucoadhesive buccal films based on a graft copolymer – A mucin-retentive hydrogel scaffold. *European Journal of Pharmaceutical Sciences*, 142, Article ID: 105142.
- Chatterjee, S., Hui, P.C.L. and Kan, C.W. 2018. Thermoresponsive hydrogels and their biomedical applications: Special insight into their applications in textile based transdermal therapy. *Polymers*, 10(5), p.480.
- Chu, X.Y., Huang, W., Wang, Y.L., Meng, L.W., Chen, L.Q., Jin, M.J., Chen, L., Gao, C.H., Ge, C., Gao, Z.G. and Gao, C.S. 2019. Improving antitumor outcomes for palliative intratumoral injection therapy through lecithin–chitosan nanoparticles loading paclitaxel–cholesterol complex. *International Journal of Nanomedicine*, 14, p.689-705.
- Deng, A., Kang, X., Zhang, J., Yang, Y. and Yang, S. 2017. Enhanced gelation of chitosan/ $\beta$ -sodium glycerophosphate thermosensitive hydrogel with sodium bicarbonate and biocompatibility evaluated. *Materials Science and Engineering: C*, 78, pp.1147-1154.
- Fang, J.Y., Hwang, T.L. and Leu, Y.L. 2003. Effect of enhancers and retarders on percutaneous absorption of flurbiprofen from hydrogels. *International Journal of Pharmaceutics*, 250(2), pp.313-325.
- Jaafar, A.M. and Thatchinamoorthi, V. 2018, October. Preparation and Characterisation of Gellan Gum Hydrogel containing Curcumin and Limonene. In *IOP Conference Series: Materials Science and Engineering* 440, No. 1, p. 012023). IOP Publishing.
- Li, C., Zhang, Y., Li, Z., Mei, E., Lin, J., Li, F., Chen, C., Qing, X., Hou, L., Xiong, L. and Hao, H. 2018. Light-Responsive Biodegradable Nanorattles for Cancer Theranostics. *Advanced Materials*, 30(8), p.1706150.

Li, J., Wang, H., Wang, Y., Gong, X., Xu, X., Sha, X., Zhang, A., Zhang, Z. and Li, Y. 2020. Tumor-Activated Size-Enlargeable Bioinspired Lipoproteins Access Cancer Cells in Tumor to Elicit Anti-Tumor Immune Responses. *Advanced Materials*, 32(38), Article ID: .2002380.

Li, M., Yue, X., Wang, Y., Zhang, J., Kan, L. and Jing, Z. 2019. Remodeling the tumor microenvironment to improve drug permeation and antitumor effects by co-delivering quercetin and doxorubicin. *Journal of Materials Chemistry B*, 7(47), pp.7619-7626.

Mu, Y., Fu, Y., Li, J., Yu, X., Li, Y., Wang, Y., Wu, X., Zhang, K., Kong, M., Feng, C. and Chen, X. 2019. Multifunctional quercetin conjugated chitosan nano-micelles with P-gp inhibition and permeation enhancement of anticancer drug. *Carbohydrate Polymers*, 203, pp.10-18.

Omura, K. 2014. Current status of oral cancer treatment strategies: surgical treatments for oral squamous cell carcinoma. *International Journal of Clinical Oncology*, 19(3), pp.423-430.

Pourjavadi, A., Doroudian, M., Ahadpour, A. and Azari, S. 2019. Injectable chitosan/k-carrageenan hydrogel designed with au nanoparticles: A conductive scaffold for tissue engineering demands. *International Journal of Biological Macromolecules*, 126, pp.310-317.

Reddy, P., Zuma, K., Shisana, O., Jonas, K. and Sewpaul, R. 2015. Prevalence of tobacco use among adults in South Africa: results from the first South African National Health and Nutrition Examination Survey. *South African Medical Journal*, 105(8), pp.648-655

Ren, Y., Liu, S., Jin, G., Yang, X. and Zhou, Y.J. 2020. Microbial production of limonene and its derivatives: Achievements and perspectives. *Biotechnology Advances*, p.107628.

Renu, K., Abilash, V.G., PB, T.P. and Arunachalam, S. 2018. Molecular mechanism of doxorubicin-induced cardiomyopathy—An update. *European Journal of Pharmacology*, 818, pp.241-253.

Schirmmcher, V. 2019. From chemotherapy to biological therapy: A review of novel concepts to reduce the side effects of systemic cancer treatment. *International Journal of Oncology*, 54(2), pp.407-419.

Scully, C. and Bagan, J. 2009. Oral squamous cell carcinoma overview. *Oral Oncology*, 45(4/5), pp.301-308.

Sung, H., Ferlay, J., Siegel, R.L., Laversanne, M., Soerjomataram, I., Jemal, A. and Bray, F. 2021. Global cancer statistics 2020: GLOBOCAN estimates of incidence and mortality worldwide for 36 cancers in 185 countries. *CA: A Cancer Journal for Clinicians*, 71(3), pp.209-249.



Valdez, J.A. and Brennan, M.T. 2018. Impact of oral cancer on quality of life. *Dental Clinics*, 62(1), pp.143-154.

Wang, H., Li, J., Wang, Z., Wang, Y., Xu, X., Gong, X., Wang, J., Zhang, Z. and Li, Y. 2021. Tumor-permeated bioinspired theranostic nanovehicle remodels tumor immunosuppression for cancer therapy. *Biomaterials*, 269, Article ID:120609.



## CHAPTER 2: LITERATURE REVIEW

*Chapter 2 reviews the literature on oral squamous cell carcinoma – its detailed structure and impact on patient health and drug delivery. The current treatment available for oral squamous cell carcinoma is discussed, along with its challenges and strategies for improvement.*

### 2.1 Introduction

Oral squamous cell carcinoma (OSCC) is a common malignant tumour of the head and neck cancer category. The treatment of OSCC involves a carefully thought out and complex treatment procedure, either involving surgery, radiation and or chemotherapy. Satisfactory treatment outcomes are substantially dependent on the correct surgical consideration and procedure, the patient's overall health and the correct choice of chemotherapy and or radiation treatment (Liu et al., 2013). Unfortunately, patients continuously report constrained living as a result of cancer treatment, especially chemotherapy (Kessler et al., 2004). Oftentimes, there is also a reoccurrence of the disease after treatment, revealing the shortcoming of chemotherapy and radiation. The physical and emotional health of the patient is greatly affected during this period and for some, their quality of life may be prioritised over long-term survival. Chang and colleagues conducted a study investigating multidisciplinary team care and patient completion of their treatment regimen for OSCC. The study revealed that up to 12% of patients with access to therapy either did not complete their treatment, interrupted their ongoing treatment, or terminated definitive treatment (Chang et al., 2021). The researchers further reported the reason to be that the patient or their families or friends were worried about the negative treatment effects (Chang et al., 2021). This contributes to the rising number of deaths caused by OSCC yearly.

From the above discourse, it is evident that the quality of life during and after treatment is an important consideration for OSCC patients when deciding to start or continue with the recommended therapy. Based on the progressive increase in new oral cancer cases yearly, it is anticipated that such challenges shall continue if OSCC treatment is not improved to preserve the patient's quality of life. For this reason, the exploration of novel drug delivery systems for effective treatment therapy is a priority, and thus, a novel DDS aimed at the treatment of OSCC is the primary focus of this study. To contextualise this study, one must first understand the reason for the undesired treatment outcomes in OSCC therapy, which sometimes lead to non-adherence and, ultimately, death. To that end, this chapter will assess the challenges of OSCC

treatment with a special focus on physiological and pharmacological reasons. The treatment modalities available, as well as formulation development considerations, will also be discussed.

## 2.2 Current treatment challenges in OSCC

The oral cavity has a complex environment and is the main port of entry for carcinogenic agents such as tobacco and alcohol, making it a good target for cancerous growth. Treatment selection in OSCC is dictated by the nature of the carcinoma and by the general health condition of the patient. More specifically, determining factors of treatment outcomes include the anatomical site affected by the carcinoma, the clinical size, the extent of local invasion, expanse of hypoxia, tumour pH, histopathological features, regional lymph node involvement and distant metastasis.

Surgery is often the first line of treatment for small, accessible OSCCs (Bijai *et al.*, 2014). However, OSCCs that have advanced in stage are treated by a combination of chemotherapy, radiotherapy, and surgery (Bijai *et al.*, 2014). The use of chemotherapy in oral cancers is very common, and it works by destroying rapidly growing cells in the body. Although cancerous cells are the intended target, normal cells like hair follicles and cells that line the digestive tract are also destroyed since they too divide rapidly. Side-effects such as immunosuppression and gastrotoxicity are therefore, common with the utilisation of chemotherapy. Additionally, the structural defects of OSCC and poor drug properties, such as low solubility and poor permeation, make it difficult for anti-cancer agents to easily access and destroy oral squamous cells. It is for this reason that scientists have targeted efforts to remedy these challenges by exploring advanced drug delivery systems and strategies. Herein, the physiological constraints and the current challenges in OSCC treatment are discussed.

### 2.2.1 Anatomy of OSCC

As the name suggests, OSCC develops in the squamous layer of the oral cavity with an initial ulcer wound around the affected area (Figure 2.1). The National Comprehensive Scientific Network allots OSCC into 7 different anatomical locations. As depicted in Figure 2.2, these are the buccal mucosa, alveolar ridge, tongue, retromolar trigone, the floor of the mouth, hard palate, and mucosa of the lips (Pfister *et al.*, 2020). All these areas within the oral cavity are lined by squamous cells and are, therefore, susceptible to the formation of squamous cell carcinoma.

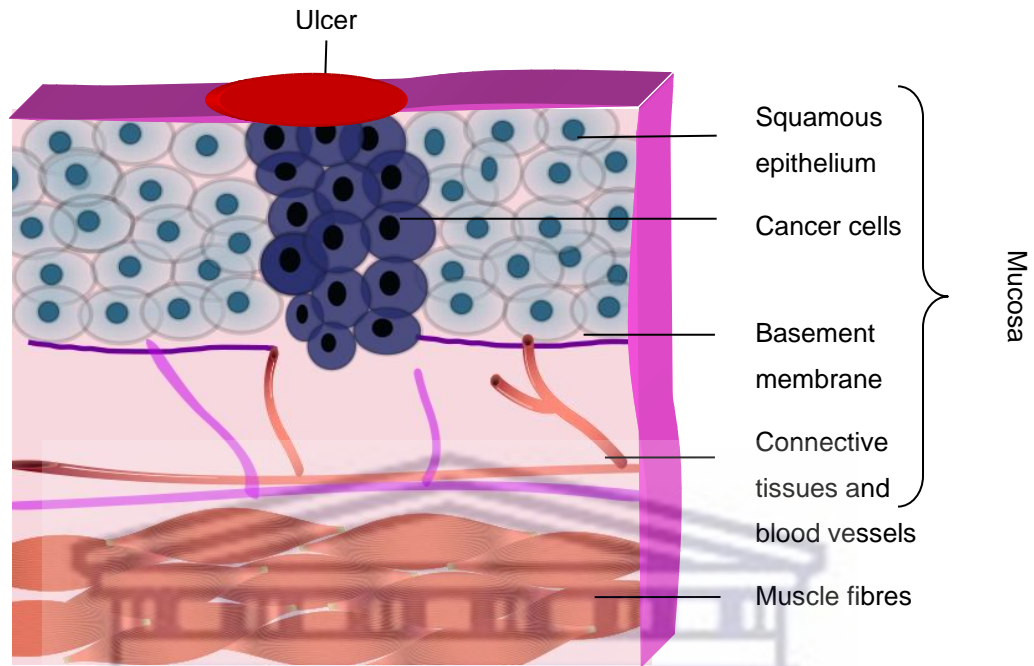


Figure 2.1: Structural representation of oral squamous cell carcinoma.

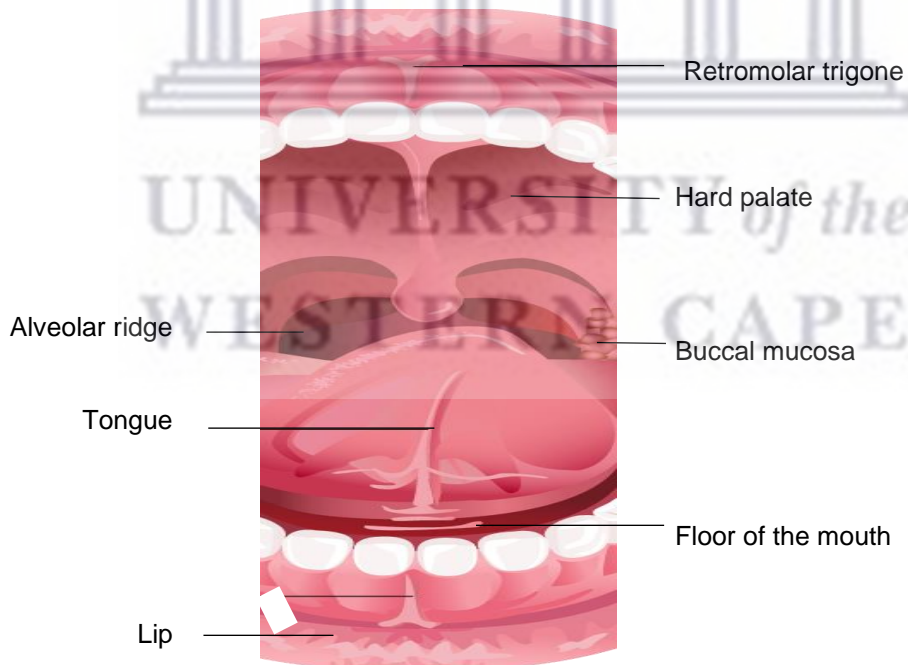


Figure 2.2: Representation of the anatomical locations of OSCC occurrence.

The anatomical location of the OSCC plays a substantial role in determining treatment and patient survival (Kerker *et al.*, 2018). According to a single centre study in Taiwan hosting 3010 OSCC patients, alveolar ridge and hard palate OSCCs carried a higher risk of mortality than OSCCs at the other subsites (Lin *et al.*, 2021). A probable explanation is that tissue adjacent to the tumour can be a channel for tumour invasion directly into the muscle, neurovascular tissue and bone, or for regional or distant node metastasis, making treatment difficult, especially the proposed intratumoral delivery. Hence early diagnosis is vital for effective treatment outcomes.

### **2.2.1.1 Tumour vasculature and hypoxia**

Irrespective of the anatomical location, the basic structure of the squamous cell tumour remains the same. OSCC presents a locally aggressive tumour with unrestrained growth and possible extensive necrotic areas, as depicted in Figure 2.3. Its blood vessels are unevenly distributed throughout the tumour, harbouring an elongated, dilated, and twisted structure with blind ends, often leading to avascular areas (Shannon *et al.*, 2003). These avascular areas in the tumour, therefore, become hypoxic and eventually necrotic. Hypoxia is a common characteristic that contributes to local and systemic cancer progression, resistance to therapy and, ultimately, poor prognosis (Qian *et al.*, 2016). For example, the primary mechanism in radiation is the creation of reactive oxygen species; hypoxic tumours are, therefore, resistant to radiation. Since the tumour has restricted vasculature due to its rapid proliferation, a diffusion barrier exists between the chemotherapeutic drug-supplying blood vessels and the tumour cells, making drug delivery to hypoxic areas difficult.

UNIVERSITY of the  
WESTERN CAPE

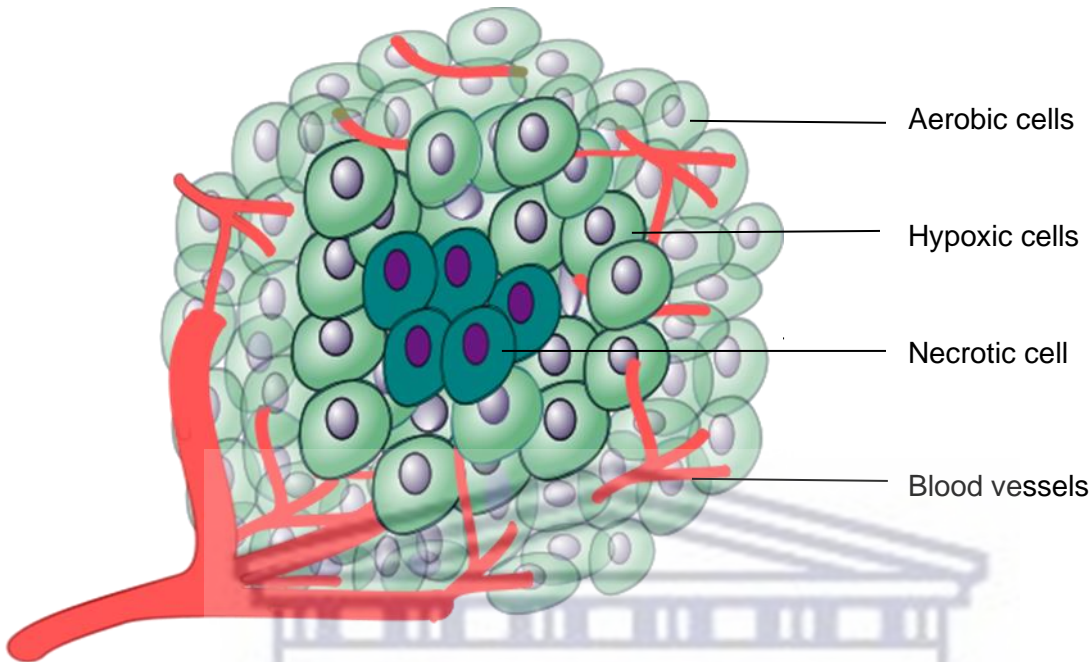


Figure 2.3: Oral squamous tumour showing necrotic and hypoxic areas.

Expanding on the topic of vasculature, its absence and/or abnormality in supportive tumour tissue generates the formation of leaky vessels and pores (Kalyane *et al.*, 2019). The poor lymphatic system is an opportunity for cancer treatment permeation, termed the enhanced permeability and retention (EPR) effect. This effect is beneficial for the delivery of nanoparticles discussed later in this review; however, it is not to be completely relied on based on the heterogeneity of tumours, which depends on a patient's pathological and physiological characteristics and clinical condition. For example, in a patient with low blood pressure, the hydrodynamic force pushing blood from the luminal side of a vessel into tumour tissue becomes significantly low, which results in a low EPR.

### 2.2.1.2 Tumour pH

The average mucosal pH in the oral cavity is 6.78 (Aframian *et al.*, 2006). This is similar to the extracellular pH of oral cancer cells, which ranges between 6.8 – 7.0 (Becelli *et al.*, 2007). Energy supply and cell constituents are crucial for the infinite proliferation of cancer cells. When oxidative phosphorylation is transformed to glycolysis to sustain energy production, lactate is generated, creating an acidic microenvironment in tumour cells (Mohajertehran *et al.*, 2019). This acidic environment is also closely connected to hypoxia in the tumour, as acidosis is more pronounced in hypoxic areas of the tumour. Furthermore, it has been reported that oral

squamous cells display enhanced glutamine metabolism, called glutaminolysis (Mohajertehran *et al.*, 2019). These findings suggest that the pH of the microenvironment around cancer cells changes according to the levels of acidic and alkaline metabolic products, such as ammonia and lactic acid (Morishima *et al.*, 2017). In oral cancer tissue, a high concentration of lactic acid was found to increase the risk of metastasis (Rai *et al.*, 2018). Most anti-cancer drugs used in OSCC are either weakly basic or weakly acidic. Specifically linking with this study, a low pH environment will inhibit the uptake of weak bases such as DOX. This is because weakly basic anti-cancer agents are ionisable at the interstitial fluid, which decreases their partitioning, and if they cross the plasma membrane, they are secluded in acidic vesicles (Mahoney *et al.*, 2003).

### 2.2.1.3 Depth of invasion and tumour thickness

The depth of invasion can be defined as the perpendicular distance between the extents of deep tumour invasion to the basement membrane of the adjacent mucosa (Chang *et al.*, 2019). The depth of invasion of the primary tumour is the most critical histologic characteristic that substantially influences therapy selection and final prognosis (Boeve *et al.*, 2019). Lesions that are *in situ* or superficially invasive have a decreased probability of regional lymph node metastasis and are highly treatable (Caldeira *et al.*, 2020; Chang *et al.*, 2019). Likewise, the influence of original tumour thickness is well shown in early-stage oral tongue and floor of mouth carcinomas. Tumour thickness represents the perpendicular distance between the highest point of the tumour surface and the deepest point of the infiltrative front of the tumour (Dirven *et al.*, 2017). Figure 2.4 demonstrates the difference between the depth of invasion and tumour thickness. Studies have not quite investigated the effect of tumour thickness on the delivery of anti-cancer treatments such as chemotherapy. Perhaps because surgery is the first option for treatment of a primary tumour, and it is difficult to retrieve reliable results, as for the same thickness size, some tumours represent a single solid mass, while others represent small, scattered masses spaced out, but grouped as one tumour. Drug permeation in the two scenarios is, therefore, difficult to assess as a function of thickness. However, investigations have focused on the correlation between tumour thickness and tumour metastasis and local recurrence, which has been shown to increase with increasing tumour thickness (Balasubramanian *et al.*, 2014).

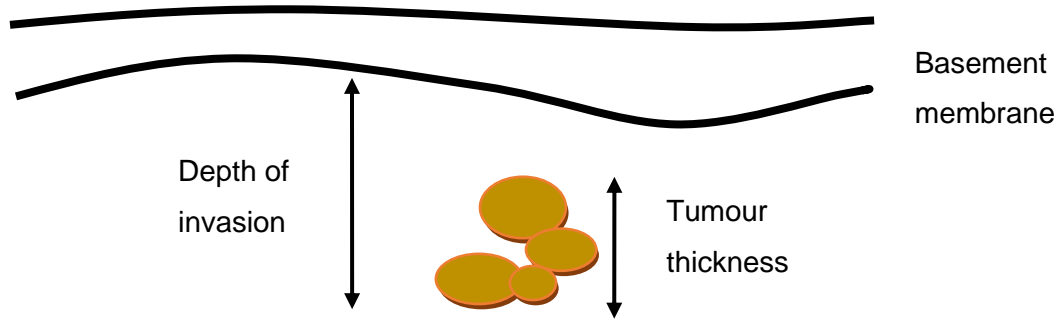


Figure 2.4: Schematic depicting the measurement of depth of invasion and tumour thickness.

#### 2.2.1.4 Histopathological differentiation

Morphological assessment of tumours can be classified based on the cancer cell differentiation into well, moderately and poorly differentiated carcinomas (Abdel Razek, and Nada, 2018; Lallas *et al.*, 2015) (Figure 2.5). The well-differentiated squamous cell carcinoma cells resemble the neighbouring benign squamous epithelium. They are large, eosinophilic, and polygonal, with a design pattern that resembles squamous cell epithelium (Bratu *et al.*, 2015). The moderately differentiating squamous cell carcinoma is less similar to normal squamous epithelium. The tumour cells are still in nests, and some larger, eosinophilic, polygonal attempt to layer themselves in a squamous manner, but the overall resemblance to normal squamous epithelium is less obvious (Lallas *et al.*, 2015). The poorly differentiated squamous cell carcinoma has lost much of its squamous epithelial features and architecture.

Well-differentiated, low-grade OSCC usually metastasises to regional lymph nodes after invading connective tissue, muscle or bone (Abdel Razek and Nada, 2018). On the other hand, poorly differentiated, high-grade oral cancer tends to be more aggressive and metastasise to regional lymph nodes early in the course of the disease (Padma *et al.*, 2017). Although unknown in OSCC, there have been reports of other cancer types supporting greater penetration and cytotoxicity of anti-cancer drugs in loosely packed well-differentiated cells as compared to moderate and poor differentiation (Grantab. and Tannock, 2012). This may be a limitation for OSCC treatment wherein most of the cells observed in patients were either moderately or poorly differentiated in a single-centre study completed by Khaleel and colleagues in 2015.



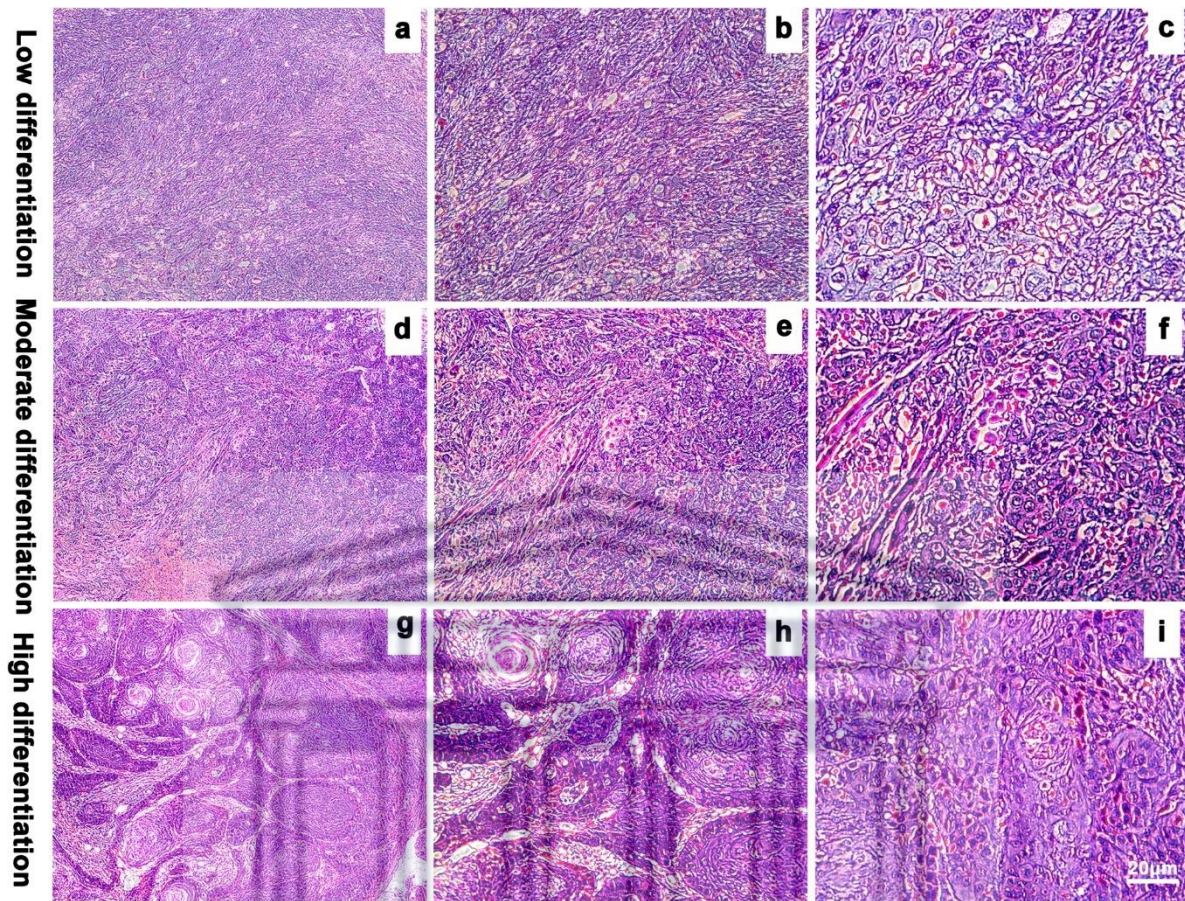


Figure 2.5: Degree of differentiation of OSCC cells across varying clinical stages (a-d) well-differentiated, (d-f) moderately differentiated, (g-l) poorly differentiated (Zhang *et al.*, 2020). Reproduced with permission from Springer Nature © 2020.

### 2.3 Clinical interventions: the challenges

When treating OSCC, it is important to strive for complete tumour eradication, while optimising aesthetic form and preserving aerodigestive function, including respiration, mastication, dental health, swallowing, and speech. To that extent, current treatments for cancer mainly rely on surgical intervention, radiotherapy, and chemotherapy. Although effective, the lack of access, poor permeation, and systemic side-effects of these treatments substantially decrease patients' quality of life and limit their treatment outcomes.

#### 2.3.1 Side-effects

The side-effects and disadvantages of cancer treatments are present across all treatment types, including surgery, radiation and chemotherapy. These side-effects promote non-adherence to

treatment regimen, or a general reduced quality of life for those who opt to continue with treatment.

### 2.3.1.1 Surgery

Surgery is the predominant treatment for oral cancer in which the bulk of the tumour is removed. However, due to inadequate cellular discrimination in most tumours, removal is often incomplete and leads to metastatic growth (Sakamoto *et al.*, 2016). Approximately two-thirds of patients with oral cancer present with stage III or IV (late stage) disease (Mackinnon, Sornalingam, and Cooper, 2021). This group of patients pose a surgical challenge, as the disease extends to more than one of the sub-sites of the oral cavity and/or has regional spread in the neck to cervical lymph nodes.

Surgical treatment in oral cancer causes several acute and chronic side-effects such as difficulty breathing, speaking, swallowing and disfigurement of the facial structure. For this reason, patients may hesitate or refuse to undergo surgery. Most OSCC patient groups with a long history of alcohol consumption, smoking and betel quid chewing often have a high association with co-morbid diseases such as heart, lung, and liver disorders, making surgery a contraindication due to their overall poor general health (Wang *et al.*, 2020).

### 2.3.1.2 Radiation

Radiation therapy utilises ionising energy to destroy cancer cells and remains a common method for the treatment of oral cancer. It is often used alone as a curative therapy or as adjuvant therapy before or after surgery or chemotherapy to reduce the risk of recurrence (Sher *et al.*, 2011; Hosni *et al.*, 2019). Although the method may be effective, radiotherapy poses several side-effects within the oral cavity. Patients suffer an increased risk of mucositis, xerostomia (dry mouth), loss of taste, fibrosis of the muscle, vascular and lymphatic tissues, and infection (Lalla *et al.*, 2017).

Mucositis is a painful and frequent complication of radiation therapy (Brandão *et al.*, 2018). It involves inflammation in the oral mucosa and can range from severe to mild depending on the dose and exposure of radiation (Arun *et al.*, 2020). Radiation-induced oral mucositis is manageable and normally subsides shortly after radiation treatment has ceased. Unfortunately, the same is not true for complications relating to xerostomia and muscle fibrosis, which are lingering effects of radiation.

Xerostomia is the most prevalent side-effect of radiation. It is prominent during the first week of radiation and can become permanent when the radiation dose exceeds 3000 cGy (Tribius *et al.*, 2013). The total dose of radiation typically prescribed for oral cancer patients is 5000 cGy to 7000 cGy (Kimple and Harari, 2014). When examining the mechanism of radiation, it is conclusive that this effect is caused by the non-targeted therapy strategy resulting in irreversible cell damage to the salivary glands. Because of the decreased production and flow of saliva, the oral cavity may be unable to naturally rinse off food particles and debris that remain in the mouth. Consequently, the mouth becomes flooded with unwanted microbiomes, resulting in increased tooth decay and oral infection (Anjali *et al.*, 2020; Lalla *et al.*, 2017). Radiation is therefore followed by a lifelong aggressive preventative measure of oral hygiene, which many patients struggle to adhere to (Levi and Lalla, 2018; Lalla *et al.*, 2017).

Fibrosis is another inconvenient and irreversible side-effect of radiation therapy. During radiation, the normal wound healing process is distorted, resulting in excessive production and deposition of extracellular matrix at the radiation injury site (Jacobson *et al.*, 2017). This leads to trismus, wherein the soft tissues such as the skin, muscles and ligaments become firm or hard (Koerdt *et al.*, 2015). Trismus is recognised by the inability to open the mouth sufficiently wide, which may interfere with eating and practising proper dental care (Ahadian *et al.*, 2020). Additionally, the bone is also affected; if a dental extraction is necessary after radiation therapy, there is a possibility that the bone will not heal properly, leading to infection. These are lifelong problems that will not resolve after radiation therapy is complete. It remains uncertain whether radiation-induced fibrosis is dose-dependent as several studies have reported contrasting results (Goldstein *et al.*, 1999; van der Geer *et al.*, 2015; Gebre-Medhin *et al.*, 2016).

### 2.3.1.3 Chemotherapy

Various chemotherapeutic drugs exist for the treatment of oral cancer, with their mode of action being an interference with the normal function of DNA and RNA. They are used alone or in combination and are usually given in cycles every few weeks. It is well established that drugs in the pharmaceutical field can be characterised using the biopharmaceutics classification system (BCS), which denotes the degree of solubility and permeation. In this system, drugs are divided into four distinct classes – class I: high solubility, high permeability; class II: low solubility, high permeability; class III: high solubility, low

permeability; class IV: low solubility, low permeability. Unfortunately, most chemotherapeutic drugs used in the treatment of oral cancer are class IV drugs. To achieve acceptable therapeutic concentrations post-administration, pharmaceutical formulations of these drugs are typically limited to parenteral formulations. This highlights the necessity for the development of novel DDS for chemotherapeutic drugs. Table 2.1 shows a list of chemotherapeutic drugs used for solid tumours, their extent of solubility and the various commercially available improved formulation types.

Table 2.1: Solubility of chemotherapeutic agents and their smart drug delivery systems

| <b>Drug</b>  | <b>Solubility in aqueous solution (mg/ml)</b> | <b>Advanced/Smart DDSs available</b>        | <b>Reference</b>  |
|--------------|---|---|---|
| Cisplatin    | ~2.5  | Lipoplatin (liposomal)                      | Jayasuriya and Darr, 2013                                   |
| Paclitaxel   | ~0.002  | Nab-paclitaxel (Albumin nanoparticle-based) | Dordunoo and Burt, 1996<br>Miwa <i>et al.</i> , 1998        |
| Doxorubicin  | 1.18  | Lipodox (liposomal)<br>Myocet (liposomal)   | Bruda <i>et al.</i> , 2017<br>D'Angelo <i>et al.</i> , 2022 |
| Docetaxel    | 0.006 – 0.007                                 | N/A   | Du <i>et al.</i> , 2007                                     |
| Daunorubicin | ~0.3  | Vyxeos (liposomal)                          | Chu <i>et al.</i> , 2016                                    |
| 5-Flouroucil | 12  | N/A   | Goindi <i>et al.</i> , 2014                                 |
| Carboplatin  | 14  | N/A   | Mittal, Chitkara, and Kumar, 2007                           |
| Tamoxifen    | ~0.0003                                       | N/A   | Öztürk-Atar, Kaplan, and Çalış, 2020                        |

The intravenous route also delivers a potentially high concentration of drugs to normal tissues, resulting in overall toxicity. Several anti-cancer agents and their excipients are biologically reactive and may trigger the release of various vasoactive substances,

sometimes resulting in life-threatening reactions (Raza *et al.*, 2019). For example, paclitaxel contains poly ethoxylated castor oil, which is associated with severe side-effects of neurotoxicity and hypersensitivity reactions (Mao *et al.*, 2021). Chemotherapeutic oral formulations are also not exempt from limitations. They have a short biological half-life, poor patient compliance, low therapeutic index, are prone to the development of resistance, lack the ability to achieve therapeutic concentrations at the target oral site and have insufficient bioavailability due to limited aqueous solubility, degradation in gastrointestinal fluids and/or affinity for intestinal and liver cytochrome P450 (CYP3A4) and P-glycoprotein (Reshma *et al.*, 2019; Li *et al.*, 2018; Tang *et al.*, 2018).

### 2.3.2 Permeation of chemotherapeutics

Permeability is defined as the ability of a drug to cross through a biological membrane. Passive diffusion controls the permeation of conventional chemotherapeutic drugs from the intravascular to the interstitial space (Borys and Dewhirst, 2021; Derieppe *et al.*, 2019) and is reliant on EPR. The EPR effect is a concept based on the accumulation of a drug in the interstitial fluid of the diseased tissue because of the structural abnormalities found in tumours, such as leaky vessels (Figure 2.6).

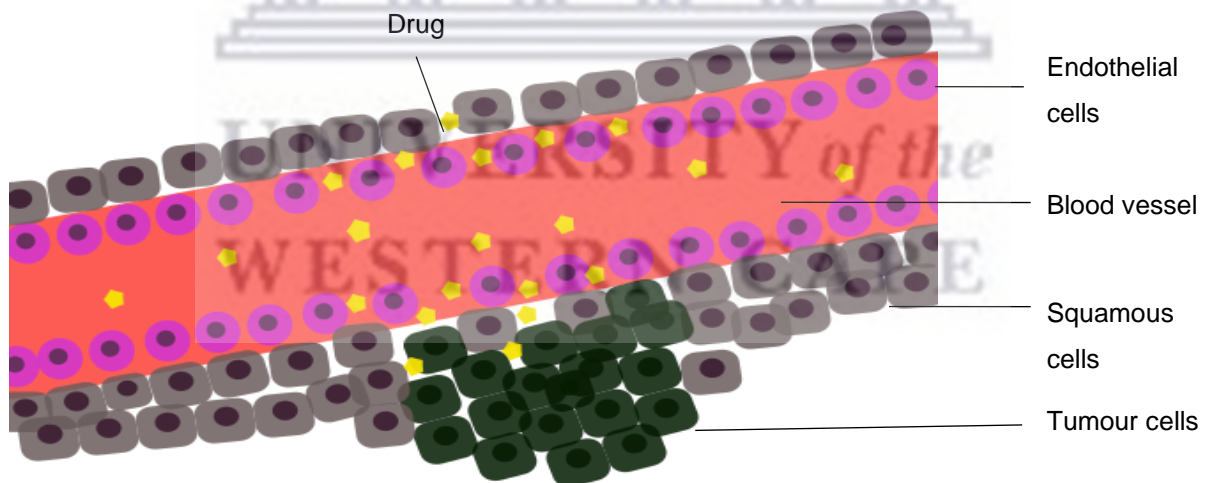


Figure 2.6: Drug permeation through passive targeting. Chemotherapeutic drugs penetrate through leaky vessels in the tumour.

Chemotherapeutic drugs have been known to exert poor permeability to their target cancer cells. Studies have revealed that these drugs generally only penetrate approximately 50  $\mu\text{m}$  from the nearest vessel, with little to no drug reaching distant tumour cells and potentially resulting in the development of drug resistance (Saggar and Tannock, 2014; Primeau *et al.*, 2005; Tannock *et al.*, 2002). Various factors can influence the potential for or degree of drug permeation. Amongst these, the p-glycoprotein (P-gp) is one of the major restrictions of permeability in cancer cells (De Vera *et al.*, 2019; Qian *et al.*, 2019b). Its mediated efflux mechanism can reduce the intracellular accumulation of chemotherapeutic drugs in most resistant cells (Kebsa *et al.*, 2018). Drugs such as DOX and cisplatin are usually isolated in the cytoplasm where they are expelled, failing to reach the nucleus (Astuti *et al.*, 2019), which is the targeted site of action for most anti-cancer drugs. Furthermore, many chemotherapeutic agents are also substrates of drug-resistant proteins such as P-gp, multidrug resistance-associated proteins, and ATP-binding cassette transporter superfamily, thus contributing to the decrease in intracellular permeation and ultimate poor drug efficacy (Jianmongkol, 2021).

Most chemotherapeutic drugs have a high molecular weight (MW), and this feature is a substantial barrier to drug penetration. For example, DOX has a MW of 544 g/mol, and paclitaxel has a MW of 853 g/mol. Therefore, these agents experience a decreased permeability into tumour cells. However, once diffused from the blood vessel into tumour tissue, the drug retains for a longer period, assisting in tumour reduction. Low MW drugs are easily diffused by the passive diffusion mechanism from blood vessels into the interstitium of tumour tissue. However, these drugs cannot be retained in tumour tissue for a sufficiently long period due to their smaller size, and they, therefore, get freely into the systemic circulation. This is especially pertinent in the use of nanoparticles for the delivery of chemotherapeutics, reported later in this chapter.

To circumvent the challenges associated with the delivery of chemotherapeutic drugs, clinicians have implemented the use of intratumoral delivery, which delivers the drug directly at the site of the cancer tumour. Although this strategy delivers the drug directly at the target site, the challenge of chemotherapeutic intratumoral delivery lies in the lack of equal dispersion throughout the tumour for an extended period. Chemotherapeutics, such as DOX, are hydrophilic, yet tumours often contain a high percentage of lipids (Halczy-Kowalik *et al.*, 2019). Aqueous formulations are therefore not well absorbed into these tumours and will leak out of the tumour and into the blood vessels, defeating the purpose of local delivery. For highly protein-bound anti-cancer agents such as DOX, actinomycin D, and vincristine, the limited drug

penetration to tumour cells that are removed from the blood supply is considered a cause of suboptimal drug effects.

### 2.3.3 Inaccessibility of treatment

Finally, despite radiotherapy, surgery and chemotherapy forming a crucial part of oral cancer treatment, many patients lack access to these treatment options. It has been reported that 28 African countries have no radiation facilities, and the existing radiotherapy centres tend to be outdated or non-operational (Zubizarreta *et al.*, 2015). Almost 60% of available radiotherapy equipment in Africa is housed in South Africa and Egypt (Bishr and Zaghloul, 2018). Issues such as poverty, political instability, and untrained personnel have led to this service sitting low on governments' priorities (Bishr and Zaghloul, 2018; Anakwenze *et al.*, 2017). This negatively impacts patients' treatment outcomes wherein therapy is delayed or simply inaccessible.

Additionally, patients in undeveloped and developing areas are unable to access medical centres with qualified personnel who are capable of the complex and comprehensive demands of oral surgery or simply, the patients may lack sufficient socioeconomic support or resources to receive surgical or chemotherapeutic treatment. Therefore, a substantial proportion of oral cancer patients still do not receive definitive anti-cancer treatment, particularly in African countries (Wang *et al.*, 2020).

### 2.4 Requirements for an ideal DDS

Despite surgical excision being the first choice of therapy for oral cancers, the permanent physiological impairment of oral and maxillofacial regions limits its preference as a treatment option. While radiation is part of supportive treatment, its access is severely limited in undeveloped and developing countries. To that end, chemotherapy remains the backbone of cancer treatment despite its poor bioavailability, as detailed previously. The design of an improved DDS for chemotherapy is therefore necessary. This would enhance treatment outcomes and extend lives. Patients would enjoy a better quality of life during and after therapy. Importantly, side-effects would be significantly reduced.

There are various drawbacks that need to be resolved to reach optimum therapeutic outcomes. Foremost, the issue of systemic toxicity must be addressed. A DDS should only deliver the drug at the oral tumour site, limiting the dreadful side-effects involved in cancer therapy; normal cells should be spared and only cancer cells targeted to achieve this effect. Secondly, the ideal system should provide maximum toxicity to cancer cells preventing further recurrence or

metastasis. This maximum toxicity can only be obtained if a high concentration (within therapeutic levels) of the drug reaches the target and remains there for a prolonged period under controlled release; and if the drug is able to permeate throughout the avascular tissue, deep into the hypoxic areas and directly into the neoplasm of the oral squamous cells, resisting microenvironmental changes inside and outside the tumour site.

Furthermore, as chemotherapy/radiation/surgery negate wound healing capacity, which is evident in the side-effects previously discussed, it is essential for an ideal cancer treatment to support wound healing or have little to no impact on the rapidly dividing tissue cells of healing wounds in the oral cavity. The delivery system should not interact adversely with the tumour environment, encouraging unnecessary microbial growth, rather, it should target/resist drug-resistant genes such as P-gp, MDRI, ABCG2 and AT3B-1 cells reportedly present in OSCC (Jianmongkol, 2021). Depending on the type of system design, certain requirements may further come into play. Finally, an ideal system should have simple preparation methods, be easy to administer, inexpensive and accessible to all OSCC patients.

## **2.5 Drug delivery systems**

The topic of improved delivery strategies in cancer therapy is not new. Researchers have tried and tested several methods over the past years for chemotherapeutic delivery. In this context, many promising tumour-targeting systems have emerged; the most prominent, broadly termed "smart drug delivery systems", are discussed further in this chapter.

### **2.5.1 Nanoparticles**

Nanoparticles have received much attention as a drug delivery strategy in cancer due to their small size (1-100 nm). They solve the problem of non-specific biodistribution, lack of targeting, lack of aqueous solubility, poor oral bioavailability, and low therapeutic indices of conventional chemotherapeutic drugs (Alavi *et al.*, 2022; Fan *et al.*, 2021; Li *et al.*, 2020). Tumour tissue vasculature tends to be leakier (gaps as large as 200 to 2000 nm between adjacent endothelial cells of a tumour), thus enabling entry and accumulation of nanoparticles at the interstitial space of the tumour (Wang *et al.*, 2018; Dewhirst and Secomb, 2017). Unfortunately, tumour structures differ depending on their type, stage and location, and hence, nanoparticles do not always succeed in reaching and delivering chemotherapeutic agents to every tumour type. The accumulation of nanoparticles in tumour tissues also depends on size, shape, surface



properties, charge, circulation half-life of the nanoparticles and the degree of angiogenesis of the tumour (Wang *et al.*, 2019; Bhattacharya *et al.*, 2020).

Although nanoparticles offer several advantages for targeted drug delivery, disadvantages include burst release, poor bio-adhesion and irreversible deformation; therefore, nanoparticles may not be suitable for long-term administration (Lai *et al.*, 2021; Hu *et al.*, 2018). Presently available are some nano-based formulations on the market for drug delivery in breast cancer and ovarian cancer, such as nab-paclitaxel, however, no system has been FDA-approved for treatment in OSCC yet. Albeit a potential nano-based system has been designed by Nanobiotex for injection directly into an OSCC tumour prior to a patient's first radiation treatment. The design has received the European conformity (CE) certification and is currently undergoing FDA investigation for approval. It is named Hensify<sup>®</sup> or NBTXR3 and is based on helium oxide nanoparticles which help to localize the cytotoxicity of radiotherapy treatment, ensuring high dose is received in the tumour (Bonvalot *et al.*, 2019). Its clinical efficacy has been proven in several studies and continues to be investigated by many researchers (Le Tourneau *et al.*, 2017; Zhang *et al.*, 2021; Hoffmann *et al.*, 2021). Currently, BNT113 in combination with pembrolizumab is also being investigated for its therapeutic efficacy in head and neck cancer (Sun *et al.*, 2021; ClinicalTrials.gov, 2021). The system is based on size and charge RNA-lipoplex nanoparticles for targeting dendritic cells to elicit immune response against oncoproteins E6 and E7 (Sun *et al.*, 2021). Participants are still being recruited for phase 2 clinical trials (ClinicalTrials.gov. (n.d.)a, 2021).

### 2.5.2 Liposomes

Liposomes have been widely explored as drug carriers for various cancers. They have a spherical structure with a hydrophilic core, which is surrounded by amphiphilic lipids. Their hydrophobic core and hydrophilic lumen enable the encapsulation of hydrophobic and hydrophilic drugs, respectively. The lipids assist with their clearance from systemic circulation (La-Beck *et al.*, 2021). The surface charge and size also affect their clearance; hydrophobic surfaced liposomes greater than 200 nm promote opsonisation and reticuloendothelial system uptake (Petrini *et al.*, 2021; Sun *et al.*, 2017). To achieve targeted delivery, liposomes rely on ligands such as peptides, transferrin, mannose, folate, asialoglycoprotein, and antibodies (d'Avanzo *et al.*, 2021; Deshpande *et al.*, 2018; Minelli *et al.*, 2018). An example of a well-studied anti-cancer liposomal agent is Doxil<sup>®</sup> which was FDA approved in 1995. Although the design has shown several benefits such as dose reduction and decrease in side-effects, it's

extremely low permeability values on the order of  $10^{-12} \text{ cm s}^{-1}$  is still cause for concern (Russell, Hultz, and Searson, 2018). Other challenges of liposomal drug delivery include the low drug loading capability, rapid liposomal structure decomposition before any therapeutic activity is achieved, and expensive preparation methods.

Liposomes can also be designed as smart delivery systems to respond to physiological stimuli. pH-sensitive liposomes are stable at physiological pH yet destabilise at acidic pH, such as at the tumour site (Park *et al.*, 2020; Nunes *et al.*, 2021). Temperature-sensitive liposomes rely on external local heating above body temperature to release the chemotherapeutic drug. Cao and coworkers designed a hybrid DDS consisting of an injectable liposomal DOX-loaded PLGA-PEG-PLGA thermogel (Cao *et al.*, 2019). The DDS was able to sustain drug release, enhance the anti-cancer efficacy through localised therapy and managed to reduce cytotoxicity, particularly cardiotoxicity (Cao *et al.*, 2019).

### 2.5.3 Hydrogels

Hydrogels have received plenty of attention since their discovery in the 1960s. More recently, they have been greatly employed in targeted cancer research because of their highly biocompatible, biodegradable and versatile nature, which allows them to respond to external stimuli (Lima-Sousa *et al.*, 2020; Rezk *et al.*, 2019; Bilalis *et al.*, 2018). These hydrogels can be injected directly at the site of the tumour, forming a semi-solid or solid gel in response to a stimulus. In addition, the well-adhering capacity of polysaccharide-based hydrogels to biological tissues and mucosal surfaces renders them a good choice for developing biomaterials in the biomedical field (Fan *et al.*, 2021). Their wound healing and tissue engineering capacity are also beneficial, considering tissue repair needed after surgery and the reduction of wound healing that accompanies chemotherapy in oral cancer. Examples of polymers used for hydrogel design are chitosan, gellan gum, xanthan gum, hyaluronic acid and methylcellulose.

#### 2.5.3.1 Stimuli-responsive hydrogels

Hydrogels can be designed to respond to various external stimuli such as pH, light, magnetic field and temperature. These systems follow the normal physiological process of tumour cells and have been explored in cancer treatment.

### 2.5.3.1.1 pH-responsive hydrogels

pH-responsive hydrogels release chemotherapeutics based on the pH of the target tumour. The polymers induced in this type of hydrogel undergo a sol-gel phase transition due to acidic functional groups, such as sulfonic acid and carboxylic acid or basic groups, such as ammonium, that accept or donate protons caused by changes in the environmental pH (Pandit *et al.*, 2021). A novel injectable, self-healing and pH-responsive hydrogel was successfully designed by combining carboxyethyl-modified chitosan and aldehyde-modified hyaluronic acid for the release of DOX (Qian *et al.*, 2019a). The pH-dependent gel swelling, and DOX release behaviour confirmed that hydrogels could release drugs in response to pH conditions within the tumour microenvironment (Qian *et al.*, 2019a).

### 2.5.3.1.2 Photosensitive hydrogels

Photosensitive hydrogels are polymeric networks that undergo physical or chemical changes in response to light. These molecules undergo a change in geometrical and macroscopic structure as a result of light exposure (Chang *et al.*, 2019). Mechanisms that control photosensitivity are photoisomerisation, photocleaving and photosensitive dimerisation (Liu *et al.*, 2019). However, human tissue is the main obstructor of phototherapy, as the penetration depth of light is only a few centimetres depending on the applied wavelength, and this can hinder the desired structural modification and, therefore, drug release (Lu *et al.*, 2020; Ji *et al.*, 2018). To overcome this challenge, Brevé and colleagues (2021), investigated the potential of *in situ* generated light, known as Cerenkov luminescence, and its employment as a drug release trigger (Brevé, *et al.*, 2021). The researchers synthesised two phenacyl bis-azide crosslinkers, which they incorporated in dextran-based hydrogels to enable photosensitivity in a type of Cerenkov emission window (Brevé, *et al.*, 2021). The system managed to produce photosensitivity, but drug release results due to Cerenkov luminescence were not demonstrated.

### 2.5.3.1.3 Magnetic-sensitive hydrogels

Magnetic-sensitive hydrogels rely on the addition of nanoparticles with paramagnetic properties. They are frequently used with either pH or thermosensitive hydrogels (Derakhshankhah *et al.*, 2021; Xie *et al.*, 2017). For example, a contractible hydroxypropyl methylcellulose/Fe<sub>3</sub>O<sub>4</sub> hydrogel with dual-response pH and magnetic properties showed enhanced cytotoxicity when encapsulated with DOX (Zhou *et al.*, 2018).

#### 2.5.3.1.4 Thermo-responsive hydrogels

Thermo-responsive/ thermosensitive hydrogels are the most investigated stimuli-responsive hydrogel designs because of their simple formulation methods, which rely on phase changes across different temperatures. Unlike radio- and photosensitive hydrogels, thermo-responsive hydrogels do not depend on the use of extra equipment or heterogenic tumour pHs to elicit a response. These hydrogels rely on the intratumoral delivery of injectable systems, which remain solution at cool temperatures and gel at physiological temperature. Intratumoral delivery provides localised therapy directly at the tumour site, preventing side-effects such as cardiotoxicity, immunotoxicity and myelosuppression associated with conventional intravenous delivery. The benefit of using intratumoral drug delivery as compared to intravenous delivery in OSCC treatment is highlighted in Figure 2.7. For hydrogels particularly, the greater advantage is the accumulation of the gel system at the tumour site, which enhances the localisation effect and significantly increases the therapeutic index of cytotoxic chemotherapeutic drugs. Intratumoral delivery does not require surgical procedures for use, however, it is unsuitable for use in internal organ cancers such as colon cancer and pancreatic cancer except if it is placed at the resected site during surgery.



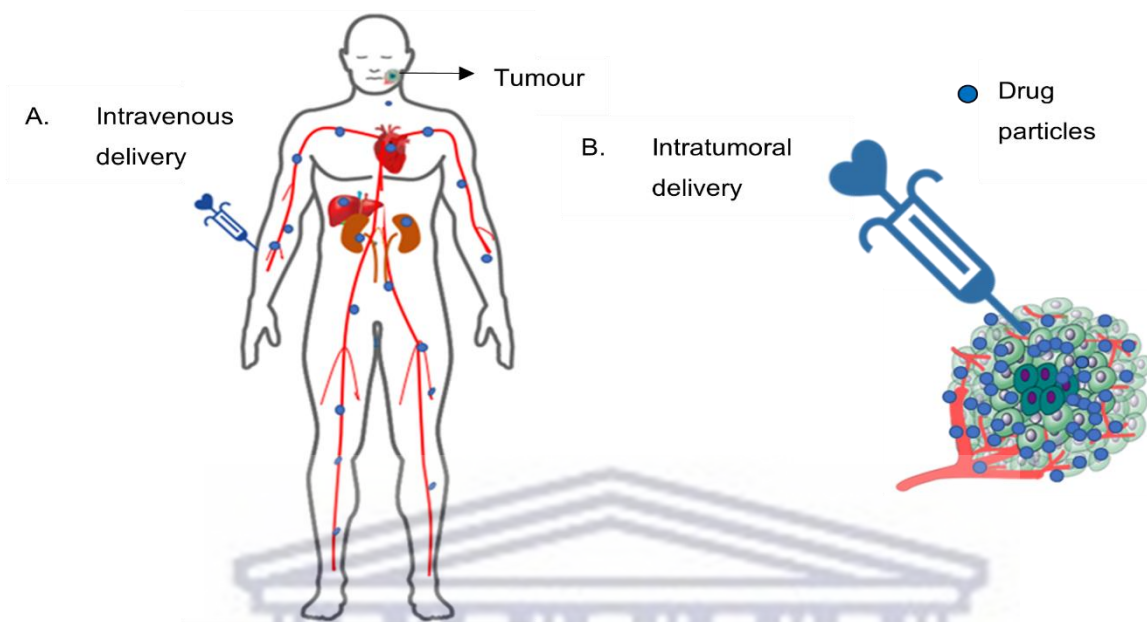


Figure 2.7: Representation of intravenous delivery and intratumoral delivery. A. Intravenous delivery: the drug is systemically circulated throughout the body. B. Intratumoral delivery: the drug remains localised within the tumour.

Synthetic polymers such as Pluronic™ F127 (PF-127), poly isopropyl acrylamide (PNIPAM), poly (D, L-lactide-co-glycolide)-b-poly (ethylene glycol)-b-poly (D, L-lactide -co-glycolide) (PLGA-PEG-PLGA), polycaprolactone, and poly (vinyl methyl ether) are well known and employed for their thermoresponsive effect. These polymers are formed through radical polymerisation and can undergo physical or chemical crosslinking with other polymers like chitosan, hyaluronic acid, and cellulose (Khan *et al.*, 2021). Physical crosslinking methods such as electrostatic interactions, hydrophobic interactions and stereocomplexation are commonly utilised as they are mostly reversible in their sol-gel behaviour (Zhou *et al.*, 2022). Chemical crosslinking methods such as click chemistry, Michael-type addition, and Schiff base reactions have poor reversibility, however, they are more stable than physically crosslinked hydrogels (Liu *et al.*, 2021; Dehghan-Baniani *et al.*, 2020; Maiti *et al.*, 2020). Additionally, the crosslinking reagents used for chemically crosslinked hydrogels such as glutaraldehyde, are often incompatible with bioactive molecules and unsafe for human use (Mitra, Sailakshmi, and Gnanamani, 2014).

The lower critical solution temperature (LCST) of a thermoresponsive hydrogel indicates the temperature at which the solution gels and is an important consideration during hydrogel preparation. As the temperature increases, the viscosity of the solution increases and the crosslinking bonds tighten until a gel is obtained, as portrayed in Figure 2.8. Most polymers used for thermal response have a very high LCST, which limits their applicability for biopharmaceutical use (Table 2.2). PNIPAM and PF-127 have become very useful in thermosensitive hydrogel formulation because their LCST is closer to physiological temperature. Additions of different polymers and changes in their ratios or polymer links have been used to alter the LCST of different hydrogels. For example, Xu *et al.*, 2018 reduced the LCST of copolymers of acrylamide, *N,N*-dimethyl acrylamide, and 3-(acrylamido)phenylboronic acid from 86 °C to 14 °C by the addition of poly (vinyl acrylamide), a polymeric additive.

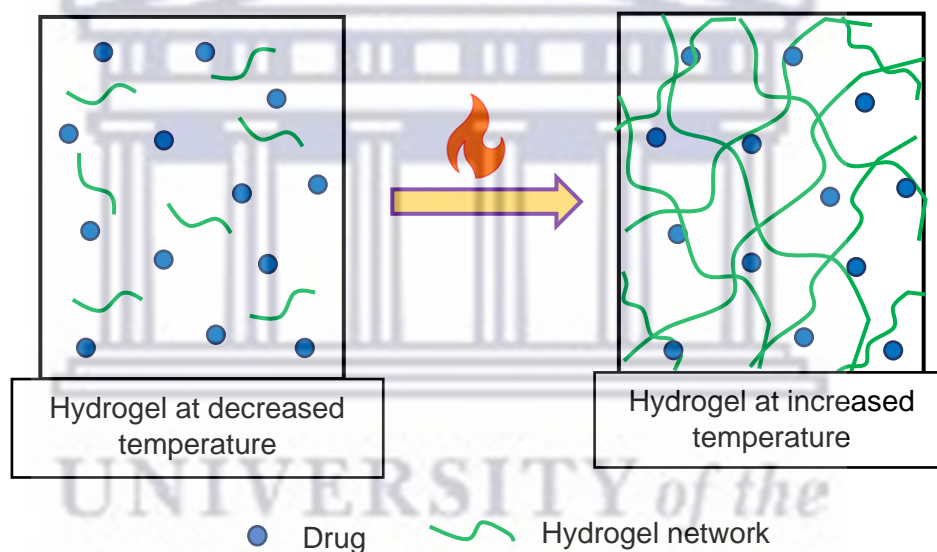


Figure 2.8: Sol-to-gel transition of thermosensitive hydrogel at low and high temperatures.

Table 2.2: LCST of commonly used polymers in water

| Polymer  | Polymer concentration in aqueous solution (% w/v) | LCST (°C) | Reference                         |
|--|---|-----------|-----------------------------------|
| Poly( <i>N</i> -isopropyl acrylamide), PNIPAM            | ~ 2.5   | ~ 32      | Fehér, Varga, and Pedersen, 2021  |
| Poly(vinyl methyl ether), PVME                           | ~ 5   | ~ 40      | Starovoytova <i>et al.</i> , 2016 |
| PLGA-PEG-PLGA  | ~ 25  | ~ 25      | Yu, Zhang, and Ding, 2006         |
| Poly( <i>N</i> -vinylcaprolactam), PNVCL                 | ~ 0.5   | ~ 30      | Marsili <i>et al.</i> , 2021.     |
| Chitosan-glycerol phosphate                              | ~ 1 CH + ~ 10 GP                                  | ~ 37      | Ahmadi, and de Bruijn, 2008       |
| Pluronic™ F127, PF-127                                   | ~ 15  | ~ 70      |                                   |
| Hydroxypropyl methylcellulose, HPMC                      | ~ 1   | ~ 70      | Joshi <i>et al.</i> , 2011        |
| Polyphosphazene derivatives                              | ~ 2   | 25 – 80   | Wilfert <i>et al.</i> , 2014      |
| Methoxy poly(ethylene glycol) (MPEG)–diblock copolymers) | ~ 1   | 32 – 42   | Chen, Lin, and Chu, 2010          |

An important factor which determines the release behaviour of the hydrogel system is the mechanical strength. While synthetic hydrogels are useful for their thermal response, their formed gel is extremely weak in strength and elasticity. This often leads to premature "burst

release" and/or unrhythmic release patterns of the drug. These synthetic polymers also have very long degradation rates, which may not be favourable for chemotherapeutic drug release (Shen *et al.*, 2017). Also, polyethylene glycol-based polymers produce acidic degradation products that may react with the chemotherapeutic drug or cause inflammation to the host tissue (Dirauf *et al.*, 2022). To circumvent these effects, researchers have relied on crosslinking synthetic polymers with natural polysaccharides such as chitosan, gellan gum, hyaluronic acid and alginate, to improve the mechanical strength and degradation rates of the hydrogel (Yap and Yang, 2016, Sohn *et al.*, 2016; Yu *et al.*, 2017; Xu *et al.*, 2020). For example, Liu and colleagues designed a thermoresponsive copolymer using alginate-*g*-poly(*N*-isopropyl acrylamide) loaded with DOX. The hydrogels were able to release DOX encapsulated micelles in a sustained manner and enhanced the cellular uptake of the drug in multidrug-resistant AT3B-1 cells (Lui *et al.*, 2017). In addition, the pure alginate-*g*-PNIPAM copolymers were non-cytotoxic in the cell lines (Lui *et al.*, 2017), showing great potential for sustained release and effective delivery of anti-cancer drugs. Recently Song *et al.*, 2020, synthesised a dual supramolecular hydrogel using PNIPAM with a  $\beta$ -cyclodextrin core and an adamantyl-terminated poly(ethylene glycol) polymer. The system managed to release a pseudo-block copolymer in the form of micelles that continued to serve as drug carriers with DOX encapsulated in the hydrophobic core. The researchers reported improved cellular uptake and anti-cancer effect than free DOX controls, even in multidrug-resistant cancer cells (Song *et al.*, 2020).

The application of injectable thermosensitive hydrogels for cancer treatment has been severely limited. Table 2.3 shows a list of thermosensitive hydrogels that have undergone clinical trials for cancer treatment. To date, only Jelymyto<sup>®</sup> has received FDA approval for upper tract urothelial carcinoma (Donin, *et al.*, 2017). Though the system relies on pyelocaliceal delivery, it still possesses the solution-to-gel transition property of thermosensitive hydrogels. Notably, only PLGA-PEG-PLGA thermosensitive polymers have undergone clinical trials for cancers, likely because they display suitable properties for encapsulating hydrophobic chemotherapeutic drugs. This is important because most chemotherapeutic drugs are hydrophobic and will therefore show poor solubility in polymer blocks with hydrophilic ends (e.g., polyethylene glycol-based polymers) (Boonlai *et al.*, 2018). Triblock copolymers such as PLGA-PEG-PLGA have 2 hydrophobic ends and will show enhanced solubility when used with hydrophobic drugs.



Table 2.3: Thermosensitive hydrogels that have undergone clinical trials for cancer treatment

| Tradename | Encapsulated drug | Thermosensitive hydrogel | Cancer type   | Status                         | References  |
|-----------|-------------------|--------------------------|---|--------------------------------|---|
| OncoGel®  | Paclitaxel        | PLGA-PEG-PLGA            | Esophageal Cancer<br>Adenocarcinoma of the Esophagus<br>Squamous Cell Carcinoma<br>Brain Neoplasms<br>Glioblastoma Multiforme | Phase 2<br><br><br><br>Phase 2 | Cho, Gao, and Kwon, 2016.<br>ClinicalTrials.gov, (n.d.)b<br><br><br><br>ClinicalTrials.gov., (n.d.)c  |
| Jelymyto® | Mytomycin         | PLGA-PEG-PLGA            | Carcinoma, Transitional Cell Transitional Cell Carcinoma of Renal Pelvis<br>Bladder Cancer                                    | Phase 3<br><br><br><br>Phase 2 | Kleinmann <i>et al.</i> , 2020<br>ClinicalTrials.gov., (n.d.)d<br><br><br>Chevli <i>et al.</i> , 2022 |

### 2.5.3.2 Multicomponent systems

There often exists various challenges in designing single component DDSs; for example, nanoparticles may easily leak through the tumour vessels. In order to combat the limitations of one response system, researchers dive into the use of multicomponent or multifunctional materials for enhanced drug delivery. For instance, a combined system of a thermosensitive hydrogel embedded with nanoparticles may be a strategy to increase drug loading and avoid rapid drug release and wastage (Pang *et al.*, 2020; Manatunga *et al.*, 2017). A remarkable study was conducted by Pang and his colleagues in which they combined the advantages of hydrogels and small-sized nanoparticles to formulate a structure transformable thermo-pH responsive co-delivery system to deliver co-loaded chemo-protein drugs to the tumour site (Pang *et al.*, 2020). The developed system was able to co-deliver two different anti-cancer drugs, facilitate tumour accumulation, and achieve tumour penetration (Pang *et al.*, 2020).

Another noteworthy mention is the design of a novel multifunctional nanoplateform comprising alginate nanogel co-loaded with cisplatin and gold nanoparticles, which was developed to combine photothermal therapy and chemotherapy (Mirrahimi *et al.*, 2019). The combined action of chemo-photothermal therapy using the nanocomplex dramatically suppressed tumour growth up to 95% of control and markedly prolonged the animal survival rate (Mirrahimi *et al.*, 2019). Despite the good results promised by multicomponent systems, their high cost, long preparation time and complex methods present some drawbacks.

## 2.6 Strategies for enhancing drug permeation

As highlighted throughout this chapter, tumour structures and factors such as large molecular weight, hydrophilicity, and drug-resistant proteins, limit the permeation of chemotherapeutic drugs. This insufficient delivery to the nucleus of OSCCs has necessitated the improvement of anti-cancer treatment. Poor permeability to nucleus cells prolongs the need for treatment, causing financial strains and continued unbearable side-effects. Permeation strategies have therefore been implemented in oral cancer therapy to increase the uptake of chemotherapeutic drugs via a range of physical and pharmacological approaches. Regarding physical approaches, the endothelial pores are widened using vasomediators or external mechanical forces like laser light, ultrasound and radiation (Dasgupta *et al.*, 2016; De Rosa *et al.*, 2000). These strategies can reconfigure the tumour microenvironment by widening vessel leakiness or destroying physical barriers in the tumour, therefore improving drug accumulation and therapeutic efficacy (Byrne, Tambe, and Coulter, 2021; Tang *et al.*, 2019).

For pharmacological modifications, the design of a delivery system and the selection of pharmaceutical excipients play a substantial role in influencing tumour permeation. The perfect excipient must be biologically safe and compatible with the active ingredient or other excipients. A delivery design may contain a lipophilic or amphiphilic excipient, reasonably because high lipophilicity increases tissue penetration. INT230-6 is an intratumoral formulation of cisplatin and vinblastine with an amphiphilic penetration enhancer designed to improve dispersion and diffusion into cancer cells (El-Khoeiry *et al.*, 2018). Intensity Therapeutics Inc. reported more rapid and improved penetration throughout the tumour, including hypoxic and nonvascularised areas, with the use of their novel permeation enhancer. Clinical trials for INT230-6 are still ongoing. Other pharmacological strategies include the use of low-dose anti-angiogenic agents to correct the structural and functional abnormalities of tumour vasculature (Li *et al.*, 2020).

Concerning drug delivery, the size, surface charge, and particle shape of nanoparticles are manipulated to enhance permeation. However, excessive manipulation of the physicochemical characteristics of nanomedicines can compromise their targeting efficiency; for example, minimising particle size below 5 nm shortens their blood circulation, and therefore, the tumour-targeting efficiency and larger nanoparticles may create a hypoxic environment, thereby weakening drug efficiency (Zhou *et al.*, 2021). Slightly negatively charged nanoparticles have a longer circulation time in the bloodstream, which enhances their tumour accumulation probabilities, but positively charged nanoparticles provide an easier uptake by tumour cells (Wu *et al.*, 2021; Zhou *et al.*, 2021). Contrasts like these have influenced the rise of designs of charge/size switchable nanomedicines. An ultrasound-triggered dual size/charge-switchable nano catalytic medicine, designated as Cu-layered double hydroxide (LDH)/hematoporphyrin monomethyl ether liposomes, was constructed by Wu *et al.*, 2021, for deep solid tumour therapy via catalytic reactive oxygen species generation. The small, positively charged Cu-LDH nanosheets ( $\approx 50$  nm) encapsulated into the cores of larger liposomes ( $\approx 200$  nm) prolonged circulatory half-life and blood circulation while ensuring infiltration deeply into the tumour tissue (Wu *et al.*, 2021).

Unlike nanoparticles, it is arguable that the mucoadhesive nature of hydrogels is an important requirement to enhance permeation, simply because the longer the system adheres to the site, the greater the exposure of drug release to the adhering tissue. However, if drug permeability is very poor, mucoadhesion alone will not be sufficient to stimulate adequate tissue absorption. Drug transport to the nucleus with the said delivery system is mostly dependent on the passive diffusion of free drug from the cytoplasm to the nucleus, which could be inefficient. The use of a chemical permeation enhancer in a hydrogel preparation to improve diffusion is therefore beneficial. Terpenes, fatty acids, fatty alcohols, alcohols, glycols, laurocapram (Azone®), sulfoxides, pyrrolidones, and surfactants have been explored for permeation enhancement and have potential for use in hydrogel preparations (Salem *et al.*, 2022; Tampucci *et al.*, 2020).

Terpenes like menthol, limonene,  $\alpha$ -bisabolol and camphor have received attention as permeation enhancers in cancer, particularly in skin cancers. Apart from their high lipophilicity, these compounds possess wound healing, antitumour, anti-inflammatory, antibiotic, and immunogenic properties which are beneficial in cancer treatment (Quintanilha *et al.*, 2017). Cosolvents like propylene glycol can increase the permeability of hydrophobic chemotherapeutic drugs across biological membranes via solvent drag. When propylene glycol is combined with another permeation enhancer, pronounced drug permeation can be expected

as it acts as a cosolvent for both permeant and enhancer and may facilitate enhanced penetration of both molecules (Wu *et al.*, 2012). This knowledge was further explored by Wu and coworkers, who evaluated mucoadhesive fenretinide-Eudragit RL PO-solubilizer-containing patches with propylene glycol and menthol for increased mucosal permeation in oral cancer both *in vitro* and *in vivo*. Saffari *et al.*, 2016 used two terpenes; limonene and cineole, to formulate nanoliposomes for gene delivery in lung cancer. Cellular uptake was increased by the cineole liposomes, while liposomal limonene showed insignificant uptake. The study quotes Moghimi *et al.*, to support that limonene has weak enhancement effects toward permeation of hydrophilic drugs through lamellar lipid structures.

The use of peptides to enhance permeation has also drawn much attention. Peptides bind to a primary, tumour-specific receptor, followed by a proteolytic cleavage and binding to the second receptor called neuropilin-1 and 2, which activates the transport pathway. Chemical enhancers like organic solvents and protonated chitosan have shown efficacy in further increasing the permeability of peptides in cancer cells (Yong *et al.*, 2018; Sonaje *et al.*, 2012).

## 2.7 Conclusion

Surgery, chemotherapy and radiation are the main treatment strategies for OSCC. While there have been some treatment improvements over the past years, OSCC treatment still leads to permanent disfigurement, decreased self-esteem, and debilitating physiological consequences. The structural barriers of tumours such as their histopathology, inconsistent oxygen supply and unrestrained blood vessels, contribute to the treatment shortcomings. Chemotherapy holds great importance as adjunct OSCC treatment, but challenges of poor permeation, inaccessibility and systemic side-effects limit its adherence and applicability. These treatment challenges have compelled the design of complex DDSs such as liposomes, nanoparticles, hydrogels, multicomponent systems, and the exploration of strategies to enhance drug permeation. To enhance drug delivery targeting, stimuli-response systems have been investigated with various anti-cancer drugs, and despite their rigorous examination and system accolades, no stimuli-responsive hydrogel systems for cancer have survived through clinical stages, showing that there is still a need for investigation of this approach. Also, xenograft models used in most research mentioned in this chapter do not accurately reproduce human oral cancer due to their limitations in terms of tumour location, microenvironment, vasculature, and metastatic growth. Hence, results achieved in several studies may not represent the true reaction of the system in humans – reasonably why many studies fail clinical trials.

The importance of intratumoral delivery for localised treatment and drug accumulation has been emphasised when used as an injectable thermosensitive hydrogel drug carrier. Consequently, drug accumulation is improved in tumours that show varying differentiation and hypoxic behaviours, as well as easy permeation of chemotherapeutic drugs. Drug designs that are currently FDA-approved for OSCC such as hydrogels, nanoparticles, and liposomes, still lack efficient delivery outcomes. The use of multicomponent systems or the inclusion of excipients with synergistic properties, such as permeation enhancers, should be further explored. The urgency continues for researchers to get an improved system through clinical trials and in the clinic.



## 2.8 References

- Abdel Razek, A.A.K. and Nada, N. 2018. Arterial spin labeling perfusion-weighted MR imaging: correlation of tumor blood flow with pathological degree of tumor differentiation, clinical stage and nodal metastasis of head and neck squamous cell carcinoma. *European Archives of Oto-Rhino-Laryngology*, 275(5), pp.1301-307.
- Aframian, D.J., Davidowitz, T. and Benoliel, R. 2006. The distribution of oral mucosal pH values in healthy saliva secretors. *Oral Diseases*, 12(4), pp.420-423.
- Ahadian, H., Yassaei, S., Bouzarjomehri, F., Targhi, M.G. and Kheirollahi, K. 2017. Oral complications of the oromaxillofacial area radiotherapy. *Asian Pacific Journal of Cancer Prevention: APJCP*, 18(3), p.721, Article ID: 10.22034/APJCP.2017.18.3.721.
- Ahmadi, R. and de Bruijn, J.D. 2008. Biocompatibility and gelation of chitosan–glycerol phosphate hydrogels. *Journal of Biomedical Materials Research*, 86(3), pp.824-832.
- Alavi, M., Rai, M., Martinez, F., Kahrizi, D., Khan, H., Rose Alencar De Menezes, I., Douglas Melo Coutinho, H. and Costa, J.G.M. 2022. The efficiency of metal, metal oxide, and metalloid nanoparticles against cancer cells and bacterial pathogens: different mechanisms of action. *Cellular, Molecular and Biomedical Reports*, 2(1), pp.10-21.
- Anakwenze, C.P., Ntekim, A., Trock, B., Uwadiae, I.B. and Page, B.R. 2017. Barriers to radiotherapy access at the University College Hospital in Ibadan, Nigeria. *Clinical and Translational Radiation Oncology*, 5, pp.1-5.
- Anjali, K., Arun, A.B., Bastian, T.S., Parthiban, R., Selvamani, M. and Adarsh, H. 2020. Oral microbial profile in oral cancer patients before and after radiation therapy in a cancer care center—A prospective study. *Journal of Oral and Maxillofacial Pathology: JOMFP*, 24(1), p.117-124.
- Arun, P., Sagayaraj, A., Mohiyuddin, S.A. and Santosh, D. 2020. Role of turmeric extract in minimising mucositis in patients receiving radiotherapy for head and neck squamous cell cancer: a randomised, placebo-controlled trial. *The Journal of Laryngology & Otology*, 134(2), pp.159-164.

Astuti, I., Torizal, G.F., Sa'adah, N., Oktriani, R., Wardana, T., Aryandono, T. and Mubarika, S. 2019. Resistance to doxorubicin correlated with dysregulation of microRNA-451 and P-glycoprotein, caspase 3, estrogen Receptor on Breast Cancer cell line. *Journal of the Medical Sciences (Berkala Ilmu Kedokteran)*, 51(4), pp.282-291.

Balasubramanian, D., Ebrahimi, A., Gupta, R., Gao, K., Elliott, M., Palme, C.E. and Clark, J.R. 2014. Tumour thickness as a predictor of nodal metastases in oral cancer: comparison between tongue and floor of mouth subsites. *Oral Oncology*, 50(12), pp.1165-1168.

Becelli, R., Renzi, G., Morello, R. and Altieri, F. 2007. Intracellular and extracellular tumor pH measurement in a series of patients with oral cancer. *Journal of Craniofacial Surgery*, 18(5), pp.1051-1054.

Bhattacharya, S., Ghosh, A., Maiti, S., Ahir, M., Debnath, G.H., Gupta, P., Bhattacharjee, M., Ghosh, S., Chattopadhyay, S., Mukherjee, P. and Adhikary, A. 2020. Delivery of thymoquinone through hyaluronic acid-decorated mixed Pluronic® nanoparticles to attenuate angiogenesis and metastasis of triple-negative breast cancer. *Journal of Controlled Release*, 322, pp.357-374.

Bijai, L.K., Mathew, P., Jayaraman, V. and Austin, R.D. 2014. Oral squamous cell carcinoma of palate—A case report and review of literature. *International Journal of Dental Sciences and Research*, 2(5), pp.106-108.

Bilalis, P., Skoulas, D., Karatzas, A., Marakis, J., Stamogiannos, A., Tsimblouli, C., Sereti, E., Stratikos, E., Dimas, K., Vlassopoulos, D. and Iatrou, H. 2018. Self-healing pH-and enzyme stimuli-responsive hydrogels for targeted delivery of gemcitabine to treat pancreatic cancer. *Biomacromolecules*, 19(9), pp.3840-3852.

Bishr, M.K. and Zaghoul, M.S. 2018. Radiation therapy availability in Africa and Latin America: two models of low and middle income countries. *International Journal of Radiation Oncology\* Biology\* Physics*, 102(3), pp.490-498.

Boeve, K., Melchers, L.J., Schuurin, E., Roodenburg, J.L., Halmos, G.B., van Dijk, B.A., van der Vegt, B. and Witjes, M.J. 2019. Addition of tumour infiltration depth and extranodal extension improves the prognostic value of the pathological TNM classification for early-stage oral squamous cell carcinoma. *Histopathology*, 75(3), pp.329-337.

Bonvalot, S., Rutkowski, P.L., Thariat, J., Carrère, S., Ducassou, A., Sunyach, M.P., Agoston, P., Hong, A., Mervoyer, A., Rastrelli, M. and Moreno, V. 2019. NBTXR3, a first-in-class radioenhancer hafnium oxide nanoparticle, plus radiotherapy versus radiotherapy alone in patients with locally advanced soft-tissue sarcoma (Act. In. Sarc): a multicentre, phase 2–3, randomised, controlled trial. *The Lancet Oncology*, 20(8), pp.1148-1159.

Boonlai, W., Tantishaiyakul, V., Hirun, N., Sangfai, T. and Suknuntha, K. 2018. Thermosensitive poloxamer 407/poly (acrylic acid) hydrogels with potential application as injectable drug delivery system. *AAPS PharmSciTech*, 19(5), pp.2103-2117.

Borys, N. and Dewhurst, M.W. 2021. Drug development of lyso-thermosensitive liposomal doxorubicin: Combining hyperthermia and thermosensitive drug delivery. *Advanced Drug Delivery Reviews*, 178, Article ID: 113985.

Brandão, T.B., Morais-Faria, K., Ribeiro, A.C.P., Rivera, C., Salvajoli, J.V., Lopes, M.A., Epstein, J.B., Arany, P.R., de Castro, G., Migliorati, C.A. and Santos-Silva, A.R. 2018. Locally advanced oral squamous cell carcinoma patients treated with photobiomodulation for prevention of oral mucositis: retrospective outcomes and safety analyses. *Supportive Care in Cancer*, 26(7), pp.2417-2423.

Brevé, T.G., Filius, M., Weerdenburg, S., van der Griend, S.J., Groeneveld, T.P., Denkova, A.G. and Eelkema, R., 2022. Light-Sensitive Phenacyl Crosslinked Dextran Hydrogels for Controlled Delivery. *Chemistry–A European Journal*, 28(10), Article, ID: e202103523.

Burade, Vinod, Subhas Bhowmick, Kuntal Maiti, Rishit Zalawadia, Harry Ruan, and Rajamannar Thennati. "Lipodox®(generic doxorubicin hydrochloride liposome injection): in vivo efficacy and bioequivalence versus Caelyx®(doxorubicin hydrochloride liposome injection) in human mammary carcinoma (MX-1) xenograft and syngeneic fibrosarcoma (WEHI 164) mouse models." *BMC Cancer* 17, no. 1 (2017): 1-12.

Byrne, N.M., Tambe, P. and Coulter, J.A. 2021. Radiation response in the tumour microenvironment: Predictive biomarkers and future perspectives. *Journal of Personalized Medicine*, 11(1), p.53, Article ID: 10.3390/jpm11010053.

Caldeira, P.C., Soto, A.M.L., de Aguiar, M.C.F. and Martins, C.C. 2020. Tumor depth of invasion and prognosis of early-stage oral squamous cell carcinoma: A meta-analysis. *Oral Diseases*, 26(7), pp.1357-1365.



Cao, D., Zhang, X., Akabar, M.D., Luo, Y., Wu, H., Ke, X. and Ci, T. 2019. Liposomal doxorubicin loaded PLGA-PEG-PLGA based thermogel for sustained local drug delivery for the treatment of breast cancer. *Artificial Cells, Nanomedicine, and Biotechnology*, 47(1), pp.181-191.

Chang, G., Zhang, H., Li, S., Huang, F., Shen, Y. and Xie, A. 2019. Effective photodynamic therapy of polymer hydrogel on tumor cells prepared using methylene blue sensitized mesoporous titania nanocrystal. *Materials Science and Engineering: C*, 99, pp.1392-1398.

Chang, W.C., Chang, C.F., Li, Y.H., Yang, C.Y., Su, R.Y., Lin, C.K. and Chen, Y.W. 2019. A histopathological evaluation and potential prognostic implications of oral squamous cell carcinoma with adverse features. *Oral Oncology*, 95, pp.65-73.

Chang, Y.L., Lin, C.Y., Kang, C.J., Liao, C.T., Chung, C.F., Yen, T.C., Peng, H.L. and Chen, S.C. 2021. Association between multidisciplinary team care and the completion of treatment for oral squamous cell carcinoma: A cohort population-based study. *European Journal of Cancer Care*, 30(2), Article ID: e13367.

Chen, C.F., Lin, C.T.Y. and Chu, I.M. 2010. Study of novel biodegradable thermo-sensitive hydrogels of methoxy-poly (ethylene glycol)-block-polyester diblock copolymers. *Polymer International*, 59(10), pp.1428-1435.

Chevli, K.K., Shore, N.D., Trainer, A., Smith, A.B., Saltzstein, D., Ehrlich, Y., Raman, J.D., Friedman, B., D'Anna, R., Morris, D. and Hu, B. 2022. Primary chemoablation of low-grade intermediate-risk nonmuscle-invasive bladder cancer using UGN-102, a mitomycin-containing reverse thermal gel (Optima II): a phase 2b, open-label, single-arm trial. *The Journal of urology*, 207(1), pp.61-69.

Cho, H., Gao, J. and Kwon, G.S. 2016. PEG-b-PLA micelles and PLGA-b-PEG-b-PLGA sol-gels for drug delivery. *Journal of Controlled Release*, 240, pp.191-201.

Chu, L.L., Pandey, R.P., Shin, J.Y., Jung, H.J. and Sohng, J.K. 2016. Synthetic analog of anticancer drug daunorubicin from daunorubicinone using one-pot enzymatic UDP-recycling glycosylation. *Journal of Molecular Catalysis B: Enzymatic*, 124, pp.1-10.

ClinicalTrials.gov. (n.d.)a. A Clinical Trial Investigating the Safety, Tolerability, and Therapeutic Effects of BNT113 in Combination With Pembrolizumab Versus Pembrolizumab Alone for

Patients With a Form of Head and Neck Cancer Positive for Human Papilloma Virus 16 and Expressing the Protein PD-L1 (AHEAD-MERIT), <https://www.clinicaltrials.gov/ct2/show/NCT04534205> (Accessed on 25 October 2021).

ClinicalTrials.gov. (n.d.)b: Efficacy and Safety of OncoGel™ Added to Chemotherapy and Radiation Before Surgery in Subjects With Esophageal Cancer, <https://www.clinicaltrials.gov/ct2/show/NCT00573131#:~:text=OncoGel%20is%20a%20new%20experimental%20drug%20delivery%20system,to%206%20weeks%20as%20it%20releases%20t%20paclitaxel> (Accessed on 25 October 2021).

ClinicalTrials.gov. (n.d.)c: A Phase 1/2 Dose Escalation Study of Locally-Administered OncoGel™ in Subjects With Recurrent Glioma, <https://clinicaltrials.gov/ct2/show/NCT00479765?term=oncogel&cond=Cancer&draw=2&rank=2> (Accessed on 25 October 2021).

ClinicalTrials.gov. (n.d.)d: The OLYMPUS Study - Optimized DeLivery of Mitomycin for Primary UTUC Study (Olympus), <https://clinicaltrials.gov/ct2/show/NCT02793128?term=Mitomycin+gel&cond=upper+tract+urothelial+carcinoma&draw=2&rank=2> (Accessed on 25 October 2021).

D'Angelo, N.A., Noronha, M.A., Câmara, M.C., Kurnik, I.S., Feng, C., Araujo, V.H., Santos, J.H., Feitosa, V., Molino, J.V., Rangel-Yagui, C.O. and Chorilli, M. 2022. Doxorubicin nanoformulations on therapy against cancer: An overview from the last 10 years. *Biomaterials Advances*, 133, p.112623.

d'Avanzo, N., Torrieri, G., Figueiredo, P., Celia, C., Paolino, D., Correia, A., Moslova, K., Teesalu, T., Fresta, M. and Santos, H.A. 2021. LinTT1 peptide-functionalized liposomes for targeted breast cancer therapy. *International Journal of Pharmaceutics*, 597, Article ID: 120346.

Dasgupta, A., Liu, M., Ojha, T., Storm, G., Kiessling, F. and Lammers, T. 2016. Ultrasound-mediated drug delivery to the brain: principles, progress and prospects. *Drug Discovery Today: Technologies*, 20, pp.41-48.

De Rosa, F.S., Marchetti, J.M., Thomazini, J.A., Tedesco, A.C. and Bentley, M.V.L.B. 2000. A vehicle for photodynamic therapy of skin cancer: influence of dimethylsulphoxide on 5-aminolevulinic acid in vitro cutaneous permeation and in vivo protoporphyrin IX accumulation determined by confocal microscopy. *Journal of Controlled Release*, 65(3), pp.359-366.

De Vera, A.A., Gupta, P., Lei, Z., Liao, D., Narayanan, S., Teng, Q., Reznik, S.E. and Chen, Z.S. 2019. Immuno-oncology agent IPI-549 is a modulator of P-glycoprotein (P-gp, MDR1, ABCB1)-mediated multidrug resistance (MDR) in cancer: In vitro and in vivo. *Cancer Letters*, 442, pp.91-103.

Dehghan-Baniani, D., Chen, Y., Wang, D., Bagheri, R., Solouk, A. and Wu, H. 2020. Injectable in situ forming kartogenin-loaded chitosan hydrogel with tunable rheological properties for cartilage tissue engineering. *Colloids and Surfaces B: Biointerfaces*, 192, Article ID: 111059.

Derakhshankhah, H., Jahanban-Esfahlan, R., Vandghanooni, S., Akbari-Nakhjavani, S., Massoumi, B., Haghshenas, B., Rezaei, A., Farnudiyan-Habibi, A., Samadian, H. and Jaymand, M. 2021. A bio-inspired gelatin-based pH-and thermal-sensitive magnetic hydrogel for in vitro chemo/hyperthermia treatment of breast cancer cells. *Journal of Applied Polymer Science*, 138(24), Article ID: 50578.

Derieppe, M., Escoffre, J.M., Denis de Senneville, B., van Houtum, Q., Rijbroek, A.B.V., van der Wurff-Jacobs, K., Dubois, L., Bos, C. and Moonen, C. 2019. Assessment of Intratumoral Doxorubicin Penetration after Mild Hyperthermia-Mediated Release from Thermosensitive Liposomes. *Contrast Media & Molecular Imaging*, 2019, Article ID: 2645928.

Deshpande, P., Jhaveri, A., Pattni, B., Biswas, S. and Torchilin, V. 2018. Transferrin and octaarginine modified dual-functional liposomes with improved cancer cell targeting and enhanced intracellular delivery for the treatment of ovarian cancer. *Drug Delivery*, 25(1), pp.517-532.

Dewhirst, M.W. and Secomb, T.W. 2017. Transport of drugs from blood vessels to tumour tissue. *Nature Reviews Cancer*, 17(12), pp.738-750.

Dirauf, M., Muljajew, I., Weber, C. and Schubert, U.S. 2022. Recent advances in degradable synthetic polymers for biomedical applications–Beyond polyesters. *Progress in Polymer Science*, p.101547.

Dirven, R., Ebrahimi, A., Moeckelmann, N., Palme, C.E., Gupta, R. and Clark, J. 2017. Tumor thickness versus depth of invasion–Analysis of the 8th edition American Joint Committee on Cancer Staging for oral cancer. *Oral Oncology*, 74, pp.30-33.

Donin, N.M., Duarte, S., Lenis, A.T., Caliliw, R., Torres, C., Smithson, A., Strauss-Ayali, D., Agmon-Gerstein, Y., Malchi, N., Said, J. and Raman, S.S. 2017. Sustained-release formulation of mitomycin C to the upper urinary tract using a thermosensitive polymer: a preclinical study. *Urology*, 99, pp.270-277.

Dordunoo, S.K. and Burt, H.M. 1996. Solubility and stability of taxol: effects of buffers and cyclodextrins. *International Journal of Pharmaceutics*, 133(1-2), pp.191-201.

Du, W., Hong, L., Yao, T., Yang, X., He, Q., Yang, B. and Hu, Y. 2007. Synthesis and evaluation of water-soluble docetaxel prodrugs-docetaxel esters of malic acid. *Bioorganic & Medicinal Chemistry*, 15(18), pp.6323-6330.

El-Khoeiry, A., Siu, L.L., Azad, N., Walters, I.B., Bender, L., Kamen, L. and Olszanski, A.J. 2018. Phase I/II evaluation of intratumoral INT230-6 for the treatment of solid tumors. *Annals of Oncology*, 29, p.viii413.

Fan, L., Wang, W., Wang, Z. and Zhao, M. 2021. Gold nanoparticles enhance antibody effect through direct cancer cell cytotoxicity by differential regulation of phagocytosis. *Nature Communications*, 12(1), pp.1-13.

Fan, M., Jia, L., Pang, M., Yang, X., Yang, Y., Kamel Elyzayati, S., Liao, Y., Wang, H., Zhu, Y. and Wang, Q. 2021. Injectable Adhesive Hydrogel as Photothermal-Derived Antigen Reservoir for Enhanced Anti-Tumor Immunity. *Advanced Functional Materials*, 31(20), p.2010587.

Fehér, B., Varga, I. and Pedersen, J.S. 2021. Effect of concentration and ionic strength on the lower critical solution temperature of poly (N-isopropylacrylamide) investigated by small-angle X-ray scattering. *Soft Materials*, pp.1-9.

Feng, L., De Dille, A., Jameson, V.J., Smith, L., Dernel, W.S. and Manning, M.C. 2004. Improved potency of cisplatin by hydrophobic ion pairing. *Cancer Chemotherapy and Pharmacology*, 54(5), pp.441-448.

Gebre-Medhin, M., Haghanegi, M., Robért, L., Kjellén, E. and Nilsson, P. 2016. Dose-volume analysis of radiation-induced trismus in head and neck cancer patients. *Acta Oncologica*, 55(11), pp.1313-1317.

Goindi, S., Arora, P., Kumar, N. and Puri, A. 2014. Development of novel ionic liquid-based microemulsion formulation for dermal delivery of 5-fluorouracil. *AAPS PharmSciTech*, 15, pp.810-821.

Goldstein, M., Maxymiw, W.G., Cummings, B.J. and Wood, R.E. 1999. The effects of antitumor irradiation on mandibular opening and mobility: a prospective study of 58 patients. *Oral Surgery, Oral Medicine, Oral Pathology, Oral Radiology, and Endodontology*, 88(3), pp.365-373.

Grantab, R.H. and Tannock, I.F. 2012. Penetration of anticancer drugs through tumour tissue as a function of cellular packing density and interstitial fluid pressure and its modification by bortezomib. *BMC Cancer*, 12(1), pp.1-11.

Halczy-Kowalik, L., Drozd, A., Stachowska, E., Drozd, R., Żabski, T. and Domagała, W. 2019. Fatty acids distribution and content in oral squamous cell carcinoma tissue and its adjacent microenvironment. *PloS One*, 14(6), p.e0218246.

Hoffmann, C., Calugaru, V., Borcoman, E., Moreno, V., Calvo, E., Liem, X., Salas, S., Doger, B., Jouffroy, T., Mirabel, X. and Rodriguez, J. 2021. Phase I dose-escalation study of NBTXR3 activated by intensity-modulated radiation therapy in elderly patients with locally advanced squamous cell carcinoma of the oral cavity or oropharynx. *European Journal of Cancer*, 146, pp.135-144.

Hosni, A., Huang, S.H., Chiu, K., Xu, W., Su, J., Bayley, A., Bratman, S.V., Cho, J., Giuliani, M., Kim, J. and O'Sullivan, B. 2019. Predictors of early recurrence prior to planned postoperative radiation therapy for oral cavity squamous cell carcinoma and outcomes following salvage intensified radiation therapy. *International Journal of Radiation Oncology\* Biology\* Physics*, 103(2), pp.363-373.

Hu, J., Youssefian, S., Obayemi, J., Malatesta, K., Rahbar, N. and Soboyejo, W. 2018. Investigation of adhesive interactions in the specific targeting of Triptorelin-conjugated PEG-coated magnetite nanoparticles to breast cancer cells. *Acta Biomaterialia*, 71, pp.363-378.

Jacobson, L.K., Johnson, M.B., Dedhia, R.D., Niknam-Bienia, S. and Wong, A.K. 2017. Impaired wound healing after radiation therapy: A systematic review of pathogenesis and treatment. *JPRAS Open*, 13, pp.92-105.

Jayasuriya, A.C. and Darr, A.J. 2013. Controlled release of cisplatin and cancer cell apoptosis with cisplatin encapsulated poly (lactic-co-glycolic acid) nanoparticles. *Journal of Biomedical Science and Engineering*, 6 (5). Article ID: 31902

Ji, C., Gao, Q., Dong, X., Yin, W., Gu, Z., Gan, Z., Zhao, Y. and Yin, M. 2018. A Size-Reducible Nanodrug with an Aggregation-Enhanced Photodynamic Effect for Deep Chemo-Photodynamic Therapy. *Angewandte Chemie*, 130(35), pp.11554-11558.

Jianmongkol, S. 2021. Overcoming P-Glycoprotein-Mediated Doxorubicin Resistance. *Advances in Precision Medicine Oncology*. IntechOpen, Article ID: 10.5772/intechopen.95553.

Joshi, S.C. 2011. Sol-gel behavior of hydroxypropyl methylcellulose (HPMC) in ionic media including drug release. *Materials*, 4(10), pp.1861-1905.

Kalyane, D., Raval, N., Maheshwari, R., Tambe, V., Kalia, K. and Tekade, R.K. 2019. Employment of enhanced permeability and retention effect (EPR): Nanoparticle-based precision tools for targeting of therapeutic and diagnostic agent in cancer. *Materials Science and Engineering: C*, 98, pp.1252-1276.

Kebsa, W., Lahouel, M., Rouibah, H., Zihlif, M., Ahram, M., Abu-Irmaileh, B., Mustafa, E., Al-Ameer, H.J. and Al Shhab, M. 2018. Reversing multidrug resistance in chemo-resistant human lung Adenocarcinoma (A549/DOX) cells by Algerian Propolis through direct inhibiting the P-gp Efflux-pump, G0/G1 cell cycle arrest and apoptosis induction. *Anti-Cancer Agents in Medicinal Chemistry (Formerly Current Medicinal Chemistry-Anti-Cancer Agents)*, 18(9), pp.1330-1337.

Kerker, F.A., Adler, W., Brunner, K., Moest, T., Wurm, M.C., Nkenke, E., Neukam, F.W. and von Wilmowsky, C. 2018. Anatomical locations in the oral cavity where surgical resections of oral squamous cell carcinomas are associated with a close or positive margin—a retrospective study. *Clinical Oral Investigations*, 22(4), pp.1625-1630.

Kessler, P.A., Bloch-Birkholz, A., Leher, A., Neukam, F.W. and Wiltfang, J. 2004. Evaluation of quality of life of patients with oral squamous cell carcinoma. Comparison of two treatment protocols in a prospective study. *Radiotherapy and Oncology*, 70(3), pp.275-282.

Khan, S., Akhtar, N., Minhas, M.U., Shah, H., Khan, K.U. and Thakur, R.R.S. 2021. A difunctional Pluronic® 127-based in situ formed injectable thermogels as prolonged and

controlled curcumin depot, fabrication, in vitro characterization and in vivo safety evaluation. *Journal of Biomaterials Science, Polymer Edition*, 32(3), pp.281-319.

Kimple, R.J. and Harari, P.M. 2014. Is radiation dose reduction the right answer for HPV-positive head and neck cancer? *Oral Oncology*, 50(6), pp.560-564.

Kleinmann, N., Matin, S.F., Pierorazio, P.M., Gore, J.L., Shabsigh, A., Hu, B., Chamie, K., Godoy, G., Hubosky, S., Rivera, M. and O'Donnell, M. 2020. Primary chemoablation of low-grade upper tract urothelial carcinoma using UGN-101, a mitomycin-containing reverse thermal gel (OLYMPUS): an open-label, single-arm, phase 3 trial. *The lancet oncology*, 21(6), pp.776-785.

Koerdts, S., Rohleder, N.H., Rommel, N., Nobis, C., Stoeckelhuber, M., Pigorsch, S., Duma, M.N., Wolff, K.D. and Kesting, M.R. 2015. An expression analysis of markers of radiation-induced skin fibrosis and angiogenesis in wound healing disorders of the head and neck. *Radiation Oncology*, 10(1), pp.1-10.

La-Beck, N.M., Liu, X., Shmeeda, H., Shudde, C. and Gabizon, A.A. 2021, January. Repurposing amino-bisphosphonates by liposome formulation for a new role in cancer treatment. In *Seminars in Cancer Biology* (Vol. 68, pp. 175-185). Academic Press.

Lai, L., Bi, G., Sun, Y., Shen, M., Su, Y., Che, X. and Meng, D. 2021. The formation and release of aurothioglucose from thioglucose-loaded gold nanoparticles by NIR irradiation: a combined anti-cancer effect of thermotherapy and chemotherapy without the risk of uncontrollable drug burst release and leakage. *New Journal of Chemistry*, 45(48), pp.22574-22578.

Lalla, R.V., Treister, N., Sollecito, T., Schmidt, B., Patton, L.L., Mohammadi, K., Hodges, J.S., Brennan, M.T. and OraRad Study Group. 2017. Oral complications at 6 months after radiation therapy for head and neck cancer. *Oral Diseases*, 23(8), pp.1134-1143.

Lallas, A., Pyne, J., Kyrgidis, A., Andreani, S., Argenziano, G., Cavaller, A., Giacomel, J., Longo, C., Malvestiti, A., Moscarella, E. and Piana, S. 2015. The clinical and dermoscopic features of invasive cutaneous squamous cell carcinoma depend on the histopathological grade of differentiation. *British Journal of Dermatology*, 172(5), pp.1308-1315.

Le Tourneau, C., Calugaru, V., Jouffroy, T., Rodriguez, J., Hoffmann, C., Dodger, B., Moreno, V. and Calvo, E. 2017. A phase 1 trial of NBTXR3 nanoparticles activated by intensity-

modulated radiation therapy (IMRT) in the treatment of advanced-stage head and neck squamous cell carcinoma (HNSCC). *Journal of Clinical Oncology*, 35(15), pp.6080-6080.

Levi, L.E. and Lalla, R.V. 2018. Dental treatment planning for the patient with oral cancer. *Dental Clinics*, 62(1), pp.121-130.

Li, Q., Wang, Y., Jia, W., Deng, H., Li, G., Deng, W., Chen, J., Kim, B., Jiang, W., Liu, Q. and Liu, J., 2020. Low-Dose Anti-Angiogenic Therapy Sensitizes Breast Cancer to PD-1 Blockade. *Clinical Cancer Research*, 26(7), pp.1712-1724.

Li, S., Yuan, S., Zhao, Q., Wang, B., Wang, X. and Li, K. 2018. Quercetin enhances chemotherapeutic effect of doxorubicin against human breast cancer cells while reducing toxic side effects of it. *Biomedicine & Pharmacotherapy*, 100, pp.441-447.

Li, Z., He, J., Li, B., Zhang, J., He, K., Duan, X., Huang, R., Wu, Z. and Xiang, G. 2020. Titanium dioxide nanoparticles induce endoplasmic reticulum stress-mediated apoptotic cell death in liver cancer cells. *Journal of International Medical Research*, 48(4), p.0300060520903652.

Lima-Sousa, R., de Melo-Diogo, D., Alves, C.G., Cabral, C.S., Miguel, S.P., Mendonça, A.G. and Correia, I.J. 2020. Injectable in situ forming thermo-responsive graphene based hydrogels for cancer chemo-photothermal therapy and NIR light-enhanced antibacterial applications. *Materials Science and Engineering: C*, 117, p.111294.

Lin, N.C., Hsien, S.I., Hsu, J.T. and Chen, M.Y. 2021. Impact on patients with oral squamous cell carcinoma in different anatomical subsites: a single-center study in Taiwan. *Scientific Reports*, 11(1), pp.1-9.

Liu, C.H., Chen, H.J., Wang, P.C., Chen, H.S. and Chang, Y.L. 2013. Patterns of recurrence and second primary tumors in oral squamous cell carcinoma treated with surgery alone. *The Kaohsiung Journal of Medical Sciences*, 29(10), pp.554-559.

Liu, M., Song, X., Wen, Y., Zhu, J.L. and Li, J. 2017. Injectable thermoresponsive hydrogel formed by alginate-g-poly (N-isopropylacrylamide) that releases doxorubicin-encapsulated micelles as a smart drug delivery system. *ACS Applied Materials & Interfaces*, 9(41), pp.35673-35682.



Liu, Q., Wang, H., Li, G., Liu, M., Ding, J., Huang, X., Gao, W. and Huayue, W. 2019. A photocleavable low molecular weight hydrogel for light-triggered drug delivery. *Chinese Chemical Letters*, 30(2), pp.485-488.

Liu, S., Wang, Y.N., Ma, B., Shao, J., Liu, H. and Ge, S. 2021. Gingipain-responsive thermosensitive hydrogel loaded with SDF-1 facilitates in situ periodontal tissue regeneration. *ACS Applied Materials & Interfaces*, 13(31), pp.36880-36893.

Lu, X., Song, X., Wang, Q., Hu, W., Shi, W., Tang, Y., Wu, Z., Fan, Q. and Huang, W. 2020. Chemiluminescent organic nanophotosensitizer for a penetration depth independent photodynamic therapy. *RSC Advances*, 10(20), pp.11861-11864.

Mackinnon, E.D., Sornalingam, S. and Cooper, M. 2021. Urgent call to prevent late stage presentation of head and neck cancer. *BMI*, 373.

Mahoney, B.P., Raghunand, N., Baggett, B. and Gillies, R.J. 2003. Tumor acidity, ion trapping and chemotherapeutics: I. Acid pH affects the distribution of chemotherapeutic agents in vitro. *Biochemical Pharmacology*, 66(7), pp.1207-1218.

Maiti, B., Abramov, A., Franco, L., Puiggali, J., Enshaei, H., Alemán, C. and Díaz, D.D. 2020. Thermoresponsive Shape-Memory Hydrogel Actuators Made by Phototriggered Click Chemistry. *Advanced Functional Materials*, 30(24), p.2001683.

Manatunga, D.C., de Silva, R.M., de Silva, K.N., de Silva, N., Bhandari, S., Yap, Y.K. and Costha, N.P. 2017. pH responsive controlled release of anti-cancer hydrophobic drugs from sodium alginate and hydroxyapatite bi-coated iron oxide nanoparticles. *European Journal of Pharmaceutics and Biopharmaceutics*, 117, pp.29-38.

Mao, Y., Zhang, Y., Luo, Z., Zhan, R., Xu, H., Chen, W. and Huang, H. 2018. Synthesis, biological evaluation and low-toxic formulation development of glycosylated paclitaxel prodrugs. *Molecules*, 23(12), p.3211.

Marsili, L., Dal Bo, M., Eisele, G., Donati, I., Berti, F. and Toffoli, G., 2021. Characterization of thermoresponsive poly-N-Vinylcaprolactam polymers for biological applications. *Polymers*, 13(16), p.2639.

Minnelli, C., Cianfruglia, L., Laudadio, E., Galeazzi, R., Pisani, M., Crucianelli, E., Bizzaro, D., Armeni, T. and Mobbili, G. 2018. Selective induction of apoptosis in MCF7 cancer-cell by targeted liposomes functionalised with mannose-6-phosphate. *Journal of Drug Targeting*, 26(3), pp.242-251.

Mirrahimi, M., Abed, Z., Beik, J., Shiri, I., Dezfuli, A.S., Mahabadi, V.P., Kamrava, S.K., Ghaznavi, H. and Shakeri-Zadeh, A. 2019. A thermo-responsive alginate nanogel platform co-loaded with gold nanoparticles and cisplatin for combined cancer chemo-photothermal therapy. *Pharmacological Research*, 143, pp.178-185.

Mittal, A., Chitkara, D. and Kumar, N. 2007. HPLC method for the determination of carboplatin and paclitaxel with cremophorEL in an amphiphilic polymer matrix. *Journal of chromatography B*, 855(2), pp.211-219.

Mitra, T., Sailakshmi, G. and Gnanamani, A. 2014. Could glutaric acid (GA) replace glutaraldehyde in the preparation of biocompatible biopolymers with high mechanical and thermal properties? *Journal of Chemical Sciences*, 126(1), pp.127-140.

Miwa, A., Ishibe, A., Nakano, M., Yamahira, T., Itai, S., Jinno, S. and Kawahara, H. 1998. Development of novel chitosan derivatives as micellar carriers of taxol. *Pharmaceutical Research*, 15(12), pp.1844-1850.

Moghimi, H.R., Williams, A.C. and Barry, B.W. 1998. Enhancement by terpenes of 5-fluorouracil permeation through the stratum comeum: model solvent approach. *Journal of Pharmacy and Pharmacology*, 50(9), pp.955-964.

Mohajertehran, F., Ayatollahi, H., Jafarian, A.H., Khazaeni, K., Soukhtanloo, M., Shakeri, M.T. and Mohtasham, N. 2019. Overexpression of lactate dehydrogenase in the saliva and tissues of patients with head and neck squamous cell carcinoma. *Reports of Biochemistry & Molecular Biology*, 7(2), p.142, Article ID: 30805393.

Morishima, H., Washio, J., Kitamura, J., Shinohara, Y., Takahashi, T. and Takahashi, N. 2017. Real-time monitoring system for evaluating the acid-producing activity of oral squamous cell carcinoma cells at different environmental pH. *Scientific Reports*, 7(1), pp.1-9.

Nunes, S.S., Miranda, S.E.M., de Oliveira Silva, J., Fernandes, R.S., de Alcântara Lemos, J., de Aguiar Ferreira, C., Townsend, D.M., Cassali, G.D., Oliveira, M.C. and de Barros, A.L.B. 2021.

pH-responsive and folate-coated liposomes encapsulating irinotecan as an alternative to improve efficacy of colorectal cancer treatment. *Biomedicine & Pharmacotherapy*, 144, p.112317.

Öztürk-Atar, K., Kaplan, M. and Çalış, S. 2020. Development and evaluation of polymeric micelle containing tablet formulation for poorly water-soluble drug: Tamoxifen citrate. *Drug Development and Industrial Pharmacy*, 46(10), pp.1695-1704.

Padma, R., Kalaivani, A., Sundaresan, S. and Sathish, P. 2017. The relationship between histological differentiation and disease recurrence of primary oral squamous cell carcinoma. *Journal of Oral and Maxillofacial Pathology: JOMFP*, 21(3), p.461, Article ID: 29391735.

Pandit, A.H., Nisar, S., Imtiyaz, K., Nadeem, M., Mazumdar, N., Rizvi, M.M.A. and Ahmad, S. 2021. Injectable, self-healing, and biocompatible N, O-carboxymethyl chitosan/Multialdehyde guar gum Hydrogels for sustained anticancer drug delivery. *Biomacromolecules*, 22(9), pp.3731-3745.

Pang, X., Liang, S., Wang, T., Yu, S., Yang, R., Hou, T., Liu, Y., He, C. and Zhang, N. 2020. Engineering thermo-ph dual responsive hydrogel for enhanced tumor accumulation, penetration, and chemo-protein combination therapy. *International Journal of Nanomedicine*, 15, p. 4739-4752.

Park, Y.I., Kwon, S.H., Lee, G., Motoyama, K., Kim, M.W., Lin, M., Niidome, T., Choi, J.H. and Lee, R. 2021. pH-sensitive multi-drug liposomes targeting folate receptor  $\beta$  for efficient treatment of non-small cell lung cancer. *Journal of Controlled Release*, 330, pp.1-14.

Petrini, M., Lokerse, W.J., Mach, A., Hossann, M., Merkel, O.M. and Lindner, L.H. 2021. Effects of Surface Charge, PEGylation and Functionalization with Dipalmitoylphosphatidylglycerol on Liposome–Cell Interactions and Local Drug Delivery to Solid Tumors via Thermosensitive Liposomes. *International Journal of Nanomedicine*, 16, p.4045-4061.

Pfister, D.G., Spencer, S., Adelstein, D., Adkins, D., Anzai, Y., Brizel, D.M., Bruce, J.Y., Busse, P.M., Caudell, J.J., Cmelak, A.J. and Colevas, A.D. 2020. Head and neck cancers, version 2.2020, NCCN clinical practice guidelines in oncology. *Journal of the National Comprehensive Cancer Network*, 18(7), pp.873-898.

Primeau, A.J., Rendon, A., Hedley, D., Lilge, L. and Tannock, I.F. 2005. The distribution of the anticancer drug Doxorubicin in relation to blood vessels in solid tumors. *Clinical Cancer Research*, 11(24), pp.8782-8788. Qian, C., Zhang, T., Gravesande, J., Baysah, C., Song, X. and Xing, J. 2019a. Injectable and self-healing polysaccharide-based hydrogel for pH-responsive drug release. *International Journal of Biological Macromolecules*, 123, pp.140-148.

Qian, J., Wenguang, X., Zhiyong, W., Yuntao, Z. and Wei, H. 2016. Hypoxia inducible factor: a potential prognostic biomarker in oral squamous cell carcinoma. *Tumor Biology*, 37(8), pp.10815-10820.

Qian, J., Xia, M., Liu, W., Li, L., Yang, J., Mei, Y., Meng, Q. and Xie, Y. 2019b. Glabridin resensitizes p-glycoprotein-overexpressing multidrug-resistant cancer cells to conventional chemotherapeutic agents. *European Journal of Pharmacology*, 852, pp.231-243.

Quintanilha, N.P., Costa, I.D.S.M., de Souza Ramos, M.F., de Oliveira Miguel, N.C. and Pierre, M.B.R. 2017.  $\alpha$ -Bisabolol improves 5-aminolevulinic acid retention in buccal tissues: Potential application in the photodynamic therapy of oral cancer. *Journal of Photochemistry and Photobiology B: Biology*, 174, pp.298-305.

Raghunand, N. and Gillies, R.J. 2000. pH and drug resistance in tumors. *Drug Resistance Updates*, 3(1), pp.39-47.

Rai, V., Mukherjee, R., Ghosh, A.K., Routray, A. and Chakraborty, C. 2018. "Omics" in oral cancer: New approaches for biomarker discovery. *Archives of Oral Biology*, 87, pp.15-34.

Raza, F., Zhu, Y., Chen, L., You, X., Zhang, J., Khan, A., Khan, M.W., Hasnat, M., Zafar, H., Wu, J. and Ge, L. 2019. Paclitaxel-loaded pH responsive hydrogel based on self-assembled peptides for tumor targeting. *Biomaterials Science*, 7(5), pp.2023-2036.

Reshma, P.L., Unnikrishnan, B.S., Preethi, G.U., Syama, H.P., Archana, M.G., Remya, K., Shiji, R., Sreekutty, J. and Sreelekha, T.T. 2019. Overcoming drug-resistance in lung cancer cells by paclitaxel loaded galactoxyloglucan nanoparticles. *International Journal of Biological Macromolecules*, 136, pp.266-274.

Rezk, A.I., Obiweluzor, F.O., Choukrani, G., Park, C.H. and Kim, C.S. 2019. Drug release and kinetic models of anticancer drug (BTZ) from a pH-responsive alginate polydopamine hydrogel:

Towards cancer chemotherapy. *International Journal of Biological Macromolecules*, 141, pp.388-400.

Russell, L.M., Hultz, M. and Searson, P.C. 2018. Leakage kinetics of the liposomal chemotherapeutic agent Doxil: The role of dissolution, protonation, and passive transport, and implications for mechanism of action. *Journal of Controlled Release*, 269, pp.171-176.

Saffari, M., Shirazi, F.H. and Moghimi, H.R. 2016. Terpene-loaded liposomes and isopropyl myristate as chemical permeation enhancers toward liposomal gene delivery in lung cancer cells; a comparative study. *Iranian Journal of Pharmaceutical Research: IJPR*, 15(3), p.261-267.

Saggar, J.K. and Tannock, I.F. 2014. Activity of the hypoxia-activated pro-drug TH-302 in hypoxic and perivascular regions of solid tumors and its potential to enhance therapeutic effects of chemotherapy. *International Journal of Cancer*, 134(11), pp.2726-2734.

Sakamoto, Y., Matsushita, Y., Yamada, S.I., Yanamoto, S., Shiraishi, T., Asahina, I. and Umeda, M. 2016. Risk factors of distant metastasis in patients with squamous cell carcinoma of the oral cavity. *Oral Surgery, Oral Medicine, Oral Pathology and Oral Radiology*, 121(5), pp.474-480.

Salem, H.F., Gamal, A., Saeed, H., Kamal, M. and Tulbah, A.S. 2022. Enhancing the Bioavailability and Efficacy of Vismodegib for the Control of Skin Cancer: In Vitro and In Vivo Studies. *Pharmaceuticals*, 15(2), p.126, Article ID: 10.3390/ph15020126.

Shannon, A.M., Bouchier-Hayes, D.J., Condrón, C.M. and Toomey, D. 2003. Tumour hypoxia, chemotherapeutic resistance and hypoxia-related therapies. *Cancer Treatment Reviews*, 29(4), pp.297-307.

Shen, W., Chen, X., Luan, J., Wang, D., Yu, L. and Ding, J. 2017. Sustained codelivery of cisplatin and paclitaxel via an injectable prodrug hydrogel for ovarian cancer treatment. *ACS Applied Materials & Interfaces*, 9(46), pp.40031-40046.

Sher, D.J., Thotakura, V., Balboni, T.A., Norris Jr, C.M., Haddad, R.I., Posner, M.R., Lorch, J., Goguen, L.A., Annino, D.J. and Tishler, R.B. 2011. Treatment of oral cavity squamous cell carcinoma with adjuvant or definitive intensity-modulated radiation therapy. *International Journal of Radiation Oncology\* Biology\* Physics*, 81(4), pp.e215-e222.

Sohn, S.S., Revuri, V., Nurunnabi, M., Kwak, K.S. and Lee, Y.K. 2016. Biomimetic and photo crosslinked hyaluronic acid/pluronic F127 hydrogels with enhanced mechanical and elastic properties to be applied in tissue engineering. *Macromolecular Research*, 24(3), pp.282-291.

Sonaje, K., Chuang, E.Y., Lin, K.J., Yen, T.C., Su, F.Y., Tseng, M.T. and Sung, H.W. 2012. Opening of epithelial tight junctions and enhancement of paracellular permeation by chitosan: microscopic, ultrastructural, and computed-tomographic observations. *Molecular Pharmaceutics*, 9(5), pp.1271-1279.

Song, X., Zhang, Z., Zhu, J., Wen, Y., Zhao, F., Lei, L., Phan-Thien, N., Khoo, B.C. and Li, J. 2020. Thermo-responsive hydrogel induced by dual supramolecular assemblies and its controlled release property for enhanced anticancer drug delivery. *Biomacromolecules*, 21(4), pp.1516-1527.

Starovoytova, L., Šťastná, J., Šturcová, A., Konefal, R., Dybal, J., Velychkivska, N., Radecki, M. and Hanyková, L. 2015. Additive effects on phase transition and interactions in poly (vinyl methyl ether) solutions. *Polymers*, 7(12), pp.2572-2583.

Sun, X., Yan, X., Jacobson, O., Sun, W., Wang, Z., Tong, X., Xia, Y., Ling, D. and Chen, X. 2017. Improved tumor uptake by optimizing liposome based RES blockade strategy. *Theranostics*, 7(2), p.319-328.

Sun, Y., Wang, Z., Qiu, S. and Wang, R. 2021. Therapeutic strategies of different HPV status in Head and Neck Squamous Cell Carcinoma. *International Journal of Biological Sciences*, 17(4), p.1104-1118.

Tampucci, S., Guazzelli, L., Burgalassi, S., Carpi, S., Chetoni, P., Mezzetta, A., Nieri, P., Polini, B., Pomelli, C.S., Terreni, E. and Monti, D. 2020. pH-responsive nanostructures based on surface active fatty acid-protic ionic liquids for imiquimod delivery in skin cancer topical therapy. *Pharmaceutics*, 12(11), p.1078, Article ID: 10.3390/pharmaceutics12111078.

Tang, J., Zhang, R., Guo, M., Shao, L., Liu, Y., Zhao, Y., Zhang, S., Wu, Y. and Chen, C. 2018. Nucleosome-inspired nanocarrier obtains encapsulation efficiency enhancement and side effects reduction in chemotherapy by using fullereneol assembled with doxorubicin. *Biomaterials*, 167, pp.205-215.

Tang, Z., Liu, Y., He, M. and Bu, W. 2019. Chemodynamic therapy: tumour microenvironment-mediated Fenton and Fenton-like reactions. *Angewandte Chemie International Edition*, 58(4), pp.946-956.

Tannock, I.F., Lee, C.M., Tunggai, J.K., Cowan, D.S. and Egorin, M.J. 2002. Limited penetration of anticancer drugs through tumor tissue: a potential cause of resistance of solid tumors to chemotherapy. *Clinical Cancer Research*, 8(3), pp.878-884.

Torralba, M.G., Aleti, G., Li, W., Moncera, K.J., Lin, Y.H., Yu, Y., Masternak, M.M., Golusinski, W., Golusinski, P., Lamperska, K. and Edlund, A. 2020. Oral microbial species and virulence factors associated with oral squamous cell carcinoma. *Microbial Ecology*, pp.1-17.

Tribius, S., Sommer, J., Prosch, C., Bajrovic, A., Muenscher, A., Blessmann, M., Kruell, A., Petersen, C., Todorovic, M. and Tennstedt, P. 2013. Xerostomia after radiotherapy. *Strahlenther Onkol* 189, pp. 216–222.

van der Geer, S.J., Kamstra, J.I., Roodenburg, J.L., van Leeuwen, M., Reintsema, H., Langendijk, J.A. and Dijkstra, P.U. 2016. Predictors for trismus in patients receiving radiotherapy. *Acta Oncologica*, 55(11), pp.1318-1323.

Wang, C.P., Liao, L.J., Chiang, C.J., Hsu, W.L., Kang, C.J., Wang, C.C., Chen, P.R., Chen, T.C., Huang, W.W. and Chien, C.Y. 2020. Patients with oral cancer do not undergo surgery as primary treatment: A population-based study in Taiwan. *Journal of the Formosan Medical Association*, 119(1), pp.392-398.

Wang, H.F., Ran, R., Liu, Y., Hui, Y., Zeng, B., Chen, D., Weitz, D.A. and Zhao, C.X. 2018. Tumor-vasculature-on-a-chip for investigating nanoparticle extravasation and tumor accumulation. *ACS Nano*, 12(11), pp.11600-11609.

Wang, Y., Wang, Z., Xu, C., Tian, H. and Chen, X. 2019. A disassembling strategy overcomes the EPR effect and renal clearance dilemma of the multifunctional theranostic nanoparticles for cancer therapy. *Biomaterials*, 197, pp.284-293.

Wilfert, S., Iturmendi, A., Henke, H., Brüggemann, O. and Teasdale, I. 2014, March. Thermoresponsive Polyphosphazene-Based Molecular Brushes by Living Cationic Polymerization. *Macromolecular Symposia* 337(1), pp. 116-123.

Wu, W., Pu, Y. and Shi, J. 2021. Dual Size/Charge-Switchable Nanocatalytic Medicine for Deep Tumor Therapy. *Advanced Science*, 8(9), Article ID: 2002816.

Wu, X., Desai, K.G.H., Mallery, S.R., Holpuch, A.S., Phelps, M.P. and Schwendeman, S.P. 2012. Mucoadhesive fenretinide patches for site-specific chemoprevention of oral cancer: enhancement of oral mucosal permeation of fenretinide by coinorporation of propylene glycol and menthol. *Molecular Pharmaceutics*, 9(4), pp.937-945.

Xie, W., Gao, Q., Guo, Z., Wang, D., Gao, F., Wang, X., Wei, Y. and Zhao, L. 2017. Injectable and self-healing thermosensitive magnetic hydrogel for asynchronous control release of doxorubicin and docetaxel to treat triple-negative breast cancer. *ACS Applied Materials & Interfaces*, 9(39), pp.33660-33673.

Xu, N., Xu, J., Zheng, X. and Hui, J. 2020. Preparation of Injectable Composite Hydrogels by Blending Poloxamers with Calcium Carbonate-Crosslinked Sodium Alginate. *ChemistryOpen*, 9(4), pp.451-458.

Xu, R., Tian, J., Guan, Y. and Zhang, Y. 2018. Extraordinarily large LCST depression converts nonthermosensitive polymer to thermosensitive. *Macromolecules*, 52(1), pp.365-375.

Yap, L.S. and Yang, M.C. 2016. Evaluation of hydrogel composing of Pluronic F127 and carboxymethyl hexanoyl chitosan as injectable scaffold for tissue engineering applications. *Colloids and Surfaces B: Biointerfaces*, 146, pp.204-211.

Yong, X., Yang, X., Emory, S.R., Wang, J., Dai, J., Yu, X., Mei, L., Xie, J. and Ruan, G. 2018. A potent, minimally invasive and simple strategy of enhancing intracellular targeted delivery of Tat peptide-conjugated quantum dots: organic solvent-based permeation enhancer. *Biomaterials science*, 6(11), pp.3085-3095.

Yu, S., Zhang, X., Tan, G., Tian, L., Liu, D., Liu, Y., Yang, X. and Pan, W. 2017. A novel pH-induced thermosensitive hydrogel composed of carboxymethyl chitosan and poloxamer cross-linked by glutaraldehyde for ophthalmic drug delivery. *Carbohydrate Polymers*, 155, pp.208-217.

Yu, L., Zhang, H. and Ding, J. 2006. A subtle end-group effect on macroscopic physical gelation of triblock copolymer aqueous solutions. *Angewandte Chemie International Edition*, 45(14), pp.2232-2235.



Zhang, B., Gao, S., Li, R., Li, Y., Cao, R., Cheng, J., Guo, Y., Wang, E., Huang, Y. and Zhang, K., 2020. Tissue mechanics and expression of TROP2 in oral squamous cell carcinoma with varying differentiation. *BMC Cancer*, 20(1), pp.1-12.

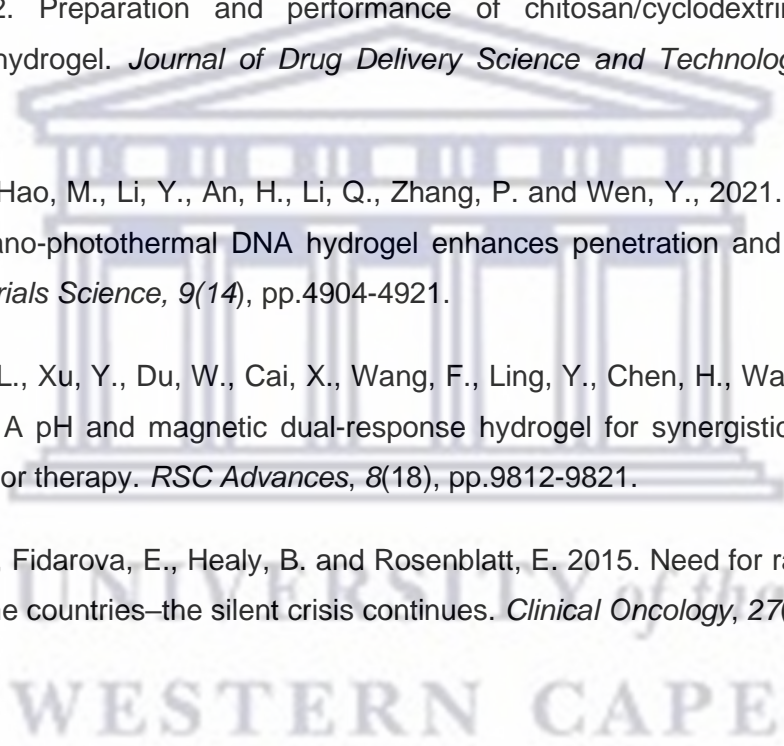
Zhang, P., Marill, J., Darmon, A., Anesary, N.M., Lu, B. and Paris, S. 2021. NBTXR3 Radiotherapy-Activated Functionalized Hafnium Oxide Nanoparticles Show Efficient Antitumor Effects Across a Large Panel of Human Cancer Models. *International Journal of Nanomedicine*, 16, p.2761-2773.

Zhou, H.Y., Tong, J.N., Ren, L.J., Hao, P.Y., Zheng, H.J., Guo, X.M., Chen, Y.W., Li, J.B. and Park, H.J. 2022. Preparation and performance of chitosan/cyclodextrin-g-glutamic acid thermosensitive hydrogel. *Journal of Drug Delivery Science and Technology*, 74, Article ID: 103504.

Zhou, L., Pi, W., Hao, M., Li, Y., An, H., Li, Q., Zhang, P. and Wen, Y., 2021. An injectable and biodegradable nano-photothermal DNA hydrogel enhances penetration and efficacy of tumor therapy. *Biomaterials Science*, 9(14), pp.4904-4921.

Zhou, X., Wang, L., Xu, Y., Du, W., Cai, X., Wang, F., Ling, Y., Chen, H., Wang, Z., Hu, B. and Zheng, Y. 2018. A pH and magnetic dual-response hydrogel for synergistic chemo-magnetic hyperthermia tumor therapy. *RSC Advances*, 8(18), pp.9812-9821.

Zubizarreta, E.H., Fidarova, E., Healy, B. and Rosenblatt, E. 2015. Need for radiotherapy in low and middle income countries—the silent crisis continues. *Clinical Oncology*, 27(2), pp.107-114.



## CHAPTER 3: MATERIALS AND METHODS

*In this chapter, the general considerations for the synthesis of thermoresponsive gels are described. The selection of materials and their concentrations within the formulation is also discussed. The synthesis method and physicochemical characterisation of the preparation are specified.*

### 3.1 Introduction

The idea to design thermosensitive hydrogels for localised drug therapy in cancer is a unique and appealing venture. However, simply having a thermal response at biological temperature does not equate to a good system design. Various bottlenecks, such as obtaining a low viscosity of the hydrogel solution, ensuring good mechanical strength and erosion of the formed gel post-administration, are paramount factors to consider in the hydrogel system design. Thermosensitive hydrogels are prone to present weakness in their ability to remain at their targeted site without breaking or tearing as a result of biological interference or design impairment (Seo *et al.*, 2021). The mechanical strength of a hydrogel system is therefore of considerable importance to maintain rigidity and structure within the tumour. This is supported by the use of chitosan (CH) and *k*-carrageenan (*k*CRG) which have been selected for their favourable biocompatible properties and their mechanical strength. The two mixtures, however, produce a mesh formed by electrostatic interactions that prevent a homogenous mixture; a method to prevent this has therefore been reported in this study.

Amongst the chemotherapeutic agents used for oral squamous cell carcinoma (OSCC), Doxorubicin HCl (DOX) shows poor permeability and due to its non-targeted intravenous delivery, it is prominent for one of the most dreadful side effects of chemotherapy – irreversible myocardial damage (Mohammadi, Arabi, and Alibolandi, 2020). To improve the accumulation of DOX in tumour tissue, the drug has been incorporated into the thermosensitive hydrogel design. Pluronic™ F127 (PF-127) possesses a very good thermal response around physiological temperature (37°C) (Cao *et al.*, 2020; Yeh *et al.*, 2017). It is considered non-toxic and has shown *in vivo* and *in vitro* success in the delivery of several chemotherapeutic agents such as cisplatin and docetaxel (Xu *et al.*, 2018; Wen *et al.*, 2020). Therefore, PF-127 was the thermosensitive polymer of choice in this study. Limonene (LIM), a natural monoterpene derived from orange peels (Siddiqui *et al.*, 2022), was also included in the hydrogel formulations as it potentially possesses the proposed permeation feature that is investigated in this study.

Research has shown that LIM has chemopreventive and chemotherapeutic activities in cancers such as lung, breast, gastric, and prostate cancer (Ren *et al.*, 2020), and may provide a synergistic cytotoxic effect with DOX. LIM is used as a flavouring agent in the food industry, which contributes to its safety for use. Its high lipophilicity leads to favourable cellular absorption and could enhance the permeation of DOX in tumour cells (Ren *et al.*, 2020). Transdermal studies have also supported the high permeability of LIM, however, studies showing the permeability of drugs in the presence of LIM are still lacking; a factor that this study will investigate (Yang *et al.*, 2013; Lu *et al.*, 2014).

The aim of this chapter was to optimise hydrogel formulations by selecting the minimum and maximum parameters for synthesising material concentrations in terms of gelation temperature, to confirm injectability and clarity of gels for easy observation of homogenisation. To ascertain knowledge of the physicochemical characterisation of the hydrogels, different analytical techniques such as thermal analysis, molecular transitions, rheological behaviour, mechanical properties, swelling and erosion capacity have been explored. This type of knowledge highlights the compatibility of DOX and the excipients for an intratumoral thermosensitive hydrogel design.

### 3.2 Materials

The active ingredient, DOX, (BN: D22204001) was purchased from DB Fine Chemicals (Pty) Ltd (Johannesburg, South Africa). LIM (BN: IF-LI-210524) and *k*CRG (BN: IF-CA-210515) were purchased from Iffect Chemphar Co., Ltd, Hongkong, P.R. China. Ethanol 96 %v/v (BN: 3202) was supplied by Laborem (Johannesburg, South Africa). Pluronic™ F127 (BN: BCCD6387), chitosan medium molecular weight (BN: STBJ3281), sodium hydroxide (NaOH) (BN: SZBF3240V), disodium hydrogen phosphate (BN: F1535286 833), potassium dihydrogen phosphate (BN: 8256-0), chromatography grade methanol (BN: I1046818942) and dimethyl sulfoxide, purity  $\geq 99.7\%$  (BN: RNBJ9739) were obtained from Sigma-Aldrich (Johannesburg, South Africa). Analytical grade glacial acetic acid, (BN: 52615) was obtained from Saarchem (Pty) Ltd (Johannesburg, South Africa). Orthophosphoric acid 85 % (BN: 45JN12099123 K26/081) was supplied by Kimix Chemicals and Laboratory Supplies (Cape Town, South Africa). Chromatography acetonitrile, purity  $\geq 99\%$  (BN: 1922928) was purchased from Labchem (Cape Town, South Africa). Deionized water was obtained from a water purification system manufactured by Lasec Group (Johannesburg, South Africa).

### 3.3 Synthesis of CH/*k*CRG/PF-127 thermoresponsive hydrogel

#### 3.3.1 Determination of concentration limits for formulation synthesis

For the successful design of the thermoresponsive hydrogels, preliminary trial formulations were carried out. A gelation temperature of  $37 \pm 2$  °C was targeted due to the physiological temperature of the oral cavity. The visible appearance of the gel formulation in terms of colour, viscosity and homogeneity of the gel system was considered. The starting choice of concentrations was carefully selected after consulting literature. For PF-127, studies have shown that concentrations of 15-25 % are best suited to achieve thermal gelation at body temperature (Braet *et al.*, 2021). Despite different formulation designs, CH and *k*CRG have usually succeeded as flexible hydrogels in cases where the concentration of *k*CRG was equal to or did not exceed that of CH (Pettinelli *et al.*, 2019; Pourjavadi *et al.*, 2019; Yu *et al.*, 2018). These considerations were used as a guide toward the selection of concentration limits for formulation synthesis. Table 3.1 provides the concentrations of the various materials used during preliminary trial formulations for hydrogel synthesis.

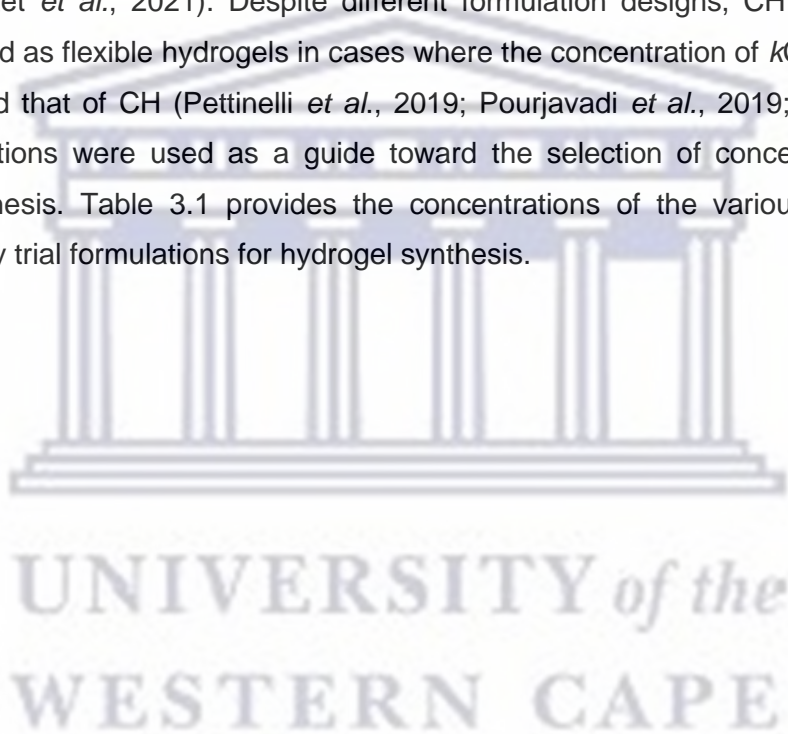


Table 3.1: Composition and observations of preliminary trial formulations

| <b>Trial formulation</b> | <b>Composition</b>  | <b>Aim</b>   | <b>Observation</b>   |
|--------------------------|---|--|--|
| <b>1</b>                 | 15%PF-127+1%LIM+0.3%CH+0.1%kCRG<br>15%PF-127+1%LIM+0.1%CH+0.3%kCRG<br>15%PF-127+1%LIM+0.1%CH+0.1%kCRG   | Preparation of thermoresponsive hydrogel.  | Gelation time from 4 °C to 37 °C too slow.<br>Phase separation present.<br>White, cloudy formulation.            |
| <b>2</b>                 | 25%PF-127+0.1%LIM+0.3%CH+0.3%kCRG,<br>20%PF-127+0.5%LIM+0.3%CH+0.3%kCRG,<br>25%PF-127+0.5%LIM+0.3%CH+0.3%kCRG,<br>15%PF-127+0.5%LIM+0.3%CH+0.3%kCRG,<br>15%PF-127+0.5%LIM+0.3%CH+0.3%kCRG,<br>15%PF-127+0.5%LIM+0.3%CH+0.3%kCRG | Enhance gelation by decreasing LIM and increasing PF-127/CH/kCRG.<br>Reduce cloudiness by decreasing LIM/kCRG. | Gelation visible at 37 °C.<br>Reduced cloudiness.<br>Phase separation present.<br>Formulation too thick at 4 °C. |
| <b>3</b>                 | 15%PF-127+<br>≤[0.5%LIM+0.3%CH+0.3%kCRG]  | Reduce viscosity of solution at 4 °C by decreasing PF-127 and CH/kCRG.   | Viscosity of solution reduced at 4 °C. Phase separation present.   |
| <b>3</b>                 | 15%PF-127+<br>≤[0.5%LIM+0.3%CH+0.3%kCRG]<br>+20%ethanol   | Avoid phase separation by addition of ethanol.   | Gelation visible at 37 °C.<br>No phase separation.   |

Based on the preliminary studies, 9 formulations which were physically crosslinked with various concentrations of CH, *k*CRG and LIM, were furthered in the study (Table 3.2). The 9 formulations were selected to perform physicochemical and *in vitro* characterisation studies to identify the ideal formulation according to rheological behaviour, mechanical strength, erosion and permeability studies.

Table 3.2: Concentration of ingredients for hydrogel formulations

| Sample no. | LIM (%v/v) | CH (%w/v) | <i>k</i> CRG (%w/v) |
|------------|------------|-----------|---------------------|
| 1          | 0.1        | 0.1       | 0.1                 |
| 2          | 0.1        | 0.3       | 0.1                 |
| 3          | 0.1        | 0.3       | 0.3                 |
| 4          | 0.3        | 0.1       | 0.1                 |
| 5          | 0.3        | 0.3       | 0.1                 |
| 6          | 0.3        | 0.3       | 0.3                 |
| 7          | 0.5        | 0.1       | 0.1                 |
| 8          | 0.5        | 0.3       | 0.1                 |
| 9          | 0.5        | 0.3       | 0.3                 |

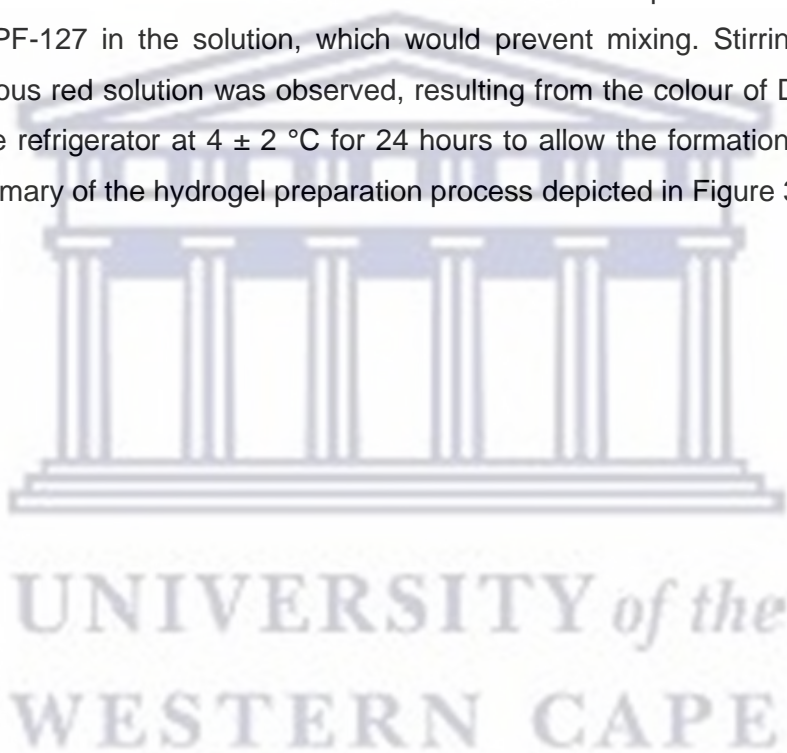
\*15 %w/v PF-127, 0.0005 %w/v DOX and 20 %v/v ethanol were used in all formulations.

### 3.3.2 Synthesis of thermoresponsive hydrogel solution

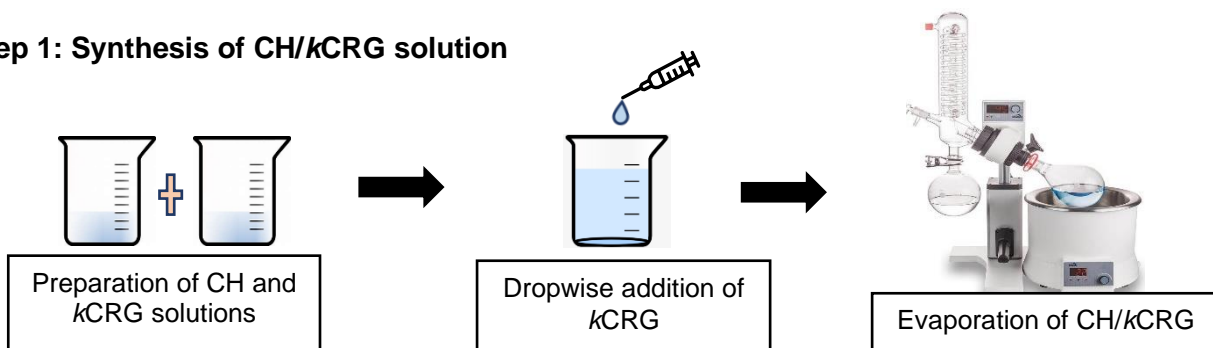
To synthesise the CH solution, 1 %v/v glacial acetic acid was prepared in 10 mL deionized water. The CH was then transferred to the resulting diluent followed by agitation of the solution at 1400 rpm for 30 min at ambient temperature using a DragonLab MS7-H550-Pro hotplate magnetic stirrer. *k*CRG solution was prepared by heating 10 mL deionized water to  $60 \pm 2$  °C followed by the addition of the polymer to the heated water under magnetic stirring at 800 rpm for 15 min; the stirring hotplate was maintained at  $60 \pm 2$  °C throughout this process to ensure complete solubilisation of the *k*CRG powder. In order to achieve a homogenous mixture of the CH/*k*CRG solution, an evaporation technique adapted from Pourjavadi *et al.*, 2019 was employed. The two polymer solutions were diluted by adding 40 mL deionized water to each solution. Subsequently, the *k*CRG solution was added dropwise (not more than 5 mL/min) to the CH solution under vigorous mixing (1400 rpm) at  $50 \pm 2$  °C in a 250 mL rotary flask. Once the *k*CRG was fully incorporated, the rotary flask containing the homogeneous solution was attached to a rotary evaporator (Büchi, Flawil, Switzerland). The water bath of the evaporator was set to a temperature of  $50 \pm 2$  °C, and once this temperature was reached, the sample was

left to rotate under vacuum for 30 min at a rotation intensity of 5 until the concentration of water was reduced to approximately 10 mL. The resulting solution was left to cool to room temperature.

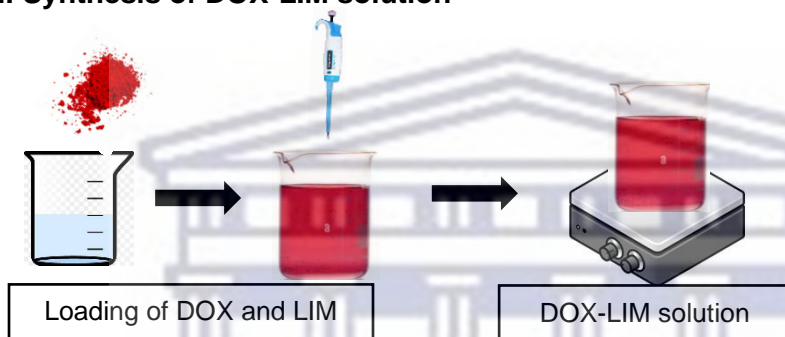
DOX (0.0005 %w/v) was added to 20 %v/v ethanol in a 50 mL glass beaker. The solution was stirred for 5 min, and thereafter, LIM was added, and mixing continued at 800 rpm at room temperature. Following this, the CH/kCRG solution initially prepared was transferred to the 50 mL beaker containing LIM-DOX. The solution was mixed for 5 min using the same agitation speed. The beaker containing the solution was then placed in an ice water bath and 15 % PF-127 was added and stirred. The ice bath was essential to prevent the gelation of the thermosensitive PF-127 in the solution, which would prevent mixing. Stirring was concluded once a homogenous red solution was observed, resulting from the colour of DOX. The solution was placed in the refrigerator at  $4 \pm 2$  °C for 24 hours to allow the formation of a transparent, red liquid. A summary of the hydrogel preparation process depicted in Figure 3.1.



**Step 1: Synthesis of CH/kCRG solution**



**Step 2: Synthesis of DOX-LIM solution**



**Step 3: Preparation of PF-127/CH/kCRG loaded with DOX-LIM**

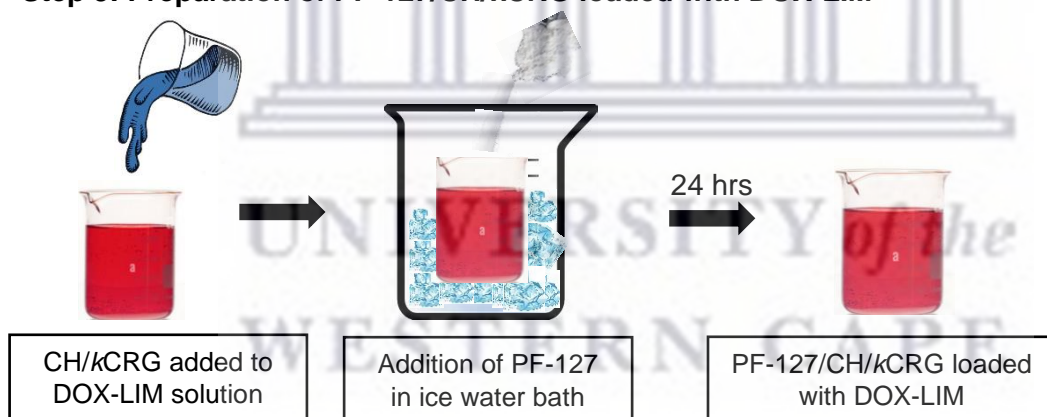


Figure 3.1: Schematic representing the synthesis of thermoresponsive PF-127/CH/kCRG hydrogel with DOX-LIM.



### 3.3.3 Adjustment of hydrogel pH

The pH of the thermoresponsive hydrogel solution was measured using a Eutech Instrument, pH 2700 digital pH meter (Paisley, UK). The hydrogel formulation remained in an ice water bath of  $4 \pm 2$  °C throughout this process to avoid gelation of the solution, which would hinder the process of recording the pH measurement. The probe was inserted into the solution and allowed to equilibrate. 2 M NaOH was used to adjust the pH of the solution between 4.4-5.5. The hydrogel solution was allowed to gel in a water bath for 3 min at  $37 \pm 2$  °C, and subsequently, the pH was recorded. The pH was measured in triplicate ( $n=3$ ).

### 3.4 Physicochemical characterisation of hydrogel constituents and formulation

Physicochemical studies were carried out using various characterisation methods. The pure compounds necessary for synthesising the hydrogels were first characterised, i.e., DOX, the polymers, and LIM, to confirm the compound purity and understand the thermal and molecular vibrational characteristics, to identify factors affecting hydrogel synthesis, and to correlate results of the pure compounds to the hydrogel formulation. This initial characterisation was performed using thermogravimetric analysis (TGA), differential scanning calorimetry (DSC), and Fourier-transform infrared spectroscopy (FTIR). After the preparation of the thermoresponsive hydrogel formulation, the same analytical techniques were utilised in characterising the hydrogels.

#### 3.4.1 Thermogravimetric Analysis (TGA)

The raw materials and the hydrogel formulations were analysed using a Perkin Elmer TGA 4000 thermogravimetric analyser (Waltham, USA), with the flow rate of nitrogen gas at 10 mL/min. An empty porcelain crucible was tared to zero, and the sample was placed into the porcelain crucible; the weight of the sample was then recorded. All samples were analysed over a temperature range of 20-600 °C at a heating rate of 10 °C/min. The data was collected and analysed using Pyris™ software (Perkin Elmer, Waltham, USA). This analysis was essential in characterising the change in weight as a function of temperature of the samples. Its correlation with DSC data assisted in determining the effect of crosslinking in relation to polymer thermal degradation properties.

### 3.4.2 Differential Scanning Calorimetry (DSC)

A Q200 DSC (TA Instruments, New Castle, Delaware, USA) equipped with Universal Analysis version 5.5.24 software was used for DSC analyses. About 1-5 mg of each sample was weighed into an aluminium pan and sealed using a mechanical crimping device. An empty aluminium pan of the same dimensions was sealed and used as a reference. The samples were analysed at a heating rate of 10 °C/min, with nitrogen as the purging gas at a flow rate of 20 mL/min. Samples were heated over a temperature range of 25-300 °C. Differences in the heat flow and phase transitions of the formulations provided insight into the effects of polymer blending and crosslinking of the chemicals.

### 3.4.3 Fourier-Transform Infrared Spectroscopy (FTIR)

Fourier-transform infrared spectroscopy was employed to confirm the chemical structures and detect molecular transitions of the hydrogel to ascertain crosslinking and interactions between DOX, LIM and the polymers used (CH, PF-127, and *k*CRG). The hydrogel samples were analysed through the collection of 3 scans across a wavenumber range of 4000-650 cm<sup>-1</sup> using a Perkin Elmer 400 FTIR instrument fitted with a diamond attenuated total reflectance (ATR) crystal. Spectrum<sup>®</sup> software version 6.3.5 (Waltham, USA) was used to control the instrument as well as for the analyses of the obtained FTIR spectra. A small quantity of the dry samples (CH, *k*CRG, and PF-127) were placed on the FTIR instrument crystal and not more than 60% pressure was applied. No pressure was applied to the liquid samples (LIM and hydrogel formulations). The FTIR spectra of the hydrogel formulations with different concentrations were compared to each other. Differences or changes in the characteristic absorbance bands of the hydrogel formulations, such as the appearance or disappearance of peaks, variations in peak intensity, peak broadening, and shifts in the wavenumbers of peaks indicate crosslinking and other interactions that aid in understanding the chemical and physical characteristics of the hydrogel formulations.

### 3.5 Gelation time

The sol-gel transition time was measured using the tube-inversion method (Figure 3.2). Vials containing 1 mL of 4 ± 2 °C hydrogel solution were immersed in a water bath at 37 ± 2 °C and at room temperature (23 ± 2 °C). The gelation time was monitored by inverting the vials horizontally at every 1 min interval. The time at which the liquid did not flow was recorded as the

gelation time. The maximum observation time was set to 1 hr. Gelation time for each sample was measured in triplicate (n=3).

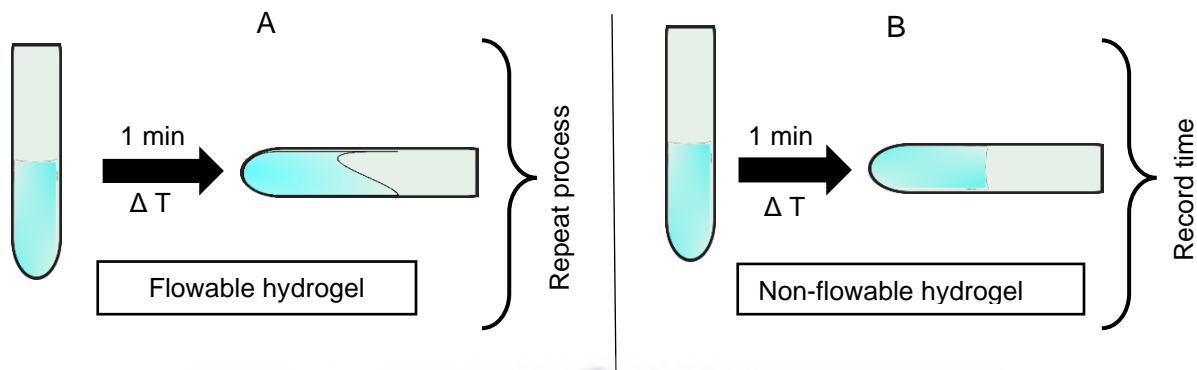


Figure 3.2: Tube-inversion method from (A) flowable hydrogel to (B) non-flowable hydrogel, where  $T = 23 \pm 2 \text{ }^\circ\text{C} / 37 \pm 2 \text{ }^\circ\text{C}$ .

### 3.6 Rheological analysis of the thermoresponsive hydrogels

The viscoelastic behaviour of the hydrogel samples was analysed using an ElastoSens™ Bio<sup>2</sup> rheometer (Rheolution Inc, Montreal, Canada) with Elastoview version 18.8 software. Hydrogel samples of 5 mL were placed in a 23 mm pan and analysed from 4-40 °C at a heating rate of 5 °C/min. The shear storage modulus ( $G'$ ) and shear loss modulus ( $G''$ ) were plotted on a graph using Microsoft Excel™. The loss tangent ( $\tan\delta$ ) values at 4 °C, 25 °C and 37 °C were recorded for each sample.

### 3.7 Determining the compressive strength of the thermoresponsive hydrogel

The compressive modulus was measured for each hydrogel sample using a Mecmesin mechanical analyser, Poly Test Instruments (Boksburg, South Africa). Five mL of each hydrogel sample was transferred to a size 6 poly top vial. The hydrogel samples were maintained in a water bath at  $37 \pm 2 \text{ }^\circ\text{C}$  and then quickly transferred to the mechanical analyser. The analysis was performed within one minute, which was enough time to preserve the gelation property of the system. Samples were compressed under a load of 20 N, speed of 10 mm/min, and displacement of 5 mm using a stainless-steel probe of 10 mm diameter. Young's modulus of elasticity, indicated by the slope of the graph, was generated from the Emperor™ Force software.

### 3.8 Swelling of thermoresponsive hydrogel samples

Phosphate buffer solution (PBS) buffered at pH 6.8 was prepared and preheated to  $37 \pm 2$  °C to facilitate swelling studies. The hydrogel samples were lyophilized by a vacuum freeze dryer at  $-80$  °C, and 0.1 g of the dry hydrogel was placed in a poly top vial with 1 mL of PBS. The hydrogel was left to swell for 72 hrs to ensure that swelling equilibrium was reached. Swelling was conducted in a humidity chamber (Labdesign Engineering (Pty) Ltd, South Africa) at  $37 \pm 2$  °C and a percentage relative humidity (% RH) of  $70 \pm 2$  %. The excess PBS was then removed from the hydrogel, and the sample was weighed. This process was repeated 3 times for each sample ( $n=3$ ). Equation 3.1 was used to calculate the swelling percentage after 72 hrs, where  $M_s$  refers to the mass of the swollen hydrogels and  $M_l$  refers to the mass of the lyophilized hydrogel.

$$\text{Swelling (\%)} = \left( \frac{M_s - M_l}{M_l} \right) \times 100 \quad \text{Equation 3.1}$$

### 3.9 Erosion of thermoresponsive hydrogel samples

For erosion studies, 50 mL PBS was preheated to  $37 \pm 2$  °C. Hydrogel samples of 1 g were transferred to a 5 mL poly top vials where they were allowed to gel in a water bath at  $37 \pm 2$  °C for 3 min. Thereafter, the samples were weighed, and the mass for each sample was recorded. Subsequently, 1 mL of the preheated PBS was added to the hydrogel sample. The hydrogel samples were left in a humidity chamber (Labdesign Engineering (Pty) Ltd, South Africa) at  $37 \pm 2$  °C and  $70 \pm 2$  %RH. For a period of six weeks, on a weekly basis, the PBS was replaced with fresh medium, and the hydrogel samples were weighed. Equation 3.2 was used to calculate the erosion percentage per week of each sample, where  $M_i$  is the initial mass of the sample and  $M_f$  is the final mass of the sample.

$$\text{Erosion (\%)} = ((M_i - M_f) \times 100) \quad \text{Equation 3.2}$$

### 3.10 Evaluation of DOX loading

High-performance liquid chromatography (HPLC) analysis was performed using a Knauer Azura HPLC (Berlin, Germany) to quantify the concentration of DOX loaded into the hydrogel samples. The HPLC method for the identification and quantification of DOX was adapted from the United States Pharmacopeia (USP), 2007. The mobile phase involved a mixture of water, acetonitrile, methanol, and phosphoric acid in the ratio 270:145:85:1. Sodium lauryl sulphate (0.5 g) was dissolved in the mixture and NaOH was used to adjust the pH to  $3.6 \pm 0.1$ . The HPLC system

was equipped with a reversed-phase (Kinetex™ C<sub>18</sub> 150 x 4.6 mm, 5 μm) column (Phenomenex, California, USA). The mobile phase flow rate was 1.5 mL/min and the detection wavelength was set to 230 nm. Two standard preparations of DOX each containing 5 mg/mL, were prepared and filtered into the HPLC vials. Thereafter, 0.5 mL of each hydrogel sample was diluted with DOX mobile phase to a volume of 25 mL. This was done to allow easy injection of the samples through the syringe filter for a clear and homogeneous solution. The diluted hydrogel samples were transferred to 1.5 mL HPLC vials, and the analysis was performed. A regression graph was plotted from the obtained results ( $r^2 = 0.999$ ) and the resulting equation was used to calculate the concentration of loaded DOX in each hydrogel sample.

### 3.11 Drug diffusion studies

The release behaviour of DOX from the hydrogel systems were determined through drug diffusion studies. During these studies an HDT 1000, Copley Vertical Diffusion Cell system (Nottingham, United Kingdom) was used. The system was set to maintain each diffusion cell at a constant temperature of  $37 \pm 0.5$  °C. Glass diffusion cells, 15 mm in diameter, with a receptor phase holding volume of 12 mL, resulting in a diffusion surface area of 1.77 cm<sup>2</sup>, were utilised. A 0.45 μm cellulose membrane (Millipore, Merck KGaA, Darmstadt, Germany) was locked in place between the donor and receptor compartments. Subsequently, 12 mL PBS (pH 6.8) was placed into each receptor compartment ensuring that the PBS remained in contact with the cellulose membrane. The diffusion study constituted a blank sample without DOX and the hydrogel samples that had passed previous analyses. A volume of 0.4 mL of each hydrogel sample was accurately transferred to the donor compartment of each diffusion cell and sealed with Parafilm™ (Bemis, Neenah, Wisconsin, USA) to avoid any evaporation or sample spillage. Subsequently the stirring of the receptor phase was initiated and maintained at 400 rpm. Drug diffusion was measured over 7 days with sample withdrawal at 1 hr, 2 hrs, 4 hrs, 8 hrs, 12 hrs, and every day for 7 days. At the set time intervals, 1 mL solution was withdrawn from the receptor compartment and transferred into HPLC vials. The same volume (1 mL) of fresh preheated PBS was carefully replaced into each receptor compartment. Due to limited sample availability, the diffusion experiment of sample 3 and 8 was completed in duplicate (n=2). The two formulations were selected because of their improved erosion and swelling compared to the other formulations. The concentration of DOX was determined using HPLC analysis, as described in paragraph 3.10.

The initial amount of drug released ( $t_1AR_1$ ) and subsequent release values ( $t_2AR_2$ ) were calculated using equations 3.3 and 3.4, respectively. The drug release rate was determined using equation 3.5.

$$t_1AR_1 = \left(\frac{AU_1}{A_S}\right) \times C_S \times 1000 \times \frac{V_C}{A_0} \quad \text{Equation 3.3}$$

$$t_2AR_2 = \left(\frac{AU_2}{A_S}\right) \times C_S \times 1000 \times \frac{V_C}{A_0} + (AR_1 \times \left(\frac{V_S}{V_C}\right)) \quad \text{Equation 3.4}$$

$$\text{Release rate} = \frac{t_2AR_2}{\sqrt{t}} \quad \text{Equation 3.5}$$

$AR$  = amount of drug released ( $\text{mg}/\text{cm}^2$ )

$AU$  = peak area of sample solution

$A_S$  = peak area of DOX standard

$C_S$  = concentration of the standard solution (5  $\text{mg}/\text{mL}$ )

$V_C$  = volume of the diffusion cell (12  $\text{mL}$ )

$A_0$  = area of the orifice (0.77  $\text{cm}^2$ )

$V_S$  = volume of sample taken (1  $\text{mL}$ )

$t$  = time (seconds)

### 3.12 Permeability studies

The parallel artificial membrane permeability assay (PAMPA) (PAMPA-096, BioAssay Systems, Hayward, USA) was used to analyse the effect of LIM on the permeability of DOX. Samples 3 and 8 were evaluated as they had better swelling and erosion capacity. A stock solution containing 1  $\text{mL}$  of 10  $\text{mM}$  DOX in DMSO was prepared. As a control, 25  $\mu\text{L}$  of the stock solution was added to 475  $\mu\text{L}$  of PBS (pH 6.8). Thereafter, 25  $\mu\text{L}$  of each hydrogel sample was diluted in 475  $\mu\text{L}$  of PBS (pH 6.8). A blank control of each hydrogel sample without LIM was also prepared by dispersing the hydrogel in the PBS. Following the sample preparation, 300  $\mu\text{L}$  of PBS was added to each well of the PAMPA acceptor plate. Subsequently, 5  $\mu\text{L}$  of 4 %w/v lecithin in dodecane solution was added directly to the surface of the well membranes. Each of the PBS-diluted samples of DOX-hydrogel initially prepared was then added to each donor wall. Due to limited sample quantities, only duplicate analyses were possible ( $n=2$ ). The donor plate was placed into the acceptor plate and the kit was transferred to an incubator (LabEcono, Johannesburg, South Africa) maintained at  $37 \pm 0.5$   $^\circ\text{C}$  for 24 hours. Subsequently, the donor plate was removed, and the acceptor solutions (in the acceptor wells) were transferred to HPLC vials for analysis.

The permeation rate of the hydrogel systems was calculated using Equation 3.6.

$$P_e = C \times -\ln\left(1 - \frac{OD_A}{OD_E}\right) \quad (\text{Equation 3.6})$$

$OD_A$  = peak area of acceptor solution

$OD_E$  = peak area of equilibrium standard

$C = 0.6912$  cm/sec



### 3.13 References

- Braet, H., Rahimi-Gorji, M., Debbaut, C., Ghorbaniasl, G., Van Wallegghem, T., Cornelis, S., Cosyns, S., Vervaet, C., Willaert, W., Ceelen, W. and De Smedt, S.C. 2021. Exploring high pressure nebulization of Pluronic F127 hydrogels for intraperitoneal drug delivery. *European Journal of Pharmaceutics and Biopharmaceutics*, 169, pp.134-143.
- Cao, J., Su, M., Hasan, N., Lee, J., Kwak, D., Kim, D.Y., Kim, K., Lee, E.H., Jung, J.H. and Yoo, J.W. 2020. Nitric Oxide-Releasing Thermoresponsive Pluronic F127/Alginate Hydrogel for Enhanced Antibacterial Activity and Accelerated Healing of Infected Wounds. *Pharmaceutics*, 12(10), p.926.
- Lu, W.C., Chiang, B.H., Huang, D.W. and Li, P.H. 2014. Skin permeation of d-limonene-based nanoemulsions as a transdermal carrier prepared by ultrasonic emulsification. *Ultrasonics Sonochemistry*, 21(2), pp.826-832.
- Mohammadi, M., Arabi, L. and Alibolandi, M. 2020. Doxorubicin-loaded composite nanogels for cancer treatment. *Journal of Controlled Release*, 328, pp.171-191.
- Pettinelli, N., Rodríguez-Llamazares, S., Abella, V., Barral, L., Bouza, R., Farrag, Y. and Lago, F. 2019. Entrapment of chitosan, pectin or κ-carrageenan within methacrylate based hydrogels: effect on swelling and mechanical properties. *Materials Science and Engineering: C*, 96, pp.583-590.
- Pourjavadi, A., Doroudian, M., Ahadpour, A. and Azari, S. 2019. Injectable chitosan/κ-carrageenan hydrogel designed with au nanoparticles: A conductive scaffold for tissue engineering demands. *International Journal of Biological Macromolecules*, 126, pp.310-317
- Ren, Y., Liu, S., Jin, G., Yang, X. and Zhou, Y.J. 2020. Microbial production of limonene and its derivatives: Achievements and perspectives. *Biotechnology Advances*, p.107628.
- Seo, J.W., Shin, S.R., Lee, M.Y., Cha, J.M., Min, K.H., Lee, S.C., Shin, S.Y. and Bae, H. 2021. Injectable hydrogel derived from chitosan with tunable mechanical properties via hybrid-crosslinking system. *Carbohydrate Polymers*, 251, p.117036.
- Siddiqui, S.A., Pahmeyer, M.J., Assadpour, E. and Jafari, S.M. 2022. Extraction and purification of d-limonene from orange peel wastes: Recent advances. *Industrial Crops and Products*, 177, p.114484.



Wen, Q., Zhang, Y., Luo, J., Xiong, K., Lu, Y., Wu, Z., Wang, B.Q., Wu, J., Chen, Y. and Fu, S. 2020. Therapeutic efficacy of thermosensitive Pluronic hydrogel for codelivery of resveratrol microspheres and cisplatin in the treatment of liver cancer ascites. *International Journal of Pharmaceutics*, 582, p.119334.

Xu, M., Mou, Y., Hu, M., Dong, W., Su, X., Wu, R. and Zhang, P. 2018. Evaluation of micelles incorporated into thermosensitive hydrogels for intratumoral delivery and controlled release of docetaxel: a dual approach for in situ treatment of tumors. *Asian Journal of Pharmaceutical Sciences*, 13(4), pp.373-382.

Yang, Z., Teng, Y., Wang, H. and Hou, H. 2013. Enhancement of skin permeation of bufalin by limonene via reservoir type transdermal patch: formulation design and biopharmaceutical evaluation. *International Journal of Pharmaceutics*, 447(1-2), pp.231-240.

Yeh, M.Y., Zhao, J.Y., Hsieh, Y.R., Lin, J.H., Chen, F.Y., Chakravarthy, R.D., Chung, P.C., Lin, H.C. and Hung, S.C. 2017. Reverse thermo-responsive hydrogels prepared from Pluronic F127 and gelatin composite materials. *RSC Advances*, 7(34), pp.21252-21257.

Yu, H.C., Zhang, H., Ren, K., Ying, Z., Zhu, F., Qian, J., Ji, J., Wu, Z.L. and Zheng, Q. 2018. Ultrathin  $\kappa$ -carrageenan/chitosan hydrogel films with high toughness and antiadhesion property. *ACS Applied Materials & Interfaces*, 10(10), pp.9002-9009.

UNIVERSITY of the  
WESTERN CAPE

## CHAPTER 4: THERMORESPONSIVE HYDROGEL SYNTHESIS AND CHARACTERISATION

*This chapter presents and discusses the results obtained from the synthesis process of the thermoresponsive hydrogel formulation. The results obtained during the characterisation of the hydrogel samples are also discussed.*

### 4.1 Introduction

The efficacy of intravenous doxorubicin (DOX) is severely limited by its systemic circulation, which causes intolerable side effects such as cardiotoxicity, immunosuppression, and hepatotoxicity. To that end, the use of a localised drug delivery system is essential to eradicate the side effects associated with conventional DOX. Amongst the drug delivery systems (DDSs) such as nanoparticles and liposomes available for localised therapy, thermosensitive hydrogels are an effective way to target primary tumours such as OSCCs. This type of DDS easily stands as the most appealing method for primary tumour targeting as it delivers the maximum concentration and retains the drug directly at the tumour site. However, the design of thermoresponsive injectables requires special procedures and distinct tests to ensure their suitability as an injectable sol-gel system. Like all pharmaceutical dosage forms, the formulation of thermoresponsive hydrogels inevitably goes hand-in-hand with initial formulation trial and error. One needs to study literature and the characteristics of potential excipients carefully to inform preliminary synthesis/ formulation processes. Considering this, a significant part of this study was dedicated towards preliminary hydrogel synthesis studies, which involved studying the characteristics of the hydrogel constituents, as well as investigating suitable concentrations for each hydrogel constituent/ excipient. Thus, the results of the trial formulations that led to hydrogel synthesis with the selected concentrations are discussed in this chapter.

The final hydrogel formulations were considered for visual properties of homogeneity and colour for easy characterisation. Formulations that did not show sol-gel behaviour were not subjected to further investigation. During the preliminary trial phase, it was important to identify the problem within the formulation, such as phase separation and lack of thermosensitivity at 37 °C and establish a way to solve it. In the next phase, the hydrogels were characterised for their physicochemical properties and compared in relation to the different ratios of ingredients. The effect of an increasing concentration of limonene (LIM), chitosan (CH), and *k*-carrageenan (*k*CRG) on various factors such as rheology, mechanical strength, swelling, and erosion were

evaluated. These analyses were performed to identify optimised hydrogels with readiness for use as a delivery system in terms of further studying, manufacturing, and handling.

## 4.2 Hydrogel synthesis

### 4.2.1 Preliminary trial formulations for hydrogel synthesis

Preliminary trial formulations were performed to identify the concentration of ingredients that allowed a thermoresponsive effect at 37 °C. Although several studies report that Pluronic™ F127 (PF-127) produces thermal response from concentrations of 15-25 %w/v, the trials in this study showed that the addition of CH and *k*CRG increased the thermal response and therefore decreased the need for a high concentration of PF-127. This was also favourable in decreasing the hydrogel's viscosity at low temperatures so that needle withdrawal would be easy and the clinician would have ample time to transfer the injection from cold storage, extract through the needle and inject at the tumour site before gelation occurs. Having a variety of concentrations for PF-127 would also complicate the identification of the effect of CH and *k*CRG on various characteristics, such as the mechanical strength of the hydrogel systems. PF-127 concentration was therefore maintained at 15 %w/v in all the formulations.

The use of ethanol became paramount in this study for its solvation ability. In the initial trials conducted without ethanol, the appearance of a cloudy white layer on top of the reaction mixture was formed, demonstrating the spontaneous separation of lipophilic LIM from the hydrophilic-base formulation (Figure 4.1). Ethanol, therefore, provided the solvation of LIM that was needed to homogenise the mixture. Although this study focuses on DOX as a model drug, the rationale to increase the concentration of ethanol was also to ensure that the system could secure maximum drug loading of both hydrophobic and hydrophilic drugs for future exploration. However, a concentration above 20 %v/v ethanol did not allow thermoresponsive sol-gel transition. This result corresponds with that of Chaibundit *et al.*, 2010 who investigated the gelling property of PF-127 at ethanol concentrations of 10-, 20-, and 30 %v/v. The researchers identified that the maximum concentration of ethanol that could accommodate gelling of PF-127 at 37 °C was 20 %v/v (Chaibundit *et al.*, 2010).

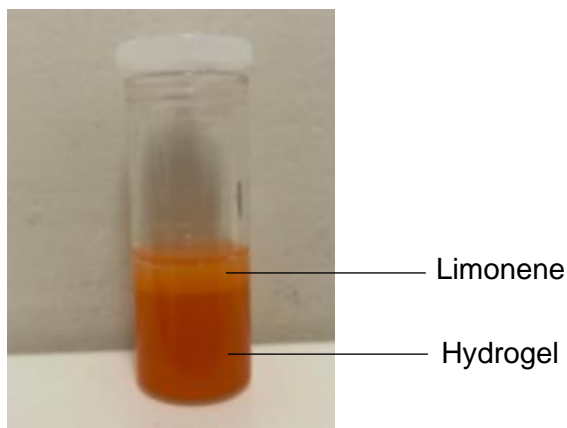


Figure 4.1: Spontaneous separation of LIM from the hydrogel formulation.

Another problem observed during trial formulations was the mesh formation during the mixing of CH and *k*CRG. This observation likely stemmed from the strong electrostatic interaction between the positively charged amine groups on CH and the negatively charged sulfate ( $\text{SO}_3^-$ ) functional groups of *k*CRG (Figure 4.2). Chitosan contains an  $\text{NH}_2$ -group which protonates to  $\text{NH}_3^+$  when exposed to acidic media (Ashrafizadeh *et al.*, 2022). Presumably, the use of acetic acid to allow solubility of CH, caused its protonation. It was identified that the speed of mixing, polymer concentration, and speed of pour influence the mesh formation and structure thereof. A higher stirring speed, lower concentration and slower pour rate led to a more dispersed mesh formation as depicted in Figure 4.3. The final CH/*k*CRG preparation as per the method adapted from Pourjavadi *et al.*, 2019, yielded a homogeneous mixture.

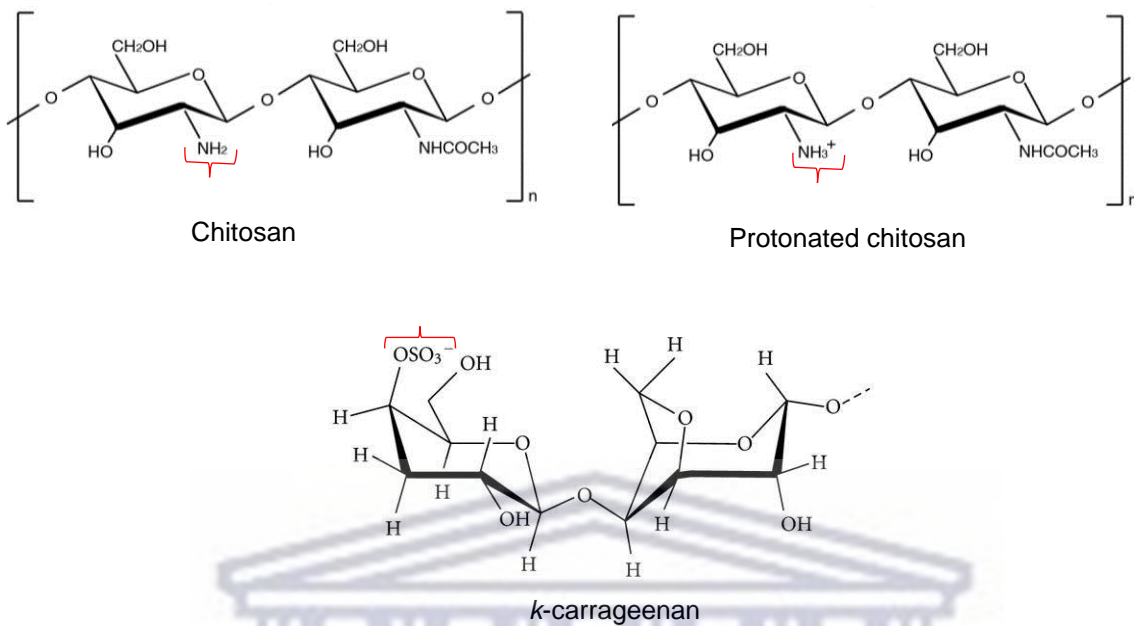


Figure 4.2: The molecular structures of CH and *k*CRG, with a depiction of the protonation of the  $\text{NH}_2$ -group on the CH molecule, rendering it in the protonated state.

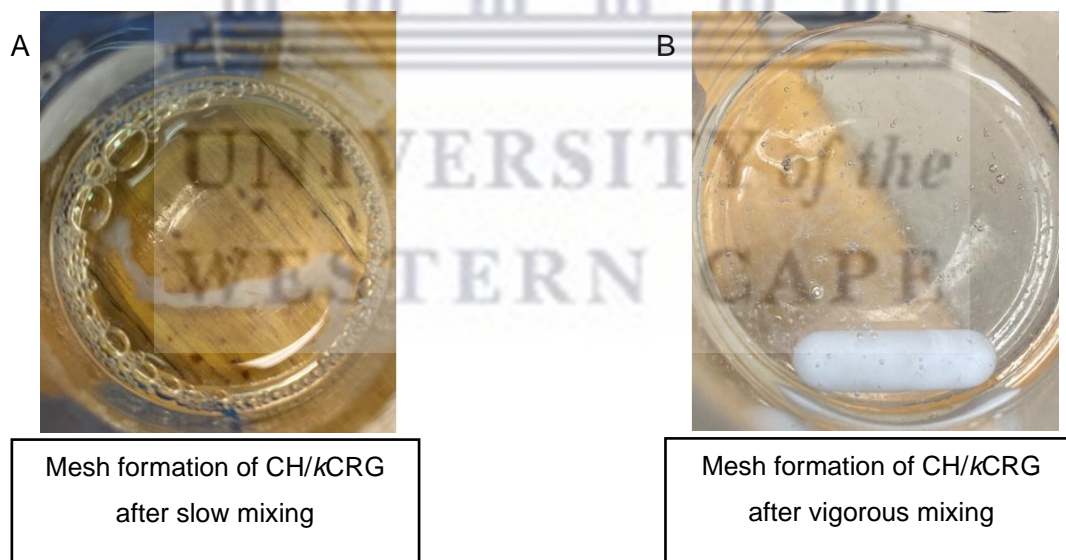


Figure 4.3: (A) Depiction of mesh formation after slow mixing (600 rpm) of CH/*k*CRG, (B) depiction of the mesh formation upon vigorous stirring (1400 rpm) of CH/*k*CRG.

### 4.2.2 Outcome of hydrogel synthesis

The preliminary trials resulted in the selection of 9 formulations (samples 1-9) with varying concentrations of polymers as reported in Chapter 3 (paragraph 3.3). All 9 samples gelled at ambient temperature and showed reversible sol-gel transition (Figure 4.4). The samples were red in colour because of the presence of DOX, and they were flowable at  $4 \pm 2$  °C. The 9 formulations were selected for physicochemical and *in vitro* characterisation studies to identify the ideal formulation according to rheological behaviour, mechanical strength, drug release and permeability studies.

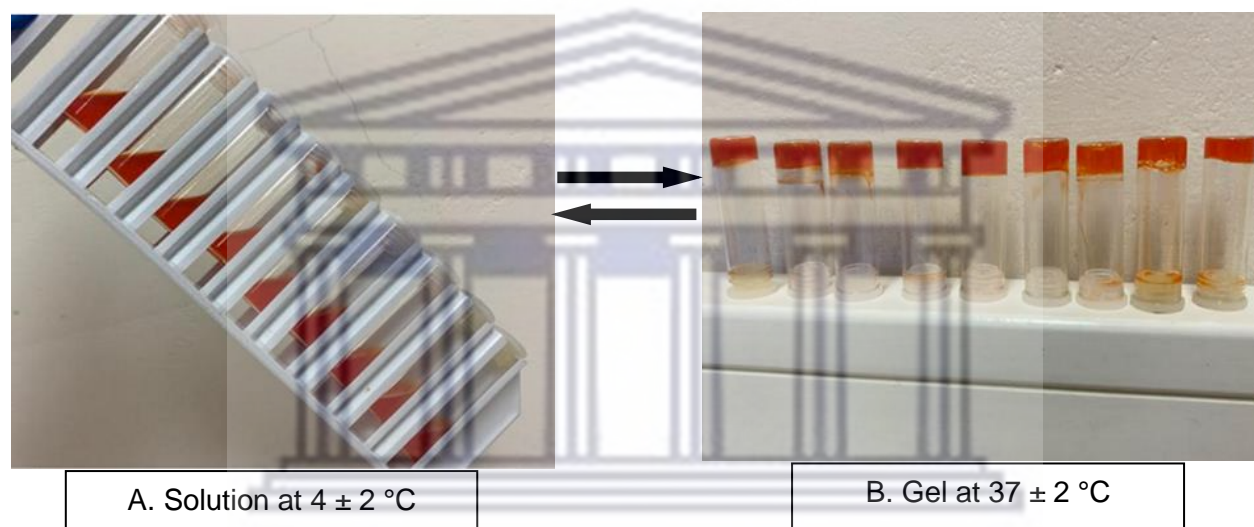


Figure 4.4: Sol-gel transition of hydrogel samples. A: flowable liquid. B: immovable gel.

### 4.2.3 pH of hydrogel formulations

All 9 hydrogel samples began to aggregate upon reaching pH 6, as shown in Figure 4.5. Because a homogenous formulation was required, this was an undesirable effect, but it also showed the pH-responsive nature of the system and the possibility to obtain a dual system of temperature and pH response for *in situ* hydrogel aggregation and gelation at the tumour site. A possible contribution to the aggregation may be due to CH's inability to solubilise at neutral-alkaline pH. At a lower pH, the configuration of polymer chains is more relaxed, enabling a more stable ionic interaction with *k*CRG (Xu and Matysiak, 2017). The main reason to emulate the pH of the tumour was to ensure that the tissues do not experience irritation. However, during DOX preparation with sodium chloride injection, USP, or 5 %w/v dextrose for intravenous injection, its pH is targeted at 3 and administered to the patient. Hence, although physiological pH is ideal, a

lower pH of the formulation will not obstruct the tumour environment and will be safe for patient use. The pH was determined after sol-gel transition at  $37 \pm 2$  °C. This was done to ensure that there is no drastic change in pH value after conversion of sol to gel, which could occur because of an undesired chemical reaction in the system. There was no difference in the pH of the solution and that of the gel. The external pH of the hardened gel does not influence its structure. This was further emphasised in erosion studies, which is discussed in paragraph 4.8. The pH values that were recorded of the 9 hydrogel formulations are tabulated in Table 4.1.

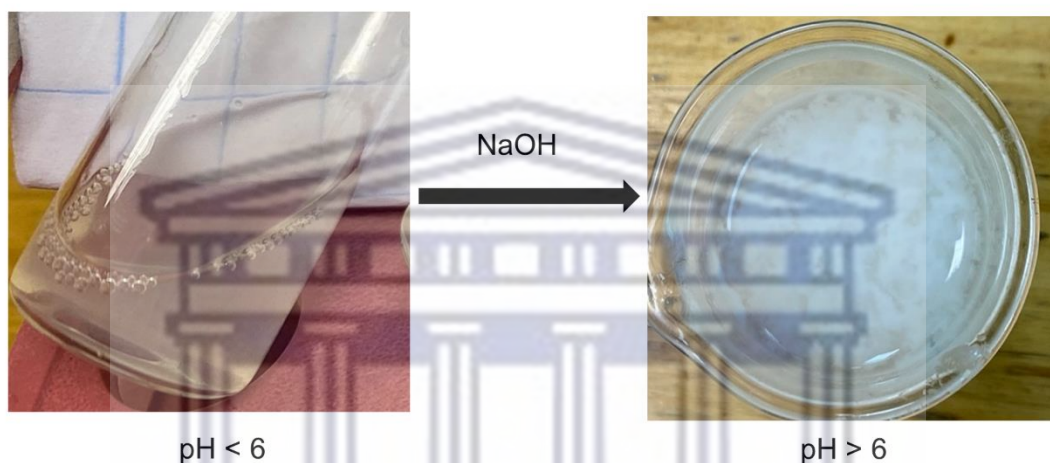


Figure 4.5: Photographic evidence depicting the instability of the prepared hydrogel with increasing pH.

UNIVERSITY of the  
WESTERN CAPE

Table 4.1: pH of the formulated hydrogel samples at  $4 \pm 2$  °C and  $37 \pm 2$  °C

| Sample | pH at $4 \pm 2$ °C (n=3) | pH at $37 \pm 2$ °C (n=3) |
|--------|--------------------------|---------------------------|
| 1      | 4.870 $\pm$ 0.014        | 4.880 $\pm$ 0.021         |
| 2      | 5.110 $\pm$ 0.009        | 5.100 $\pm$ 0.000         |
| 3      | 4.880 $\pm$ 0.021        | 4.880 $\pm$ 0.000         |
| 4      | 4.450 $\pm$ 0.000        | 4.450 $\pm$ 0.000         |
| 5      | 4.640 $\pm$ 0.025        | 4.640 $\pm$ 0.000         |
| 6      | 4.720 $\pm$ 0.009        | 4.740 $\pm$ 0.004         |
| 7      | 4.620 $\pm$ 0.000        | 4.620 $\pm$ 0.000         |
| 8      | 4.580 $\pm$ 0.012        | 4.570 $\pm$ 0.009         |
| 9      | 4.470 $\pm$ 0.005        | 4.470 $\pm$ 0.005         |

### 4.3 Fourier-transform infrared spectroscopy (FTIR)

The 9 hydrogel formulations were characterised by FTIR to identify the molecular vibrations of the hydrogels and validate the electrostatic interactions between the polymers. The important spectroscopic peaks identified from the FTIR data are tabulated in Table 4.2. Figure 4.6 shows the FTIR spectra obtained for CH, PF-127, kCRG, LIM, and DOX used in this study. With this foundation, the FTIR spectra for all 9 hydrogel formulations were plotted and evaluated (Figure 4.7).

Table 4.2: Selected FTIR data for CH, kCRG, LIM and DOX

| Wavenumber (cm <sup>-1</sup> ): functional group |                            |              |              |              |
|--|----------------------------|--------------|--------------|--------------|
| CH   | kCRG                       | PF-127       | LIM          | DOX          |
| 3300.41: O-H, N-H                                | 3300.02: N-H               | 1100.01: C-O | 1450.00: C-H | 3450.00: N-H |
| 2900.12: C-H                                     | 2900.00: C-H               | 2900.23: C-H | 3000.00: C=C | 3330.00: O-H |
|  | 1249.00: S=O               |              | 2900.00: C-H | 1100.00: C-H |
|  | 1600.00: C-O               |              |              |              |
|  | 1030.00: C-O               |              |              |              |
|  | 844.00: C-OSO <sub>3</sub> |              |              |              |



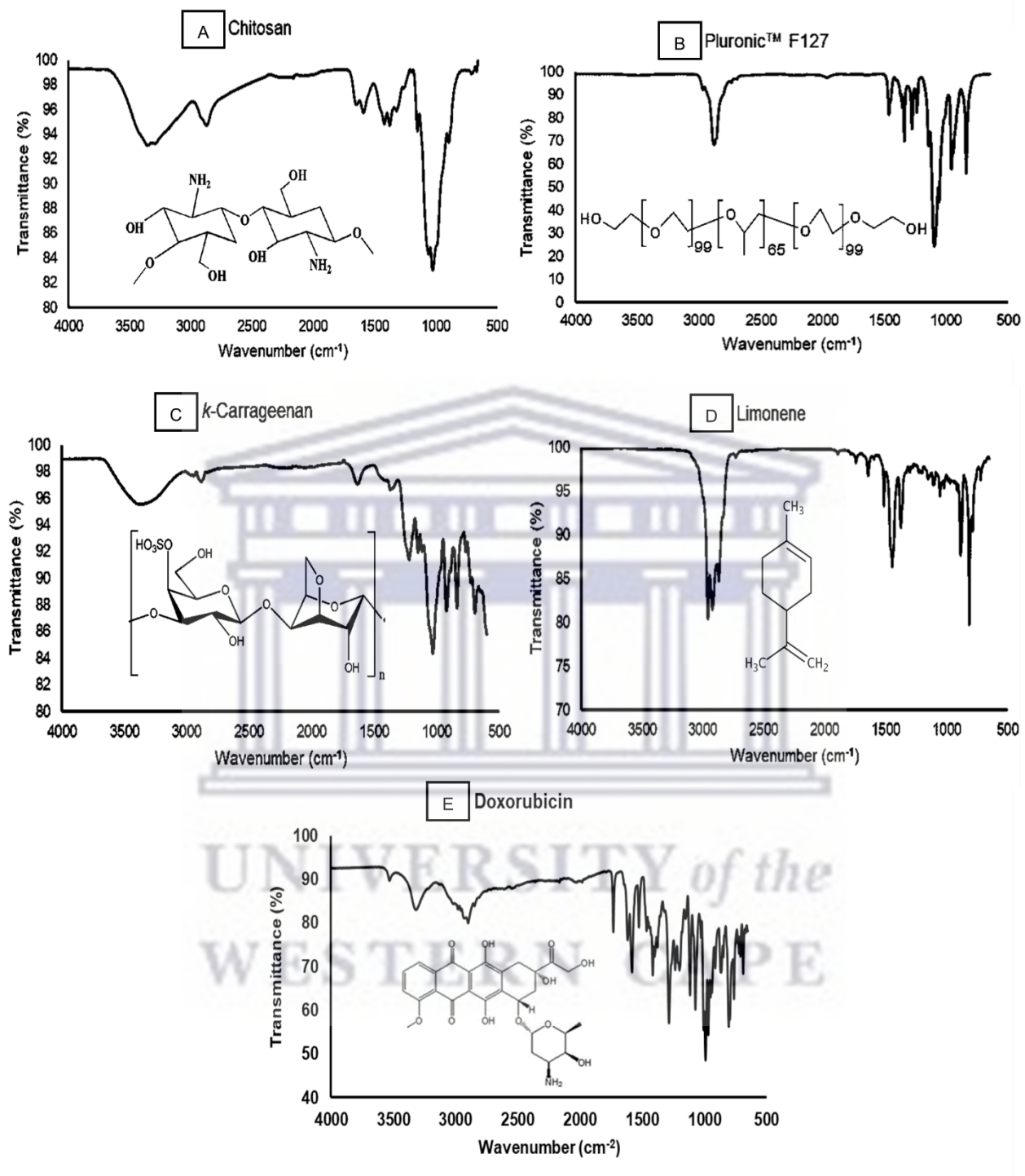


Figure 4.6: FTIR spectra of individual hydrogel constituents – A: CH, B: PF-127, C: *k*CRG, D: LIM, and E: DOX.

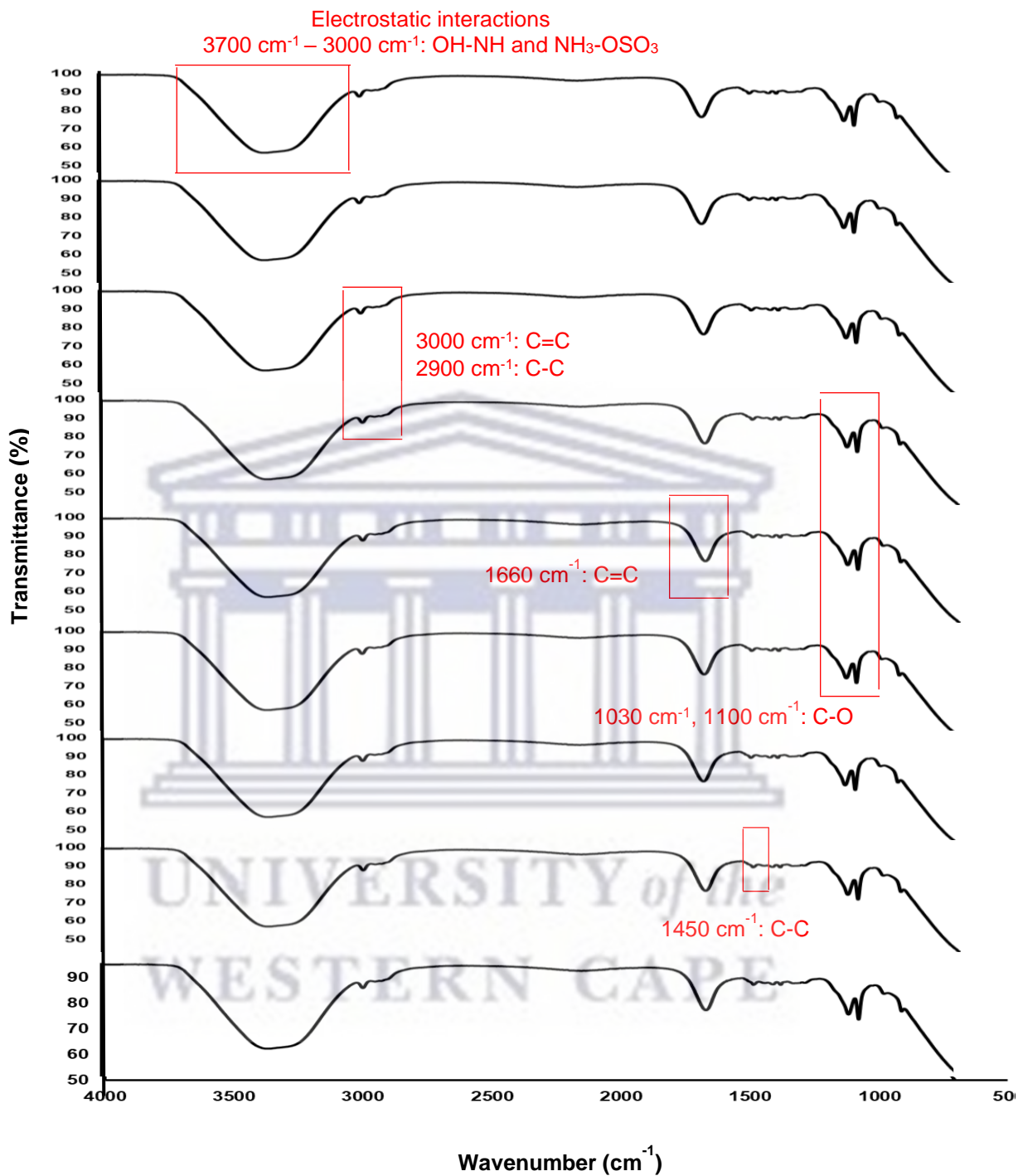


Figure 4.7 FTIR spectra of the 9 hydrogel formulations indicating peak similarities to CH, *k*CRG, PF-127, and LIM.

The spectra of crosslinked polymers with LIM and DOX were represented in the hydrogel preparation. According to Figure 4.7, all 9 hydrogel samples maintained identical absorbance peaks despite variations in the ratios of the polymers. Therefore, concentration changes of the hydrogel constituents did not affect the intensity or broadening of the FTIR peaks. The characteristic broad peaks of CH at  $3300\text{ cm}^{-1}$  showing the amine and alcohol functional groups, as well as the alcohol in *k*CRG, were represented in the FTIR spectra of the formulations. There was a notable increase in the peak intensity around this wavenumber ( $3300\text{ cm}^{-1}$ - $3700\text{ cm}^{-1}$ ) in the final formulations, most likely indicating the electrostatic interaction that occurred with the combination of CH and *k*CRG (transmittance intensity of CH and *k*CRG  $\approx 94\%$ , final formulation transmittance intensity  $\approx 57\%$ ), which facilitated extensive bonding of  $\text{NH}_3^+$  and  $\text{OSO}_3^-$ , respectively. Further support of the presence of *k*CRG is represented by the peaks at 844, 925, 1030, and  $1249\text{ cm}^{-1}$  indicating the stretching bands of C- $\text{OSO}_3$  of d-galactose-4-sulfate, CO of 3,6 anhydro d-galactose, glycoside bands of saccharide moiety, and S=O of sulfate, respectively (Pourjavadi *et al.*, 2019). The presence of PF-127 in the formulation was clearly evidenced by the broad peak at  $1100\text{ cm}^{-1}$ , which is assigned to the ether functional group. The characteristic alkane peak of LIM was also featured in the hydrogel formulation at  $2900\text{ cm}^{-1}$  and a weak peak at  $1450\text{ cm}^{-1}$ . The medium  $2900\text{ cm}^{-1}$  peak likely represents the alkane formation between PF-127, CH, and LIM. The  $1660\text{ cm}^{-1}$  peak was further assigned to the alkene group in LIM. DOX was characterised by the peaks at  $3450\text{ cm}^{-1}$  due to NH stretching vibrations for the primary amine structure and at  $3330\text{ cm}^{-1}$  due to OH stretching vibrations. The CH and *k*CRG peak intensity at  $1000$ - $1100\text{ cm}^{-1}$  were present but significantly reduced in the final formulations, suggesting reduced ether interaction of the polymers with the other constituents. The reduced peak can also be attributed to the high concentration of PF-127 in the formulation, wherein the PF-127 (Figure 4.3: B) shows a small peak at  $1100\text{ cm}^{-1}$ , which is replicated in the final formulation. Overall, all distinct functional groups of the hydrogel excipients were present in the 9 formulations and the changes in intensities of characteristic peaks, as compared to that of the individual constituents, are proof of their crosslinking.

## 4.4 Thermal analysis

### 4.4.1 Thermogravimetric analysis (TGA)

The thermal stability of the hydrogel formulations with varying concentrations of polymers was investigated using TGA. Initially, individual constituents of CH, *k*CRG, PF-127, LIM and DOX were analysed (Figure 4.8) to gain insight into their thermal behaviour. The final formulations

were then analysed, and thermograms were obtained as shown in Figures 4.9a and 4.9b. In the first step, a rapid mass loss of 19-22 % was observed because of the presence of absorbed water in the hydrogel network and the volatile LIM. As the temperature increased to 350 °C, a second mass loss of 27-30 % was observed due to polymer degradation. This degradation at high temperatures indicates the extensive crosslinking of the polymers and high stability over a wide temperature range. However, the early evaporation at 20 °C supports the need for refrigeration of the hydrogel. Unfortunately, the confirmation of hydrogel stability between 4-20 °C was impossible due to instrument limitations. However, based on the presence of LIM, water, and ethanol, the commencement of evaporation is expected, although at an extremely small mass loss. It was interesting to note that all 9 hydrogels showed the same thermal behaviour despite variations in the concentrations of the constituents. This correlates with the FTIR data, wherein no changes in molecular vibrations were observed despite the differences in polymer concentrations. Jaafar and Thatchinamoorthi, 2018 observed opposing thermal results when they prepared a gellan gum hydrogel containing LIM and curcumin. They identified that as the concentration of LIM increased, the mass loss increased (Jaafar and Thatchinamoorthi, 2018). While their results are sensible, the difference in thermal observations could stem from the extremely small concentration differences of LIM in the different formulations used in this study which may make it difficult to detect changes in thermal behaviour. However, whether the small thermal changes are present or not, the most important consideration is the proven thermal stability of the hydrogel formulations.

UNIVERSITY of the  
WESTERN CAPE

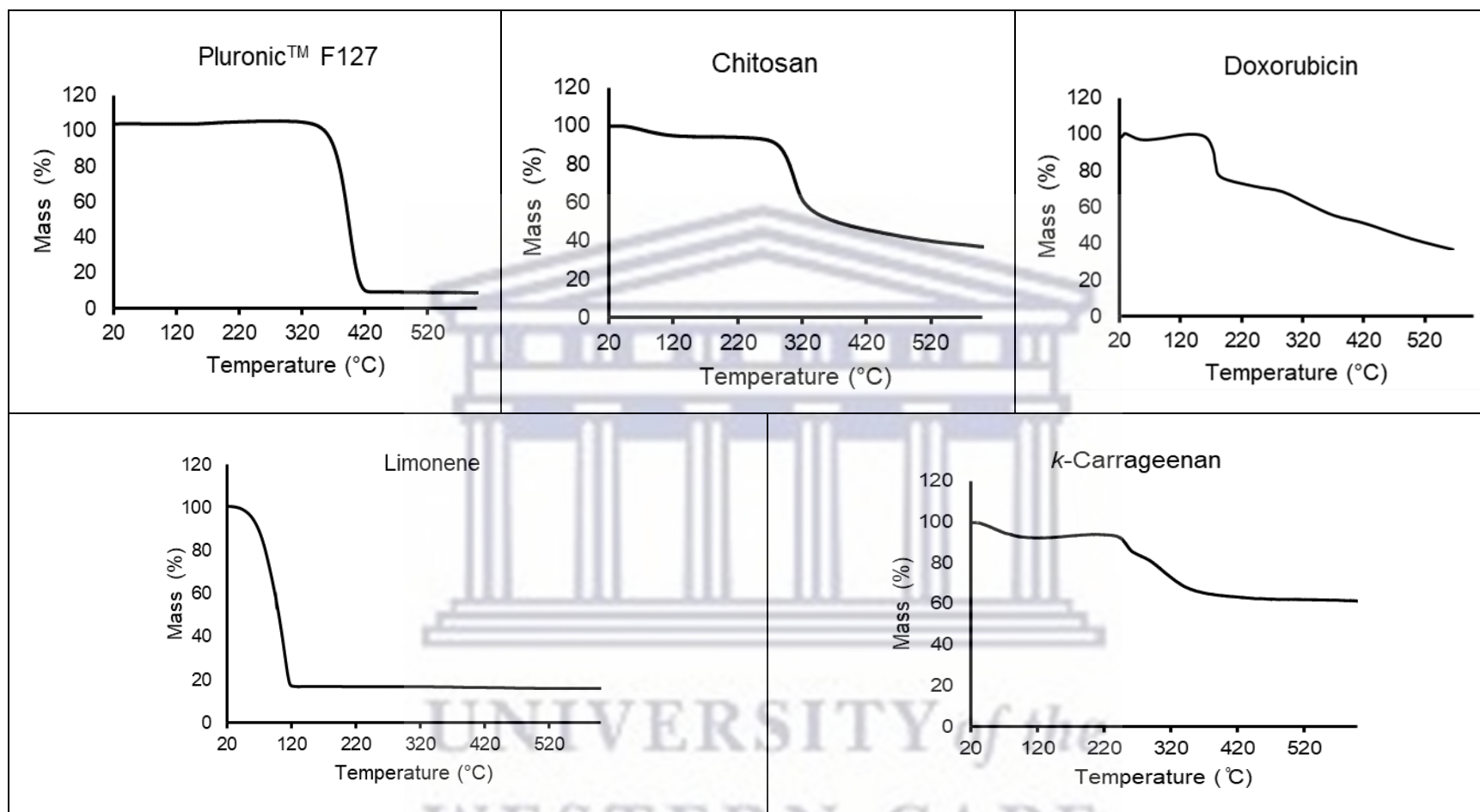


Figure 4.8: Thermogravimetric thermograms obtained with CH, kCRG, PF-127, LIM and DOX during heating from ambient temperature to 600 °C.

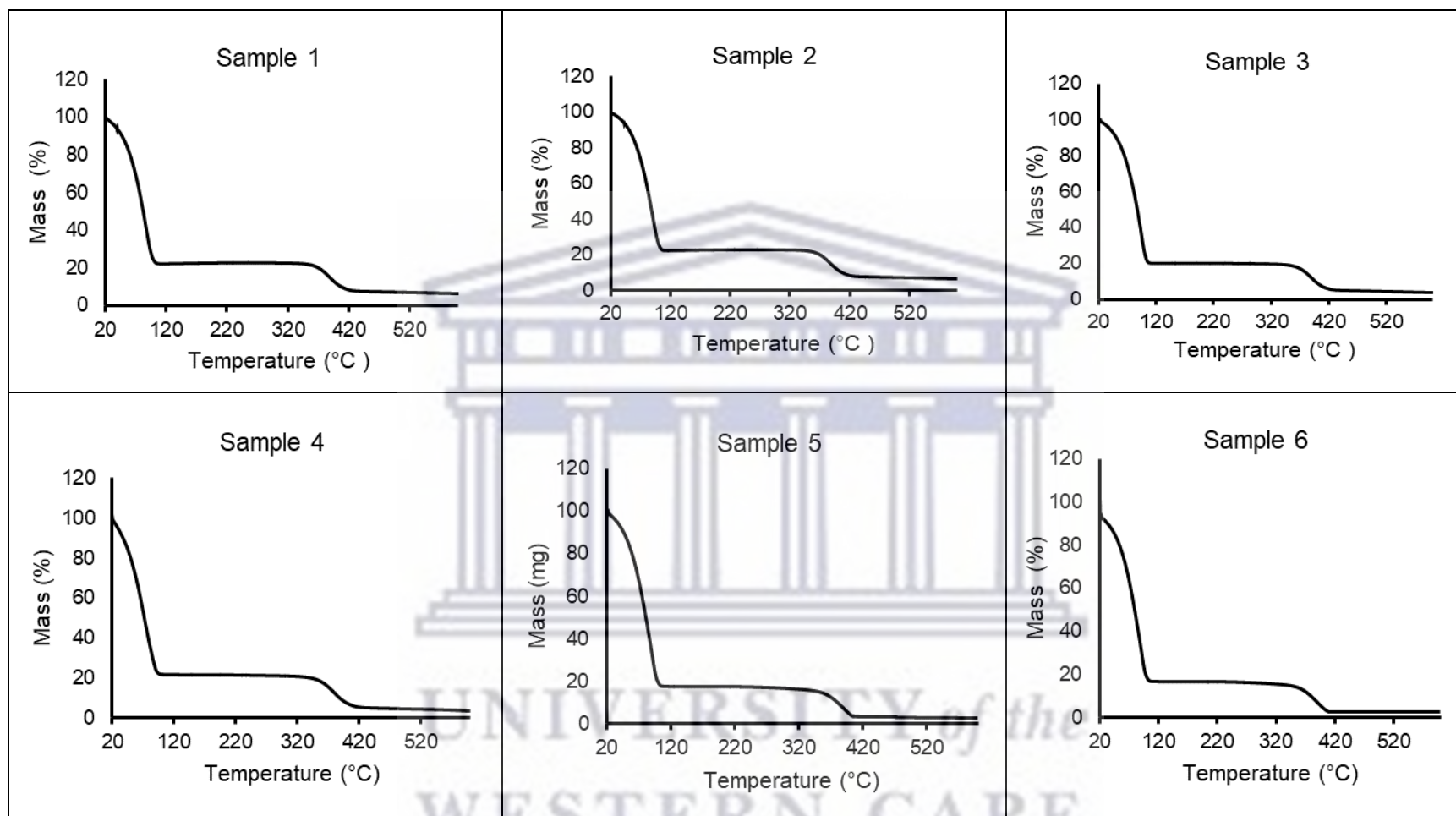


Figure 4.9a: TGA thermograms of hydrogel formulations 1-6 from a temperature of 20 °C to 600 °C.

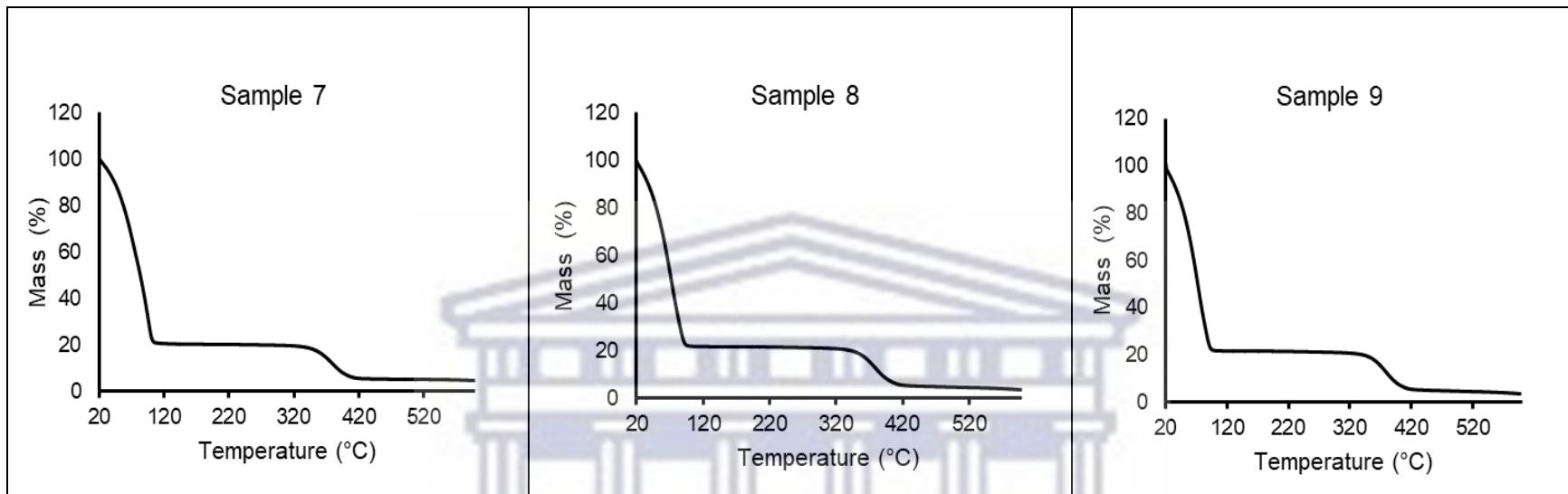


Figure 4.9b: TGA thermograms of hydrogel formulations 7-9 from a temperature of 20 °C to 600 °C.

UNIVERSITY of the  
WESTERN CAPE

#### 4.4.2 Differential scanning calorimetry (DSC)

DSC was employed to further confirm the thermal behaviour of the hydrogel constituents and to confirm compatibility of DOX with the polymers. Figure 4.10 shows the DSC traces of the individual polymers and the drug. The DSC thermogram obtained for DOX (Figure 4.10(a)) revealed an endothermic event at 238.70 °C, which corresponded with the melting point of DOX as reported by Obireddy and Lai *et al.*, 2022. Figure 4.10(b) exhibits the thermal trace for PF-127 which clearly indicates the melting point of 56.40 °C. This correlated well with literature, which reports a melting point around of 55 °C (da Silva *et al.*, 2021). The DSC thermogram obtained for *k*CRG showed a broad endothermic event ranging from onset of heating up to 125 °C. Various literature sources reported that this first thermal event is associated with the melting of *k*CRG (Savadekar *et al.*, 2012). This event was followed by an exothermic event at 242.14 °C, correlating with the onset of degradation observed during TGA analysis (Figure 4.8). Interestingly, CH showed a very similar thermal trace to that observed with *k*CRG. However, the endothermic event showing a peak temperature at 72.18 °C was identified as loss of surface water. This corresponded with the first small weight loss step visible in the TGA trace of CH (Figure 4.8). The following exothermic event is attributed to the degradation of the amine groups associated with the CH molecule (Tahira *et al.*, 2019). From the thermal data obtained for each individual compound, it was concluded that DOX shows thermal stability until  $\approx$  239 °C, whilst PF-127 and *k*CRG melt at fairly low temperatures, 30-60 °C, and CH remains stable well above 200 °C. Considering this, it is apparent that the hydrogel formulation process will result in complete melting of PF-127 and *k*CRG and no degradation of any of the components will be triggered.

Figure 4.11 shows the DSC thermograms obtained with mixtures containing DOX and the polymers. Three samples were prepared by weighing and mixing of the constituents to obtain a physical powder mixture. Sample 1 consisted of 0.0005 %w/w DOX, 15 %w/w PF-127, 0.1 %w/w CH and 0.1 %w/w *k*CRG. This powder mixture corresponded to the DOX:polymer ratios used in the formulation of hydrogels 1, 4, and 7. Sample 2 consisted of 0.0005 %w/w DOX, 15 %w/w PF-127, 0.3 %w/w CH and 0.1 %w/w *k*CRG, corresponding to the drug:polymer ratios used in the formulation of hydrogels 2, 5, and 8. Lastly, Sample 3 consisted of 0.0005 %w/w DOX, 15 %w/w PF-127, 0.3 %w/w CH and 0.3 %w/w *k*CRG corresponding to the DOX:polymer ratios used in the preparation of hydrogels 3, 6 and 9.



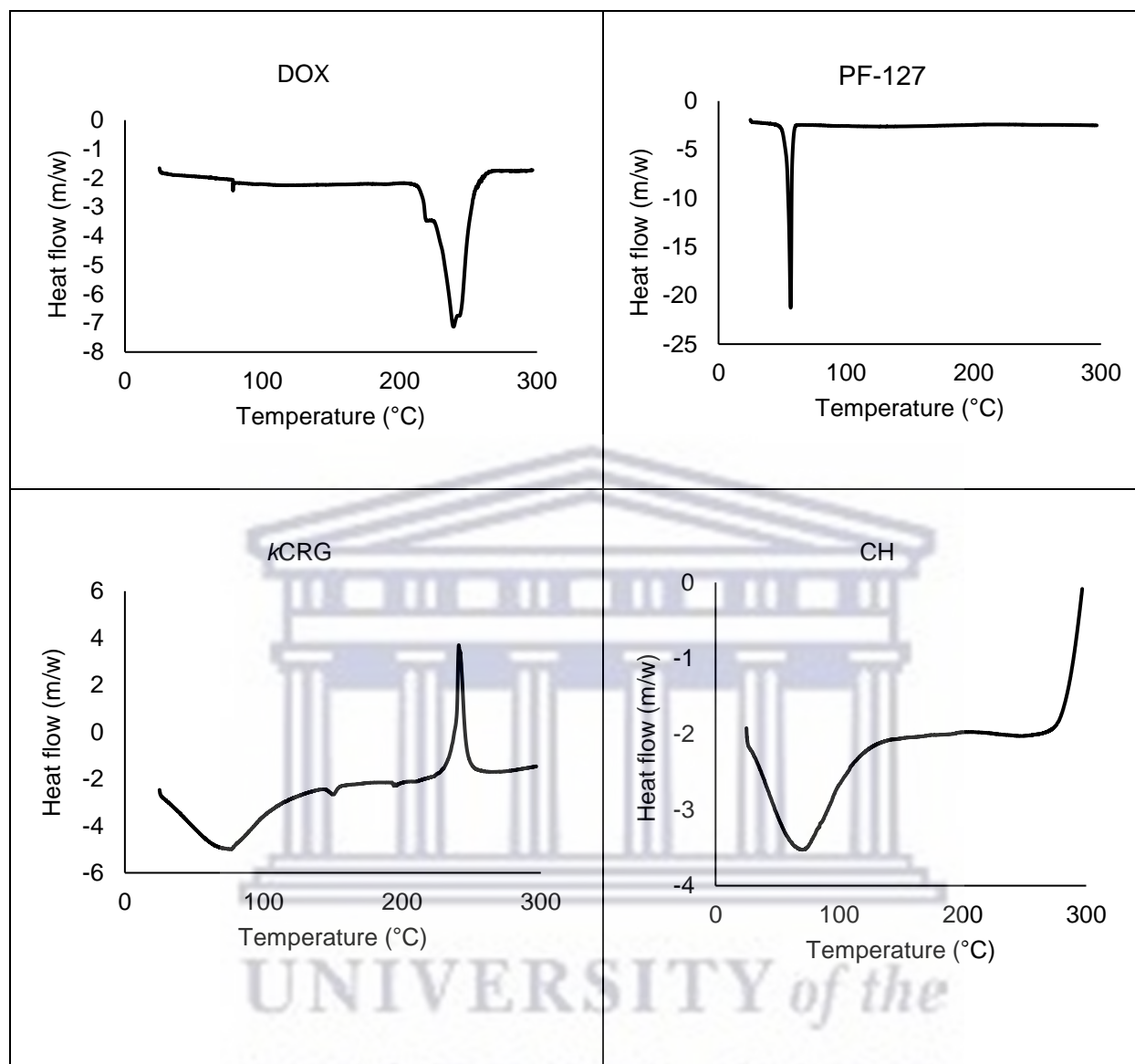


Figure 4.10: DSC thermograms of CH, kCRG, PF-127 and DOX from a temperature of 25 °C to 300 °C.

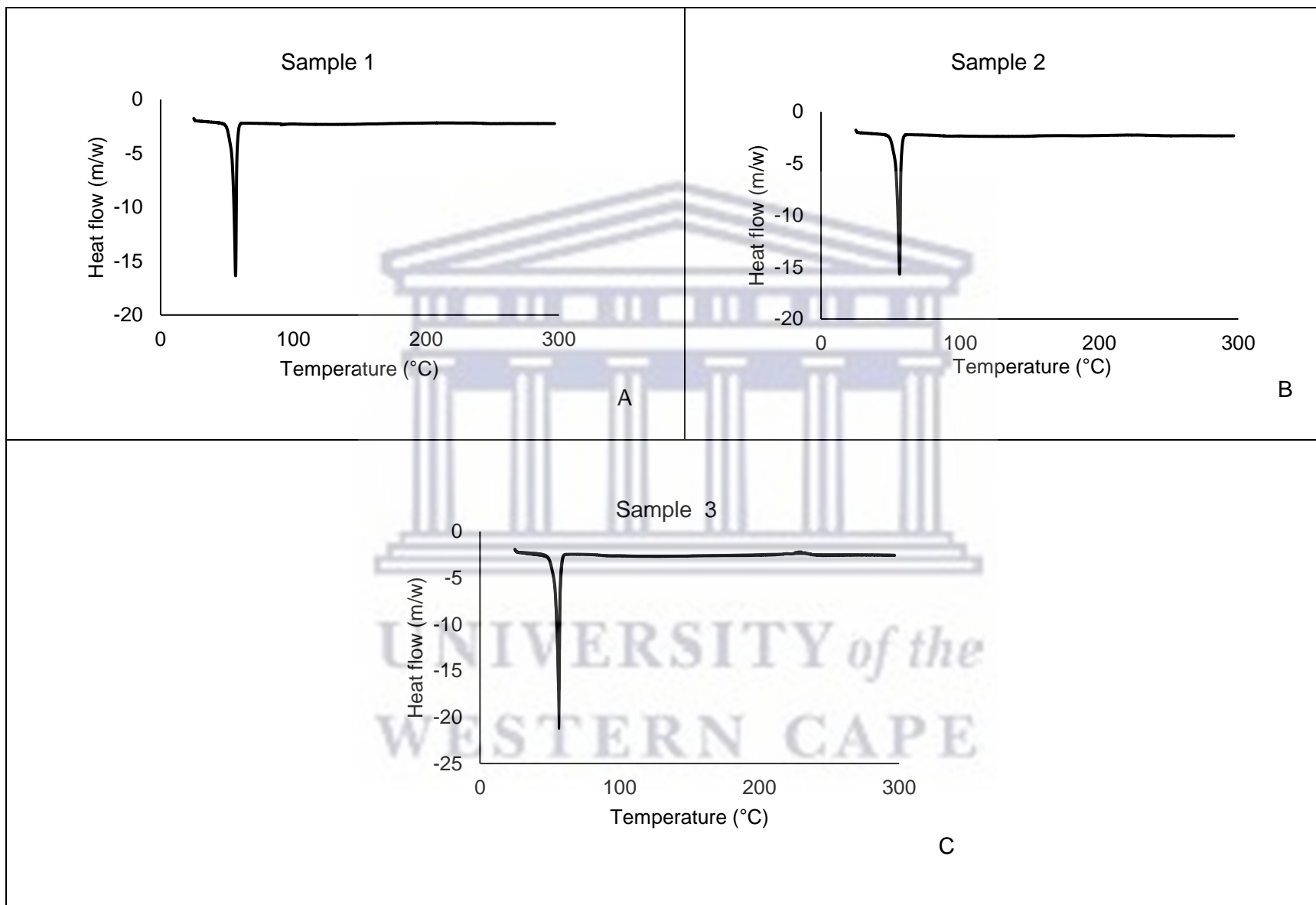


Figure 4.11: DSC thermograms of thermosensitive hydrogel formulations (sample 1-3) from a temperature of 25 °C to 300 °C.

Interestingly, the concentration variations of PF-127 and *k*CRG did not affect the measured thermal behaviour. For Samples 1 and 2, a single endothermic peak at 56.40 °C was observed and based on observations made during the DSC analysis of the individual compounds, this thermal event was identified as the melting of PF-127. The prominence of this melting peak was expected based on the concentration thereof ( $\approx 98\%$ ) in the drug:polymer mixtures. In sample 3, a slight exothermic peak was observed at 232.95 °C indicating the degradation of *k*CRG as confirmed by TGA (Figure 4.8) and DSC analysis (Figure 4.10). This observation is understandable since this sample contained the highest concentration of *k*CRG.

#### 4.5 Gelation time

The gelation time of thermoresponsive hydrogels is an important consideration for injectability and drug release. Slow gelation may cause the drugs embedded in the hydrogel to escape from the tumour into systemic circulation, while fast gelation may clog the injection needle and limit homogeneous tissue integration, which further negates drug release. The samples were analysed at room temperature  $23 \pm 2$  °C and at physiological temperature of  $37 \pm 2$  °C. Table 4.3 shows the results obtained within 1 hr of the observation. The point at which there was no flow of the hydrogel's meniscus after tilting was considered the gelation time. Hydrogels 1-3 remained in a liquid state at  $23 \pm 2$  °C throughout the 1 hr period because of the low LIM concentration and increase in water to meet the required volume of the hydrogels. Reasonably, the increase in water decreased the gelling capacity of PF-127, and a decrease in the water concentration and increase of CH and *k*CRG led to a more viscous solution and, ultimately, quicker gelation. All the samples showed rapid gelation, within 1-3 min, at  $37 \pm 2$  °C, indicating the likelihood of an initial stable release of the drug from the hydrogel system. Hydrogels 4-9 showed the shortest gelling time. Another notable pattern is that as temperature increases, the gelling time decreases. This is due to attractive hydrophobic and hydrogen bonding between the polymer chains, which aggregate as temperature increases (Ahmad *et al.*, 2019).

Table 4.3: Gelation time of hydrogels 1-9 at  $23 \pm 2$  °C and  $37 \pm 2$  °C after 1 hr observation

| Sample | Gelation time at $23 \pm 2$ °C<br>(min) (n=3) | Gelation time at $37 \pm 2$ °C<br>(min) (n=3) |
|--------|---|---|
| 1      | Remains liquid, no gelation                   | $3 \pm 0.000$                                 |
| 2      | Remains liquid, no gelation                   | $3 \pm 0.000$                                 |
| 3      | Remains liquid, no gelation                   | $3 \pm 0.000$                                 |
| 4      | $15 \pm 1.528$                                | $1 \pm 0.000$                                 |
| 5      | $9 \pm 0.577$                                 | $1 \pm 0.000$                                 |
| 6      | $5 \pm 0.000$                                 | $1 \pm 0.000$                                 |
| 7      | $5 \pm 0.577$                                 | $1 \pm 0.000$                                 |
| 8      | $3 \pm 0.000$                                 | $1 \pm 0.000$                                 |
| 9      | $3 \pm 0.000$                                 | $1 \pm 0.000$                                 |

#### 4.6 Rheological analysis of the hydrogel samples

Rheological analysis was performed to identify the effect of temperature on the gelation behaviour of the hydrogels. Figures 4.12 (a-c) show the results obtained from the analysis. Shear storage modulus ( $G'$ ) and shear loss modulus ( $G''$ ) were used to express the changes in deformity of the hydrogel. The orange arrows on the graphs indicate the lower critical solution temperature (LCST) of the hydrogel samples, and the green arrows represent  $G'$  at 37 °C.

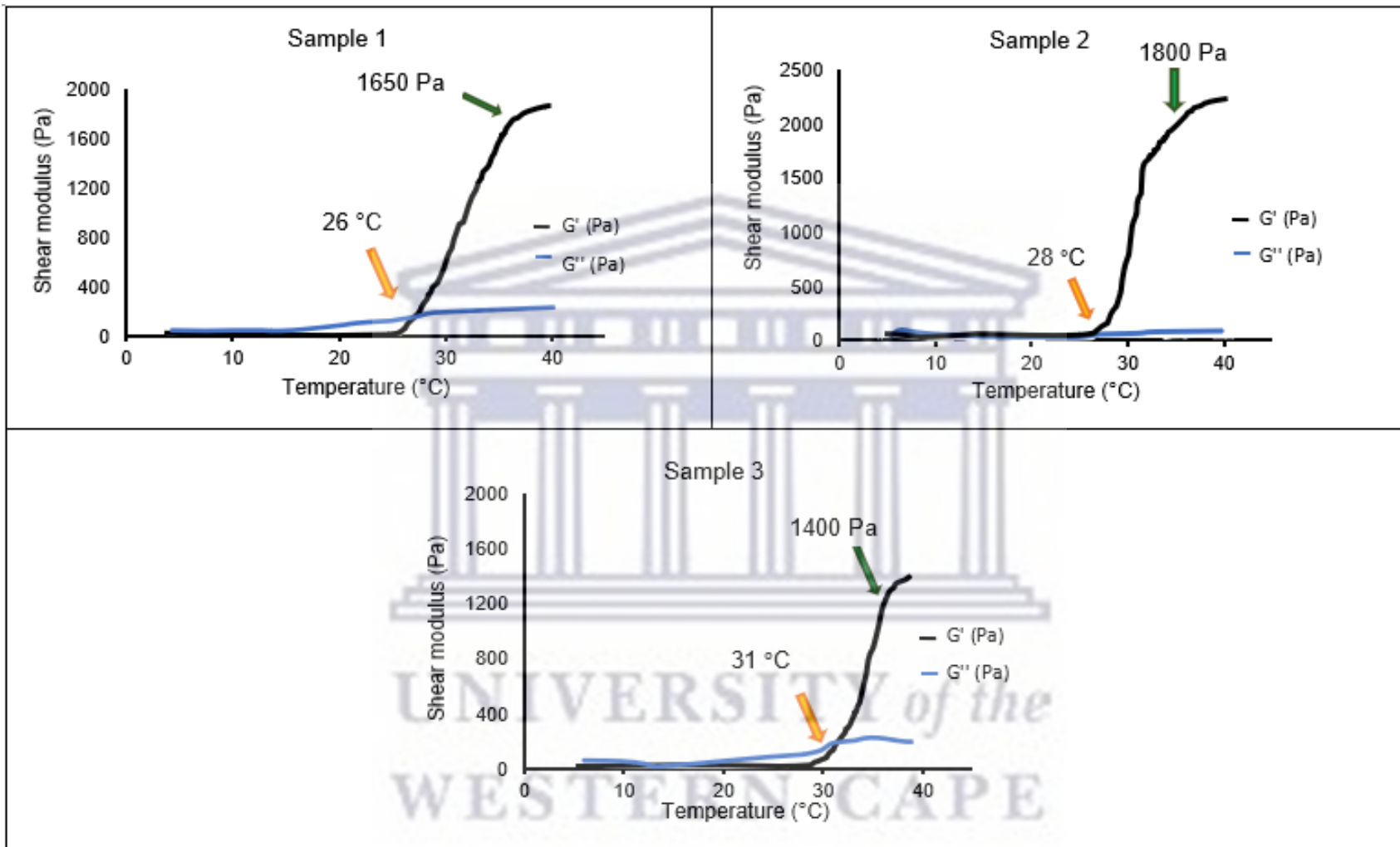


Figure 4.12 (a): Shear storage ( $G'$ ) and shear loss ( $G''$ ) modulus as a function of temperature (4-40 °C) for hydrogel samples 1-3  
 Sample 1: 01%LIM;0.1%CH;0.1%*k*CRG, sample 2: 01%LIM;0.3%CH;0.1%*k*CRG, sample 3: 0.1%LIM;0.3%CH;0.3%*k*CRG.

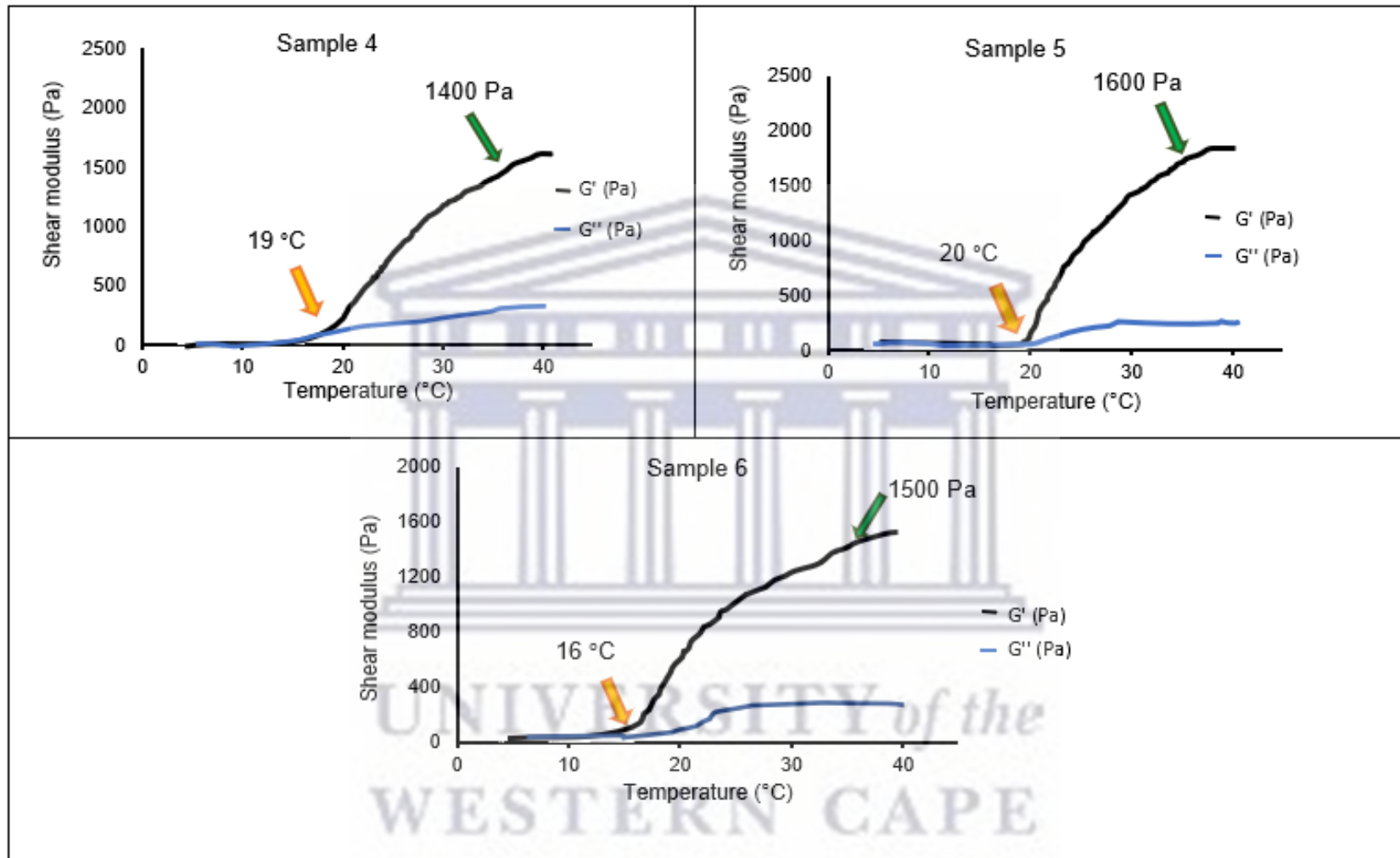


Figure 4.12 (b): Shear storage ( $G'$ ) and shear loss ( $G''$ ) modulus variation as a function of temperature (4-40 °C) for hydrogel samples 4-6. Sample 4: 0.3%LIM;0.1%CH;0.1%kCRG, sample 5: 0.3%LIM;0.3%CH;0.1%kCRG, sample 6: 0.3%LIM;0.3%CH;0.3%kCRG.

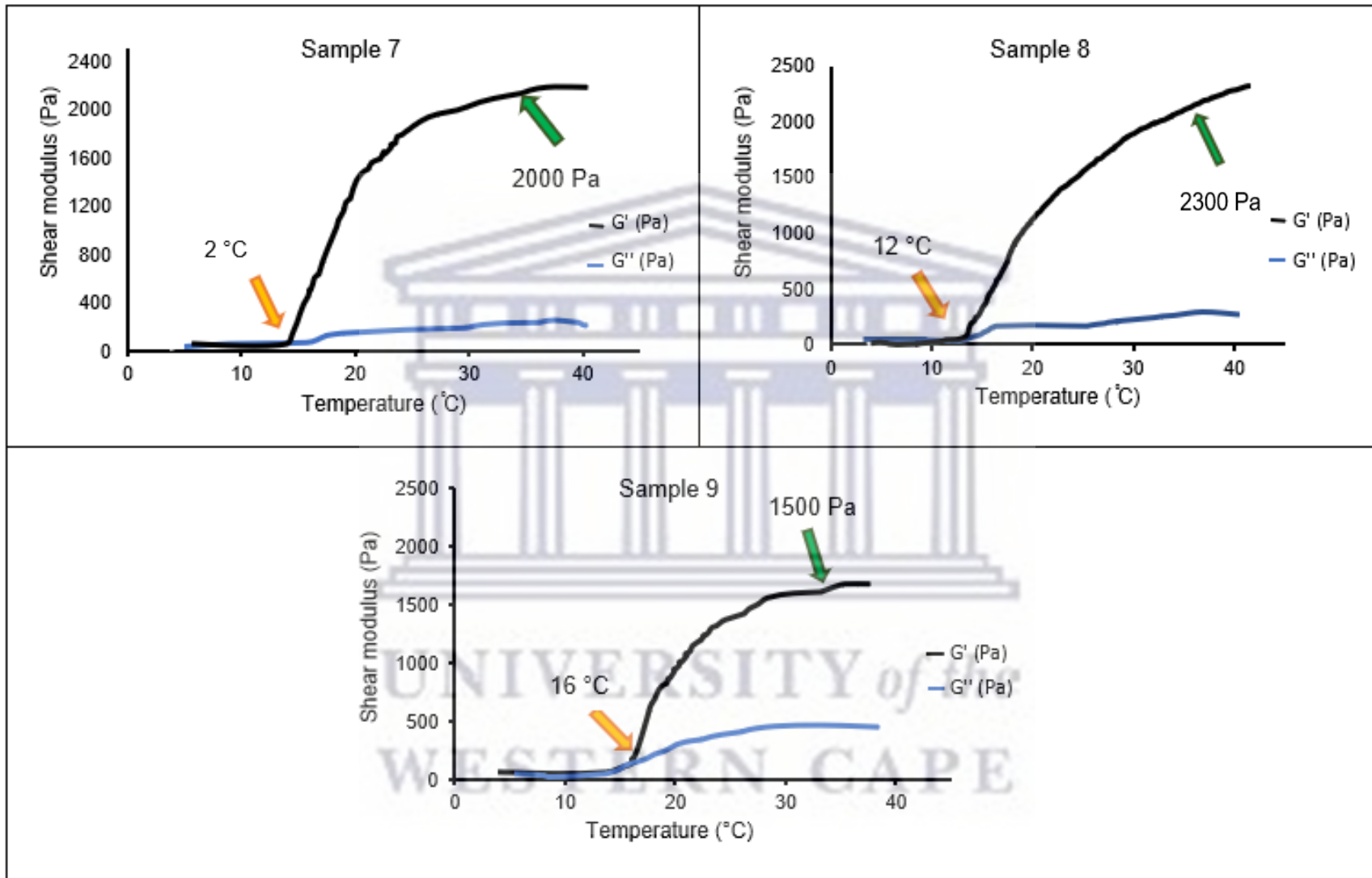


Figure 4.12 (c): Shear storage ( $G'$ ) and shear loss ( $G''$ ) modulus as a function of temperature (4-40 °C) for hydrogel samples 7-9. Sample 7: 0.5%LIM;0.1%CH;0.1%kCRG, sample 8: 0.5%LIM;0.3%CH;0.1%kCRG, sample 9: 0.5%LIM;0.3%CH;0.3%kCRG.

Rheological analysis predicts fundamental aspects of the manufacturing process, handling, and potential clinical use of thermoresponsive hydrogels. The analysis assisted in understanding the viscoelastic properties of the hydrogel system. This is important to ascertain the exact temperature at which the hydrogel gels (LCST) and their resistance towards elastic deformation upon the addition of stress –  $G'$  and  $G''$  assist with this identification. The sudden increase of  $G'$  confirms the thermoresponsive nature of all 9 hydrogels and indicates their LCST. The LCST decreased with increasing LIM and increasing CH and  $kCRG$ . Samples 1-3 showed an LCST above room temperature of  $23\text{ }^{\circ}\text{C}$ , while samples 4-9 had an LCST below room temperature. Therefore, samples 1-3 will still be in a liquid phase at room temperature ( $23 \pm 2\text{ }^{\circ}\text{C}$ ), enabling easy administration, but samples 4-9 will gel once exposed to room temperature and may prove difficult for administration as the solution must be injected before gelling occurs. However, according to the gel time obtained for the hydrogel samples at  $23 \pm 2\text{ }^{\circ}\text{C}$ , administration within a limited period of 3-15 min is still possible at room temperature. For samples 7-9 with an LCST of  $\sim 12\text{ }^{\circ}\text{C}$ , strict storage of the samples at  $4\text{ }^{\circ}\text{C}$  will be required for the hydrogel to maintain a liquid phase, as any increase in temperature may lead to undesired premature gelling.

For all 9 samples,  $G'$  was greater than the  $G''$ , which confirms the more elastic deformative property of the hydrogels. By comparing hydrogel 1 with hydrogel 2, hydrogel 4 with hydrogel 5, and hydrogel 7 with hydrogel 8, it was observed that  $G'$  and  $G''$  increased slightly at  $37\text{ }^{\circ}\text{C}$ . This can be attributed to increasing CH concentration. Several articles have reported the significant improvement of  $G'$  with the inclusion of CH (Di Maro *et al.*, 2020), and this study supports those results. Like PF-127, CH demonstrates thermal response (Moura, Figueiredo, and Gil, 2008) and thickens upon increasing polymer concentration. The thickening represents increment of the entanglement of the CH molecular chains, which increases the strength of the system (Rwei, and Lien, 2014.). However, upon equal CH and  $kCRG$  concentrations at 0.3 %w/v each (samples 3, 6 and 9), the viscoelasticity is severely decreased. According to this report, when crosslinked with CH and PF-127,  $kCRG$  does not improve the viscoelasticity of the hydrogels at a temperature of  $37\text{ }^{\circ}\text{C}$ . Despite being thermoresponsive, the gelation behaviour of  $kCRG$  is based on the reduction of temperature, unlike that of PF-127, which relies on increasing temperature to facilitate gelation. CH produces high viscoelasticity, however, when crosslinked with  $kCRG$ , its ability to offer viscoelastic properties is limited due to their opposing thermal response behaviour. A recommendation is to use  $kCRG$  in cases where the hydrogel polymer has a very high LCST and its reduction is needed. The increase of CH did not significantly affect



the LCST of the hydrogels (samples 2, 5, and 7), possibly due to the decrease in viscosity of CH with increasing temperature (Baratpour *et al.*, 2016).

Overall, the  $G'$  of the results obtained showed excellent elasticity. The lowest value reported is 1500 Pa (sample 4), and the highest is 2300 Pa at 37 °C (sample 8). Pourjavadi, *et al.*, 2019, also crosslinked CH and  $kCRG$  and reported a 470 Pa strength of PNIPAM when crosslinked with CH and  $kCRG$  for the development of an injectable thermosensitive hydrogel; however, despite the poor  $G'$ , the LCST was 37 °C, which is remarkably better than that obtained herein.

As part of rheology studies,  $\tan\delta$  values were obtained at 4 °C, 23 °C and 37 °C, as tabulated in Table 4.4.  $\tan\delta$  values further substantiate the viscoelastic properties of the samples and confirm their phase transition from liquid to gel. As expected, all 9 hydrogels showed initial liquid-like behaviour at 4 °C with  $\tan\delta$  values less than or equal to 1.000, indicating the predominantly viscous property of the hydrogel formulations. As the temperature increased to 23 °C and 37 °C, the  $\tan\delta$  decreased drastically, indicating gelling of the hydrogels and its transition towards elastic behaviour. For the first 3 samples, the higher  $\tan\delta$  at 23 °C compared to samples 4-9 support the gelation time results, which showed that the hydrogel maintained some viscous behaviour imparted by slower gelation times and higher LCSTs. The lower  $\tan\delta$  values of samples 4-9 ( $\leq 0.178$ ) at 23 °C and 37 °C are cause for concern regarding the hydrogels' administration and deformability at the tumour site; however, the gelation time results are significantly important to consider when analysing the dismissal or retainment of these samples in the study. Although the hydrogels show predominantly elastic behaviour at 23 °C and 37 °C, the gelation time has proven that this does not happen immediately but over a period of 3-15 min or 1-3 min at  $23 \pm 2$  °C and  $37 \pm 2$  °C, respectively. Therefore, adequate administration and deformability of the hydrogel is still possible within this time range.

Table 4.4: Tan- $\delta$  values for hydrogel formulations at 4 °C, 23 °C and 37 °C

| Sample no. | Tan- $\delta$ |       |       |
|------------|---------------|-------|-------|
|            | 4 °C          | 23 °C | 37 °C |
| 1          | 1.000         | 0.210 | 0.066 |
| 2          | 1.000         | 0.305 | 0.026 |
| 3          | 0.999         | 0.294 | 0.067 |
| 4          | 1.000         | 0.178 | 0.110 |
| 5          | 1.000         | 0.121 | 0.113 |
| 6          | 0.999         | 0.097 | 0.047 |
| 7          | 0.999         | 0.136 | 0.078 |
| 8          | 0.999         | 0.112 | 0.095 |
| 9          | 1.000         | 0.167 | 0.052 |

#### 4.7 Compression strength

The compression strength is a type of mechanical analysis for thermosensitive hydrogels which assists in the determination of rigidity – a property that could influence water penetration, swelling and drug release behaviour. Gels with low compression strength will release the drug too quickly, whereas those with high mechanical strength will release the drug over a longer period. A system that is too rigid and resistant to deformation may irritate the area of injection and cause further discomfort for the patient and restrained mobility at the affected site, such as mastication in the oral cavity. The peak values and Young's modulus (E) (represented by the slope of the graph) were obtained from the Emperor™ Force software. Unlike storage modulus, Young's modulus measures the compressive stiffness of a solid when the force is applied lengthwise. Figures 4.13 (a) and 4.13 (b) provide the results obtained from the compression test. The arrows represent the peak force and the Young's modulus is denoted by "E".

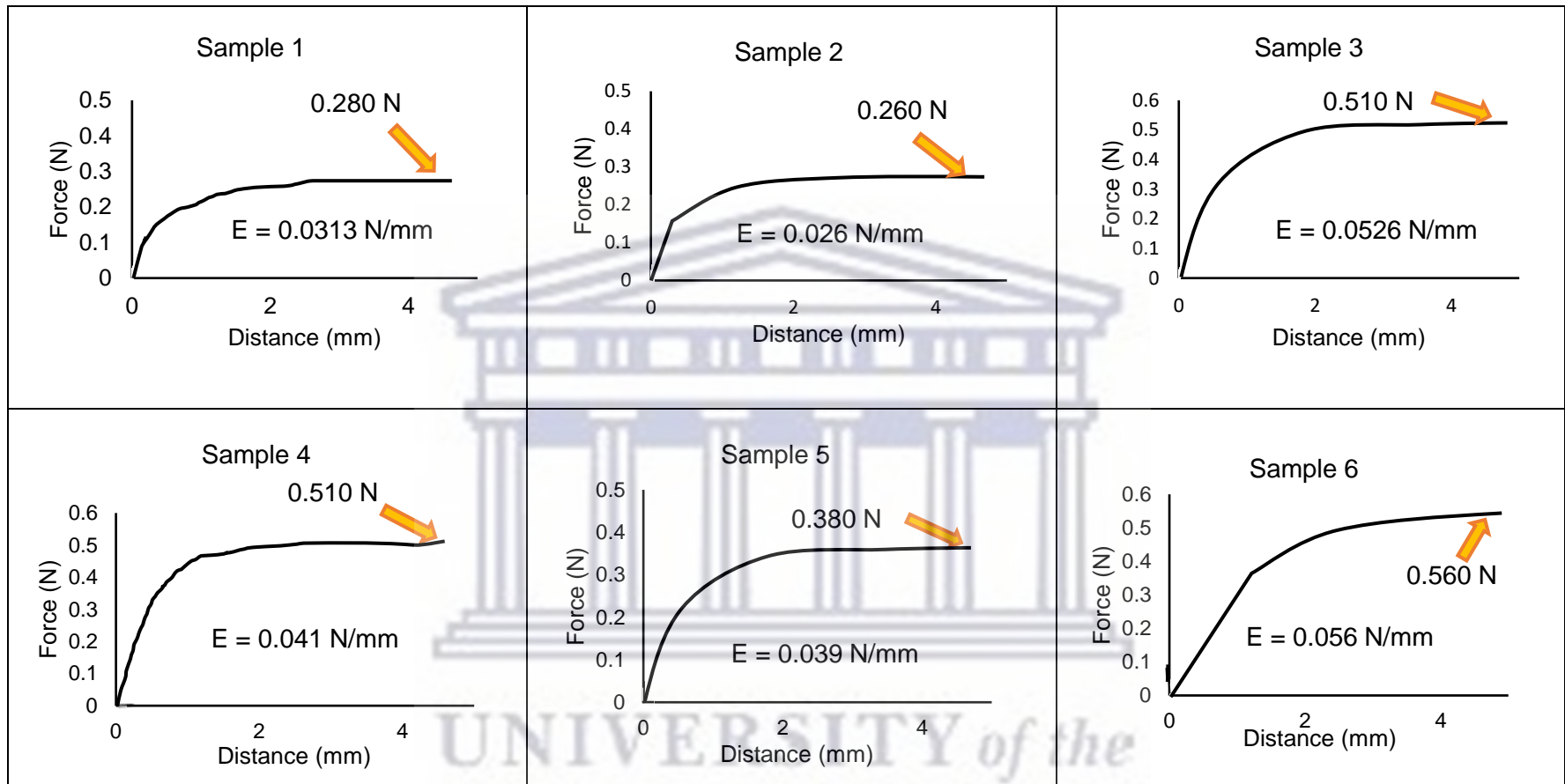


Figure 4.13 (a) Compression results indicating the peak and Young's modulus ( $E$ ) of the hydrogel samples at 37 °C, over a force of 20 N and a displacement of 5 mm for samples 1-6. Sample 1: 0.1%LIM;0.1%CH;0.1%*k*CRG, sample 2: 0.1%LIM;0.3%CH;0.1%*k*CRG, sample 3: 0.1%LIM;0.3%CH;0.3%*k*CRG, sample 4: 0.3%LIM;0.1%CH;0.1%*k*CRG, sample 4: 0.3%LIM;0.1%CH;0.1%*k*CRG, sample 5: 0.3%LIM;0.3%CH;0.1%*k*CRG, sample 6: 0.3%LIM;0.3%CH;0.3%*k*CRG.

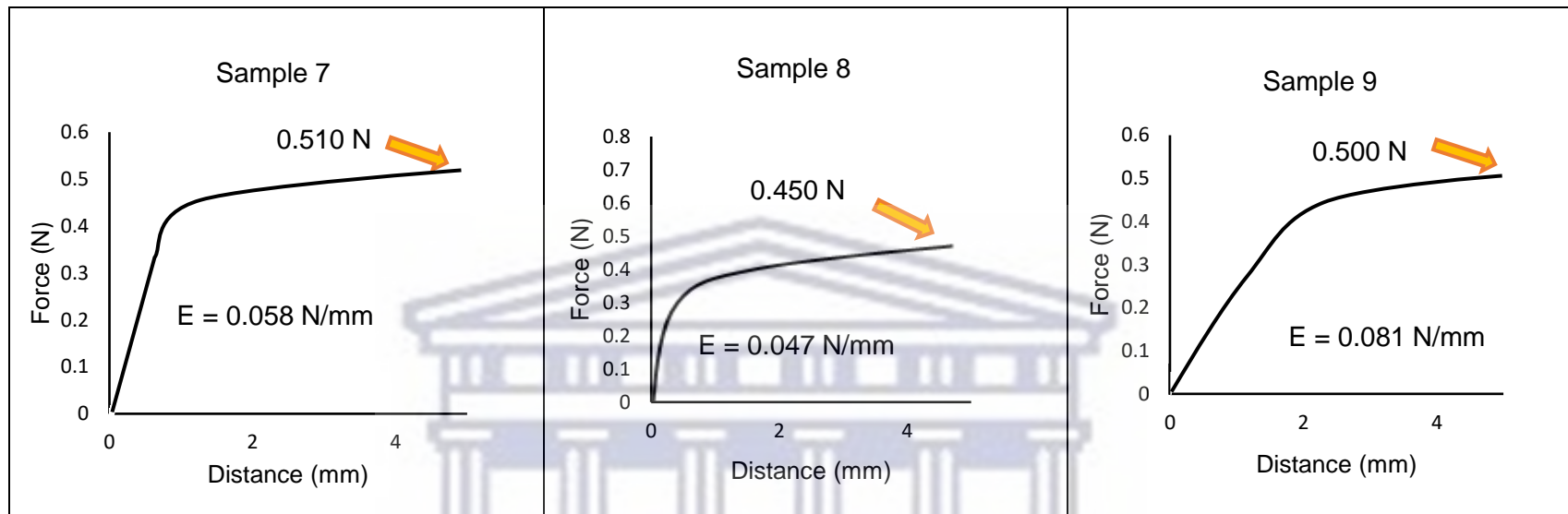


Figure 4.13 (b): Compression results indicating the peak and Young's modulus ( $E$ ) of the hydrogel samples at 37 °C, over a force of 20 N and a displacement of 5 mm for samples 7-9. Sample 7: 0.5%LIM;0.1%CH;0.1%kCRG, sample 8: 0.5%LIM;0.3%CH;0.1%kCRG, sample 9: 0.5%LIM;0.3%CH;0.3%kCRG.

UNIVERSITY of the  
WESTERN CAPE

The tumour is subject to internal and external mechanical forces such as interstitial fluid pressure and basic touching or movements in the oral cavity, which may distort the gel system and hinder drug delivery. Because tumours are significantly heterogeneous in shape, size and type, it is difficult to quantify their mechanical strength; however, studies have shown that the stiffness of tumour extracellular matrix ranges anywhere from 1000 Pa to 70000 Pa (Jain, Martin, and Stylianopoulos, 2014). The tensile strength of the facial skin was reported as 1400 Pa (Mazza *et al.*, 2005). The thermosensitive hydrogel must therefore mimic these values while ensuring that there is no physical irritation to the tissue area. The mechanical results show that all the samples experienced plastic deformation and did not break during compression analysis. According to peak values at 5 mm, samples 3, 6 and 9 (formulations with an increased concentration of CH and *k*CRG) can withstand a higher force than the other samples. The samples will therefore require a greater amount of force to undergo physical deformation. This high force can be attributed to the intensified compactness of the hydrogel structure due to increased polymer concentration, which resulted in denser packing of the incorporated molecules. The compressive force of the peak of the hydrogel samples was within the range of the skin and tumour tissue.

The Young's modulus obtained for samples 3, 6, 7 and 9 (0.0526, 0.056, 0.058 and 0.081, respectively) is high compared to the other samples, indicating slightly higher rigidity. The increase in rigidity due to increasing *k*CRG is supported by several studies, including that of Derkach *et al.*, 2015, and Lim *et al.*, 2017. Young's modulus also increased with increasing LIM, and this may be attributed to the increasing hydrophobic interactions. Mredha *et al.*, 2019 noted that hydrophobic-rich components were able to impart stiffness and strength to hydrogels. Increasing CH reduced rigidity according to compressive mechanical analysis but increased elastic behaviour, according to rheology. From these studies, it can be confirmed that CH imparts elasticity to the hydrogels whereas *k*CRG contributes to compressive strength and rigidity. When considering variations in body temperatures between 37-40 °C, the steadiness of  $G'$  within that temperature range indicates that each sample will have a similar mechanical profile.

#### 4.8 Swelling and erosion

The swelling and erosion capacity of hydrogels are important factors which control drug release patterns from hydrogel networks. Aside from mechanical strength, CH and *k*CRG were employed as natural polymers to enhance the biocompatibility of the hydrogels by improving their swelling and erosion capacities. It is important to note that the hydrogel formulations used in this part of the study did not include DOX due to its high cost and therefore limited availability. It is hypothesised that the exclusion of DOX is unlikely to affect the erosion and swelling capacity of the gel system because of the low DOX concentration (0.0005 %w/v) that is loaded into the hydrogels. Additionally, the low DOX concentration did not affect the chemical properties of the hydrogel formulation, as observed in DSC and FTIR. Thus, DOX will not affect swelling and erosion of the hydrogel formulations. However, if it does, we can assume that results will still follow the same trend since the quantity of DOX is the same for all 9 hydrogels. Tables 4.5 and 4.6 represent the results obtained from the swelling and erosion studies, respectively, performed at  $37 \pm 2$  °C.

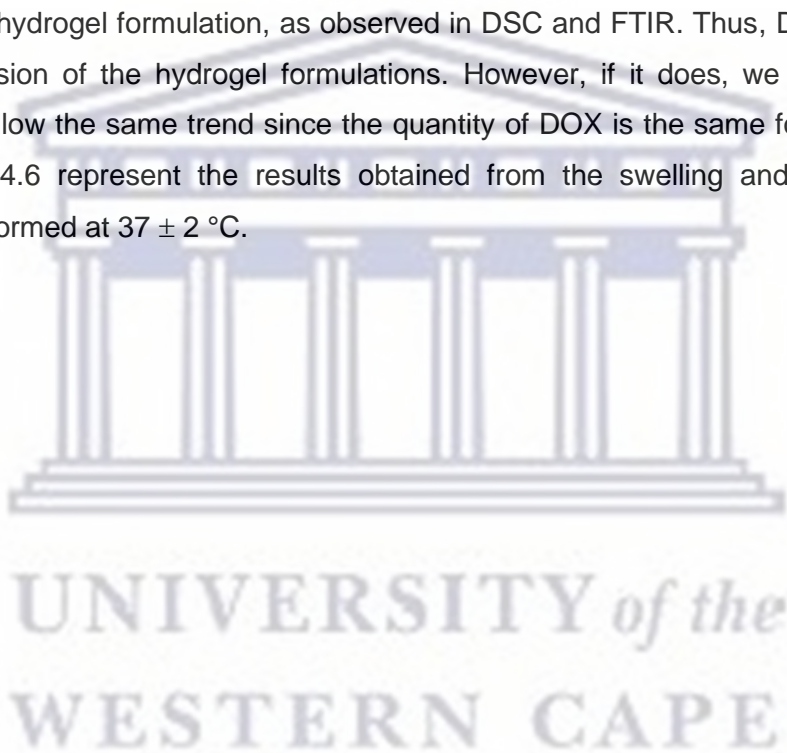


Table 4.5: Swelling of hydrogels 1-9 after 72 hrs at  $37 \pm 2^\circ\text{C}$ 

| Sample no. | Average initial mass of hydrogels (g) (n=3) | Average final mass gain after 72 hrs | Average % mass gain after 72 hrs (%) |
|------------|---|--------------------------------------|--------------------------------------|
| 1          | 0.1003<br>$\pm 0.0000$                      | N/A                                  | N/A                                  |
| 2          | 0.1002<br>$\pm 0.0000$                      | N/A                                  | N/A                                  |
| 3          | 0.1001<br>$\pm 0.0001$                      | 0.1445<br>$\pm 0.0062$               | 44.5000<br>$\pm 6.2110$              |
| 4          | 0.1003<br>$\pm 0.0001$                      | N/A                                  | N/A                                  |
| 5          | 0.1003<br>$\pm 0.0001$                      | N/A                                  | N/A                                  |
| 6          | 0.1002<br>$\pm 0.0001$                      | 0.1359<br>$\pm 0.0042$               | 35.9162<br>$\pm 4.1515$              |
| 7          | 0.1002<br>$\pm 0.0002$                      | N/A                                  | N/A                                  |
| 8          | 0.1002<br>$\pm 0.0002$                      | 0.1286<br>$\pm 0.0050$               | 28.5572<br>$\pm 5.0051$              |
| 9          | 0.1004<br>$\pm 0.0001$                      | 0.1276<br>$\pm 0.0060$               | 27.6218<br>$\pm 6.0030$              |

Many studies claim that swelling is the most important characteristic of hydrogels (Rufato *et al.*, 2018; Zhang, Feng, and Jin, 2020). It is generally accepted that a high crosslinking density of polymers leads to lower swelling and a low crosslinking density leads to higher swelling (Hafeez *et al.*, 2018). This is reasonable since, for higher crosslinking density, the internal crosslinking points of the hydrogel networks are reduced, restricting their ability to absorb moisture. Contrary to many studies, a high crosslinking density of CH and *k*CRG of the thermoresponsive hydrogels resulted in a high swelling capacity. More specifically, an increase in the

concentration of CH and *k*CRG led to an increase in the swelling ratio, but as the concentration of LIM increased, the swelling percentage decreased. This was easily identifiable as the lyophilised samples with lower crosslinking polymer density/ elasticity and rigidity (samples 1, 2, 4, 5 and 7) dissolved in the PBS solution, meaning that although crosslinking density may be significant, the strength of these linkages to hold the hydrophilic media was not sufficient. It is also important to recall that CH and *k*CRG undergo protonation at lower pH, which strengthens their electrostatic interaction, but the PBS was prepared to mimic the tumour environment of pH 6.8. The high pH may have contributed to weakening the strength of the intermolecular forces between these polymers, which further affected their ability to sustain maximum swelling. A similar effect was observed by Ahmad *et al.*, 2019, who crosslinked CH with PNIPAM. Their study continued to compare the swelling of the hydrogels at low and high pH, and they concluded that deprotonation of the amino group occurred at high pH, which reduced the swelling ratio of the hydrogel (Ahmad *et al.*, 2019). A study completed by Varshosaz *et al.*, 2021 also supports the notion that increasing the crosslinking density of polymers leads to increased swelling. Nonetheless, the decreased swelling observed with the increased concentration of LIM can be related to its hydrophobicity, which further decreases PBS absorption.

The observed differences in swelling behaviour may also affect deformability of the thermoresponsive hydrogels. For formulations which swelled (sample 3, 6, 8 and 9), the hydrogel may expand into neighbouring tissue, compromising DOX targeting; although this largely depends on the quantity of drug-hydrogel volume that will be administered and the tumour size – factors to be further evaluated after quantifying drug loading. Additionally, the increased swelling could lead to superficial exposure of the drug-hydrogel system, which in the case of OSCC may be transferred to the oral cavity where the patient may swallow or discard the drug, even though this will depend on the location of the tumour. With these considerations, non-swelling could serve as a preference for injectable hydrogels. Therefore, both non-swollen and swollen hydrogels were analysed for erosion. In their review, Zhan *et al.*, 2021 discussed the incompatibility of hydrogel swelling in several biomedical applications. Though injectable hydrogels did not form part of their discussion, their findings on the non-swelling of double network structures and multiple crosslinked polymers emphasise that low/no swelling of hydrogels is possible and acceptable depending on the required application and properties, such as mechanical strength and elasticity.



Table 4.6: Erosion of hydrogel samples 1-9 for 5 weeks at 37 °C

| Sample no. | Average initial mass of hydrogels (g) (n=3) | Average mass loss after 1 week (%) | Average mass loss after 2 weeks (%) | Average mass loss after 3 weeks (%) | Average mass loss after 4 weeks (%) | Average mass loss after 5 weeks (%) |
|------------|---|------------------------------------|-------------------------------------|-------------------------------------|-------------------------------------|-------------------------------------|
| 1          | 1.080<br>± 0.033                            | N/A                                | N/A                                 | N/A                                 | N/A                                 | N/A                                 |
| 2          | 0.966<br>± 0.053                            | 17.242<br>± 5.048                  | 43.320<br>± 4.285                   | N/A                                 | N/A                                 | N/A                                 |
| 3          | 0.997<br>± 0.026                            | 2.261<br>± 1.799                   | 18.269<br>± 4.042                   | 50.500<br>± 7.231                   | 60.497<br>± 2.790                   | 87.070<br>± 3.120                   |
| 4          | 0.968<br>± 0.058                            | N/A                                | N/A                                 | N/A                                 | N/A                                 | N/A                                 |
| 5          | 1.030<br>± 0.008                            | 23.049<br>± 1.262                  | 68.574<br>± 2.132                   | N/A                                 | N/A                                 | N/A                                 |
| 6          | 1.018<br>± 0.075                            | 7.3250<br>± 4.155                  | 59.678<br>± 6.750                   | 68.097<br>± 6.216                   | 73.280<br>± 1.489                   | 78.720<br>± 4.010                   |
| 7          | 0.964<br>± 0.128                            | 49.125<br>± 4.001                  | N/A                                 | N/A                                 | N/A                                 | N/A                                 |
| 8          | 0.979<br>± 0.031                            | 15.253<br>± 2.005                  | 48.521<br>± 4.004                   | 68.932<br>± 5.211                   | 77.995<br>± 2.043                   | 88.880<br>± 0.810                   |
| 9          | 0.950<br>± 0.114                            | 14.239<br>± 3.703                  | 47.224<br>± 5.001                   | 67.326<br>± 3.174                   | 73.363<br>± 2.999                   | 79.280<br>± 1.360                   |

Formulations with increased swelling (sample 3, 6, 8 and 9) demonstrated increased erosion. As the water penetration increased, the hydrogel network became weaker and therefore eroded more. Additionally, the erosion results show a parallel relationship to mechanical strength. The samples which demonstrated poor mechanical strength (samples 1, 4, and 7) were unable to maintain their structure within the first week and became completely dissolved in the PBS. Figure 4.14 illustrates the destruction of the hydrogel system after 1 week. The destruction of the hydrogel network paved an opportunity for elimination of the samples from the study as they would lead to poor DOX release. Samples 2 and 5 (higher concentrations of CH) had an initial erosion of 17.242 % and 23.049 %, followed by 43.320 % and 68.574 %, respectively, after 2 weeks. By the third week, the hydrogels de-structured and were therefore eliminated from the study. Samples 3, 6, and 9, which showed high rigidity because of their enhanced *kCRG* concentration, were very slow to erode during the first week, demonstrating a mass loss of 2.261 %, 7.325 %, and 15.253 %. The increase in mass loss with the increasing LIM concentration corresponds with TGA results wherein LIM mass loss is already evident at 37 °C (see Figure 4.8). Sample 8 also showed initial rapid degradation of 15.253 %, which is similar to that of sample 9 (14.253 %) because of the equal amount of LIM. Despite the low concentration of *kCRG* in sample 8, the high CH concentration, which drastically enhanced the shear storage modulus to 2300 Pa, was able to maintain the hydrogel structure with minor initial mass loss. By week 5, samples 3, 6, 8 and 9 were able to erode up to 72-88 % of their initial mass (see Figure 4.15). The samples were fragmented into tiny pieces and could not be weighed by the sixth week. Rasool and colleagues (2019) also identified fragmentation during drug release experiments of *kCRG* and poly(vinyl alcohol) (PVA). Notably, the erosion rapidly increased by the second week compared to weeks 3, 4 and 5. A probable reason is that the surface area of the hydrogel that was exposed for degradation in the initial weeks was larger and as time progressed and the hydrogel decreased in size, the exposed area became smaller, and therefore, a smaller mass loss was observed. Ultimately, samples 3, 6, 8, and 9 showed better erosion capacity for potential long-term drug release. However, because only sample 3 and 8 showed the maximum degradation over 5 weeks (87.070 % and 88.880 %, respectively), they were, therefore, maintained in the study. Erosion studies also proved a fundamental aspect of the effect of the high pH of PBS on the gelled hydrogels. The solid gels maintained their initial structure when immersed in PBS, unlike the lumping observed when the gels are in liquid state and adjusted with NaOH to 6.8. Perhaps, a higher pH of the gelled system would affect erosion, but like in the case of swelling, that exploration would be beyond the scope of this study.

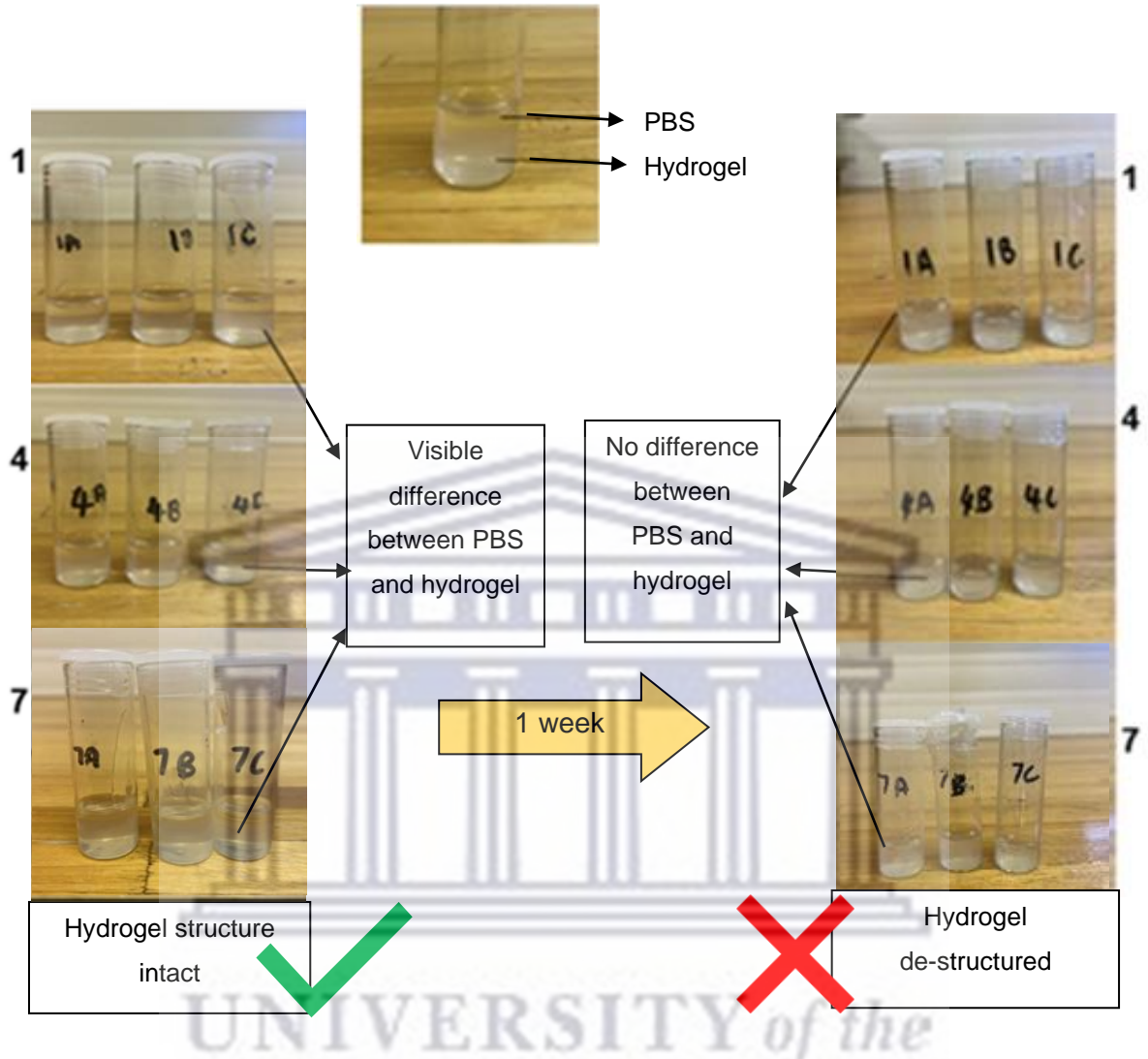


Figure 4.14: Hydrogel samples 1, 4 and 7 immersed in PBS after 1 week of erosion studies. Hydrogel de-structured: no difference between PBS and gel.

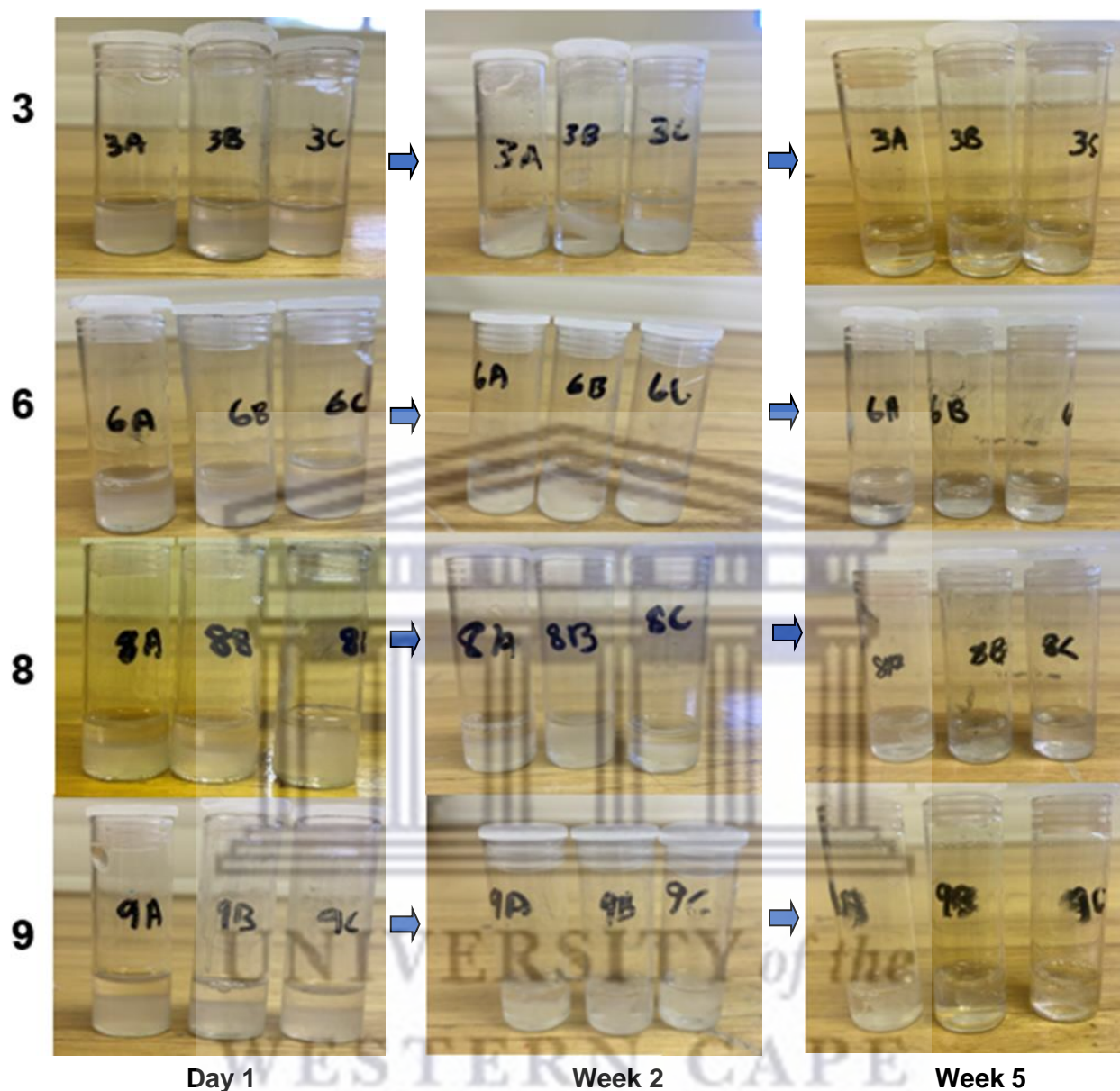


Figure 4.15: Hydrogel samples 3, 6, 8 and 9 after 2 and 5 weeks, respectively, after erosion.

#### 4.9 Evaluation of drug loading efficiency

Despite its potency in cancer treatments such as OSCC, DOX is amongst the poorly soluble chemotherapeutics (Soltantabar *et al.*, 2020). This drawback makes it a target for drug-loading improvements. Although it would be an added advantage, this study did not aim to improve the drug-loading capacity of DOX, therefore, the hydrochloride salt form was used. The salt form of DOX has shown increased solubility of 50 mg/mL (D' Angelo *et al.*, 2022), however, only

5 mg/mL of DOX was loaded into the hydrogel system due to the limited quantity available for this study. HPLC was then used to detect whether the drug was successfully loaded in samples 3 and 8. HPLC analysis was essential in identifying the hydrogel system's ability to load the drug as well as quantifying a potential dosage range expected with this loading concentration. Table 4.7 shows the concentration of DOX available in the hydrogel samples as quantified through HPLC analysis. The regression curve used for the calculation of the DOX concentration is plotted in Figure 4.16.

Table 4.7: Concentration of DOX in hydrogel

| Sample no. | Concentration of DOX (mg/mL) |
|------------|------------------------------|
| 3          | 5.035                        |
| 6          | 4.864                        |
| 8          | 4.947                        |
| 9          | 4.914                        |

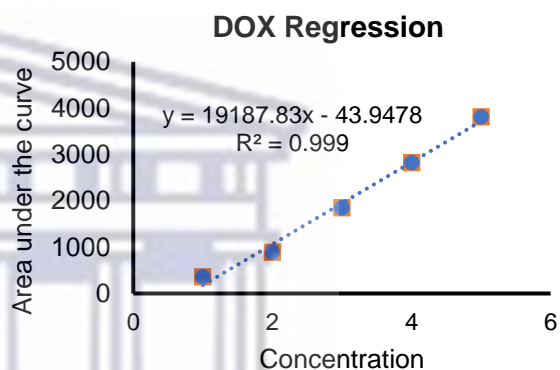


Figure 4.16: DOX regression curve obtained from HPLC data

The DOX concentrations loaded into the hydrogel formulations averaged at 5 mg/mL. This was noted to be close to 100 % of the actual weighed and added DOX concentration, thus showing that the hydrogel formulation process results in excellent drug incorporation. The use of PF-127 as the thermosensitive polymer of choice is a suitable candidate for the DOX drug loading. As detailed in Chapter 2, section 2.5.3.1.4, hydrophilic drugs tend to show good solubility and encapsulation capacity in polymer blocks with hydrophilic ends. PF-127 is a triblock copolymer with one hydrophobic moiety and two hydrophilic ends, and DOX is also a hydrophilic drug. This similarity increases the capacity for hydrophilic DOX attachment to the hydrophilic ends of PF-127 (Figure 4.17). Therefore, there is a possibility of loading a significantly higher concentration of DOX into the hydrogel system.

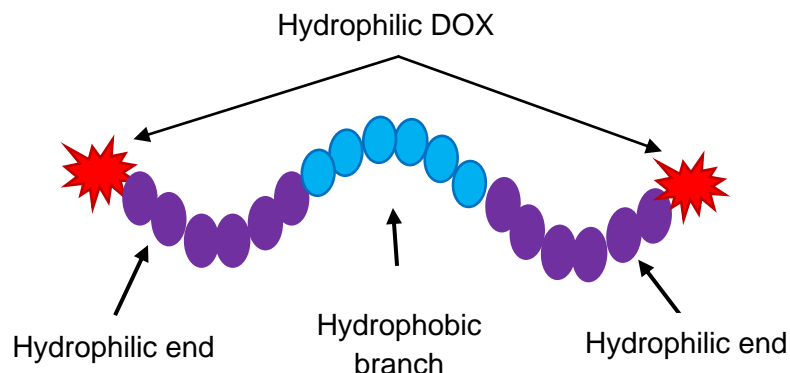


Figure 4.17: Schematic depicting PF-127 triblock copolymer with 2 hydrophilic ends and hydrophilic DOX binding to the hydrophilic end of the triblock.

On the other hand, the small quantity of drug loaded in this study could compromise the dosing requirement of DOX. Oral tumours are  $\leq 2$  cm in size with a depth of invasion of 10 mm for stage 1-2 cancers (Anderson, Sisson, and Moncrieff, 2015). The low concentration of loaded DOX could prove challenging for administration to these early-stage tumours. According to the Food and Drug Administration (FDA), the recommended dose for DOX varies between 40-90 mg/m<sup>2</sup> every 21-28 days, depending on factors such as age, stage, and drug combination (Food and Drug Administration, 2023). Table 4.8 details the expected volume of the thermosensitive hydrogel when 5 mg/mL of DOX is loaded. According to Table 4.8, a patient would need to inject a minimum of 8 mL and a maximum of 18 mL of the thermoresponsive hydrogel at 5.00 mg/mL, which will accumulate beyond the tumour alone and into neighbouring tissue, further compromising the aim for targeted therapy. The injection of a large volume of viscous liquid into a small area could also be a painful experience for the patient. Therefore, higher concentration of DOX should be explored in further studies.

Table 4.8: Thermosensitive hydrogel volume required with 5 mg/mL DOX.

| DOX dose (mg/m <sup>2</sup> ) | Thermosensitive hydrogel volume (mL) |
|-------------------------------|--------------------------------------|
| 40                            | 8                                    |
| 60                            | 12                                   |
| 75                            | 15                                   |
| 90                            | 18                                   |

\*Hydrogel volume = DOX dose/ concentration of DOX in hydrogel formulation

#### 4.10 Drug diffusional release studies

Drug release studies were completed over 7 days using a Franz cell diffusion apparatus to ensure efficient drug release from the hydrogel matrix and through the synthetic membrane at 37 °C. The donor compartment was loaded with 2 mg of DOX (0.4 mL hydrogel volume). Figure 4.18 shows the concentration of drug released over 7 days for sample 3 and 8, including a blank. The rate of drug release, represented by the slope of the graph, was calculated according to USP, 2014.

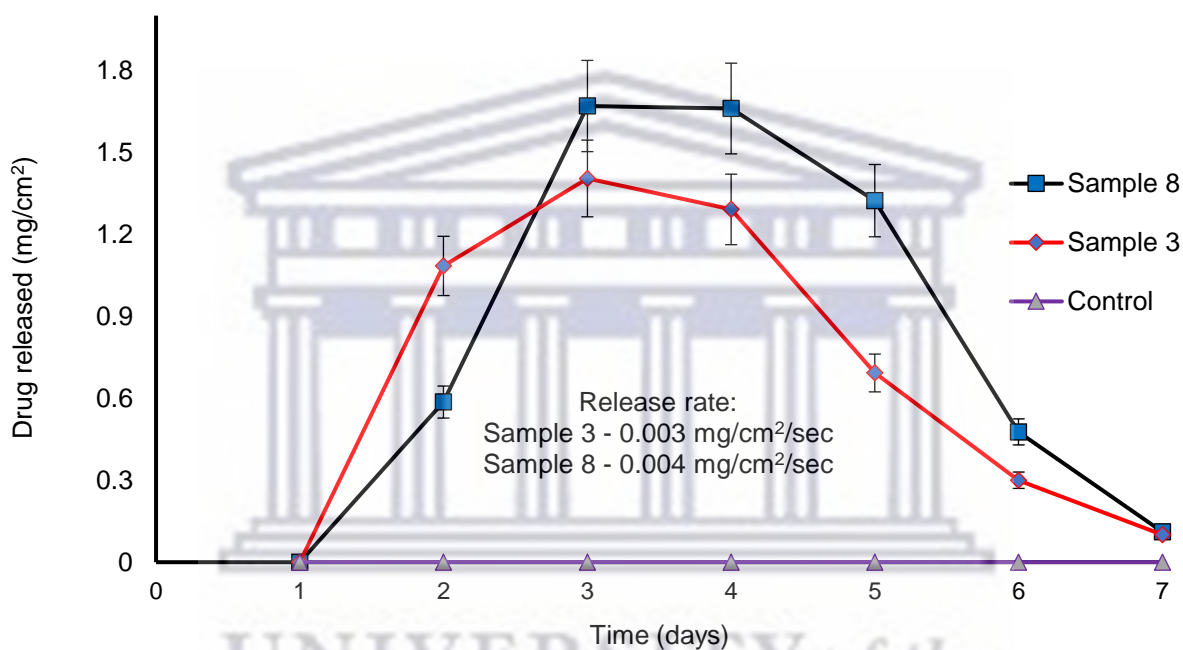


Figure 4.18: DOX release profile of samples 3 and 8, at 37 °C, over 7 days.

No DOX was detected in the receiver compartment of the diffusion cell for samples 3 and 8 within the first 24 hrs. The initial delayed release could stem from the high stiffness of the hydrogels (0.053 N and 0.047 N for samples 3 and 8, respectively, as obtained in compression analysis), which kept the system intact for a long time, causing the hindrance of DOX release. The delayed release may not be favourable for OSCC patients as immediate treatment is usually necessary, however the physician would need to consider the stage of cancer and whether a 24-hour delay of drug release will negatively impact the patient. It is also important to note that the cellulose membrane does not accurately mimic the tumour as described in Chapter 2, it was emphasised that tumours are made of complex porous tissue, with high interstitial

pressure, which may likely assist in the physical breakdown of the hydrogel, thus facilitating drug release *in vivo*. Therefore, *in vivo*, DOX release from the hydrogel may be quicker than the result provided herein.

The extended exposure of the samples to the release media contributed to softening of the hydrogel network, and therefore fostering DOX release of  $0.586 \pm 0.052$  mg/cm<sup>2</sup> and  $1.084 \pm 0.080$  mg/cm<sup>2</sup> for samples 3 and 8 respectively by the 2<sup>nd</sup> day. The release on day 2 indicated the common phenomenon of “burst release” associated with stimuli-responsive hydrogel formulations. García-Couce *et al.*, 2022, explained that burst release is likely to occur because the drug closer to the surface of the membrane can escape more easily into the diffusion media due to the rapid interaction and hydration of the hydrogel front with the diffusion media. The difference in the burst release of the samples can be attributed to the high swelling observed within 72 hrs in sample 3 (44.500 %) compared to that of sample 8 (28.557 %). The high swelling in sample 3 resulted in rapid hydration of the hydrogel front and subsequent release of drug molecules at the surface of the hydrogel. The release of DOX was associated with a visible colour change of the diffusion medium for both samples.

Further softening of the polymer network caused an increase in the release concentration for both samples on the 3<sup>rd</sup> day. This can be indicated by the increase in swelling and erosion of the hydrogels. Sample 8 released the maximum drug concentration of  $1.669 \pm 0.062$  mg/mL (85 %) and sample 3 released  $1.404 \pm 0.070$  mg/mL (70 %) of the drug. The slope of the graphs specifies the release rate of 0.003 mg/cm<sup>2</sup>/sec and 0.004 mg/cm<sup>2</sup>/sec for samples 3 and 8, respectively. From these studies, it appears that DOX release is dependent on the erosion of the hydrogel rather than swelling, because sample 3 underwent more swelling (44.500 %) compared to sample 8 (28.557 %) within 3 days but released less drug than sample 8. Whereas sample 8 eroded (15.235 %) more than sample 3 (2.262 %) within the first week and further released more DOX.

The slower release rate of sample 3 could also stem from the strong electrostatic interaction between the NH<sub>3</sub><sup>+</sup> of CH and OSO<sub>3</sub><sup>-</sup> of *k*CRG, which kept the drug entrapped in the hydrogel network. The preliminary studies wherein the two polymers were mixed revealed the strength of the polymer complexation (refer to Figure 4.3). FTIR results also confirmed the strength of this interaction with increasing intensity between 3300-3700 cm<sup>-1</sup>. The lower drug release of sample 3 could be due to the high crosslinking between the CH and *k*CRG polymers wherein equal concentrations of CH could interact with equal concentrations of *k*CRG (0.3 CH: 0.3 *k*CRG), to form a strong complexation. In sample 8, the concentration of CH and *k*CRG varied (0.3 CH: 0.1



*k*CRG), therefore the entanglement between these polymers may have been slightly reduced, with less DOX entrapped within the polymer network, and therefore, more drug being released (see Figure 4.19). Liu and colleagues also reported lower release for stronger polyelectrolyte complexations between alginate-g-poly(N-isopropyl acrylamide) and CH (Liu *et al.*, 2022).

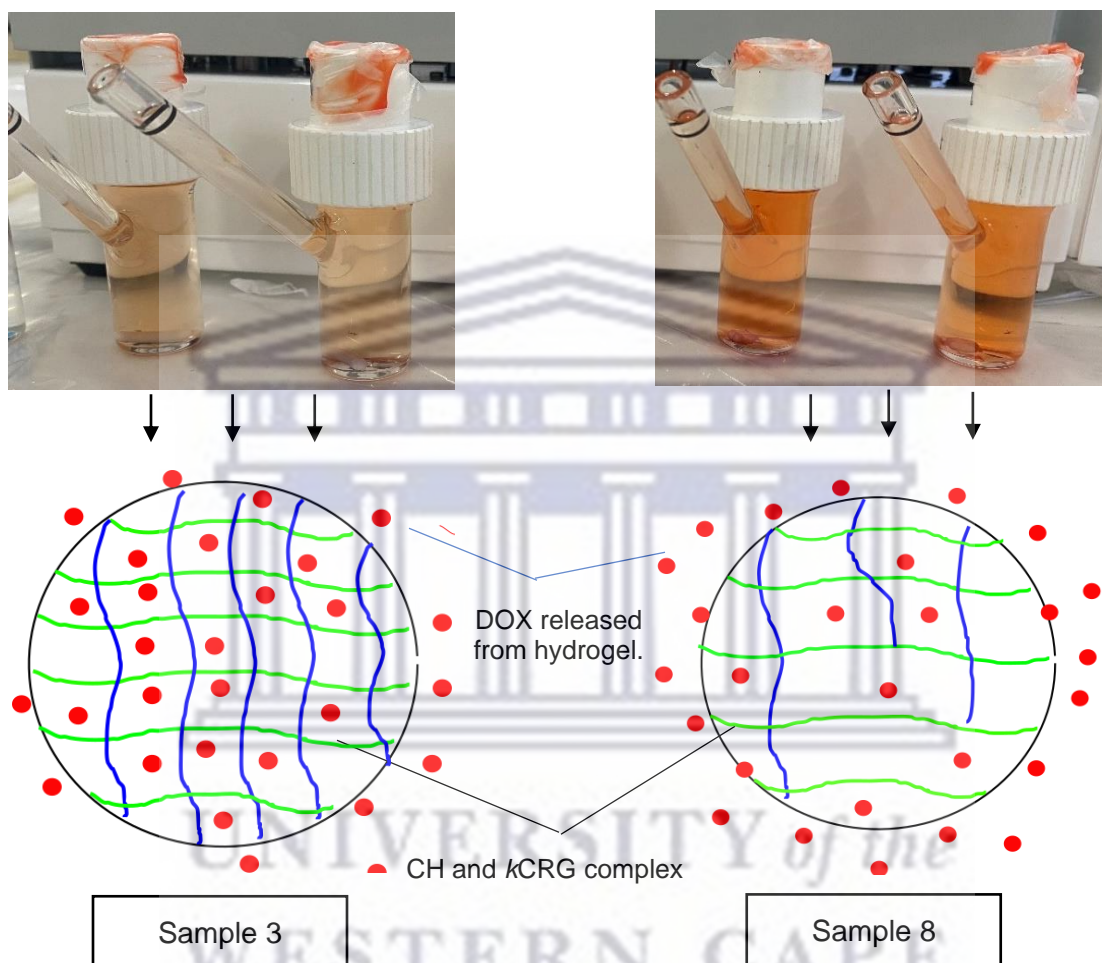


Figure 4.19: Schematic of drug release from hydrogel matrix. Sample 3 – 1 CH: 1 *k*CRG, with higher drug entrapment capacity and less drug release. Sample 8 – 3 CH: 1 *k*CRG, with lower drug entrapment capacity and more drug released.

It is also likely that the increased concentration of LIM in sample 8 assisted in the release of DOX from the hydrogel matrix. The high lipophilicity of LIM could have improved the diffusion of DOX through the cellulose membrane. To the best of our knowledge, studies regarding the effect of LIM on drug release rates are lacking. Samples 3 and 8 both maintained their maximum released concentration between day 3 and 4 of the release study, which suggests a

controlled release of the drug. However, DOX concentration decreased thereafter because all the sample in the donor compartment were depleted by the 5<sup>th</sup> day. It is important to note that the drug release curve is dependent on several factors including the amount of sample available for the test and thus, the seemingly short period of drug release is congruent with the small sample quantity in the donor compartment. The quick release of the samples compared to their long erosion time indicates that DOX will release to its maximum capacity before the hydrogel fully degrades. Overall, samples 3 and 8 demonstrated a delayed and extended-release behaviour of the hydrogel system. Chung and colleagues also designed thermosensitive PF-127 (25 %) hydrogel for DOX release (Chung *et al.*, 2020). The researchers obtained a similar release behaviour of up to 5 days and a release of 50 % DOX within 24 hrs (Chung *et al.*, 2020). A comparison of this study to their results reveals that the crosslinking of PF-127 with CH, kCRG and LIM, has had an effect in delaying the release of DOX.

#### 4.11 Permeability

The PAMPA kit was used to analyse the effect of LIM on the permeation rate of DOX through biological membranes facilitated by the hydrogel drug delivery system. PAMPA does not accurately mimic OSCC tumours because it lacks pores and active transport mechanisms, however, it can provide insight on the trend of drug permeation through passive diffusion. DOX must travel through the avascular tumour tissue, deep into the hypoxic areas and directly into the neoplasm of the oral squamous cell to effectuate complete tumour cytotoxicity. However, the drug's BCS III classification compromises this possibility. Several studies have reported the cytotoxic and hydrophobic properties of LIM which can facilitate transdermal permeation and cytotoxicity of tumour cells (Campos *et al.*, 2022; Shah *et al.*, 2019; Lu *et al.*, 2014). Therefore, it was fitting to investigate the potential effect of lipophilic LIM within the hydrogel system. Drug permeation from DOX-loaded hydrogel formulations (sample 3 and 8) with and without LIM were compared to the permeation of DOX from a PBS solution of pH 6.8 (control) as depicted in Figure 4.20.

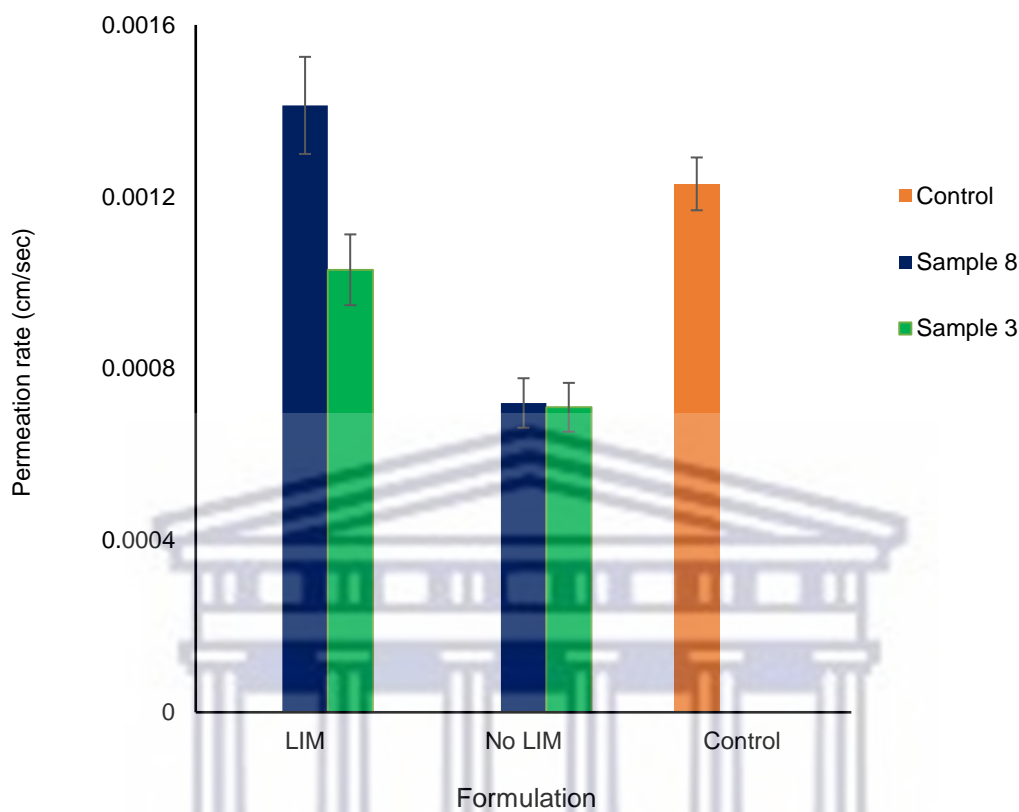


Figure 4.20: DOX permeability rate of hydrogel samples 3 and 8 for PAMPA analysis.

Literature dictates that DOX exhibits high solubility and low permeability (Kim *et al.*, 2021). Upon comparison of DOX control to the hydrogel formulations with or without LIM, it is evident that the permeation rate decreased when drug is entrapped within the hydrogel. One study designed tretinoin as a liquid and semi-solid hydrogel formulation to reduce its skin permeability through nanoencapsulation (Ourique *et al.*, 2011). Although their focus was on the effect of nanoencapsulation, a closer look at their results reveals that the permeation rate of tretinoin decreased in the Carbopol<sup>®</sup>-based hydrogel formulation as compared to the liquid formulation. The reason for this observation is unclear, especially because many researchers report increasing drug permeability with the formulation of hydrogels (Fernández-Romero *et al.*, 2020; Wu *et al.*, 2022). However, it can be hypothesised that in comparison with a liquid formulation drug permeation from a hydrogel formulation not only relies on drug diffusion but also on the erosion behaviour, mechanical integrity thereof and the ability of the hydrogel to carry the drug to and through the molecular membranes. Despite this result, the aim to improve DOX targeting

and reduce its associated side effects, are crucial factors which cannot dismiss the need for a thermosensitive hydrogel design.

When comparing the formulations (samples 3 and 8), to their controls, it is apparent that LIM increased the permeation rate of DOX in these hydrogels. Sample 3 showed a permeation rate of  $1.032 \times 10^{-3}$  cm/sec, which is a third increment higher compared to its “no LIM” control. For sample 8, the formulation showed a 100 % increase in the permeation rate of DOX in the hydrogel –  $1.413 \times 10^{-3}$  cm/sec, showing an increased permeation rate even in comparison with the DOX control. Although LIM increased the permeation of DOX in the hydrogel formulations, the degree of permeation seems to be controlled by the concentration of LIM within the hydrogel samples. Sample 8 had a higher concentration of LIM (0.5 %v/v) and thus could permeate more extensively than sample 3, which had only 0.1 %v/v LIM. This improvement is substantial in increasing the delivery of DOX in OSCC, especially since only 20 % of a conventional DOX dose reaches tumour cells (Greene *et al.*, 1983). In most research where significant permeation was observed in transdermal studies, LIM concentrations remained between 5-12 % (Lu *et al.*, 2014; Yang *et al.*, 2013). For example, Yang *et al.*, 2013, reported a 22-fold increase of bufalin in rat skin when 10 %v/v LIM was used with a Carbopol® gel for the design of a transdermal patch. Another study compared the effect of increasing LIM concentration for the delivery of transdermal testosterone (Charoensumran *et al.*, 2020). The investigators reported a significant permeability increase when LIM was increased up to 10 %v/v (Charoensumran *et al.*, 2020). In this study, however, increasing the LIM concentration would compromise the hydrogel's thermosensitivity, as observed from the trial formulations. Further studies would therefore need to modify the system to ensure that higher concentrations of LIM is loaded (> 0.5 %) and the thermosensitive property of the hydrogel is maintained while allowing maximum permeability.

Furthermore, in their review, Hmingthansanga *et al.*, 2022, reported that the non-polar group containing terpenes such as LIM seemed to enhance permeation more rapidly in hydrophobic drugs than hydrophilic drugs. This phenomenon would explain the low increase in the permeation rates of the hydrogels when compared to the DOX control. Consequently, hydrophobic chemotherapeutic drugs may show more statistically significant permeability increase in the thermosensitive hydrogels and should therefore be explored.

#### 4.12 Conclusion

Nine PF-127-based thermoresponsive hydrogel samples containing varying concentrations of CH/*k*CRG and LIM were successfully designed. FTIR analysis confirmed the crosslinking of the polymers. Despite similar molecular profiles according to FTIR, the hydrogel samples displayed different physicochemical behaviours based on the concentration of the materials. The tube inversion method and rheological studies revealed that the sol-gel transition of the hydrogel samples occurred at temperatures below 37 °C and a gelling time between 1-3 min. The viscoelastic nature of the system was proven by the high values of  $G'$  when compared to  $G''$  for all sample ratios after reaching the LCST. CH and *k*CRG played a pivotal role in enhancing the elasticity and rigidity of the hydrogels, respectively. However, the enhanced strength decreased the LCST of the hydrogel formulations. The samples with greater elasticity and rigidity showed enhanced swelling and erosion capacity of the hydrogels. The most optimal samples based on physical characterisation were samples 3, and 8 because they possessed favourable properties for injectable hydrogel manufacture and use, such as high mechanical strength, reasonable gelation times, a slow degradation rate and 100 % drug incorporation. Samples 3 and 8 also demonstrated delayed release of 24 hours due to the high crosslinking of the CH and *k*CRG polymers. Sample 8 could release up to 85 % of DOX within 3 days and a comparison between the release of samples 3 and 8, revealed that the hydrogel system underwent an erosion-mediated diffusion behaviour. Ultimately, the most optimal formulation was sample 8 as it showed higher permeation of DOX after PAMPA assay. LIM favourably enhanced the permeation rate of DOX and has potential to enhance the drug's transport to OSCC cells. The system holds promise for cytotoxic synergic activity between DOX and LIM.

#### 4.13 References

- Ahmad, U., Sohail, M., Ahmad, M., Minhas, M.U., Khan, S., Hussain, Z., Kousar, M., Mohsin, S., Abbasi, M., Shah, S.A. and Rashid, H. 2019. Chitosan based thermosensitive injectable hydrogels for controlled delivery of loxoprofen: development, characterization and in-vivo evaluation. *International Journal of Biological Macromolecules*, 129, pp.233-245.
- Anderson, C.R., Sisson, K. and Moncrieff, M. 2015. A meta-analysis of margin size and local recurrence in oral squamous cell carcinoma. *Oral Oncology*, 51(5), pp.464-469.
- Ashrafizadeh, M., Hushmandi, K., Mirzaei, S., Bokaie, S., Bigham, A., Makvandi, P., Rabiee, N., Thakur, V.K., Kumar, A.P., Sharifi, E. and Varma, R.S. 2022. Chitosan-based nanoscale systems for doxorubicin delivery: Exploring biomedical application in cancer therapy. *Bioengineering & Translational Medicine*, Article ID: e10325.
- Baratpour, M., Karimipour, A., Afrand, M. and Wongwises, S. 2016. Effects of temperature and concentration on the viscosity of nanofluids made of single-wall carbon nanotubes in ethylene glycol. *International Communications in Heat and Mass Transfer*, 74, pp.108-113.
- Campos, E.V., Proença, P.L., da Costa, T.G., de Lima, R., Fraceto, L.F. and de Araujo, D.R. 2022. Using Chitosan-Coated Polymeric Nanoparticles-Thermosensitive Hydrogels in association with Limonene as Skin Drug Delivery Strategy. *BioMed Research International*, 2022. Article ID: 9165443
- Chung, C.K., García-Couce, J., Campos, Y., Kralisch, D., Bierau, K., Chan, A., Ossendorp, F. and Cruz, L.J. 2020. Doxorubicin loaded poloxamer thermosensitive hydrogels: chemical, pharmacological and biological evaluation. *Molecules*, 25(9), Article ID: 10.3390/molecules25092219.
- Charoensumran, P. and Ajiro, H. 2020. Controlled release of testosterone by polymer-polymer interaction enriched organogel as a novel transdermal drug delivery system: Effect of limonene/PG and carbon-chain length on drug permeability. *Reactive and Functional Polymers*, 148, p.104461.
- D'Angelo, N.A., Noronha, M.A., Câmara, M.C., Kurnik, I.S., Feng, C., Araujo, V.H., Santos, J.H., Feitosa, V., Molino, J.V., Rangel-Yagui, C.O. and Chorilli, M. 2022. Doxorubicin nanoformulations on therapy against cancer: An overview from the last 10 years. *Biomaterials Advances*, 133, p.112623.

da Silva, J.B., Dos Santos, R.S., da Silva, M.B., Braga, G., Cook, M.T. and Bruschi, M.L. 2021. Interaction between mucoadhesive cellulose derivatives and Pluronic F127: Investigation on the micelle structure and mucoadhesive performance. *Materials Science and Engineering: C*, 119, p.111643.

Derkach, S.R., Ilyin, S.O., Maklakova, A.A., Kulichikhin, V.G. and Malkin, A.Y. 2015. The rheology of gelatin hydrogels modified by  $\kappa$ -carrageenan. *LWT-Food Science and Technology*, 63(1), pp.612-619.

Di Maro, M., Faga, M.G., Malucelli, G., Mussano, F.D., Genova, T., Morsi, R.E., Hamdy, A. and Duraccio, D. 2020. Influence of chitosan on the mechanical and biological properties of HDPE for biomedical applications. *Polymer Testing*, 91, Article ID: 106610.

Fernández-Romero, A.M., Maestrelli, F., García-Gil, S., Talero, E., Mura, P., Rabasco, A.M. and González-Rodríguez, M.L., 2021. Preparation, Characterization and Evaluation of the Anti-Inflammatory Activity of Epichlorohydrin- $\beta$ -Cyclodextrin/Curcumin Binary Systems Embedded in a Pluronic®/Hyaluronate Hydrogel. *International Journal of Molecular Sciences*, 22(24), p.13566.

Food and Drug Administration. 2023. Doxorubicin Hydrochloride for Injection for intravenous use. Available at [https://www.accessdata.fda.gov/drugsatfda\\_docs/label/2020/050467s078,050629s030lbl.pdf](https://www.accessdata.fda.gov/drugsatfda_docs/label/2020/050467s078,050629s030lbl.pdf) (Accessed: 30/01/2023)

García-Couce, J., Tomás, M., Fuentes, G., Que, I., Almirall, A. and Cruz, L.J. 2022. Chitosan/Pluronic F127 thermosensitive hydrogel as an injectable dexamethasone delivery carrier. *Gels*, 8(1), p.44.

Greene, R.F., Collins, J.M., Jenkins, J.F., Speyer, J.L. and Myers, C.E. 1983. Plasma pharmacokinetics of adriamycin and adriamycinol: implications for the design of in vitro experiments and treatment protocols. *Cancer research*, 43(7), pp.3417-3421.

Hafeez, S., Islam, A., Gull, N., Ali, A., Khan, S.M., Zia, S., Anwar, K., Khan, S.U. and Jamil, T. 2018.  $\gamma$ -Irradiated chitosan based injectable hydrogels for controlled release of drug (Montelukast sodium). *International Journal of Biological Macromolecules*, 114, pp.890-897.

Hmingthansanga, V., Singh, N., Banerjee, S., Manickam, S., Velayutham, R. and Natesan, S. 2022. Improved Topical Drug Delivery: Role of Permeation Enhancers and Advanced Approaches. *Pharmaceutics*, 14(12), p.2818.

Kalaria, D.R., Sharma, G., Beniwal, V. and Ravi Kumar, M.N.V. 2009. Design of biodegradable nanoparticles for oral delivery of doxorubicin: in vivo pharmacokinetics and toxicity studies in rats. *Pharmaceutical Research*, 26, pp.492-501.

Kim, M.K., Ki, D.H., Na, Y.G., Lee, H.S., Baek, J.S., Lee, J.Y., Lee, H.K. and Cho, C.W. 2021. Optimization of mesoporous silica nanoparticles through statistical design of experiment and the application for the anticancer drug. *Pharmaceutics*, 13(2), p.184.

Jaafar, A.M. and Thatchinamoorthi, V. 2018. Preparation and Characterisation of Gellan Gum Hydrogel containing Curcumin and Limonene. *IOP Conference Series: Materials Science and Engineering*, 440, Article ID: 012023.

Jain, R.K., Martin, J.D. and Stylianopoulos, T. 2014. The role of mechanical forces in tumor growth and therapy. *Annual Review of Biomedical Engineering*, 16, p.321-346.

Lim, H.P., Ooi, C.W., Tey, B.T. and Chan, E.S. 2017. Controlled delivery of oral insulin aspart using pH-responsive alginate/k-carrageenan composite hydrogel beads. *Reactive and Functional Polymers*, 120, pp.20-29.

Liu, M., Zhu, J., Song, X., Wen, Y. and Li, J. 2022. Smart Hydrogel Formed by Alginate-g-Poly (N-isopropylacrylamide) and Chitosan through Polyelectrolyte Complexation and Its Controlled Release Properties. *Gels*, 8(7), p.441.

Lu, W.C., Chiang, B.H., Huang, D.W. and Li, P.H. 2014. Skin permeation of d-limonene-based nanoemulsions as a transdermal carrier prepared by ultrasonic emulsification. *Ultrasonics sonochemistry*, 21(2), pp.826-832.

Mazza, E., Papes, O., Rubin, M.B., Bodner, S.R. and Binur, N.S. 2005. Nonlinear elastic-viscoplastic constitutive equations for aging facial tissues. *Biomechanics and Modeling in Mechanobiology*, 4(2), pp.178-189.

Mredha, M.T.I., Pathak, S.K., Cui, J. and Jeon, I. 2019. Hydrogels with superior mechanical properties from the synergistic effect in hydrophobic–hydrophilic copolymers. *Chemical Engineering Journal*, 362, pp.325-338.

Moura, M.J., Figueiredo, M.M. and Gil, M.H. 2008. Rheology of chitosan and genipin solutions. In *Materials Science Forum*, 587, pp. 27-31. Trans Tech Publications Ltd.

Obireddy, S.R. and Lai, W.F. 2022. ROS-generating amine-functionalized magnetic nanoparticles coupled with carboxymethyl chitosan for pH-responsive release of doxorubicin. *International Journal of Nanomedicine*, pp.589-601.



Ourique, A.F., Melero, A., da Silva, C.D.B., Schaefer, U.F., Pohlmann, A.R., Guterres, S.S., Lehr, C.M., Kostka, K.H. and Beck, R.C.R., 2011. Improved photostability and reduced skin permeation of tretinoin: development of a semisolid nanomedicine. *European Journal of Pharmaceutics and biopharmaceutics*, 79(1), pp.95-101.

Pourjavadi, A., Doroudian, M., Ahadpour, A. and Azari, S. 2019. Injectable chitosan/k-carrageenan hydrogel designed with au nanoparticles: A conductive scaffold for tissue engineering demands. *International Journal of Biological Macromolecules*, 126, pp.310-317.

Rasool, A., Ata, S., Islam, A. and Khan, R.U. 2019. Fabrication of novel carrageenan based stimuli responsive injectable hydrogels for controlled release of cephadrine. *RSC Advances*, 9(22), pp.12282-12290.

Rufato, K.B., Galdino, J.P., Ody, K.S., Pereira, A.G., Corradini, E., Martins, A.F., Paulino, A.T., Fajardo, A.R., Aouada, F.A., La Porta, F.A. and Rubira, A.F. 2018. Hydrogels based on chitosan and chitosan derivatives for biomedical applications. In *Hydrogels-smart Materials for Biomedical Applications*. IntechOpen.

Rwei, S.P. and Lien, C.C. 2014. Synthesis and viscoelastic characterization of sulfonated chitosan solutions. *Colloid and Polymer Science*, 292(4), pp.785-795.

Savadekar, N.R., Karande, V.S., Vigneshwaran, N., Bharimalla, A.K. and Mhaske, S.T. 2012. Preparation of nano cellulose fibers and its application in kappa-carrageenan based film. *International journal of biological macromolecules*, 51(5), pp.1008-1013.

Shah, B., Shaikh, M.V., Chaudagar, K., Nivsarkar, M. and Mehta, A., 2019. D-limonene possesses cytotoxicity to tumor cells but not to hepatocytes. *Polish Annals of Medicine*, 26(2).

Soltantabar, P., Calubaquib, E.L., Mostafavi, E., Biewer, M.C. and Stefan, M.C. 2020. Enhancement of loading efficiency by co-loading of doxorubicin and quercetin in thermoresponsive polymeric micelles. *Biomacromolecules*, 21(4), pp.1427-1436.

Tahira, I., Aslam, Z., Abbas, A., Monim-ul-Mehboob, M., Ali, S. and Asghar, A. 2019. Adsorptive removal of acidic dye onto grafted chitosan: a plausible grafting and adsorption mechanism. *International journal of biological macromolecules*, 136, pp.1209-1218.

Varshosaz, J., Sajadi-Javan, Z.S., Kouhi, M. and Mirian, M. 2021. Effect of bassorin (derived from gum tragacanth) and halloysite nanotubes on physicochemical properties and the osteoconductivity of methylcellulose-based injectable hydrogels. *International Journal of Biological Macromolecules*, 192, pp.869-882.

Wu, H., Wei, G., Luo, L., Li, L., Gao, Y., Tan, X., Wang, S., Chang, H., Liu, Y., Wei, Y. and Song, J. 2022. Ginsenoside Rg3 nanoparticles with permeation enhancing based chitosan derivatives were encapsulated with doxorubicin by thermosensitive hydrogel and anti-cancer evaluation of peritumoral hydrogel injection combined with PD-L1 antibody. *Biomaterials Research*, 26(1), pp.1-21.

Xu, H. and Matysiak, S. 2017. Effect of pH on chitosan hydrogel polymer network structure. *Chemical Communications*, 53(53), pp.7373-7376.

Xu, X., Chen, J., Li, Y., Yang, X., Wang, Q., Wen, Y., Yan, M., Zhang, J., Xu, Q., Wei, Y. and Chen, W. 2021. Targeting epigenetic modulation of cholesterol synthesis as a therapeutic strategy for head and neck squamous cell carcinoma. *Cell death & disease*, 12(5), p.482.

Yang, Z., Teng, Y., Wang, H. and Hou, H. 2013. Enhancement of skin permeation of bufalin by limonene via reservoir type transdermal patch: formulation design and biopharmaceutical evaluation. *International journal of pharmaceutics*, 447(1-2), pp.231-240.

Zhan, Y., Fu, W., Xing, Y., Ma, X. and Chen, C. 2021. Advances in versatile anti-swelling polymer hydrogels. *Materials Science and Engineering: C*, 127, Article ID: 112208.

Zhang, K., Feng, W. and Jin, C. 2020. Protocol efficiently measuring the swelling rate of hydrogels. *MethodsX*, 7, Article ID: 100779.



UNIVERSITY of the  
WESTERN CAPE

## CHAPTER 5: CONCLUSION

*This chapter provides the overall conclusion to the study. A summary of the study is provided, along with its limitations and recommendations.*

### 5.1 Summary

In this study, oral squamous cell carcinoma (OSCC) was identified as the most common and aggressive carcinoma of the head and neck category. Intravenous chemotherapeutic drugs, such as doxorubicin (DOX), were discussed as the main treatment option for OSCC, but poor permeation into tumorous tissues and side-effects such as immunotoxicity, cardiotoxicity, and gastrotoxicity were established to significantly limit their applicability. This study, therefore, aimed to design a target-specific delivery system that would possibly enhance permeation to OSCC by using a thermoresponsive hydrogel system and a novel permeation enhancer.

Thermosensitive hydrogels were designed by crosslinking chitosan (CH), *k*-carrageenan (*k*CRG), Pluronic™ F127 (PF-127) and limonene (LIM). Nine formulations which contained varying ratios of the constituents were characterised to identify the most optimal hydrogel samples with qualities for a lower critical solution temperature (LCST) around physiological temperature, rapid gelation at 37 °C, slow drug release and good permeation potential. To gain this knowledge, various characterisation techniques such as gelation time, mechanical strength, rheology, swelling, erosion, drug release and permeation studies were employed. Physicochemical analysis of the samples also shed light on the polymer crosslinking as revealed by FTIR, TGA and DSC.

The findings of this study revealed that the crosslinking of CH and *k*CRG with PF-127, can enhance the mechanical properties and reduce the degradation rate of the hydrogel system. More specifically, CH improves hydrogel elasticity, and *k*CRG improves gel stiffness. The main disadvantage of their implementation, however, is the decrease in LCST as their concentration increases. The system was able to maintain a delayed and extended release of DOX, however, the high burst release observed may lead to toxicity and therefore indicates that further modification of the hydrogel formulation is required to adjust drug release rates. LIM was able to demonstrate a concentration dependent increase in permeation. A concentration of 0.5 %v/v of LIM could improve the permeation of DOX within the hydrogel by 100 %, according to PAMPA, suggesting that the terpene could be used as a permeation enhancer for chemotherapeutic

drugs. Table 5.1 summarises the effect of CH, *k*CRG and LIM on the physicochemical properties of the hydrogel.

Table 5.1: A summary of the effect of CH, *k*CRG and LIM on the physicochemical properties of the thermosensitive hydrogel

|                            | CH        | <i>k</i> -CRG | LIM       |
|----------------------------|-----------|---------------|-----------|
| <b>Gelation time</b>       | ↓Decrease | ↓Decrease     | ↓Decrease |
| <b>LCST</b>                | ↓Decrease | ↓Decrease     | ↓Decrease |
| <b>Mechanical strength</b> | ↑Increase | ↑Increase     | ↑Increase |
| <b>Swelling</b>            | ↑Increase | ↑Increase     | ↑Increase |
| <b>Erosion</b>             | ↓Decrease | ↓Decrease     | ↑Increase |
| <b>Drug release</b>        | ↓Decrease | ↓Decrease     | -         |
| <b>Permeation</b>          | -         | -             | ↑Increase |

The study has presented a novel strategy where LIM can be used within a thermosensitive hydrogel system to improve the permeation of drugs. The issue of poor mechanical strength often posed by hydrogels has also been addressed by employing polymers such as CH and *k*CRG. The excellent drug incorporation shows that the system could be valuable for highly soluble drugs or other poorly soluble low dose drugs that require site specific delivery. The hydrogel system could serve as a promising strategy to improve treatment outcomes in OSCC and various types of solid cancers. Overall, the thermosensitive hydrogels were successfully designed, and with further improvements in hydrogel formulation and release behaviour, the system will have better potential for clinical translation.

## 5.2 Limitations

The thermosensitive hydrogel system that was designed, as well as the methods used in this study, were not without limitations. Foremost, the high cost of DOX prevented the purchase and use of ample drug to engage in sufficient trial and error of preformulation studies as well as the use of relevant clinical amounts for the characterisation studies such as drug release and erosion. Further to this, the erosion of hydrogels depends on their volume/surface area of exposure. Therefore, the results described in this study may not reflect the true degradation of

the hydrogels *in vitro*; however, the trend of erosion over an extended period will likely still be applicable. Fortunately, the use of natural constituents with non-toxic synthetic PF-127, holds promise for the safe use of the system over a long period.

As a result of resource constraints, gelation time was dependent on an old-fashioned method of tube inversion, which could not adequately measure the rheology as a function of time to determine an exact timeframe of gelling. Additionally, financial and time limitations restricted the employment of OSCC cells to investigate drug permeation. Because of the low LCST of the most optimal hydrogels, a drawback could be their reduced applicability in warm areas, especially countries on the equator where surrounding temperatures are very high, because hydrogels would easily gel before injection at the intended site. The extremely high temperatures in these areas may significantly reduce the already low gelation times of the hydrogel based on the results obtained, wherein the gelation time decreased with increasing temperature. The thermoresponsive hydrogel would have to remain in an area with controlled cooling systems to maintain its temperature – a facility that may be lacking in undeveloped and developing countries. In South Africa, where the lack of trustworthy electricity supply resulted in the declaration of a national state of disaster, the inability to maintain a cold chain may be a significant concern for thermosensitive hydrogels. Currently, there are no international standards for the injection of hydrogels, therefore all characterisation studies were based on their comparison to existing literature. Finally, the use of this hydrogel system is limited to primary, early-stage tumours as the system would not be able to target metastatic cancers.

### 5.3 Recommendations and future outlook

The next phase of this study will aim to explore higher concentrations of LIM that can exist within the hydrogel without compromising its thermosensitivity. This will be done to enhance the permeation of DOX. A diblock copolymer for thermal response could also be employed to enhance the possible attachment of lipophilic LIM to the hydrophobic diblock end, so that ample concentration of LIM can be loaded. Furthermore, OSCC cell culture must be employed to determine a more precise effect of the terpene on DOX permeation.

To gauge better understanding of the delivery system, a recommendation is to investigate the cytotoxicity of the drug-loaded hydrogel in OSCC cell culture to determine its effectiveness toward these cancer cells. For these modifications, a larger drug quantity will need to be purchased to cater for formulation trials, and to ensure that characterisation results are not compromised. The study has also highlighted several challenges which are opportunities for

further research. For example, during trial formulations, it was discovered that PF-127 is unable to maintain its thermal property in many laboratory solvents. Some research into appropriate solvent combinations that can allow polymer thermal response while solubilising a maximum concentration of drug, would overcome this difficult challenge for researchers and would provide an easier route to improve the solubility of drugs in thermosensitive hydrogels. Another unique observation was the undesired “lumping” with increasing pH – this could be further explored to design a dual pH and thermosensitive hydrogel.



## APPENDICES

### Appendix A1

#### Design of a Thermoresponsive Hydrogel for Enhanced Intratumoral Permeation of a Model Drug in Oral Squamous Cell Carcinoma

Sandrine Tanga<sup>1</sup>, Marique Aucamp<sup>1</sup>, Poornima Ramburrun<sup>2</sup>

<sup>1</sup>Department of Pharmaceutics, University of the Western Cape, Bellville, South Africa

<sup>2</sup>Department of Pharmacy and Pharmacology, University of Witwatersrand, Johannesburg, South Africa

Email address: 3723884@myuwc.ac.za

**Purpose:** Oral squamous cell carcinoma (OSCC) is the most common and aggressive cancer occurring in the oral cavity. Intravenous chemotherapy remains a pivotal part of treatment for the disease, however, these drugs cause debilitating systemic side effects and are unable to permeate into the deep compact layers of tumorous tissue cells. Herein, the intratumoral delivery of a model drug using a novel hydrogel blend, of chitosan/*k*-carrageenan and Pluronic™ F127, for a rapid solution-to-gel thermoresponsive transition at 37°C is proposed to achieve tumour-specific delivery and controlled drug release. For enhanced permeation, a novel monoterpene with high lipophilicity and anticancer effect is combined with the hydrogel system.

**Methods:** Physicochemical characterization was performed to investigate the crosslinking and thermal behaviour of the polymer blend. The most optimal hydrogel systems were investigated through mechanical studies. Drug release from the hydrogel system was evaluated through drug diffusion and hydrogel degradation studies. Finally, the parallel artificial membrane permeability assay was utilized to assess the *in vitro* permeation of the drug through the thermoresponsive hydrogel system.

**Results:** The addition of chitosan/*k*-carrageenan increases the mechanical strength and allows for slow degradation of the hydrogel system, thus enabling a controlled release of the model drug. The blend also enables rapid gelation at room temperature with a slight pH response. Permeation studies are expected to reveal the effect of the novel monoterpene on the permeation of the drug.

**Conclusion:** The delivery system demonstrates good solution-gel behaviour with controlled and sustained drug release. Therefore, the system is an excellent candidate for locally injectable gel-depot systems and could improve treatment outcomes in OSCC.



**Appendix A2****Design of a Thermoresponsive Hydrogel for Enhanced Intratumoral Permeation of a Model Drug in Oral Squamous Cell Carcinoma**

Sandrine Tanga<sup>1</sup>, Marique Aucamp<sup>1</sup>, Poornima Ramburrun<sup>2</sup>

<sup>1</sup>Department of Pharmaceutics, University of the Western Cape, Bellville, South Africa

<sup>2</sup>Department of Pharmacy and Pharmacology, University of Witwatersrand, Johannesburg, South Africa

Email: 3723884@myuwc.ac.za

**Introduction:** Oral squamous cell carcinoma (OSCC) is the most common and aggressive cancer occurring in the oral cavity. Intravenous chemotherapy remains a pivotal part of treatment for the disease, however, these drugs cause debilitating systemic side effects and are unable to permeate into the deep compact layers of tumorous tissue cells. Herein, the intratumoral delivery of a model drug using a novel hydrogel blend, of chitosan/*k*-carrageenan and Pluronic<sup>TM</sup> F127, for a rapid solution-to-gel thermoresponsive transition at 37°C is proposed to achieve tumour-specific delivery and controlled drug release. For enhanced permeation, a novel monoterpene with high lipophilicity and anticancer effect is combined with the hydrogel system.

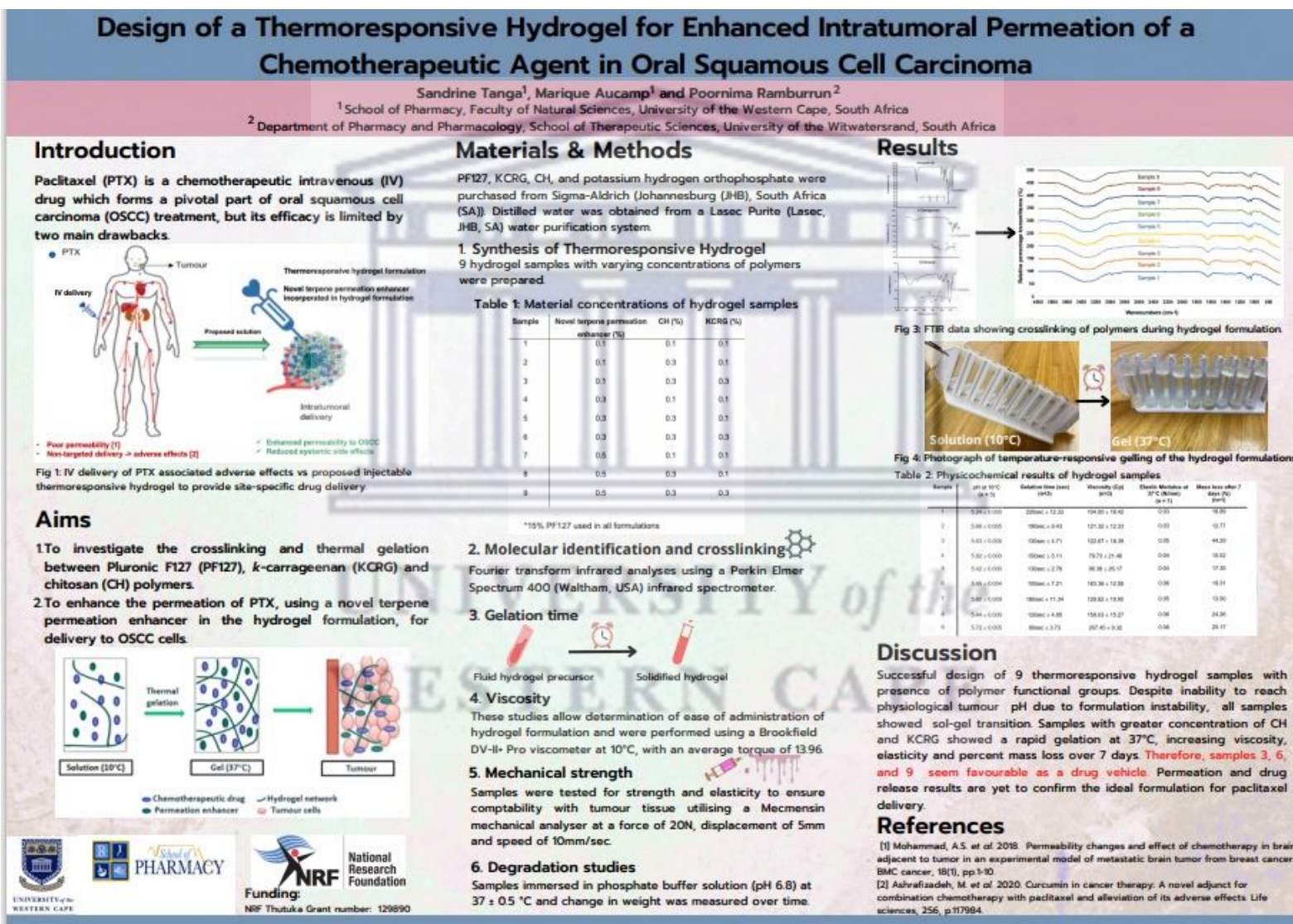
**Methods:** Physicochemical characterization was performed to investigate the crosslinking and thermal behaviour of the polymer blend. The most optimal hydrogel systems were investigated through mechanical studies. Drug release from the hydrogel system was evaluated through drug diffusion and hydrogel degradation studies. Finally, the parallel artificial membrane permeability assay was utilized to assess the in vitro permeation of the drug through the thermoresponsive hydrogel system.

**Results:** The addition of chitosan/*k*-carrageenan increases the mechanical strength and allows for slow degradation of the hydrogel system, thus enabling a controlled release of the model drug. The blend also enables rapid gelation at room temperature with a slight pH response. Permeation studies are expected to reveal the effect of the novel monoterpene on the permeation of the drug.

**Conclusions:** The delivery system demonstrates good solution-gel behaviour with controlled and sustained drug release. Therefore, the system is an excellent candidate for locally injectable gel-depot systems and could improve treatment outcomes in OSCC.



## Appendix A3



## Appendix A4

The review paper entitled: “*Injectable Thermoresponsive Hydrogels for Cancer Therapy: Challenges and Prospects*” was prepared according to the stipulated Author Guidelines of the MDPI Journal Gels, as outlined below:

Manuscript Submission Overview (Available at: <https://www.mdpi.com/journal/gels/instructions>)

### Types of Publications

Full experimental details must be provided so that the results can be reproduced. *Gels* requires that authors publish all experimental controls and make full datasets available where possible (see the guidelines on [Supplementary Materials](#) and references to unpublished data).

Manuscripts submitted to *Gels* should neither be published previously nor be under consideration for publication in another journal. The main article types are listed below and a comprehensive list of article types can be found [here](#).

- **Article:** These are original research manuscripts. The work should report scientifically sound experiments and provide a substantial amount of new information. The article should include the most recent and relevant references in the field. The structure should include an Abstract, Keywords, Introduction, Materials and Methods, Results, Discussion, and Conclusions (optional) sections, with a suggested minimum word count of 4000 words. Please refer to the journal webpages for specific instructions and templates.
- **Review:** Reviews offer a comprehensive analysis of the existing literature within a field of study, identifying current gaps or problems. They should be critical and constructive and provide recommendations for future research. No new, unpublished data should be presented. The structure can include an Abstract, Keywords, Introduction, Relevant Sections, Discussion, Conclusions, and Future Directions, with a suggested minimum word count of 4000 words.

### Submission Process

Manuscripts for *Gels* should be submitted online at [susy.mdpi.com](https://susy.mdpi.com). The submitting author, who is generally the corresponding author, is responsible for the manuscript during the submission and peer-review process. The submitting author must ensure that all eligible co-authors have been included in the author list (read the [criteria to qualify for authorship](#)) and that they have all read and approved the submitted version of the manuscript. To submit your manuscript, register and log in to the [submission website](#). Once you have registered, [click here to go to the submission form for Gels](#). All co-authors can see the manuscript details in the submission system, if they register and log in using the e-mail address provided during manuscript submission.

### Accepted File Formats

Authors are encouraged to use the [Microsoft Word template](#) or [LaTeX template](#) to prepare their manuscript. Using the template file will substantially shorten the time to complete copy-editing and publication of accepted manuscripts. The total amount of data for all files must not exceed 120 MB. If this is a problem, please contact the Editorial Office [gels@mdpi.com](mailto:gels@mdpi.com). Accepted file formats are:

- **Microsoft Word:** Manuscripts prepared in Microsoft Word must be converted into a single file before submission. When preparing manuscripts in Microsoft Word, we encourage you to use the [Gels Microsoft Word template file](#). Please insert your graphics (schemes, figures, etc.) in the main text after the paragraph of its first citation.
- **LaTeX:** Manuscripts prepared in LaTeX must be collated into one ZIP folder (including all source files and images, so that the Editorial Office can recompile the submitted PDF). When preparing manuscripts in LaTeX, we encourage you to use the [Gels LaTeX template files](#). You can now also use the online application [writeLaTeX](#) to submit articles directly to *Gels*. The MDPI LaTeX template file should be selected from the [writeLaTeX template gallery](#).
- **Supplementary files:** May be any format, but it is recommended that you use common, non-proprietary formats where possible (see [below](#) for further details).

**Disclaimer: Usage of these templates is exclusively intended for submission to the journal for peer-review, and strictly limited to this purpose and it cannot be used for posting online on preprint servers or other websites.**

### Free Format Submission

*Gels* now accepts free format submission:

- We do not have strict formatting requirements, but all manuscripts must contain the required sections: Author Information, Abstract, Keywords, Introduction, Materials & Methods, Results, Conclusions, Figures and Tables with Captions, Funding Information, Author Contributions, Conflict of Interest and other Ethics Statements. Check the Journal [Instructions for Authors](#) for more details.
- Your references may be in any style, provided that you use the consistent formatting throughout. It is essential to include author(s) name(s), journal or book title, article or chapter title (where required), year of publication, volume and issue (where appropriate) and pagination. DOI numbers (Digital Object Identifier) are not mandatory but highly encouraged. The bibliography software package *EndNote*, [Zotero](#), *Mendeley*, *Reference Manager* are recommended.
- When your manuscript reaches the revision stage, you will be requested to format the manuscript according to the journal guidelines.

### Cover Letter

A cover letter must be included with each manuscript submission. It should be concise and explain why the content of the paper is significant, placing the findings in the context of existing work. It should explain why the manuscript fits the scope of the journal.

Any prior submissions of the manuscript to MDPI journals must be acknowledged. If this is the case, it is strongly recommended that the previous manuscript ID is provided in the submission system, which will ease your current submission process. The names of proposed and excluded reviewers should be provided in the submission system, not in the cover letter.

All cover letters are required to include the statements:

- We confirm that neither the manuscript nor any parts of its content are currently under consideration or published in another journal.
- All authors have approved the manuscript and agree with its submission to (journal name).

### Author Biography

Authors are encouraged to add a biography (maximum 150 words) to the submission and post it to [SciProfiles](#). This should be a single paragraph and should contain the following points:

1. Authors' full names followed by current positions;
2. Education background including institution information and year of graduation (type and level of degree received);
3. Work experience;
4. Current and previous research interests;
5. Memberships of professional societies and awards received.

### Manuscript Preparation

#### General Considerations

- **Research manuscripts** should comprise:
  - [Front matter](#): Title, Author list, Affiliations, Abstract, Keywords.

- [Research manuscript sections](#): Introduction, Materials and Methods, Results, Discussion, Conclusions (optional).
- [Back matter](#): Supplementary Materials, Acknowledgments, Author Contributions, Conflicts of Interest, [References](#).
- **Review manuscripts** should comprise the [front matter](#), literature review sections and the [back matter](#). The template file can also be used to prepare the front and back matter of your review manuscript. It is not necessary to follow the remaining structure. Structured reviews and meta-analyses should use the same structure as research articles and ensure they conform to the [PRISMA](#) guidelines.
- **Graphical Abstract:**

A graphical abstract (GA) is an image that appears alongside the text abstract in the Table of Contents. In addition to summarizing the content, it should represent the topic of the article in an attention-grabbing way. Moreover, it should not be exactly the same as the Figure in the paper or just a simple superposition of several subfigures. Note that the GA must be original and unpublished artwork. Any postage stamps, currency from any country, or trademarked items should not be included in it.

The GA should be a high-quality illustration or diagram in any of the following formats: PNG, JPEG, TIFF, or SVG. Written text in a GA should be clear and easy to read, using one of the following fonts: Times, Arial, Courier, Helvetica, Ubuntu or Calibri.

The minimum required size for the GA is 560 × 1100 pixels (height × width). The size should be of high quality in order to reproduce well.

- **Acronyms/Abbreviations/Initialisms** should be defined the first time they appear in each of three sections: the abstract; the main text; the first figure or table. When defined for the first time, the acronym/abbreviation/initialism should be added in parentheses after the written-out form.
- **SI Units** (International System of Units) should be used. Imperial, US customary and other units should be converted to SI units whenever possible.
- **Equations:** If you are using Word, please use either the Microsoft Equation Editor or the MathType add-on. Equations should be editable by the editorial office and not appear in a picture format.
- **Research Data and supplementary materials:** Note that publication of your manuscript implies that you must make all materials, data, and protocols associated with the publication available to readers. Disclose at the submission stage any restrictions on the availability of materials or information. Read the information about [Supplementary Materials](#) and Data Deposit for additional guidelines.
- **Preregistration:** Where authors have preregistered studies or analysis plans, links to the preregistration must be provided in the manuscript.
- **Guidelines and standards:** MDPI follows standards and guidelines for certain types of research. See [https://www.mdpi.com/editorial\\_process](https://www.mdpi.com/editorial_process) for further information.

## Front Matter

These sections should appear in all manuscript types

- **Title:** The title of your manuscript should be concise, specific and relevant. It should identify if the study reports (human or animal) trial data, or is a systematic review, meta-analysis or replication study. Please do not include abbreviated or short forms of the title, such as a running title or head. These will be removed by our Editorial Office.
- **Author List and Affiliations:** Authors' full first and last names must be provided. The initials of any middle names can be added. The PubMed/MEDLINE standard format is used for affiliations: complete address information including city, zip code, state/province, and country. At least one author should be designated as the corresponding author. The email addresses of all authors will be displayed on published papers, and hidden by Captcha on the website as standard. It is the responsibility of the corresponding author to ensure that consent for the display of email addresses is obtained from all authors. If an author (other than the corresponding author) does not wish to have their email addresses displayed in this way, the corresponding author must indicate as such during proofreading. After acceptance, updates to author names or affiliations may not be permitted. Equal Contributions: authors who have contributed equally should be marked with a superscript symbol (†). The symbol must be included below the affiliations, and the following statement

added: “These authors contributed equally to this work”. The equal roles of authors should also be adequately disclosed in the author contributions statement. Please read the criteria to qualify for authorship.

- **Abstract:** The abstract should be a total of about 200 words maximum. The abstract should be a single paragraph and should follow the style of structured abstracts, but without headings: 1) Background: Place the question addressed in a broad context and highlight the purpose of the study; 2) Methods: Describe briefly the main methods or treatments applied. Include any relevant preregistration numbers, and species and strains of any animals used. 3) Results: Summarize the article’s main findings; and 4) Conclusion: Indicate the main conclusions or interpretations. The abstract should be an objective representation of the article: it must not contain results which are not presented and substantiated in the main text and should not exaggerate the main conclusions.
- **Keywords:** Three to ten pertinent keywords need to be added after the abstract. We recommend that the keywords are specific to the article, yet reasonably common within the subject discipline.

### Research Manuscript Sections

- **Introduction:** The introduction should briefly place the study in a broad context and highlight why it is important. It should define the purpose of the work and its significance, including specific hypotheses being tested. The current state of the research field should be reviewed carefully and key publications cited. Please highlight controversial and diverging hypotheses when necessary. Finally, briefly mention the main aim of the work and highlight the main conclusions. Keep the introduction comprehensible to scientists working outside the topic of the paper.
- **Materials and Methods:** They should be described with sufficient detail to allow others to replicate and build on published results. New methods and protocols should be described in detail while well-established methods can be briefly described and appropriately cited. Give the name and version of any software used and make clear whether computer code used is available. Include any pre-registration codes.
- **Results:** Provide a concise and precise description of the experimental results, their interpretation as well as the experimental conclusions that can be drawn.
- **Discussion:** Authors should discuss the results and how they can be interpreted in perspective of previous studies and of the working hypotheses. The findings and their implications should be discussed in the broadest context possible and limitations of the work highlighted. Future research directions may also be mentioned. This section may be combined with Results.
- **Conclusions:** This section is not mandatory but can be added to the manuscript if the discussion is unusually long or complex.
- **Patents:** This section is not mandatory but may be added if there are patents resulting from the work reported in this manuscript.

### Back Matter

- **Supplementary Materials:** Describe any supplementary material published online alongside the manuscript (figure, tables, video, spreadsheets, etc.). Please indicate the name and title of each element as follows Figure S1: title, Table S1: title, etc.
- **Funding:** All sources of funding of the study should be disclosed. Clearly indicate grants that you have received in support of your research work and if you received funds to cover publication costs. Note that some funders will not refund article processing charges (APC) if the funder and grant number are not clearly and correctly identified in the paper. Funding information can be entered separately into the submission system by the authors during submission of their manuscript. Such funding information, if available, will be deposited to FundRef if the manuscript is finally published. Please add: “This research received no external funding” or “This research was funded by [name of funder] grant number [xxx]” and “The APC was funded by [XXX]” in this section. Check carefully that the details given are accurate and use the standard spelling of funding agency names at <https://search.crossref.org/funding>, any errors may affect your future funding.
- **Acknowledgments:** In this section you can acknowledge any support given which is not covered by the author contribution or funding sections. This may include administrative and technical support, or donations in kind (e.g., materials used for experiments).
- **Author Contributions:** Each author is expected to have made substantial contributions to the conception or design of the work; or the acquisition, analysis, or interpretation of data; or the creation of new software used in the work; or have drafted the work or substantively revised it; AND has approved the submitted version (and version substantially edited by journal staff that involves the author’s contribution to the study); AND agrees to be personally accountable for the author’s own contributions and for ensuring that questions

related to the accuracy or integrity of any part of the work, even ones in which the author was not personally involved, are appropriately investigated, resolved, and documented in the literature. For research articles with several authors, a short paragraph specifying their individual contributions must be provided. The following statements should be used "Conceptualization, X.X. and Y.Y.; Methodology, X.X.; Software, X.X.; Validation, X.X., Y.Y. and Z.Z.; Formal Analysis, X.X.; Investigation, X.X.; Resources, X.X.; Data Curation, X.X.; Writing – Original Draft Preparation, X.X.; Writing – Review & Editing, X.X.; Visualization, X.X.; Supervision, X.X.; Project Administration, X.X.; Funding Acquisition, Y.Y.", please turn to the [CRediT taxonomy](#) for the term explanation. For more background on CRediT, see [here](#). **"Authorship must include and be limited to those who have contributed substantially to the work. Please read the section concerning the [criteria to qualify for authorship](#) carefully".**

- **Institutional Review Board Statement:** In this section, please add the Institutional Review Board Statement and approval number for studies involving humans or animals. Please note that the Editorial Office might ask you for further information. Please add "The study was conducted according to the guidelines of the Declaration of Helsinki, and approved by the Institutional Review Board (or Ethics Committee) of NAME OF INSTITUTE (protocol code XXX and date of approval)." OR "Ethical review and approval were waived for this study, due to REASON (please provide a detailed justification)." OR "Not applicable" for studies not involving humans or animals. You might also choose to exclude this statement if the study did not involve humans or animals.
- **Informed Consent Statement:** Any research article describing a study involving humans should contain this statement. Please add "Informed consent was obtained from all subjects involved in the study." OR "Patient consent was waived due to REASON (please provide a detailed justification)." OR "Not applicable" for studies not involving humans. You might also choose to exclude this statement if the study did not involve humans. Written informed consent for publication must be obtained from participating patients who can be identified (including by the patients themselves). Please state "Written informed consent has been obtained from the patient(s) to publish this paper" if applicable.
- **Data Availability Statement:** In this section, please provide details regarding where data supporting reported results can be found, including links to publicly archived datasets analyzed or generated during the study. Please refer to suggested Data Availability Statements in section "[MDPI Research Data Policies](#)". You might choose to exclude this statement if the study did not report any data.
- **Conflicts of Interest:** Authors must identify and declare any personal circumstances or interest that may be perceived as influencing the representation or interpretation of reported research results. If there is no conflict of interest, please state "The authors declare no conflict of interest." Any role of the funding sponsors in the choice of research project; design of the study; in the collection, analyses or interpretation of data; in the writing of the manuscript; or in the decision to publish the results must be declared in this section. *Gels* does not publish studies funded partially or fully by the tobacco industry. Any projects funded by industry must pay special attention to the full declaration of funder involvement. If there is no role, please state "The sponsors had no role in the design, execution, interpretation, or writing of the study". For more details please see [Conflict of Interest](#).
- **References:** References must be numbered in order of appearance in the text (including table captions and figure legends) and listed individually at the end of the manuscript. We recommend preparing the references with a bibliography software package, such as [EndNote](#), [ReferenceManager](#) or [Zotero](#) to avoid typing mistakes and duplicated references. We encourage citations to data, computer code and other citable research material. If available online, you may use reference style 9. below.
- Citations and References in Supplementary files are permitted provided that they also appear in the main text and in the reference list.

In the text, reference numbers should be placed in square brackets [ ], and placed before the punctuation; for example [1], [1–3] or [1,3]. For embedded citations in the text with pagination, use both parentheses and brackets to indicate the reference number and page numbers; for example [5] (p. 10). or [6] (pp. 101–105).

The reference list should include the full title, as recommended by the ACS style guide. Style files for [Endnote](#) and [Zotero](#) are available.

References should be described as follows, depending on the type of work:

Journal Articles:

1. Author 1, A.B.; Author 2, C.D. Title of the article. *Abbreviated Journal Name* **Year**, *Volume*, page range.

Books and Book Chapters:

2. Author 1, A.; Author 2, B. *Book Title*, 3rd ed.; Publisher: Publisher Location, Country, Year; pp. 154–196.

3. Author 1, A.; Author 2, B. Title of the chapter. In *Book Title*, 2nd ed.; Editor 1, A., Editor 2, B., Eds.; Publisher: Publisher Location, Country, Year; Volume 3, pp. 154–196.
  - Unpublished materials intended for publication:
4. Author 1, A.B.; Author 2, C. Title of Unpublished Work (optional). Correspondence Affiliation, City, State, Country. year, *status (manuscript in preparation; to be submitted)*.
5. Author 1, A.B.; Author 2, C. Title of Unpublished Work. *Abbreviated Journal Name* year, *phrase indicating stage of publication (submitted; accepted; in press)*.
  - Unpublished materials not intended for publication:
6. Author 1, A.B. (Affiliation, City, State, Country); Author 2, C. (Affiliation, City, State, Country). Phase describing the material, year. (phase: Personal communication; Private communication; Unpublished work; etc.)
  - Conference Proceedings:
7. Author 1, A.B.; Author 2, C.D.; Author 3, E.F. Title of Presentation. In *Title of the Collected Work* (if available), Proceedings of the Name of the Conference, Location of Conference, Country, Date of Conference; Editor 1, Editor 2, Eds. (if available); Publisher: City, Country, Year (if available); Abstract Number (optional), Pagination (optional).
  - Thesis:
8. Author 1, A.B. Title of Thesis. Level of Thesis, Degree-Granting University, Location of University, Date of Completion.
  - Websites:
9. Title of Site. Available online: URL (accessed on Day Month Year). Unlike published works, websites may change over time or disappear, so we encourage you create an archive of the cited website using a service such as [WebCite](#). Archived websites should be cited using the link provided as follows:
10. Title of Site. URL (archived on Day Month Year). See the [Reference List and Citations Guide](#) for more detailed information.

### Preparing Figures, Schemes and Tables

- File for Figures and Schemes must be provided during submission in a single zip archive and at a sufficiently high resolution (minimum 1000 pixels width/height, or a resolution of 300 dpi or higher). Common formats are accepted, however, TIFF, JPEG, EPS and PDF are preferred.
- *Gels* can publish multimedia files in articles or as supplementary materials. Please contact the editorial office for further information.
- All Figures, Schemes and Tables should be inserted into the main text close to their first citation and must be numbered following their number of appearance (Figure 1, Scheme I, Figure 2, Scheme II, Table 1, *etc.*).
- All Figures, Schemes and Tables should have a short explanatory title and caption.
- All table columns should have an explanatory heading. To facilitate the copy-editing of larger tables, smaller fonts may be used, but no less than 8 pt. in size. Authors should use the Table option of Microsoft Word to create tables.
- Authors are encouraged to prepare figures and schemes in color (RGB at 8-bit per channel). There is no additional cost for publishing full color graphics.

### Supplementary Materials, Data Deposit and Software Source Code

#### *MDPI Research Data Policies*

MDPI is committed to supporting open scientific exchange and enabling our authors to achieve best practices in sharing and archiving research data. We encourage all authors of articles published in MDPI journals to share their research data. Individual journal guidelines can be found at the journal 'Instructions for Authors' page. Data sharing policies concern the minimal dataset that supports the central findings of a published study. Generated data should be publicly available and cited in accordance with journal guidelines.

MDPI data policies are informed by [TOP Guidelines](#) and [FAIR Principles](#).

Where ethical, legal or privacy issues are present, data should not be shared. The authors should make any limitations clear in the Data Availability Statement upon submission. Authors should ensure that data shared are in accordance with consent provided by participants on the use of confidential data.

Data Availability Statements provide details regarding where data supporting reported results can be found, including links to publicly archived datasets analyzed or generated during the study.

Below are suggested Data Availability Statements:

- Data available in a publicly accessible repository  
The data presented in this study are openly available in [repository name e.g., FigShare] at [doi], reference number [reference number].
- Data available in a publicly accessible repository that does not issue DOIs. Publicly available datasets were analyzed in this study. This data can be found here: [link/accession number]
- Data available on request due to restrictions eg privacy or ethical . The data presented in this study are available on request from the corresponding author. The data are not publicly available due to [insert reason here]
- 3<sup>rd</sup> Party Data  
Restrictions apply to the availability of these dat. Data was obtained from [third party] and are available [from the authors / at URL] with the permission of [third party].
- Data sharing not applicable. No new data were created or analyzed in this study. Data sharing is not applicable to this article.
- Data is contained within the article or supplementary material. The data presented in this study are available in [insert article or supplementary material here]

Data citation:

- [dataset] Authors. Year. Dataset title; Data repository or archive; Version (if any); Persistent identifier (e.g., DOI).

#### *Computer Code and Software*

For work where novel computer code was developed, authors should release the code either by depositing in a recognized, public repository or uploading as supplementary information to the publication. The name and version of all software used should be clearly indicated.

#### *Supplementary Material*

Additional data and files can be uploaded as "Supplementary Files" during the manuscript submission process. The supplementary files will also be available to the referees as part of the peer-review process. Any file format is acceptable, however we recommend that common, non-proprietary formats are used where possible. For more information on supplementary materials, please refer to [https://www.mdpi.com/authors/layout#\\_bookmark83](https://www.mdpi.com/authors/layout#_bookmark83).

#### *Unpublished Data*

Restrictions on data availability should be noted during submission and in the manuscript. "Data not shown" should be avoided: authors are encouraged to publish all observations related to the submitted manuscript as Supplementary Material. "Unpublished data" intended for publication in a manuscript that is either planned, "in preparation" or "submitted" but not yet accepted, should be cited in the text and a reference should be added in the References section. "Personal Communication" should also be cited in the text and reference added in the References section. (see also the MDPI reference list and citations style guide).

#### *Remote Hosting and Large Data Sets*

Data may be deposited with specialized service providers or institutional/subject repositories, preferably those that use the DataCite mechanism. Large data sets and files greater than 60 MB must be deposited in this way. For a list of other repositories specialized in scientific and experimental data, please consult [databib.org](http://databib.org) or [re3data.org](http://re3data.org). The data repository name, link to the data set (URL) and accession number, doi or handle number of the data set must be provided in the paper. The journal [Data](#) also accepts submissions of data set papers.

#### *References in Supplementary Files*

Citations and References in Supplementary files are permitted provided that they also appear in the reference list of the main text.



## Research and Publication Ethics

### Research Ethics

#### Research Involving Human Subjects

When reporting on research that involves human subjects, human material, human tissues, or human data, authors must declare that the investigations were carried out following the rules of the Declaration of Helsinki of 1975 (<https://www.wma.net/what-we-do/medical-ethics/declaration-of-helsinki/>), revised in 2013. According to point 23 of this declaration, an approval from the local institutional review board (IRB) or other appropriate ethics committee must be obtained before undertaking the research to confirm the study meets national and international guidelines. As a minimum, a statement including the project identification code, date of approval, and name of the ethics committee or institutional review board must be stated in Section 'Institutional Review Board Statement' of the article.

Example of an ethical statement: "All subjects gave their informed consent for inclusion before they participated in the study. The study was conducted in accordance with the Declaration of Helsinki, and the protocol was approved by the Ethics Committee of XXX (Project identification code)."

For non-interventional studies (e.g. surveys, questionnaires, social media research), all participants must be fully informed if the anonymity is assured, why the research is being conducted, how their data will be used and if there are any risks associated. As with all research involving humans, ethical approval from an appropriate ethics committee must be obtained prior to conducting the study. If ethical approval is not required, authors must either provide an exemption from the ethics committee or are encouraged to cite the local or national legislation that indicates ethics approval is not required for this type of study. Where a study has been granted exemption, the name of the ethics committee which provided this should be stated in Section 'Institutional Review Board Statement' with a full explanation regarding why ethical approval was not required.

A written informed consent for publication must be obtained from participating patients. Data relating to individual participants must be described in detail, but private information identifying participants need not be included unless the identifiable materials are of relevance to the research (for example, photographs of participants' faces that show a particular symptom). Patients' initials or other personal identifiers must not appear in any images. For manuscripts that include any case details, personal information, and/or images of patients, authors must obtain signed informed consent for publication from patients (or their relatives/guardians) before submitting to an MDPI journal. Patient details must be anonymized as far as possible, e.g., do not mention specific age, ethnicity, or occupation where they are not relevant to the conclusions. A [template permission form](#) is available to download. A blank version of the form used to obtain permission (without the patient names or signature) must be uploaded with your submission. Editors reserve the right to reject any submission that does not meet these requirements.

You may refer to our sample form and provide an appropriate form after consulting with your affiliated institution. For the purposes of publishing in MDPI journals, a consent, permission, or release form should include unlimited permission for publication in all formats (including print, electronic, and online), in sublicensed and reprinted versions (including translations and derived works), and in other works and products under open access license. To respect patients' and any other individual's privacy, please do not send signed forms. The journal reserves the right to ask authors to provide signed forms if necessary.

If the study reports research involving vulnerable groups, an additional check may be performed. The submitted manuscript will be scrutinized by the editorial office and upon request, documentary evidence (blank consent forms and any related discussion documents from the ethics board) must be supplied. Additionally, when studies describe groups by race, ethnicity, gender, disability, disease, etc., explanation regarding why such categorization was needed must be clearly stated in the article.

#### Ethical Guidelines for the Use of Animals in Research

The editors will require that the benefits potentially derived from any research causing harm to animals are significant in relation to any cost endured by animals, and that procedures followed are unlikely to cause offense to the majority of readers. Authors should particularly ensure that their research complies with the commonly-accepted '3Rs [1]':

- Replacement of animals by alternatives wherever possible,

- Reduction in number of animals used, and
- Refinement of experimental conditions and procedures to minimize the harm to animals.

Authors must include details on housing, husbandry and pain management in their manuscript.

For further guidance authors should refer to the Code of Practice for the Housing and Care of Animals Used in Scientific Procedures [2], American Association for Laboratory Animal Science [3] or European Animal Research Association [4].

If national legislation requires it, studies involving vertebrates or higher invertebrates must only be carried out after obtaining approval from the appropriate ethics committee. As a minimum, the project identification code, date of approval and name of the ethics committee or institutional review board should be stated in Section 'Institutional Review Board Statement'. Research procedures must be carried out in accordance with national and institutional regulations. Statements on animal welfare should confirm that the study complied with all relevant legislation. Clinical studies involving animals and interventions outside of routine care require ethics committee oversight as per the American Veterinary Medical Association. If the study involved client-owned animals, informed client consent must be obtained and certified in the manuscript report of the research. Owners must be fully informed if there are any risks associated with the procedures and that the research will be published. If available, a high standard of veterinary care must be provided. Authors are responsible for correctness of the statements provided in the manuscript.

If ethical approval is not required by national laws, authors must provide an exemption from the ethics committee, if one is available. Where a study has been granted exemption, the name of the ethics committee that provided this should be stated in Section 'Institutional Review Board Statement' with a full explanation on why the ethical approval was not required.

If no animal ethics committee is available to review applications, authors should be aware that the ethics of their research will be evaluated by reviewers and editors. Authors should provide a statement justifying the work from an ethical perspective, using the same utilitarian framework that is used by ethics committees. Authors may be asked to provide this even if they have received ethical approval.

MDPI endorses the ARRIVE guidelines ([arriveguidelines.org/](http://arriveguidelines.org/)) for reporting experiments using live animals. Authors and reviewers must use the ARRIVE guidelines as a checklist, which can be found at <https://arriveguidelines.org/sites/arrive/files/documents/ARRIVE%20Compliance%20Questionnaire.pdf>. Editors reserve the right to ask for the checklist and to reject submissions that do not adhere to these guidelines, to reject submissions based on ethical or animal welfare concerns or if the procedure described does not appear to be justified by the value of the work presented.

1. NSW Department of Primary Industries and Animal Research Review Panel. Three Rs. Available online: <https://www.animaethics.org.au/three-rs>
2. Home Office. Animals (Scientific Procedures) Act 1986. Code of Practice for the Housing and Care of Animals Bred, Supplied or Used for Scientific Purposes. Available online: [https://assets.publishing.service.gov.uk/government/uploads/system/uploads/attachment\\_data/file/388535/CoPanimalsWeb.pdf](https://assets.publishing.service.gov.uk/government/uploads/system/uploads/attachment_data/file/388535/CoPanimalsWeb.pdf)
3. American Association for Laboratory Animal Science. The Scientific Basis for Regulation of Animal Care and Use. Available online: <https://www.aalas.org/about-aalas/position-papers/scientific-basis-for-regulation-of-animal-care-and-use>
4. European Animal Research Association. EU regulations on animal research. Available online: <https://www.eara.eu/animal-research-law>

### Research Involving Cell Lines

Methods sections for submissions reporting on research with cell lines should state the origin of any cell lines. For established cell lines the provenance should be stated and references must also be given to either a published paper or to a commercial source. If previously unpublished *de novo* cell lines were used, including those gifted from another laboratory, details of institutional review board or ethics committee approval must be given, and confirmation of written informed consent must be provided if the line is of human origin.

An example of Ethical Statements:

The HCT116 cell line was obtained from XXXX. The MLH1<sup>+</sup> cell line was provided by XXXXX, Ltd. The DLD-1 cell line was obtained from Dr. XXXX. The DR-GFP and SA-GFP reporter plasmids were obtained from Dr. XXX and the Rad51K133A expression vector was obtained from Dr. XXXX.

### Research Involving Plants

Experimental research on plants (either cultivated or wild) including collection of plant material, must comply with institutional, national, or international guidelines. We recommend that authors comply with the [Convention on Biological Diversity](#) and the [Convention on the Trade in Endangered Species of Wild Fauna and Flora](#).

For each submitted manuscript supporting genetic information and origin must be provided. For research manuscripts involving rare and non-model plants (other than, e.g., *Arabidopsis thaliana*, *Nicotiana benthamiana*, *Oryza sativa*, or many other typical model plants), voucher specimens must be deposited in an accessible herbarium or museum. Vouchers may be requested for review by future investigators to verify the identity of the material used in the study (especially if taxonomic rearrangements occur in the future). They should include details of the populations sampled on the site of collection (GPS coordinates), date of collection, and document the part(s) used in the study where appropriate. For rare, threatened or endangered species this can be waived but it is necessary for the author to describe this in the cover letter.

Editors reserve the rights to reject any submission that does not meet these requirements.

An example of Ethical Statements:

*Torenia fournieri* plants were used in this study. White-flowered Crown White (CrW) and violet-flowered Crown Violet (CrV) cultivars selected from 'Crown Mix' (XXX Company, City, Country) were kindly provided by Dr. XXX (XXX Institute, City, Country).

*Arabidopsis* mutant lines (SALKxxxx, SAILxxxx,...) were kindly provided by Dr. XXX, institute, city, country).

### Clinical Trials Registration

#### Registration

MDPI follows the International Committee of Medical Journal Editors (ICMJE) [guidelines](#) which require and recommend registration of clinical trials in a public trials registry at or before the time of first patient enrollment as a condition of consideration for publication.

Purely observational studies do not require registration. A clinical trial not only refers to studies that take place in a hospital or involve pharmaceuticals, but also refer to all studies which involve participant randomization and group classification in the context of the intervention under assessment.

Authors are strongly encouraged to pre-register clinical trials with an international clinical trials register and cite a reference to the registration in the Methods section. Suitable databases include [clinicaltrials.gov](#), [the EU Clinical Trials Register](#) and those listed by the World Health Organisation [International Clinical Trials Registry Platform](#).

Approval to conduct a study from an independent local, regional, or national review body is not equivalent to prospective clinical trial registration. MDPI reserves the right to decline any paper without trial registration for further peer-review. However, if the study protocol has been published before the enrolment, the registration can be waived with correct citation of the published protocol.

#### CONSORT Statement

MDPI requires a completed CONSORT 2010 [checklist](#) and [flow diagram](#) as a condition of submission when reporting the results of a randomized trial. Templates for these can be found here or on the CONSORT website (<http://www.consort-statement.org>) which also describes several CONSORT checklist extensions for different designs and types of data beyond two group parallel trials. At minimum, your article should report the content addressed by each item of the checklist.

## Sex and Gender in Research

We encourage our authors to follow the '[Sex and Gender Equity in Research – SAGER – guidelines](#)' and to include sex and gender considerations where relevant. Authors should use the terms sex (biological attribute) and gender (shaped by social and cultural circumstances) carefully in order to avoid confusing both terms. Article titles and/or abstracts should indicate clearly what sex(es) the study applies to. Authors should also describe in the background, whether sex and/or gender differences may be expected; report how sex and/or gender were accounted for in the design of the study; provide disaggregated data by sex and/or gender, where appropriate; and discuss respective results. If a sex and/or gender analysis was not conducted, the rationale should be given in the Discussion. We suggest that our authors consult the full [guidelines](#) before submission.

## Borders and Territories

Potential disputes over borders and territories may have particular relevance for authors in describing their research or in an author or editor correspondence address, and should be respected. Content decisions are an editorial matter and where there is a potential or perceived dispute or complaint, the editorial team will attempt to find a resolution that satisfies parties involved.

MDPI stays neutral with regard to jurisdictional claims in published maps and institutional affiliations.

## Publication Ethics Statement

*Ge/s* is a member of the Committee on Publication Ethics ([COPE](#)). We fully adhere to its [Code of Conduct](#) and to its [Best Practice Guidelines](#).

The editors of this journal enforce a rigorous peer-review process together with strict ethical policies and standards to ensure to add high quality scientific works to the field of scholarly publication. Unfortunately, cases of plagiarism, data falsification, image manipulation, inappropriate authorship credit, and the like, do arise. The editors of *Ge/s* take such publishing ethics issues very seriously and are trained to proceed in such cases with a zero tolerance policy.

Authors wishing to publish their papers in *Ge/s* must abide to the following:

- Any facts that might be perceived as a possible conflict of interest of the author(s) must be disclosed in the paper prior to submission.
- Authors should accurately present their research findings and include an objective discussion of the significance of their findings.
- Data and methods used in the research need to be presented in sufficient detail in the paper, so that other researchers can replicate the work.
- Raw data should preferably be publicly deposited by the authors before submission of their manuscript. Authors need to at least have the raw data readily available for presentation to the referees and the editors of the journal, if requested. Authors need to ensure appropriate measures are taken so that raw data is retained in full for a reasonable time after publication.
- Simultaneous submission of manuscripts to more than one journal is not tolerated.
- The journal accepts exact translations of previously published work. All submissions of translations must conform with our [policies on translations](#).
- If errors and inaccuracies are found by the authors after publication of their paper, they need to be promptly communicated to the editors of this journal so that appropriate actions can be taken. Please refer to our [policy regarding Updating Published Papers](#).
- Your manuscript should not contain any information that has already been published. If you include already published figures or images, please obtain the necessary permission from the copyright holder to publish under the CC-BY license. For further information, see the [Rights and Permissions](#) page.
- Plagiarism, data fabrication and image manipulation are not tolerated.
  - **Plagiarism is not acceptable** in *Ge/s* submissions.

Plagiarism includes copying text, ideas, images, or data from another source, even from your own publications, without giving any credit to the original source.

Reuse of text that is copied from another source must be between quotes and the original source must be cited. If a study's design or the manuscript's structure or language has been inspired by previous works, these works must be explicitly cited.

All MDPI submissions are checked for plagiarism using the industry standard software iThenticate. If plagiarism is detected during the peer review process, the manuscript may be rejected. If plagiarism is detected after publication, an investigation will take place and action taken in accordance with our policies.

- **Image files must not be manipulated or adjusted in any way** that could lead to misinterpretation of the information provided by the original image.

Irregular manipulation includes: 1) introduction, enhancement, moving, or removing features from the original image; 2) grouping of images that should obviously be presented separately (e.g., from different parts of the same gel, or from different gels); or 3) modifying the contrast, brightness or color balance to obscure, eliminate or enhance some information.

If irregular image manipulation is identified and confirmed during the peer review process, we may reject the manuscript. If irregular image manipulation is identified and confirmed after publication, we may correct or retract the paper.

Our in-house editors will investigate any allegations of publication misconduct and may contact the authors' institutions or funders if necessary. If evidence of misconduct is found, appropriate action will be taken to correct or retract the publication. Authors are expected to comply with the best ethical publication practices when publishing with MDPI.

### Citation Policy

Authors should ensure that where material is taken from other sources (including their own published writing) the source is clearly cited and that where appropriate permission is obtained.

Authors should not engage in excessive self-citation of their own work.

Authors should not copy references from other publications if they have not read the cited work.

Authors should not preferentially cite their own or their friends', peers', or institution's publications.

Authors should not cite advertisements or advertorial material.

In accordance with COPE guidelines, we expect that "original wording taken directly from publications by other researchers should appear in quotation marks with the appropriate citations." This condition also applies to an author's own work. COPE have produced a discussion document on [citation manipulation](#) with recommendations for best practice.

### Reviewer Suggestions

During the submission process, please suggest five potential reviewers with the appropriate expertise to review the manuscript. The editors will not necessarily approach these referees. Please provide detailed contact information (address, homepage, phone, e-mail address). The proposed referees should neither be current collaborators of the co-authors nor have published with any of the co-authors of the manuscript within the last five years. Proposed reviewers should be from different institutions to the authors. You may identify appropriate Editorial Board members of the journal as potential reviewers. You may suggest reviewers from among the authors that you frequently cite in your paper.

### English Corrections

To facilitate proper peer-reviewing of your manuscript, it is essential that it is submitted in grammatically correct English. Advice on some specific language points can be found [here](#).

MDPI provides minor English editing by native English speakers for all accepted papers, included in the APC. The APC does not cover extensive English editing. Your paper could be returned to you at the English editing stage of the publication process if extensive editing is required. You may choose to use a paid language-editing service, such as MDPI's [Author Services](#), before submitting your paper for publication. If you use an alternative service that provides a confirmation certificate, please send a copy to the Editorial Office. Authors from economically developing countries or nations should consider registration with [AuthorAid](#), a global research community that provides networking, mentoring, resources and training for researchers.

### Preprints and Conference Papers

*Ge/s* accepts submissions that have previously been made available as preprints provided that they have not undergone peer review. A preprint is a draft version of a paper made available online before submission to a journal.

MDPI operates [Preprints](#), a preprint server to which submitted papers can be uploaded directly after completing journal submission. Note that *Preprints* operates independently of the journal and posting a preprint does not affect the peer review process. Check the *Preprints* [instructions for authors](#) for further information.

Expanded and high-quality conference papers can be considered as articles if they fulfill the following requirements: (1) the paper should be expanded to the size of a research article; (2) the conference paper should be cited and noted on the first page of the paper; (3) if the authors do not hold the copyright of the published conference paper, authors should seek the appropriate permission from the copyright holder; (4) authors are asked to disclose that it is conference paper in their cover letter and include a statement on what has been changed compared to the original conference paper. *Ge/s* does not publish pilot studies or studies with inadequate statistical power.

Unpublished conference papers that do not meet the above conditions are recommended to be submitted to the [Proceedings Series journals](#).

### Authorship

MDPI follows the International Committee of Medical Journal Editors ([ICMJE](#)) guidelines which state that, in order to qualify for authorship of a manuscript, the following criteria should be observed:

- Substantial contributions to the conception or design of the work; or the acquisition, analysis, or interpretation of data for the work; AND
- Drafting the work or revising it critically for important intellectual content; AND
- Final approval of the version to be published; AND
- Agreement to be accountable for all aspects of the work in ensuring that questions related to the accuracy or integrity of any part of the work are appropriately investigated and resolved.

Those who contributed to the work but do not qualify for authorship should be listed in the acknowledgments. More detailed guidance on authorship is given by the [International Council of Medical Journal Editors \(ICMJE\)](#).

Any change to the author list should be approved by all authors including any who have been removed from the list. The corresponding author should act as a point of contact between the editor and the other authors and should keep co-authors informed and involve them in major decisions about the publication. We reserve the right to request confirmation that all authors meet the authorship conditions.

For more details about authorship please check [MDPI ethics website](#).

### Reviewers Recommendation

Authors can recommend potential reviewers. Journal editors will check to make sure there are no conflicts of interest before contacting those reviewers, and will not consider those with competing interests. Reviewers are asked to declare any conflicts of interest. Authors can also enter the names of potential peer reviewers they wish to exclude

from consideration in the peer review of their manuscript, during the initial submission progress. The editorial team will respect these requests so long as this does not interfere with the objective and thorough assessment of the submission.

## **Editorial Independence**

### **Lack of Interference With Editorial Decisions**

Editorial independence is of utmost importance and MDPI does not interfere with editorial decisions. All articles published by MDPI are peer reviewed and assessed by our independent editorial boards, and MDPI staff are not involved in decisions to accept manuscripts. When making an editorial decision, we expect the academic editor to make their decision based only upon:

- The suitability of selected reviewers;
- Adequacy of reviewer comments and author response;
- Overall scientific quality of the paper.

In all of our journals, in every aspect of operation, MDPI policies are informed by the mission to make science and research findings open and accessible as widely and rapidly as possible.

### **Editors and Editorial Staff as Authors**

Editorial staff or editors shall not be involved in processing their own academic work. Submissions authored by editorial staff/editors will be assigned to at least two independent outside reviewers. Decisions will be made by other Editorial Board Members who do not have a conflict of interest with the author. Journal staff are not involved in the processing of their own work submitted to any MDPI journals.

### **Conflicts of Interest**

According to The International Committee of Medical Journal Editors, “Authors should avoid entering into agreements with study sponsors, both for-profit and non-profit, that interfere with authors’ access to all of the study’s data or that interfere with their ability to analyze and interpret the data and to prepare and publish manuscripts independently when and where they choose.”

All authors must disclose all relationships or interests that could inappropriately influence or bias their work. Examples of potential conflicts of interest include but are not limited to financial interests (such as membership, employment, consultancies, stocks/shares ownership, honoraria, grants or other funding, paid expert testimonies and patent-licensing arrangements) and non-financial interests (such as personal or professional relationships, affiliations, personal beliefs).

Authors can disclose potential conflicts of interest via the online submission system during the submission process. Declarations regarding conflicts of interest can also be collected via the [MDPI disclosure form](#). The corresponding author must include a summary statement in the manuscript in a separate section “Conflicts of Interest” placed just before the reference list. The statement should reflect all the collected potential conflicts of interest disclosures in the form.

See below for examples of disclosures:

Conflicts of Interest: Author A has received research grants from Company A. Author B has received a speaker honorarium from Company X and owns stocks in Company Y. Author C has been involved as a consultant and expert witness in Company Z. Author D is the inventor of patent X.

If no conflicts exist, the authors should state:

Conflicts of Interest: The authors declare no conflicts of interest.

## Editorial Procedures and Peer-Review

### *Initial Checks*

All submitted manuscripts received by the Editorial Office will be checked by a professional in-house *Managing Editor* to determine whether they are properly prepared and whether they follow the ethical policies of the journal. Manuscripts that do not fit the journal's ethics policy or do not meet the standards of the journal will be rejected before peer-review. Manuscripts that are not properly prepared will be returned to the authors for revision and resubmission. After these checks, the *Managing Editor* will consult the journals' *Editor-in-Chief* or *Associate Editors* to determine whether the manuscript fits the scope of the journal and whether it is scientifically sound. No judgment on the potential impact of the work will be made at this stage. Reject decisions at this stage will be verified by the *Editor-in-Chief*.

### *Peer-Review*

Once a manuscript passes the initial checks, it will be assigned to at least two independent experts for peer-review. A single-blind review is applied, where authors' identities are known to reviewers. Peer review comments are confidential and will only be disclosed with the express agreement of the reviewer.

In the case of regular submissions, in-house assistant editors will invite experts, including recommendations by an academic editor. These experts may also include *Editorial Board Members* and Guest Editors of the journal. Potential reviewers suggested by the authors may also be considered. Reviewers should not have published with any of the co-authors during the past three years and should not currently work or collaborate with any of the institutions of the co-authors of the submitted manuscript.

### *Optional Open Peer-Review*

The journal operates optional open peer-review: *Authors are given the option for all review reports and editorial decisions to be published alongside their manuscript. In addition, reviewers can sign their review, i.e., identify themselves in the published review reports.* Authors can alter their choice for open review at any time before publication, but once the paper has been published changes will only be made at the discretion of the *Publisher* and *Editor-in-Chief*. We encourage authors to take advantage of this opportunity as proof of the rigorous process employed in publishing their research. To guarantee impartial refereeing, the names of referees will be revealed only if the referees agree to do so, and after a paper has been accepted for publication.

### *Editorial Decision and Revision*

All the articles, reviews and communications published in MDPI journals go through the peer-review process and receive at least two reviews. The in-house editor will communicate the decision of the academic editor, which will be one of the following:

- *Accept after Minor Revisions:*  
The paper is in principle accepted after revision based on the reviewer's comments. Authors are given five days for minor revisions.
- *Reconsider after Major Revisions:*  
The acceptance of the manuscript would depend on the revisions. The author needs to provide a point by point response or provide a rebuttal if some of the reviewer's comments cannot be revised. A maximum of two rounds of major revision per manuscript is normally provided. Authors will be asked to resubmit the revised paper within a suitable time frame, and the revised version will be returned to the reviewer for further comments. If the required revision time is estimated to be longer than 2 months, we will recommend that authors withdraw their manuscript before resubmitting so as to avoid unnecessary time pressure and to ensure that all manuscripts are sufficiently revised.
- *Reject and Encourage Resubmission:*  
If additional experiments are needed to support the conclusions, the manuscript will be rejected and the authors will be encouraged to re-submit the paper once further experiments have been conducted.
- *Reject.*  
The article has serious flaws, and/or makes no original significant contribution. No offer of resubmission to the journal is provided.



All reviewer comments should be responded to in a point-by-point fashion. Where the authors disagree with a reviewer, they must provide a clear response.

#### *Author Appeals*

Authors may appeal a rejection by sending an e-mail to the Editorial Office of the journal. The appeal must provide a detailed justification, including point-by-point responses to the reviewers' and/or Editor's comments using an [appeal form](#). Appeals can only be submitted following a "reject and decline resubmission" decision and should be submitted within three months from the decision date. Failure to meet these criteria will result in the appeal not being considered further. The *Managing Editor* will forward the manuscript and related information (including the identities of the referees) to a designated *Editorial Board Member*. The Academic Editor being consulted will be asked to provide an advisory recommendation on the manuscript and may recommend acceptance, further peer-review, or uphold the original rejection decision. This decision will then be validated by the *Editor-in-Chief*. A reject decision at this stage is final and cannot be reversed.

#### *Production and Publication*

Once accepted, the manuscript will undergo professional copy-editing, English editing, proofreading by the authors, final corrections, pagination, and, publication on the [www.mdpi.com](http://www.mdpi.com) website.

#### **Promoting Equity, Diversity and Inclusiveness Within MDPI Journals**

Our Managing Editors encourage the Editors-in-Chief and Associate Editors to appoint diverse expert Editorial Boards. This is also reflective in our multi-national and inclusive workplace. We are proud to create equal opportunities without regard to gender, ethnicity, sexual orientation, age, religion, or socio-economic status. There is no place for discrimination in our workplace and editors of MDPI journals are to uphold these principles in high regard.



Review

# Injectable Thermoresponsive Hydrogels for Cancer Therapy: Challenges and Prospects

Sandrine Tanga<sup>1</sup>, Marique Aucamp<sup>1</sup> and Poornima Ramburrun<sup>2,\*</sup>

<sup>1</sup> School of Pharmacy, Faculty of Natural Sciences, University of the Western Cape, Bellville, 7535, South Africa; 3723884@myuwc.ac.za, maucamp@uwc.ac.za

<sup>2</sup> Wits Advanced Drug Delivery Platform Research Unit, Department of Pharmacy and Pharmacology, School of Therapeutic Science, Faculty of Health Sciences, University of Witwatersrand, 7 York Road Parktown, Johannesburg, 2193, South Africa; poornima.ramburrun@wits.ac.za

\* Correspondence: poornima.ramburrun@wits.ac.za

**Abstract:** The enervating side effects of chemotherapeutic drugs have necessitated the use of targeted drug delivery in cancer therapy. To that end, thermoresponsive hydrogels have been employed to improve the accumulation and maintenance of drug release at the tumour site. Despite their efficiency, very few thermoresponsive hydrogel-based drugs have undergone clinical trials, and even fewer have received FDA approval for cancer treatment. This review discusses the challenges of designing thermoresponsive hydrogels for cancer treatment and offers suggestions for these challenges as available in literature. Furthermore, the argument for drug accumulation is challenged by the revelation of structural and functional barriers in tumours that may not support targeted drug release from hydrogels. Other highlights involve the demanding preparation process of thermoresponsive hydrogels, which often involve poor drug loading and difficulties in controlling the lower critical solution temperature and gelation kinetics. Additionally, the shortcomings in the administration process of thermosensitive hydrogels are examined, and special insight into the injectable thermosensitive hydrogels that reached clinical trials for cancer treatment is provided.

**Keywords:** thermoresponsive hydrogels, cancer, injectable hydrogels, chemotherapy, polymers, intratumoral hydrogels

## 1. Introduction

Since their introduction in the 1960s, injectable thermoresponsive/thermosensitive hydrogels have been employed for the delivery of chemotherapeutic drugs for cancer therapy. The ability of thermoresponsive hydrogels to remain at the tumour site upon injection has demonstrated their efficiency for targeted therapy and subsequent success over conventional injectable chemotherapeutics. Thermoresponsive hydrogels are able to limit systemic circulation, which causes debilitating side effects such as cardiotoxicity, gastrototoxicity, nephrotoxicity, immunosuppression, and myelosuppression, which stem from the use of intravenously injected chemotherapeutic drugs. The thermal response of injectable hydrogels relies on the transition of solution to solid/ semi-solid

**Citation:** To be added by editorial staff during production.

Academic Editor: Firstname  
Lastname

Received: date  
Revised: date  
Accepted: date  
Published: date



**Copyright:** © 2023 by the authors. Submitted for possible open access publication under the terms and conditions of the Creative Commons Attribution (CC BY) license (<https://creativecommons.org/licenses/by/4.0/>).

physiological temperature ( $\sim 37$  °C). These hydrogels are often reversible; therefore, temperature changes control their chemical and physical state. Figure 1 demonstrates the physical and chemical changes of thermoresponsive hydrogels from solution to gel state. Examples of thermoresponsive hydrogels used in cancer therapy include natural polymers, proteins or polypeptides, poly(N-isopropyl acrylamide) (PNIPAM), and poly(ethylene glycol) (PEG)-based block copolymers [1–3]. These polymers demonstrate a lower critical solution temperature (LCST) or an upper critical solution temperature (UCST). Below the LCST, the polymers remain in a solution state and become more viscous as the temperature increases. Above the LCST, the polymers undergo a state of gelation. This change from hydrophilic to hydrophobic properties demonstrates the amphiphilic nature of thermoresponsive polymers. Several factors can influence this transition process including the ratio of polymer to hydrophilic components, the dispersion medium and the concentration of hydrophobic contents [4]. Hydrogels that are formed upon cooling of a polymer solution have an upper critical solution temperature (e.g. gelatin), but this approach may not be suited for intratumoral cancer treatment due to their lack of solidification at normal body temperature and the inability to inject a solid gel. These systems also require high temperatures to prepare the formulation, which may cause instability of the loaded drug and other excipients.

Compared to other stimuli-responsive hydrogels like photo-, pH-, and radio-sensitive hydrogels, temperature-responsive hydrogels are easier to manipulate, do not need additional reagents or equipment to elicit the desired effect, and have wider applicability. These hydrogels simply rely on physiological temperature to undergo physical transition at approximately 37 °C. The enhanced applicability of thermosensitive hydrogels for cancer treatment is evidenced in their rigorous examination in literature compared to other stimuli-responsive hydrogels. Despite their relevance, thermoresponsive hydrogels present challenges in their design strategy, with drug loading hurdles, deficient degradation, poor mechanical strength, instability, and administration difficulties.

This review discusses the current challenges in the design and use of thermoresponsive hydrogels in cancer therapy and provides an overview of their future prospects. Knowledge in this area will help researchers understand pertinent matters to consider when undertaking research and development in thermoresponsive hydrogels for cancer treatment and thus guide them in forming new strategies to overcome the challenges discussed herein. The unique approach of this review is in its considerations of physiological barriers and the provision of a detailed evaluation of thermoresponsive injectable hydrogels that have been translated to clinical use.

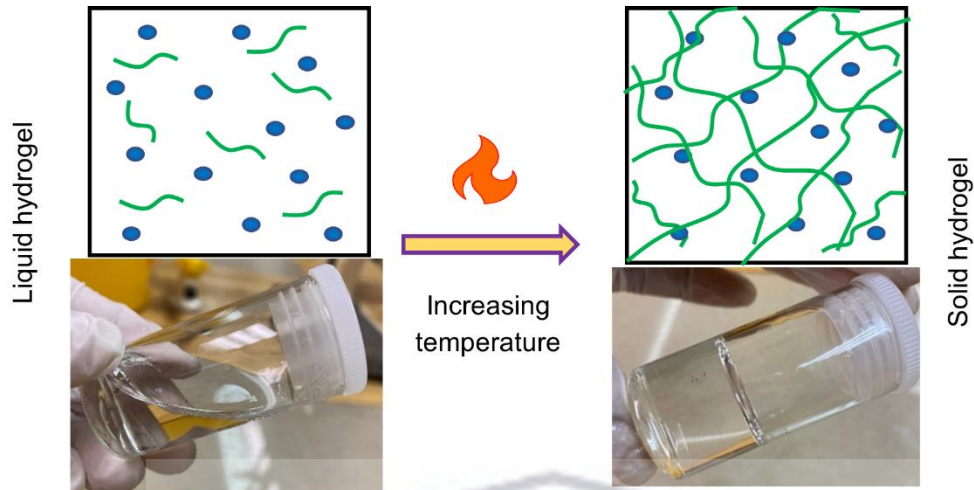


Figure 1: Sol-gel transition of a thermoresponsive hydrogel.

## 2. Physiological barriers to drug delivery in cancerous tumours

Intratumoral delivery provides a significant advantage over intravenous delivery of chemotherapeutics. Direct injection at the site of the tumour can limit systemic circulation and maximise the drug concentration at the target site, thus reducing the side effects of chemotherapeutics and their dosing frequency (Figure 2). Despite these benefits, tumorous tissue has several physical barriers that may obstruct the efficacy of chemotherapeutics by intratumoral delivery from thermoresponsive hydrogels.

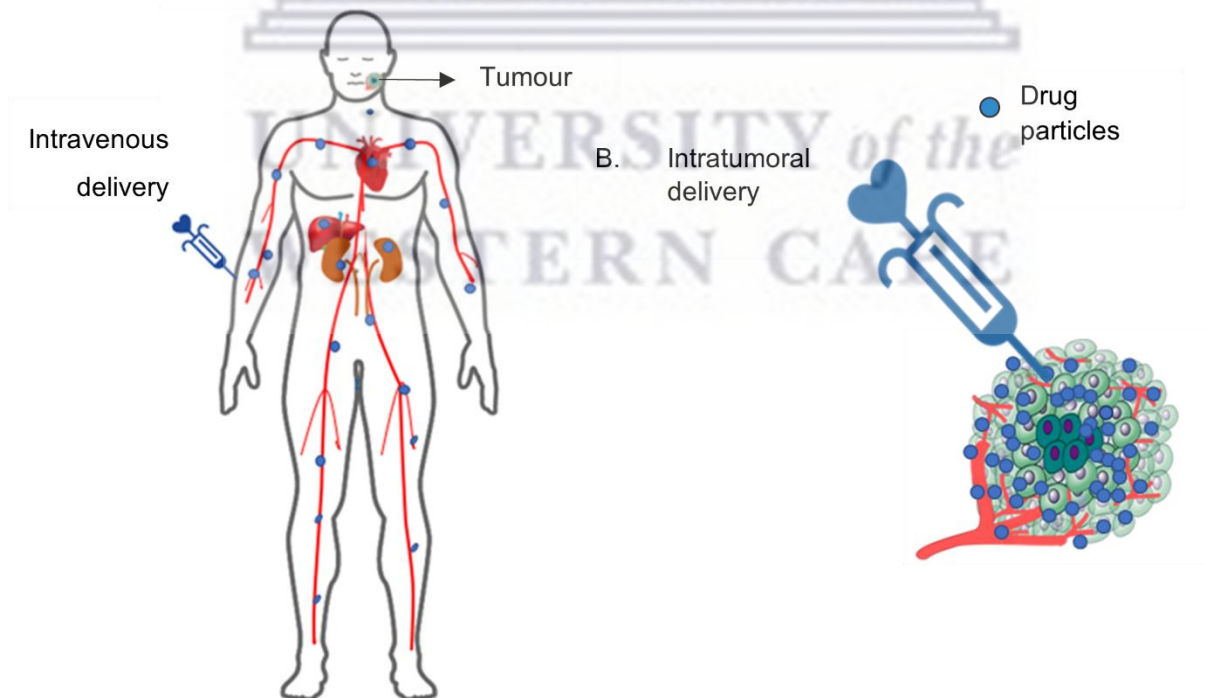


Figure 2: Intravenous delivery and intratumoral delivery. A. Intravenous delivery: the drug is systemically circulated throughout the body. B. Intratumoral delivery: the drug remains localised within the tumour.

The tumour is characterised by abnormal vascular growth, a leaky interstitial fluid-filled space with high pressure, and a hypoxic and acidic hostile microenvironment, as depicted in Figure 3. While the interstitial space is advantageous for the accumulation of solidified thermosensitive gels, it can also pose a challenge to drug distribution. Thermosensitive hydrogels with low viscosity and a long gelation time can easily flow out of the tumour and into the systemic circulation via the high-pressure flow in the interstitial space. Additionally, there is a risk of such systems leaking out through the injection site. The hypoxic environment and acidic variations from the tumour surface to the tumour core may affect drug efficacy at the tumour site [5]. Thermosensitive hydrogels often have a pH-dependent release behaviour with improved release kinetics at lower pH ranges [6]. With the core of a tumour being the most acidic region, thermosensitive hydrogels may demonstrate enhanced performance and drug release kinetics with that acidic microenvironment, yet the core has the least need for chemotherapy due to its necrotic centre. The surface of the tumour is the least acidic region and may be slightly affected with reduced efficacy even though it has the greatest need for chemotherapy since it hosts viable cancer cells. The size of the tumour may also affect the dosing requirements of thermosensitive hydrogels. Selecting the most appropriate dosing regimen may vary based on the agent or combination of agents utilised and the size of the tumour. A larger tumour may need a larger volume of the delivery vehicle so that the whole tumour area is targeted, while smaller tumours or resected tumours may need a smaller volume of the delivery system to avoid unnecessary contact with healthy tissues. Tumours located in areas that endure movements, such as oral cancer and cancerous arthritis located in the joints, require gels that have excellent mechanical strength, elasticity, and adhesion capacity, else there is a risk of displacing the gel system to non-targeted areas.

Tumours are largely heterogeneous based on their location, size and functional requisites. However, the physiological challenges of tumours are minor compared to the benefits of drug accumulation promised by thermosensitive hydrogels.

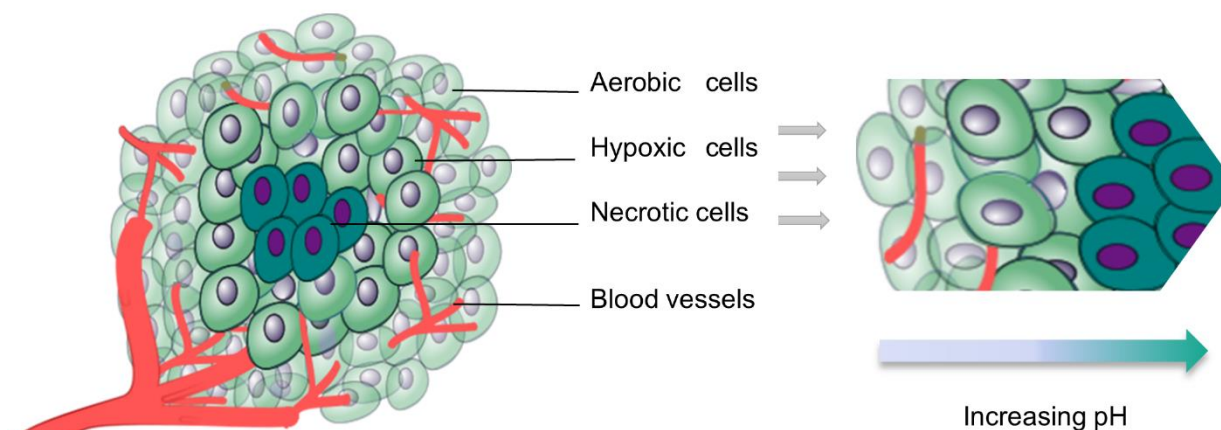


Figure 3: Tumour structure showing hypoxic and acidic variations in different regions.

### 3. Selection and preparation of injectable thermosensitive hydrogels

The design of injectable thermosensitive hydrogels involves careful consideration of the type of polymers and the type of crosslinking method used. Factors such as rheological behaviour and release kinetics are determined by these selections and ultimately influence the behaviour of the thermosensitive hydrogel during preparation and dictate their *in vivo* and *in vitro* success.

#### - Physical vs chemical crosslinking

Thermosensitive hydrogels can either be prepared via physical or chemical crosslinking. Physical crosslinking entails the linking of one polymer chain to another to produce a thermosensitive effect through non-covalent bonding. These hydrogels undergo electrostatic interactions, hydrophobic interactions, stereocomplexation and van der Waals forces, which enable them to exhibit a reversible response to temperature [7–9]. Unlike physical crosslinking, chemical crosslinking occurs through the formation of covalent bonds, such as click chemistry, Michael-type addition, Schiff base reactions, photopolymerisation and disulfide bond formation [10–12]. Chemically crosslinked hydrogels are not reversible, which may be undesirable for laboratory preparation and clinical use, because once removed from cold storage, the hydrogel must be used, and no further modifications can be made to the formulation. However, the covalent bond formed between the chains of chemically crosslinked polymers enhances their stability in physiological conditions. This stability permits their dissolution within surrounding fluids, thus limiting their degradation and release rate of drug molecules by diffusion. Physically crosslinked hydrogels suffer poor stability and tunability limitations, whereas hydrogels obtained via chemical crosslinking possess better injectability properties and improved stability [13]. A remarkable study by Han and

colleagues portrayed the superior tunability of chemically crosslinked hydrogels. In their study, a chemically crosslinked injectable thermosensitive hydrogel was successfully designed using dialdehyde-functionalised polyethylene and  $\beta$ -glycerophosphate crosslinked chitosan for the delivery of intratumoral doxorubicin [14]. Due to Schiff's reaction, the thermosensitive hydrogels could achieve self-restoration after their destruction and were able to provide sustained release of the drug while maintaining the integrity and function of the hydrogel [14]. The swelling behaviour in physically crosslinked gels is less significant than in chemically crosslinked hydrogels [15]. Consequently, chemically crosslinked hydrogels perform more consistently *in vivo* and *in vitro* than physically crosslinked hydrogels. Nonetheless, despite the accolades of chemically crosslinked thermosensitive hydrogels, the requirement of enzymes, crosslinking agents, and/ or organic solvents, has potentially toxic effects; they may undergo cross-reactivity with components of the biological system, damage cells and denature incorporated bioactive molecules, which may limit the overall application of the injectable hydrogel.

#### - Natural vs synthetic hydrogels

Natural polysaccharide polymers, such as chitosan, hyaluronic acid, alginate and cellulose, have the general advantage of excellent biocompatibility and biodegradability, which makes them preferred candidates for thermoresponsive hydrogel carriers. These polymers are abundant in nature, with good swelling and healing properties. However, their limitation lies in their extremely poor thermal response and therefore restricted applicability. For example, chitosan must be used with glycerophosphate to enhance thermal sensitivity [16–18]. This strategy produces a very slow gelation time (~10min) which may lead to premature drug release upon injection and potential toxicity [19]. If the system is injected and remains a solution for an extended period, it may travel to neighbouring blood vessels outside the tumour and release the drug before it gels. Chitosan-glycerophosphate produces a fast release of low molecular weight drugs owing to its poor mechanical strength, making it undesirable for chemotherapeutics where long-term drug release is desired [19, 20]. Moreover, the system's inability to completely reverse from gel to solution after sol-gel transition, was reported by Lu and colleagues [21]. Hyaluronic acid does not favour long-term release as it possesses a very short half-life due to its fast enzymatic degradation by hyaluronidase. Butanediol diglycidyl ether and divinyl sulfone are used to slow the degradation rate of hyaluronic acid al-[22]. A common attribute between chitosan and hyaluronic acid is that chemical modifications, covalent crosslinking, and gelling agents must be used with these polymers to obtain a gel since they are unable to form hard gels on their own [23, 24]. For cellulose, increasing its alkyl groups increases the gelation rate. Methylcellulose, carboxymethyl cellulose, and hydroxypropyl cellulose have shown similar sol-gel behaviour and have been investigated as chemotherapeutic drug carriers [25–27]. Interestingly, chitosan and carboxymethyl cellulose have shown dual sensitivity to pH and temperature [28].

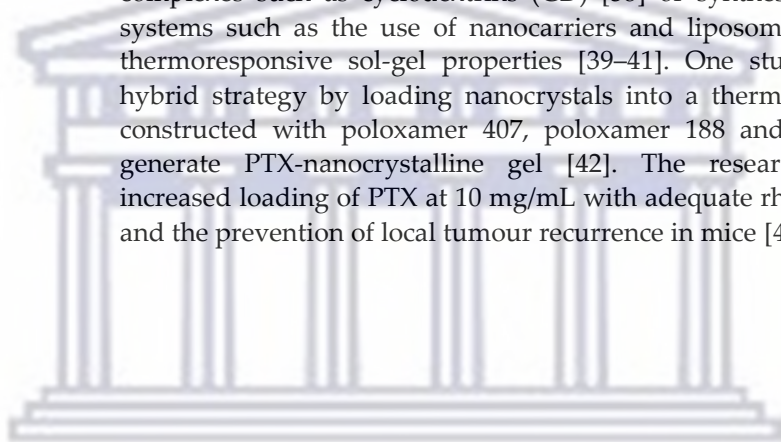
The gelation shortcomings of natural hydrogels have necessitated the introduction of synthetic polymers such as PNIPAM and triblock polymers based on polycaprolactone (PCL), poly(D,L-lactide) (PLA), poly(ethylene glycol) (PEG) and poly(amino ester urethane). These polymers can demonstrate rapid thermal response at body temperature and have greater versatility. In contrast to natural thermoresponsive polymers, the greatest weakness of synthetic polymers is their poor biocompatibility and biodegradability. Researchers generally rely on both natural and synthetic polymers for the design of hybrid thermoresponsive hydrogels to obtain desired effects of the biocompatible properties of natural polymers and the tunable properties of synthetic polymers. However, composite hydrogel blends of natural and synthetic polymers may yield viscous gels that are both difficult and painful to inject. There are also concerns of the toxicity of synthetic hydrogel monomers [29]. Extensive work has been conducted to improve the mechanical strength and degradability of synthetic hydrogels while limiting their toxicity. Patenaude and Hoare [30] reported the design of aldehyde-hydrazide-functionalised PNIPAM oligomers with molecular weights below the renal cutoff. The modified PNIPAM was able to degrade over several weeks into non-toxic, low molecular-weight oligomers. Synthetic-natural thermosensitive hydrogels have reported improved system functions such as mechanical strength and rheological behaviour compared to their individual counterparts [2, 31, 32].

- The drug-loading dilemma

Most chemotherapeutic drugs are classified under the biopharmaceutics classification system (BCS) as either class II or IV, with low solubility. A single chemotherapeutic agent is often approved for multiple cancer types – increasing their market demand. For example, paclitaxel (PTX) shows anti-cancer activity against breast, colon, and ovarian cancer, yet it is ranked amongst the lowest soluble chemotherapeutic drugs. Table 1 outlines the poor solubility of chemotherapeutic drugs and their uses in cancer. The extremely low solubility data confirms that there is an increased need for improved delivery of poorly soluble chemotherapeutics since their solubility challenges have severely limited their clinical translation. In contrast, thermoresponsive polymers are mostly soluble in water and their thermoresponsive effect is significantly decreased by the addition of chemotherapeutic drug solvents such as methanol, ethanol, tertiary-butanol and dimethyl sulfoxide [33, 34]. Three common types of thermosensitive hydrogels are often employed for thermosensitive hydrogel constructs: diblock copolymers like poly(ethylene glycol)-b-poly(D, L-lactide-co-glycolide) (PEG-b-PLGA), triblock copolymers like poloxamers, and PNIPAM. Diblock copolymers are generally composed of a hydrophilic PEG block and a hydrophobic attachment, for example, methoxy poly(ethylene glycol)-poly-ε-caprolactone (MPEG-PCL) [35]. The PEG component introduces compatibility and controls the drug release, while the hydrophobic segment can introduce biodegradability and mediate the encapsulation of hydrophobic drugs. Although the presence of the hydrophilic moiety is essential for sol-gel transition, it also contributes to



poor drug loading of hydrophobic chemotherapeutics. This concept is further exaggerated in triblock copolymers, which contain a hydrophobic A-block and a hydrophilic B-block unit. Poloxamers such as poloxamer 407, 188, and 388 are made of only one poly(propylene oxide) group and two hydrophilic blocks [36]; thus, the loading of hydrophobic chemotherapeutics into poloxamer-based hydrogels is therefore severely limited. Insoluble drugs may also become heterogeneously distributed within the hydrogels, leading to variabilities and non-uniformity of drug release rates from hydrogel samples. Consequently, hydrogel matrices with hydrophilic end blocks exhibit poor solubility, limited drug-carrying capacity and stability to sustain drug release for prolonged periods. Figure 4 depicts the sol-gel transition and drug loading of diblock and triblock copolymers. Attempts to improve this deficiency in amphiphilic thermosensitive hydrogels have been explored by combining block copolymers of differing molecular weights and ratios [37], including complexes such as cyclodextrins (CD) [38] or synthesising dual delivery systems such as the use of nanocarriers and liposomes, with targets for thermoresponsive sol-gel properties [39–41]. One study maximised this hybrid strategy by loading nanocrystals into a thermosensitive hydrogel constructed with poloxamer 407, poloxamer 188 and carbomer 974P to generate PTX-nanocrystalline gel [42]. The researchers reported an increased loading of PTX at 10 mg/mL with adequate rheological behaviour and the prevention of local tumour recurrence in mice [42].



UNIVERSITY *of the*  
WESTERN CAPE

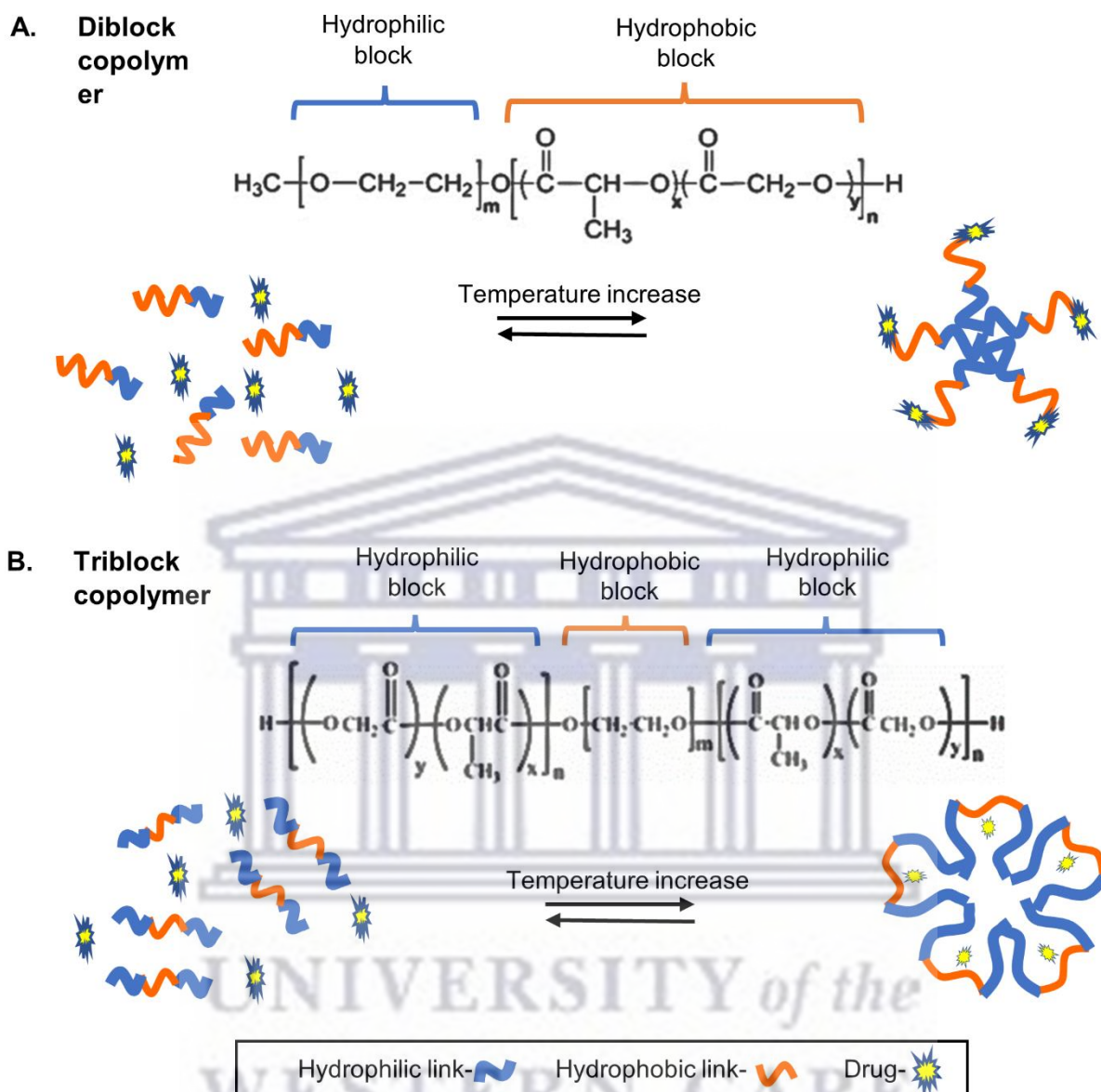


Figure 4. Schematic representation of sol-gel transition mechanisms and hydrophobic drug loading of diblock and triblock copolymers. A) Diblock copolymers (PEG-PLGA) gelate at higher temperatures with hydrophobic drugs bonded at hydrophobic end. More hydrophobic linkages present than hydrophilic ends. B) Triblock copolymers (PLGA-PEG-PLGA) gelate at increased temperature with more hydrophilic linkages and no hydrophobic ends.

Table 1. Solubility of chemotherapeutics and their examples in thermosensitive hydrogel systems

| Drug | Type of cancer commonly indicated for | Solubility in aqueous solution | Examples of thermoresponsive delivery systems | Reference |
|------|---------------------------------------|--------------------------------|---|-----------|
|------|---------------------------------------|--------------------------------|---|-----------|

|                     |   | (mg/mL)     |   |              |
|---------------------|---|-------------|---|--------------|
| <b>Cisplatin</b>    | Prostate, ovarian and bladder cancer  | ~1          | Co-delivery of resveratrol microspheres and cisplatin into pluronic-F127 hydrogel against H22 cells.                        | [43, 44]     |
| <b>Paclitaxel</b>   | Breast, colon and recurrent ovarian cancer  | ~0.002      | Paclitaxel nanocrystals loaded into poloxamer 407, poloxamer 188 and carbomer 974P against breast cancer.                   | [42, 45, 46] |
| <b>Doxorubicin</b>  | Leukemia, breast cancer, soft tissue and bone sarcoma, ovarian, bladder, thyroid, and gastric carcinoma | ~10         | Co-delivery of doxorubicin and cisplatin loaded in PLGA-PEG-PLGA hydrogel against Saos-2 and MG-63 cells.                   | [47, 48]     |
| <b>Docetaxel</b>    | Prostate cancer, metastatic breast cancer, gastric cancer   | 0.006-0.007 | Black phosphorus nanosheets and micelle docetaxel loaded in PF-127 thermoreversible hydrogel for chemophotodynamic therapy. | [49, 50]     |
| <b>Daunorubicin</b> | Leukemia  | ~0.3        | -   | [51]         |
| <b>Tamoxifen</b>    | Breast Cancer   | ~0.0003     | Tamoxifen nanoparticles loaded in PLGA-PEG-PLGA against MCF-7 cells in breast cancer.                                       | [52, 53]     |

- Lower critical solution temperature

For a thermosensitive hydrogel system to excel in its intended application, gelation must occur above room temperature but below body temperature, i.e., 26 -36 °C. However, achieving an LCST within the narrow range of 26 -36 °C is challenging. If the gelation temperature of the injectable gel is below 26 °C, gelation occurs at room temperature, leading to difficulties in manufacturing and handling. The premature gelation also risks needle clogging and consequent administration difficulties, which are elaborated on further in this review. Also, high LCSTs produced through physical crosslinking are usually accompanied by low mechanical strength at physiological temperatures [54, 55]. Many thermoresponsive polymers are restricted in their use due to their high LCSTs as presented in Table 2. However, during hydrogel preparation and drug loading, the introduction of crosslinkers, manipulations in material concentrations, polymer ratio [4] and the type of dispersion media used play a substantial role in determining the LCST of the designed hydrogel carrier. The LCST can also be manipulated by changing the copolymer block length. Increasing the block length increases the aggregation tendency of the copolymer in water, resulting in a lower LCST and quick onset of gelation at a lower

concentration [56–58]. For PEG-based amphiphilic copolymers, a lengthy polyester block, shorter PEG block, and increased hydrophobicity or crystallizability of the polyester block lead to a higher LCST. In general, increasing the ratio of hydrophobic groups results in a low LCST, while decreasing the ratio of hydrophilic groups produces a higher LCST [59]

Table 2. Lower critical solution temperature of commonly used thermosensitive polymers and polymer blends in water.

| Polymer  | Polymer concentration in aqueous solution (% w/v) | LCST (°C) | Reference |
|--|---|-----------|-----------|
| Poly( <i>N</i> -isopropyl acrylamide), PNIPAM            | ~ 2.5   | ~ 32      | [60]      |
| Poly(vinyl methyl ether), PVME                           | ~ 5   | ~ 40      | [61]      |
| PLGA-PEG-PLGA  | ~ 25  | ~ 25      | [62]      |
| Poly( <i>N</i> -vinylcaprolactam), PNVCL                 | ~ 0.5   | ~ 30      | [63]      |
| Chitosan–glycerol phosphate                              | ~ 1 CH + ~ 10 GP                                  | ~ 37      | [64]      |
| Pluronic-F127, PF-127                                    | ~ 15  | ~ 25      | -         |
| Hydroxypropyl methylcellulose, HPMC                      | ~ 1   | ~ 70      | [65]      |
| Polyphosphazene derivatives                              | ~ 2   | 25-80     | [66]      |
| Methoxy poly(ethylene glycol) (MPEG)–diblock copolymers) | ~ 1   | 32-42     | [67]      |

#### - Dynamics of drug release

The drug release behaviour of chemotherapeutics through the hydrogel matrix is impacted by various factors including hydrophobicity, mechanical strength, pore size and degradation rate. Synthetic thermoresponsive hydrogels demonstrate the rapid release of hydrophobic chemotherapeutic drugs and struggle to achieve prolonged, on-demand, and rhythmic drug delivery [6, 44, 68]. Moreover, the contrast of hydrophobic drugs in hydrophilic systems often generates a fast release rate and is characterised by an initial burst effect [69]. A synthetic hydrogel like PNIPAM is characterised by hydrophilic amide and hydrophobic propyl groups. Below its LCST, its polymer chains extend due to hydrogen bonding between the amide groups and the water molecules. Increasing the temperature weakens the hydrogen bonds between the amide and water molecules and increases the hydrogen bonding between hydrophobic interactions among the propyl groups [70]. However, PNIPAM-based hydrogels' separation from solvent and shrinkage above the LCST may permit the uncontrolled release of drug molecules [71, 72]. This poor release behaviour is also true for pluronics which encounter burst release due to their low molecular weight and mechanical strength. The many hydrogen bonds between thermosensitive polymer chains form a relatively loose and

porous three-dimensional network which allows drug molecules to easily diffuse out of the gel matrix [73]. Resolutions to this challenge are the use of hydrophobic moieties or the addition of complexing agents like CDs that allow the hydrogel system to be homogeneously incorporated with the hydrophobic drug [59, 72, 74–76]. Fiorica *et al.*, [69] designed an injectable hydrogel by using hyaluronic acid with vinyl sulfone functionalised  $\beta$ -CDs as a crosslinking agent to obtain a thermal response. Doxorubicin was loaded into the system and investigated for its use in locoregional tumours. The system maintained a sustained release of doxorubicin when tested in colorectal carcinoma micro masses. Recently, an inclusion complexation between polymerised  $\beta$ -CD and hydrophobic cholesterol end-capping polyethylene glycol, loaded with 5-fluorouracil/methotrexate was constructed as a thermoresponsive hydrogel [77]. The researchers stated that the benefit of polymerised  $\beta$ -CD, cholesterol end-capping PEG in cancer delivery had not been fully reported yet. Therefore, they sought to provide *in vitro* and *in vivo* application of the modified hydrogel in breast cancer management for the first time. Figure 5 shows the *in vitro* release profiles obtained for the two anti-cancer drugs (5-fluorouracil/methotrexate), which revealed an extended-release behaviour of up to 21 days. The novel study demonstrates the impact of the newly assembled hydrogel for controlled release and efficient delivery of the two loaded drugs. These studies also emphasise the importance of CDs in controlling the release behaviour of thermosensitive hydrogels due to their hydrophilic surface and hydrophobic core, which helps to encapsulate hydrophobic drugs.

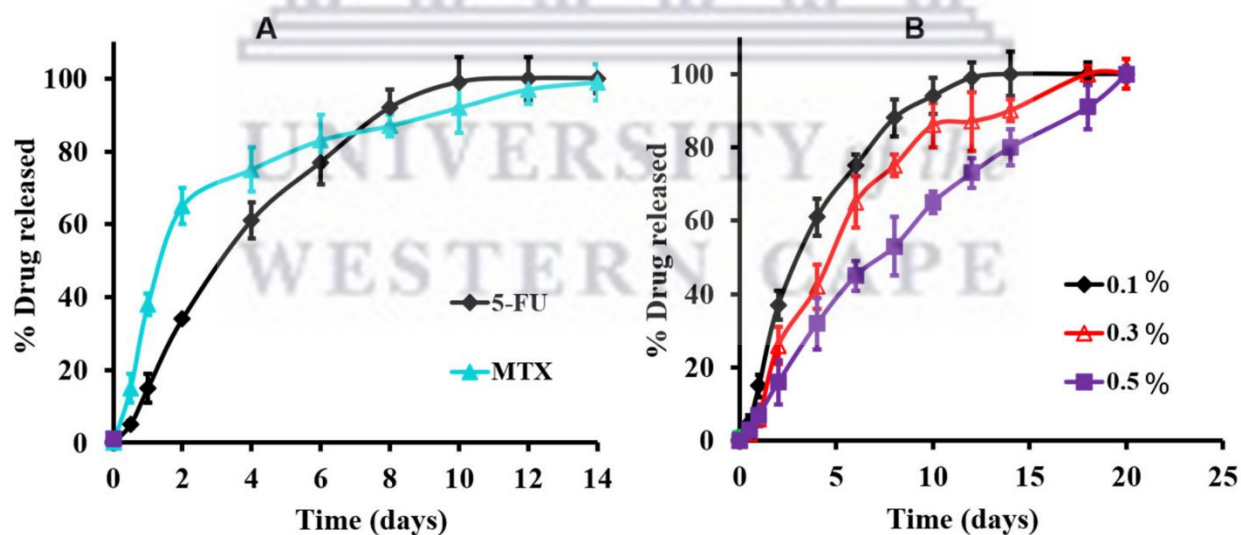


Figure 5. (A) *In vitro* release profiles of the individual 5-fluorouracil and methotrexate from the modified hydrogel at 37 °C in PBS at 0.1% drug concentration, and (B) the release profile of 5-Fluorouracil as a function of drug concentration in PBS at 37 °C [77]. Reproduced with permission from Almawash, El Hamd, and Osman 2022 © Creative Commons CC BY 4.0.

The mechanical strength of hydrogels also plays a pivotal role in determining drug release rates. Hard gels release chemotherapeutics at a slower rate, while softer gels release chemotherapeutics faster [78, 79]. As the gel hardens, the degree of porosity decreases, restricting the flow of water and drugs out of the hydrogel matrix. Sustained drug release is beneficial in cancer treatment because chemotherapeutics often require a long treatment period. Achieving this slow drug release rate through the mechanical enhancement of injectable hydrogels is difficult. While most synthetic thermosensitive systems promote rapid gelation, their formed gel severely lacks in strength [80]. This demands the need for a greater concentration of the polymer or inclusion of crosslinkers in the hydrogel system [81–85] which affects rheology, and restricts the flow of the liquid at cooler temperatures and decreases the LCST. Also, increasing synthetic polymer concentration makes the gel hard but brittle, leading to breakage of the hydrogel system and, ultimately, unsteady drug release [82]. Jiang *et al.*, [73] compared the drug release behaviour of PTX-CD loaded in chitosan (CS)/glycerol phosphate disodium salt (GP) and CS/PVA/glutaraldehyde (GA)/GP. Figure 6 shows that the mechanical strength of CS/GP was lower than that of CS/PVA/GA/GP, and consequently, the release time of PTX increased as the hardness of the hydrogel increased. Therefore, the strength and elasticity of the system hold great importance wherein the matrix remains accumulated in one area and maintains its shape within the tumour structure while retaining the drug for a prolonged period.

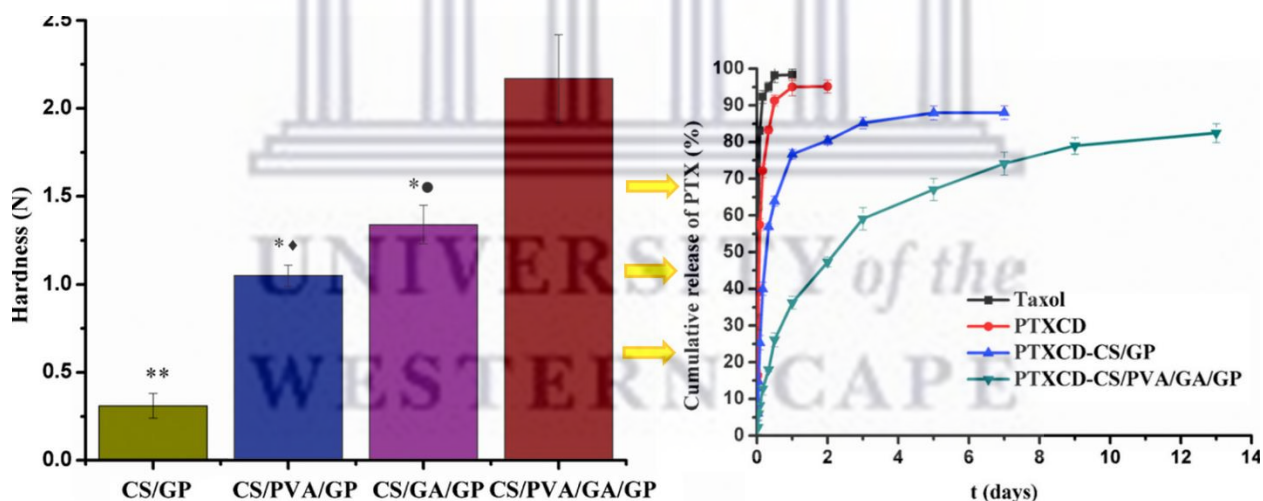


Figure 6. Drug release-dependent behaviour on mechanical strength for PTX-CD loaded hydrogels [73]. Reproduced with permission from Elsevier B.V. Ltd. © 2016

The release of chemotherapeutics is substantially influenced by the degradation rate of the thermosensitive hydrogel. This rate depends on the polymer composition, crystallinity, and topology. The issue of hydrogel degradation is of concern because most synthetic polymers possess poor biodegradation properties with rates that do not correspond to the dosing frequency of the loaded chemotherapeutic drug. Also, synthetic polymers

like PEG/polyesters produce acidic molecules that may impair drug performance [86] or promote inflammatory responses by host tissues. Their degradation time can also be very long [87], thus impeding the transport of drug molecules to the tumour via an erosion-based release mechanism. The chemical structure of the thermosensitive hydrogel [88], the inclusion of natural components like citric acid [89] or even the use of natural polymers can be exploited to develop hydrogels with tailored degradation rates and drug release behaviour. Amongst synthetic polymers, poly(lactic-co-glycolic acid) (PLGA) based hydrogels have reported the best degradation results for thermosensitive hydrogels [90, 91]

- Physical mixing hurdles

Another challenge with preparing injectable hydrogels is the large quantity requirement of the polymer concentration needed to achieve a thermal response at 37 °C, particularly for triblock copolymers [2, 92]. This is caused by the polymer's high critical micelle concentration due to weak bonds with the hydrophobic blocks. Studies report that at least 15-30% pluronic-F127 (PF-127) [44, 93, 94], 20% poly(l-lactide-co-glycolide)-poly(ethylene glycol)-poly(l-lactide-co-glycolide) (PLGA-PEG-PLGA) [95, 96], and 10% poly(organophosphazene) (PPZ) [97] are required to obtain a thermal response at physiological conditions. Hydrogels with LCST around 25 °C may also pose mixing challenges due to their high viscosity at ambient temperature. This further demands cold mixing, which may be difficult to control and maintain during the fabrication process. PEG/PLGA and polyphosphazene polymers have a paste-like consistency which hampers weighing and poses mixing challenges with the drug and other excipients. Poly( $\epsilon$ -caprolactone)-poly(ethylene glycol)-poly( $\epsilon$ -caprolactone) (PCL-PEG-PCL) has a strong crystallinity and therefore needs to be dissolved in an aqueous solution at a temperature above its melting point (60 °C). Thereafter, the polymer must be incubated at 4 °C for 24 hours to obtain a thermosensitive hydrogel – a multi-step preparation process which may limit its large-scale manufacturing and clinical translation.

#### 4. Administration of injectable thermosensitive hydrogels

The administration process of hydrogels may pose several challenges to patients and clinicians. In an attempt to reach optimal gelation properties, such as improved mechanical strength, the concentration of polymer is often increased [98]. Also, the high critical micelle concentrations of thermosensitive polymers necessitate a high concentration of copolymers to obtain gelation [99, 100], leading to a more viscous solution below the LCST. This increase in viscosity warrants the need for a large injection needle that is inserted at the tumour site, allowing the viscous hydrogel solution to flow and press against the extravascular tumour tissue as it fills the space. This is a painful experience and undoubtedly affects the patient's determination to allow repeated treatment at the tumour site. However, the use of a local anaesthetic may help prevent this scenario. If the thermosensitive gel has a low LCST, gelation of the hydrogel will occur at room temperature, causing the system to become clogged in the needle and therefore wasted. Clinicians

would have to hasten administering the injection to ensure that the gel is removed from cold storage and injected within a limited time frame before the system gels. This may be an even greater concern in undeveloped and developing tropical countries where ambient temperatures are often elevated, and there is lack of reliable cooling systems.

Another regretful administration challenge with injectable hydrogels is that they are inaccessible to internal organ cancers such as liver, pancreatic and oesophageal cancer. If a need for the system is established in such a case, the use of specialised techniques like endoscopic ultrasonography-guided fine-needle injection is required to allow direct access to the tissues. Surgery is employed for inaccessible sites such as brain and ovarian cancers. These processes require a specialist medical professional, and this can be costly and inconvenient for the patient. Metastatic cancers are also non-benefactors of injectable thermosensitive systems since they only localise at the injected tumour site. In this case, the hailed benefit of thermosensitive drug accumulation reaches a limitation. Also, for a thermosensitive hydrogel to be employed, imaging techniques must precisely identify the cancer tumour, else there is a risk of treating one tumour site while another area, unidentified by imaging, is left untreated.

#### **5. Thermoresponsive hydrogels in clinical trials: an update**

To date, clinical trials on injectable thermosensitive hydrogels for cancer treatment have been severely limited (Table 3). UroGen Pharma commercialised ReGel<sup>®</sup>; a (PLGA-PEG-PLGA)-based formulation that can undergo sol-gel transition at 37 °C. The strength of the system is in its ability to solubilise poorly soluble drugs [101, 102], and based on this advantage, OncoGel<sup>®</sup> was fabricated. OncoGel<sup>®</sup> is a chromophore free, paclitaxel formulation of triblock copolymer (PLGA-PEG-PLGA) (ReGel<sup>®</sup>) intended for local tumour management [103]. It increases paclitaxel drug loading by more than 400-fold (>10 mg/mL) and reports excellent release results and degradation over 4-6 weeks [104]. OncoGel<sup>®</sup> is currently the only existing injectable thermosensitive hydrogel that has undergone clinical trials for cancer treatment [105]. Despite efforts to make OncoGel<sup>®</sup> applicable, its phase 2 clinical trial was terminated. The researchers noted that, although safe, overall survival or tumour response remained the same when the gel was used with cisplatin/5-fluorouracil and radiation therapy in patients with previously untreated, resectable, local or local-regional adenocarcinoma or squamous cell carcinoma [106]. A dose escalation study of OncoGel<sup>®</sup> was unsuccessful in another phase 2 clinical trial when evaluated within a tumour resection cavity in the brain following surgical removal of the tumour [107].

Although not for direct injection, UGN-101 (Jelymyto<sup>®</sup>) was constructed with thermoresponsive sol-gel properties for the delivery of mitomycin in upper tract urothelial carcinoma [108]. The system is based on ReGel<sup>®</sup> and has an LCST around body temperature [109]. UGN-101 overcomes the physio-anatomical constraints of the urinary tract, where continuous urine production prevents drug retention [109]. After favourable phase 3 clinical trials, which revealed significant disease eradication and reduced nephrotoxicity [110], the system received FDA approval under the



orphan drug designation [111]. Jelymyto® has since been registered for a clinical trial to assess its efficacy and safety in recurrent patients who already received the drug for upper tract urothelial carcinoma, however, the study was withdrawn due to a lack of participants; owing to the rarity of the disease [112]. Another clinical trial was recently completed for the thermosensitive mitomycin in nonsurgical primary chemoablation of nonmuscle-invasive bladder cancer [113, 114]. The system remained durable and achieved significant recovery with no reoccurrence within one year in 65% of the patients [113].

The clinical trials presented herein validate the safety and relevance of thermosensitive hydrogels towards cancer treatment. The failed studies do not prove that thermosensitive hydrogels are ineffective, rather that more hydrogels with improved release qualities should be designed and various systems should be investigated for different cancer types. The lesson is also to look beyond the concept of intratumoral delivery and propose specialised methods to deliver thermosensitive hydrogels for various cancer types, as Jelymyto® has demonstrated.

Table 3: Thermosensitive hydrogels that have undergone clinical trials for cancer treatment

| Tradename | Encapsulated drug | Thermosensitive hydrogel | Cancer type  | Status  | References |
|-----------|-------------------|--------------------------|--|---------|------------|
| OncoGel®  | Paclitaxel        | PLGA-PEG-PLGA            | Esophageal cancer<br>Adenocarcinoma of the esophagus<br>Squamous cell carcinoma<br>Brain neoplasms | Phase 2 | [103, 105] |
|           |                   |                          | Glioblastoma Multiforme  | Phase 2 | [107]      |
| Jelymyto® | Mitomycin         | PLGA-PEG-PLGA            | Carcinoma<br>Transitional cell<br>Transitional cell<br>Carcinoma of renal pelvis<br>Bladder cancer | Phase 3 | [108, 110] |
|           |                   |                          |  | Phase 2 | [113]      |

## 6 Conclusion and future outlook

Injectable thermosensitive hydrogels are currently a popular research venture, however, there is a significant lack in their clinical translation. The challenges of tumour structural barriers, poor loading of chemotherapeutics, unsustained drug release, and inefficient gel rheology have limited their clinical efficacy. However, their promise for targeted

drug delivery at the tumour site remains the backbone of their rigorous laboratory examination. Synthetic polymers have paved the way for the enhancement and tunability of injectable thermosensitive hydrogels, but qualities of poor biocompatibility and degradability restrict their successful implementation. Natural polymers or additives for the promotion of these limitations are encouraged for use with synthetic thermosensitive hydrogels and the balancing of hydrophilic and hydrophobic components is an integral part of sol-gel behaviour. Hybrid systems like the use of nanocarriers, extravesicular carriers and inclusion complexes like cyclodextrins can tackle poor drug loading of thermosensitive hydrogels. Furthermore, the heterogeneity of different tumour types emphasises the need for personalised treatment plans.

A critical need for improved systems in the field of thermosensitive hydrogels still exists, and future research should focus on improving current or designing new synthetic polymers for the increased drug loading of hydrophobic chemotherapeutics while maintaining good mechanical strength, sol-gel transition, and biodegradable and biocompatible properties. Additional anti-cancer drugs, such as dostarlimab (recently approved for endometrial cancer), should be explored for thermosensitive hydrogel formulation. Researchers should also consider the repurposing of drug agents for thermosensitive hydrogel designs, such as aspirin and terbinafine, which have shown efficacy toward cancer cells [115, 116]. Thermosensitive hydrogels still have a long way to go in the field of advanced drug delivery. As research advances in the field of stimuli-responsive hydrogels to overcome the associated challenges, it is anticipated that more thermosensitive systems will be studied in clinical trials.

**Author Contributions:** Sandrine Tanga conceptualised, wrote, and edited the review paper. Poornima Ramburrun and Marique Aucamp reviewed and edited the paper.

**Funding:** This research received no external funding

**Conflicts of Interest:** The authors declare no conflict of interest.

## References

1. García-Couce, J.; Tomás, M.; Fuentes, G.; Que, I.; Almirall, A.; Cruz, L. J. Chitosan/Pluronic F127 Thermosensitive Hydrogel as an Injectable Dexamethasone Delivery Carrier. *Gels* **2022**, *8* (1), 44. <https://doi.org/10.3390/gels8010044>.
2. Liu, M.; Song, X.; Wen, Y.; Zhu, J.-L.; Li, J. Injectable Thermoresponsive Hydrogel Formed by Alginate-g-Poly(N-Isopropylacrylamide) That Releases Doxorubicin-Encapsulated Micelles as a Smart Drug Delivery System. *ACS Appl Mater Interfaces* **2017**, *9* (41), 35673-35682. <https://doi.org/10.1021/acsami.7b12849>.
3. Yu, S.; Zhang, D.; He, C.; Sun, W.; Cao, R.; Cui, S.; Deng, M.; Gu, Z.; Chen, X. Injectable Thermosensitive Polypeptide-Based CDDP-Complexed Hydrogel for Improving Localized Antitumor Efficacy. *Biomacromolecules* **2017**, *18* (12), 4341-4348. <https://doi.org/10.1021/acs.biomac.7b01374>.
4. Darge, H. F.; Andrgie, A. T.; Hanurrry, E. Y.; Birhan, Y. S.; Mekonnen, T. W.; Chou, H.-Y.; Hsu, W.-H.; Lai, J.-Y.; Lin, S.-Y.; Tsai, H.-C. Localized Controlled Release of Bevacizumab and Doxorubicin by Thermo-Sensitive Hydrogel for Normalization of Tumor Vasculature and to Enhance the Efficacy of Chemotherapy. *Int J Pharm* **2019**, *572*, 118799. <https://doi.org/10.1016/j.ijpharm.2019.118799>.

5. Petrova, V.; Annicchiarico-Petruzzelli, M.; Melino, G.; Amelio, I. The Hypoxic Tumour Microenvironment Hypoxia and Hypoxia-Inducible Factors. *Oncogenesis* **2018**, *7* (1), 1–13. <https://doi.org/10.1038/s41389-017-0011-9>.
6. Liu, H.; Shi, X.; Wu, D.; Kahsay Khshen, F.; Deng, L.; Dong, A.; Wang, W.; Zhang, J. Injectable, Biodegradable, Thermosensitive Nanoparticles-Aggregated Hydrogel with Tumor-Specific Targeting, Penetration, and Release for Efficient Postsurgical Prevention of Tumor Recurrence. *ACS Appl Mater Interfaces* **2019**, *11* (22), 19700–19711. <https://doi.org/10.1021/acsami.9b01987>.
7. Shi, X.; Wu, J.; Wang, Z.; Song, F.; Gao, W.; Liu, S. Synthesis and Properties of a Temperature-Sensitive Hydrogel Based on Physical Crosslinking via Stereocomplexation of PLLA-PDLA. *RSC Adv* **2020**, *10* (34), 19759–19769. <https://doi.org/10.1039/d0ra01790f>.
8. Abdolmaleki, A.; Gharibi, H.; Molavian, M. R.; Norouzi, M.; Asefifeyzabadi, N. Physicochemical Modification of Hydroxylated Polymers to Develop Thermosensitive Double Network Hydrogels. *J Appl Polym Sci* **2021**, *138* (32), 50778. <https://doi.org/10.1002/app.50778>.
9. Choi, J.; Yoon, J.; Ahn, K. H.; Choi, S.-H.; Char, K. Injectable Hydrogels with Improved Mechanical Property Based on Electrostatic Associations. *Colloid Polym Sci* **2021**, *299* (3), 575–584. <https://doi.org/10.1007/s00396-020-04726-0>.
10. Dehghan-Baniani, D.; Chen, Y.; Wang, D.; Bagheri, R.; Solouk, A.; Wu, H. Injectable in Situ Forming Kartogenin-Loaded Chitosan Hydrogel with Tunable Rheological Properties for Cartilage Tissue Engineering. *Colloids Surf B Biointerfaces* **2020**, *192*, 111059. <https://doi.org/10.1016/j.colsurfb.2020.111059>.
11. Maiti, B.; Abramov, A.; Franco, L.; Puiggali, J.; Enshaei, H.; Alemán, C.; Díaz Díaz, D.; Maiti, B.; Abramov, A.; Díaz, D. D.; Franco, L.; Puiggali, J.; Enshaei, H.; Alemán, C. Thermoresponsive Shape-Memory Hydrogel Actuators Made by Phototriggered Click Chemistry. *Adv Funct Mater* **2020**, *30* (24), 2001683. <https://doi.org/10.1002/adfm.202001683>.
12. Liao, S.; Tang, L.; Qu, J. Schiff-base-functionalized Polymeric Hydrogel with High Stretchability and Multifunction. *Polym Adv Technol* **2021**, *32* (4), 1844–1852. <https://doi.org/10.1002/pat.5225>.
13. Wu, S. W.; Liu, X.; Miller, A. L.; Cheng, Y. S.; Yeh, M. L.; Lu, L. Strengthening Injectable Thermo-Sensitive NIPAAm-g-Chitosan Hydrogels Using Chemical Cross-Linking of Disulfide Bonds as Scaffolds for Tissue Engineering. *Carbohydr Polym* **2018**, *192*, 308–316. <https://doi.org/10.1016/j.carbpol.2018.03.047>.
14. Han, X.; Meng, X.; Wu, Z.; Wu, Z.; Qi, X. Dynamic Imine Bond Cross-Linked Self-Healing Thermosensitive Hydrogels for Sustained Anticancer Therapy via Intratumoral Injection. *Materials Science and Engineering: C* **2018**, *93*, 1064–1072. <https://doi.org/10.1016/j.msec.2018.08.064>.
15. Panyamao, P.; Ruksiriwanich, W.; Sirisa-Ard, P.; Charumanee, S. Injectable Thermosensitive Chitosan/Pullulan-Based Hydrogels with Improved Mechanical Properties and Swelling Capacity. *Polymers (Basel)* **2020**, *12* (11), 2514. <https://doi.org/10.3390/polym12112514>.
16. Ramírez Barragán, C. A.; Macías Balleza, E. R.; García-Uriostegui, L.; Andrade Ortega, J. A.; Toríz, G.; Delgado, E. Rheological Characterization of New Thermosensitive Hydrogels Formed by Chitosan, Glycerophosphate, and Phosphorylated  $\beta$ -Cyclodextrin. *Carbohydr Polym* **2018**, *201*, 471–481. <https://doi.org/10.1016/j.carbpol.2018.08.076>.
17. Han Qin; Wang, J.; Wang, T.; Gao, X.; Wan, Q.; Pei, X. Preparation and Characterization of Chitosan/ $\beta$ -Glycerophosphate Thermal-Sensitive Hydrogel Reinforced by Graphene Oxide. *Front Chem* **2018**, *6*. <https://doi.org/10.3389/fchem.2018.00565>.
18. Abrami, M.; Siviello, C.; Grassi, G.; Larobina, D.; Grassi, M. Investigation on the Thermal Gelation of Chitosan/ $\beta$ -Glycerophosphate Solutions. *Carbohydr Polym* **2019**, *214*, 110–116. <https://doi.org/10.1016/j.carbpol.2019.03.015>.
19. Deng, A.; Kang, X.; Zhang, J.; Yang, Y.; Yang, S. Enhanced Gelation of Chitosan/ $\beta$ -Sodium Glycerophosphate Thermosensitive Hydrogel with Sodium Bicarbonate and Biocompatibility Evaluated. *Materials Science and Engineering: C* **2017**, *78*, 1147–1154. <https://doi.org/10.1016/j.msec.2017.04.109>.
20. Guo, B.; Wu, Y.; M Valente, A. J.; Pei, X.; Qin, H.; Wang, J.; Wang, T.; Gao, X.; Wan, Q. Preparation and Characterization of Chitosan/ $\beta$ -Glycerophosphate Thermal-Sensitive Hydrogel Reinforced by Graphene Oxide. *Frontiers in Chemistry | www.frontiersin.org* **2018**, *6*, 565. <https://doi.org/10.3389/fchem.2018.00565>.
21. Lu, S.; Yang, Y.; Yao, J.; Shao, Z.; Chen, X. Exploration of the Nature of a Unique Natural Polymer-Based Thermosensitive Hydrogel. *Soft Matter* **2016**, *12* (2), 492–499. <https://doi.org/10.1039/C5SM01947H>.
22. Al-Sibani, M.; Al-Harrasi, A.; Neubert, R. H. H. Evaluation of In-Vitro Degradation Rate of Hyaluronic Acid-Based Hydrogel Cross-Linked with 1, 4-Butanediol Diglycidyl Ether (BDDE) Using RP-HPLC and UV-Vis Spectroscopy. *J Drug Deliv Sci Technol* **2015**, *29*, 24–30. <https://doi.org/10.1016/j.jddst.2015.05.013>.

23. Jhan, H.-J.; Liu, J.-J.; Chen, Y.-C.; Liu, D.-Z.; Sheu, M.-T.; Ho, H.-O. Novel Injectable Thermosensitive Hydrogels for Delivering Hyaluronic Acid–Doxorubicin Nanocomplexes to Locally Treat Tumors. *Nanomedicine* **2015**, *10* (8), 1263–1274. <https://doi.org/10.2217/nnm.14.211>.
24. Sheu, M. T.; Jhan, H. J.; Su, C. Y.; Chen, L. C.; Chang, C. E.; Liu, D. Z.; Ho, H. O. Codelivery of Doxorubicin-Containing Thermosensitive Hydrogels Incorporated with Docetaxel-Loaded Mixed Micelles Enhances Local Cancer Therapy. *Colloids Surf B Biointerfaces* **2016**, *143*, 260–270. <https://doi.org/10.1016/J.COLSURFB.2016.03.054>.
25. Kyoung Kim, J.; Won, Y.-W.; Suk Lim, K.; Kim, Y.-H. Low-Molecular-Weight Methylcellulose-Based Thermo-Reversible Gel/Pluronic Micelle Combination System for Local and Sustained Docetaxel Delivery. *Pharm Res* **2012**, *29* (2), 52529–534. <https://doi.org/10.1007/s11095-011-0581-8>.
26. Dai, L.; Liu, R.; Hu, L.-Q.; Wang, J.-H.; Si, C.-L. Self-Assembled PEG-Carboxymethylcellulose Nanoparticles/ $\alpha$ -Cyclodextrin Hydrogels for Injectable and Thermosensitive Drug Delivery †. *RSC Adv* **2017**, *7* (5), 2905–2912. <https://doi.org/10.1039/c6ra25793c>.
27. Zhang, D.; Chu, Y.; Qian, H.; Qian, L.; Shao, J.; Xu, Q.; Yu, L.; Li, R.; Zhang, Q.; Wu, F.; Liu, B.; Liu, Q. Antitumor Activity of Thermosensitive Hydrogels Packaging Gambogic Acid Nanoparticles and Tumor-Penetrating Peptide IRGD Against Gastric Cancer. *Int J Nanomedicine* **2020**, *15*, 735–747. <https://doi.org/10.2147/IJN.S231448>.
28. Huangqin Chen; Mingwen Fan. Novel Thermally Sensitive PH-Dependent Chitosan/ Carboxymethyl Cellulose Hydrogels. *J Bioact Compat Polym* **2008**, *23* (1), 38–48. <https://doi.org/10.1177/0883911507085070>.
29. Mellati, A.; Valizadeh Kiamahalleh, M.; Dai, S.; Bi, J.; Jin, B.; Zhang, H. Influence of Polymer Molecular Weight on the in Vitro Cytotoxicity of Poly (N-Isopropylacrylamide). *Materials Science and Engineering: C* **2016**, *59*, 509–513. <https://doi.org/10.1016/J.MSEC.2015.10.043>.
30. Patenaude, M.; Hoare, T. Injectable, Degradable Thermoresponsive Poly(N-Isopropylacrylamide) Hydrogels. *ACS Macro Lett* **2012**, *1* (3), 409–413. <https://doi.org/10.1021/mz200121k>.
31. Rezazadeh, M.; Akbari, V.; Amuaghae, E.; Emami, J. *Preparation and Characterization of an Injectable Thermosensitive Hydrogel for Simultaneous Delivery of Paclitaxel and Doxorubicin*; 2018; Vol. 13.
32. Jin, X.; Fu, Q.; Gu, Z.; Zhang, Z.; Lv, H. Injectable Corilagin/Low Molecular Weight Chitosan/PLGA-PEG-PLGA Thermosensitive Hydrogels for Localized Cancer Therapy and Promoting Drug Infiltration by Modulation of Tumor Microenvironment. *Int J Pharm* **2020**, *589*, 119772. <https://doi.org/10.1016/j.ijpharm.2020.119772>.
33. Chiraphon Chaibundit; Nágila M. P. S. Ricardo; Nádja M. P. S. Ricardo; Flávia de M. L. L. Costa; Marcus G. P. Wong; Daniel Hermida-Merino; Jose Rodriguez-Perez; Ian W. Hamley; Stephen G. Yeates; Colin Booth. Effect of Ethanol on the Micellization and Gelation of Pluronic P123. *Langmuir* **2008**, *24* (21), 12260–12266. <https://doi.org/https://doi.org/10.1021/la8022425>.
34. Lee, C. H.; Bae, Y. C. Thermodynamic Framework for Switching the Lower Critical Solution Temperature of Thermo-Sensitive Particle Gels in Aqueous Solvent. *Polymer (Guildf)* **2020**, *195*, 122428. <https://doi.org/10.1016/J.POLYMER.2020.122428>.
35. Shan Xu; Xiaobo Du; Gang Feng; Yu Zhang; Jie Li; Binwei Lin; Linglin Yang; Shaozhi Fu; Jingbo Wu. Efficient Inhibition of Cervical Cancer by Dual Drugs Loaded in Biodegradable Thermosensitive Hydrogel Composites. *Oncotarget* **2018**, 282–292.
36. Boonlai, W.; Tantishaiyakul, V.; Hirun, N.; Sangfai, T.; Suknuntha, K. Thermosensitive Poloxamer 407/Poly(Acrylic Acid) Hydrogels with Potential Application as Injectable Drug Delivery System. *AAPS PharmSciTech* **2018**, *19* (5), 2103–2117. <https://doi.org/10.1208/s12249-018-1010-7>.
37. Carrillo-Castillo, T. D.; Luna-Velasco, A.; Zaragoza-Contreras, E. A.; Castro-Carmona, J. S. Thermosensitive Hydrogel for *in Situ* -Controlled Methotrexate Delivery. *e-Polymers* **2021**, *21* (1), 910–920. <https://doi.org/10.1515/epoly-2021-0085>.
38. Yang, Z.; Liu, J.; Lu, Y. Doxorubicin and CD-CUR Inclusion Complex Co-loaded in Thermosensitive Hydrogel PLGA-PEG-PLGA Localized Administration for Osteosarcoma. *Int J Oncol* **2020**, *57* (2), 433–444. <https://doi.org/10.3892/ijo.2020.5067>.
39. Xu, S.; Wang, W.; Li, X.; Liu, J.; Dong, A.; Deng, L. Sustained Release of PTX-Incorporated Nanoparticles Synergized by Burst Release of DOX·HCl from Thermosensitive Modified PEG/PCL Hydrogel to Improve Anti-Tumor Efficiency. *European Journal of Pharmaceutical Sciences* **2014**, *62*, 267–273. <https://doi.org/10.1016/J.EJPS.2014.06.002>.
40. Mao, Y.; Li, X.; Chen, G.; Wang, S. Thermosensitive Hydrogel System With Paclitaxel Liposomes Used in Localized Drug Delivery System for In Situ Treatment of Tumor: Better Antitumor Efficacy and Lower Toxicity. *J Pharm Sci* **2016**, *105* (1), 194–204. <https://doi.org/10.1002/JPS.24693>.

41. Zhou, X.; He, X.; Shi, K.; Yuan, L.; Yang, Y.; Liu, Q.; Ming, Y.; Yi, C.; Qian, Z. Injectable Thermosensitive Hydrogel Containing Erlotinib-Loaded Hollow Mesoporous Silica Nanoparticles as a Localized Drug Delivery System for NSCLC Therapy. *Advanced Science* **2020**, *7* (23), 2001442. <https://doi.org/10.1002/advs.202001442>.
42. Fan, R.; Sun, W.; Zhang, T.; Wang, R.; Tian, Y.; Zhang, H.; Li, J.; Zheng, A.; Song, S. Paclitaxel-Nanocrystals-Loaded Network Thermosensitive Hydrogel for Localised Postsurgical Recurrent of Breast Cancer after Surgical Resection. *Biomedicine & Pharmacotherapy* **2022**, *150*, 113017. <https://doi.org/10.1016/j.biopha.2022.113017>.
43. Feng Alexandra De Dille AE Vicky J Jameson Leia Smith AE William S Dernell AE Mark C Manning, L. A. Improved Potency of Cisplatin by Hydrophobic Ion Pairing. *Cancer Chemother Pharmacol* **2004**, *54* (5), 441–448. <https://doi.org/10.1007/s00280-004-0840-z>.
44. Wen, Q.; Zhang, Y.; Luo, J.; Xiong, K.; Lu, Y.; Wu, Z. X.; Wang, B. Q.; Wu, J. B.; Chen, Y.; Fu, S. Z. Therapeutic Efficacy of Thermosensitive Pluronic Hydrogel for Codelivery of Resveratrol Microspheres and Cisplatin in the Treatment of Liver Cancer Ascites. *Int J Pharm* **2020**, *582*, 119334. <https://doi.org/10.1016/J.IJPHARM.2020.119334>.
45. Dordunoo, S. K.; Burt, H. M. Solubility and Stability of Taxol: Effects of Buffers and Cyclodextrins. *Int J Pharm* **1996**, *133* (1–2), 191–201. [https://doi.org/10.1016/0378-5173\(96\)04443-2](https://doi.org/10.1016/0378-5173(96)04443-2).
46. Akio Miwa; Atsuo Ishibe; Mari Nakano; Tomohiro Yamahira; Shigeru Itai; Shuji Jinno; Hiroyuki Kawahara. Development of Novel Chitosan Derivatives as Micellar Carriers of Taxol. *Pharm Res* **1998**, *15* (12), 1844–1850.
47. Si, M.; Xia, Y.; Cong, M.; Wang, D.; Hou, Y.; Ma, H. In Situ Co-Delivery of Doxorubicin and Cisplatin by Injectable Thermosensitive Hydrogels for Enhanced Osteosarcoma Treatment. *International Journal of Nanomedicine*, **2022**, *17*, 1309. <https://doi.org/10.2147/IJN.S356453>.
48. Cell Signaling Technology. Doxorubicin. <https://media.cellsignal.com/pdf/5927.pdf#:~:text=Solubility%3ASoluble%20in%20DMSO%20at%20100%20mg%2Fml%3B%20very%20poorly,Use%3A%20Doxorubicin%20is%20supplied%20as%20a%20lyophilized%20powder> (accessed 2022-06-06).
49. Du, W.; Hong, L.; Yao, T.; Yang, X.; He, Q.; Yang, B.; Hu, Y. Synthesis and Evaluation of Water-Soluble Docetaxel Prodrugs-Docetaxel Esters of Malic Acid. *Bioorg Med Chem* **2007**, *15* (18), 6323–6330. <https://doi.org/10.1016/j.bmc.2007.04.002>.
50. Li, R.; Shan, L.; Yao, Y.; Peng, F.; Jiang, S.; Yang, D.; Ling, G.; Zhang, P. Black Phosphorus Nanosheets and Docetaxel Micelles Co-Incorporated Thermoreversible Hydrogel for Combination Chemo-Photodynamic Therapy. *Drug Delivery and Translational Research*, *11*(3), pp. **2021**, *11* (3), 1133–1143. <https://doi.org/10.1007/s13346-020-00836-y>.
51. Chu, L. L.; Pandey, R. P.; Shin, J. Y.; Jung, H. J.; Sohng, J. K. Synthetic Analog of Anticancer Drug Daunorubicin from Daunorubicinone Using One-Pot Enzymatic UDP-Recycling Glycosylation. *J Mol Catal B Enzym* **2016**, *124*, 1–10. <https://doi.org/10.1016/j.molcatb.2015.11.020>.
52. Oztürk Urk-Atar, K. E.; Kaplan, M.; Çalis, S. C. Development and Evaluation of Polymeric Micelle Containing Tablet Formulation for Poorly Water-Soluble Drug: Tamoxifen Citrate. *Drug Dev Ind Pharm* **2020**, *46* (10), 1695–1704. <https://doi.org/10.1080/03639045.2020.1820037>.
53. Meng, D.; Lei, H.; Zheng, X.; Han, Y.; Sun, R.; Zhao, D.; Liu, R. A Temperature-Sensitive Phase-Change Hydrogel of Tamoxifen Achieves the Long-Acting Antitumor Activation on Breast Cancer Cells. *Oncotargets Ther* **2019**, *12*, 3919. <https://doi.org/10.2147/OTT.S201421>.
54. Zhang, N.; Zheng, S.; Pan, Z.; Liu, Z. Phase Transition Effects on Mechanical Properties of NIPA Hydrogel. *Polymers (Basel)* **2018**, *10* (4), 358. <https://doi.org/10.3390/polym10040358>.
55. Guo, Y.; Gao, Z.; Liu, Y.; Huang, Z.; Chai, C.; Hao, J. Multiple Cross-Linking-Dominated Metal-Ligand Coordinated Hydrogels with Tunable Strength and Thermosensitivity. *ACS Appl Polym Mater* **2019**, *1* (9), 2370–2378. <https://doi.org/10.1021/acsapm.9b00490>.
56. Zeinali, E.; Haddadi-Asl, V.; Roghani-Mamaqani, H. Synthesis of Dual Thermo- and PH-Sensitive Poly( N -Isopropylacrylamide- Co -Acrylic Acid)-Grafted Cellulose Nanocrystals by Reversible Addition-Fragmentation Chain Transfer Polymerization. *J Biomed Mater Res A* **2018**, *106* (1), 231–243. <https://doi.org/10.1002/jbm.a.36230>.
57. Higashi, N.; Matsubara, S.; Nishimura, S.; Koga, T. Stepwise Thermo-Responsive Amino Acid-Derived Triblock Vinyl Polymers: ATRP Synthesis of Polymers, Aggregation, and Gelation Properties via Flower-Like Micelle Formation. *Materials* **2018**, *11* (3), 424. <https://doi.org/10.3390/ma11030424>.

58. Razmimanesh, F.; Sodeifian, G. Investigation of Temperature-Responsive Tocosomal Nanocarriers as the Efficient and Robust Drug Delivery System for Sunitinib Malate Anti-Cancer Drug: Effects of MW and Chain Length of PNIPAAm on LCST and Dissolution Rate. *J Pharm Sci* **2022**, *111* (7), 1937–1951. <https://doi.org/10.1016/j.xphs.2021.12.022>.
59. Khan, S.; Minhas, M. U.; Ahmad, M.; Sohail, M. Self-Assembled Supramolecular Thermoreversible  $\beta$ -Cyclodextrin/Ethylene Glycol Injectable Hydrogels with Difunctional Pluronic® 127 as Controlled Delivery Depot of Curcumin. Development, Characterization and in Vitro Evaluation. *Journal of Biomaterials science* **2018**, *29* (1), 1–34. <https://doi.org/10.1080/09205063.2017.1396707>.
60. Fehér, B.; Varga, I.; Pedersen, J. S. Effect of Concentration and Ionic Strength on the Lower Critical Solution Temperature of Poly(N-Isopropylacrylamide) Investigated by Small-Angle X-Ray Scattering. *Soft Mater* **2022**, *20* (sup1), S10–S18. <https://doi.org/10.1080/1539445X.2021.1979041>.
61. Starovoytova, L.; Št'astná, J.; Šturcová, A.; Konefal, R.; Dybal, J.; Velychkivska, N.; Radecki, M.; Hanyková, L. Additive Effects on Phase Transition and Interactions in Poly(Vinyl Methyl Ether) Solutions. *Polymers*, *7*(12), pp.2572-2583.2015 **2016**, *7* (12), 2572–2583. <https://doi.org/10.3390/polym7121533>.
62. Lin Yu; Huan Zhang; Jiandong Ding. A Subtle End-group Effect on Macroscopic Physical Gelation of Triblock Copolymer Aqueous Solutions. *Angewandte Chemie International Edition* **2006**, *45* (14), 2232–2235.
63. Marsili, L.; Dal Bo, M.; Eisele, G.; Donati, I.; Berti, F.; Toffoli, G.; Stadler, F. J. Characterization of Thermoresponsive Poly-N-Vinylcaprolactam Polymers for Biological Applications Academic Editors: Mattia Sponchioni. *Polymers (Basel)* **2021**, *13* (16), .2639. <https://doi.org/10.3390/polym13162639>.
64. Ahmadi, R.; de Bruijn, J. D. Biocompatibility and Gelation of Chitosan–Glycerol Phosphate Hydrogels. *J Biomed Mater Res A* **2008**, *86A* (3), 824–832. <https://doi.org/10.1002/jbm.a.31676>.
65. Joshi, S. C. Sol-Gel Behavior of Hydroxypropyl Methylcellulose (HPMC) in Ionic Media Including Drug Release. *Materials* **2011**, *4* (10), 1861–1905. <https://doi.org/10.3390/ma4101861>.
66. Wilfert, S.; Iturmendi, A.; Henke, H.; Brüggemann, O.; Teasdale, I. Thermoresponsive Polyphosphazene-Based Molecular Brushes by Living Cationic Polymerization. *Macromol Symp* **2014**, *337* (1), 116–123. <https://doi.org/10.1002/masy.201450314>.
67. Chen, C. F.; Tsai, C.; Lin, Y.; Chu, M. Study of Novel Biodegradable Thermo-Sensitive Hydrogels of Methoxy-Poly(Ethylene Glycol)-Block-Polyester Diblock Copolymers †. *Polym Int* **2010**, *55* (10), 1428–1435. <https://doi.org/10.1002/pi.2886>.
68. Zheng, L.; Li, C.; Huang, X.; Lin, X.; Lin, W.; Yang, F.; Chen, T. Thermosensitive Hydrogels for Sustained-Release of Sorafenib and Selenium Nanoparticles for Localized Synergistic Chemoradiotherapy. *Biomaterials* **2019**, *216*, 119220. <https://doi.org/10.1016/j.biomaterials.2019.05.031>.
69. Fiorica, C.; Palumbo, F. S.; Pitarresi, G.; Puleio, R.; Condorelli, L.; Collura, G.; Giammona, G. A Hyaluronic Acid/Cyclodextrin Based Injectable Hydrogel for Local Doxorubicin Delivery to Solid Tumors. *Int J Pharm* **2020**, *589*, 119879. <https://doi.org/10.1016/j.ijpharm.2020.119879>.
70. Gheysoori, P.; Paydayesh, A.; Jafari, M.; Peidayesh, H. Thermoresponsive Nanocomposite Hydrogels Based on Gelatin/Poly (N-Isopropylacrylamide) (PNIPAM) for Controlled Drug Delivery. *Eur Polym J* **2023**, *186*, 111846. <https://doi.org/10.1016/j.eurpolymj.2023.111846>.
71. Gallagher, S.; Florea, L.; Fraser, K.; Diamond, D. Swelling and Shrinking Properties of Thermo-Responsive Polymeric Ionic Liquid Hydrogels with Embedded Linear PNIPAAm. *Int J Mol Sci* **2014**, *15* (4), 5337–5349. <https://doi.org/10.3390/ijms15045337>.
72. Wang, J.; Williamson, G. S.; Yang, H. Branched Polyrotaxane Hydrogels Consisting of Alpha-Cyclodextrin and Low-Molecular-Weight Four-Arm Polyethylene Glycol and the Utility of Their Thixotropic Property for Controlled Drug Release. *Colloids Surf B Biointerfaces* **2018**, *165*, 144–149. <https://doi.org/10.1016/j.colsurfb.2018.02.032>.
73. Jiang, Y.; Meng, X.; Wu, Z.; Qi, X. Modified Chitosan Thermosensitive Hydrogel Enables Sustained and Efficient Anti-Tumor Therapy via Intratumoral Injection. *Carbohydr Polym* **2016**, *144*, 245–253. <https://doi.org/10.1016/j.carbpol.2016.02.059>.
74. Yi, P.; Wang, Y.; He, P.; Zhan, Y.; Sun, Z.; Li, Y.; Zhang, Y. Study on  $\beta$ -Cyclodextrin-Complexed Nanogels with Improved Thermal Response for Anticancer Drug Delivery. *Materials Science and Engineering: C* **2017**, *78*, 773–779. <https://doi.org/10.1016/j.msec.2017.04.096>.
75. Gami, P.; Kundu, D.; Seera, S. D. K.; Banerjee, T. Chemically Crosslinked Xylan- $\beta$ -Cyclodextrin Hydrogel for the in Vitro Delivery of Curcumin and 5-Fluorouracil. *Int J Biol Macromol* **2020**, *158*, 18–31. <https://doi.org/10.1016/j.ijbiomac.2020.04.237>.
76. Torchio, A.; Cassino, C.; Lavella, M.; Gallina, A.; Stefani, A.; Boffito, M.; Ciardelli, G. Injectable Supramolecular Hydrogels Based on Custom-Made Poly(Ether Urethane)s and  $\alpha$ -Cyclodextrins as Efficient

- Delivery Vehicles of Curcumin. *Materials Science and Engineering: C* **2021**, *127*, 112194. <https://doi.org/10.1016/J.MSEC.2021.112194>.
77. Almawash, S.; El Hamd, M. A.; Osman, S. K. Polymerized  $\beta$ -Cyclodextrin-Based Injectable Hydrogel for Sustained Release of 5-Fluorouracil/Methotrexate Mixture in Breast Cancer Management: In Vitro and In Vivo Analytical Validations. *Pharmaceutics* **2022**, *14* (4), 817. <https://doi.org/10.3390/pharmaceutics14040817>.
  78. Babaei, M.; Davoodi, J.; Dehghan, R.; Zahiri, M.; Abnous, K.; Taghdisi, S. M.; Ramezani, M.; Alibolandi, M. Thermosensitive Composite Hydrogel Incorporated with Curcumin-Loaded Nanopolymersomes for Prolonged and Localized Treatment of Glioma. *J Drug Deliv Sci Technol* **2020**, *59*, 101885. <https://doi.org/10.1016/J.JDDST.2020.101885>.
  79. Li, R.; Lin, Z.; Zhang, Q.; Zhang, Y.; Liu, Y.; Lyu, Y.; Li, X.; Zhou, C.; Wu, G.; Ao, N.; Li, L. Injectable and In Situ-Formable Thiolated Chitosan-Coated Liposomal Hydrogels as Curcumin Carriers for Prevention of In Vivo Breast Cancer Recurrence. *Cite This: ACS Appl. Mater. Interfaces* **2020**, *12*, 17936–17948. <https://doi.org/10.1021/acsami.9b21528>.
  80. Duan, J.; Huang, Y.; Zong, S.; Jiang, J. Preparation and Drug Release Properties of a Thermo Sensitive GA Hydrogel. *Polymers (Basel)* **2020**, *13* (1), 119. <https://doi.org/10.3390/polym13010119>.
  81. Liu, L.; Li, L.; Qing, Y.; Yan, N.; Wu, Y.; Li, X.; Tian, C. Mechanically Strong and Thermosensitive Hydrogels Reinforced with Cellulose Nanofibrils. *Polym Chem* **2016**, *7* (46), 7142–7151. <https://doi.org/10.1039/C6PY01652A>.
  82. Jung, Y.; Park, W.; Park, H.; Lee, D.-K.; Na, K. Thermo-Sensitive Injectable Hydrogel Based on the Physical Mixing of Hyaluronic Acid and Pluronic F-127 for Sustained NSAID Delivery. *Carbohydr Polym* **2017**, *156*, 403–408. <https://doi.org/10.1016/j.carbpol.2016.08.068>.
  83. Wu, W.-X.; Huang, Y.-C.; Lee, W.-F. Effect of Poly(Ethylene Glycol)-Derived Crosslinkers on the Properties of Thermosensitive Hydrogels. *Iranian Polymer Journal* **2020**, *29*, 679–691. <https://doi.org/10.1007/s13726-020-00831-7>.
  84. Thakur, S.; Singh, H.; Singh, A.; Kaur, S.; Sharma, A.; Singh, S. K.; kaur, S.; Kaur, G.; Jain, S. K. Thermosensitive Injectable Hydrogel Containing Carboplatin Loaded Nanoparticles: A Dual Approach for Sustained and Localized Delivery with Improved Safety and Therapeutic Efficacy. *J Drug Deliv Sci Technol* **2020**, *58*, 101817. <https://doi.org/10.1016/J.JDDST.2020.101817>.
  85. Seo, J. W.; Shin, S. R.; Lee, M. Y.; Cha, J. M.; Min, K. H.; Lee, S. C.; Shin, S. Y.; Bae, H. Injectable Hydrogel Derived from Chitosan with Tunable Mechanical Properties via Hybrid-Crosslinking System. *Carbohydr Polym* **2021**, *251*, 117036. <https://doi.org/10.1016/J.CARBPOL.2020.117036>.
  86. Dirauf, M.; Muljajew, I.; Weber, C.; Schubert, U. S. Recent Advances in Degradable Synthetic Polymers for Biomedical Applications - Beyond Polyesters. *Prog Polym Sci* **2022**, *129*, 101547. <https://doi.org/10.1016/j.progpolymsci.2022.101547>.
  87. Shen, W.; Chen, X.; Luan, J.; Wang, D.; Yu, L.; Ding, J. Sustained Codelivery of Cisplatin and Paclitaxel via an Injectable Prodrug Hydrogel for Ovarian Cancer Treatment. *ACS applied Materials & Interfaces* **2017**, *9* (46), 40031–40046. <https://doi.org/10.1021/acsami.7b11998>.
  88. Hozumi, T.; Kageyama, T.; Ohta, S.; Fukuda, J.; Ito, T. Injectable Hydrogel with Slow Degradability Composed of Gelatin and Hyaluronic Acid Cross-Linked by Schiff's Base Formation. *Biomacromolecules* **2017**, *19* (2), 288–297. <https://doi.org/10.1021/acs.biomac.7b01133>.
  89. Wang, M.; Chen, M.; Niu, W.; Winston, D. D.; Cheng, W.; Lei, B. Injectable Biodegradation-Visual Self-Healing Citrate Hydrogel with High Tissue Penetration for Microenvironment-Responsive Degradation and Local Tumor Therapy. *Biomaterials* **2020**, *261*, 120301. <https://doi.org/10.1016/J.BIOMATERIALS.2020.120301>.
  90. Ma, H.; He, C.; Cheng, Y.; Li, D.; Gong, Y.; Liu, J.; Tian, H.; Chen, X. PLK1shRNA and Doxorubicin Co-Loaded Thermosensitive PLGA-PEG-PLGA Hydrogels for Osteosarcoma Treatment. *Biomaterials* **2014**, *35* (30), 8723–8734. <https://doi.org/10.1016/J.BIOMATERIALS.2014.06.045>.
  91. Cao, D.; Zhang, X.; Luo, Y.; Wu, H.; Ke, X.; Ci, T. Artificial Cells, Nanomedicine, and Biotechnology Liposomal Doxorubicin Loaded PLGA-PEG-PLGA Based Thermogel for Sustained Local Drug Delivery for the Treatment of Breast Cancer Liposomal Doxorubicin Loaded PLGA-PEG-PLGA Based Thermogel for Sustained Local Drug Delivery for the Treatment of Breast Cancer. *Nanomedicine, and Biotechnology* **2019**, *47* (1), 181–191. <https://doi.org/10.1080/21691401.2018.1548470>.
  92. Li, T.; Zhang, M.; Wang, J.; Wang, T.; Yao, Y.; Zhang, X.; Zhang, C.; Zhang, N. Thermosensitive Hydrogel Co-Loaded with Gold Nanoparticles and Doxorubicin for Effective Chemoradiotherapy. *The AAPS journal*, *18*(1), pp. **2016**, *18* (1), 146–155. <https://doi.org/10.1208/s12248-015-9828-3>.
  93. Lin, Z.; Gao, W.; Hu, H.; Ma, K.; He, B.; Dai, W.; Wang, X.; Wang, J.; Zhang, X.; Zhang, Q. Novel Thermo-Sensitive Hydrogel System with Paclitaxel Nanocrystals: High Drug-Loading, Sustained Drug Release and

- Extended Local Retention Guaranteeing Better Efficacy and Lower Toxicity. *Journal of Controlled Release* **2014**, *174* (1), 161–170. <https://doi.org/10.1016/J.JCONREL.2013.10.026>.
94. Turabee, M. H.; Jeong, T. H.; Ramalingam, P.; Kang, J. H.; Ko, Y. T. N,N,N-Trimethyl Chitosan Embedded in Situ Pluronic F127 Hydrogel for the Treatment of Brain Tumor. *Carbohydr Polym* **2019**, *203*, 302–309. <https://doi.org/10.1016/J.CARBPOL.2018.09.065>.
  95. Ma, H.; He, C.; Cheng, Y.; Yang, Z.; Zang, J.; Liu, J.; Chen, X. Localized Co-Delivery of Doxorubicin, Cisplatin, and Methotrexate by Thermosensitive Hydrogels for Enhanced Osteosarcoma Treatment. *ACS Appl Mater Interfaces* **2015**, *7* (49), 27040–27048. <https://doi.org/10.1021/acsami.5b09112>.
  96. Pan, A.; Wang, Z.; Chen, B.; Dai, W.; Zhang, H.; He, B.; Wang, X.; Wang, Y.; Zhang, Q. Localized Co-Delivery of Collagenase and Trastuzumab by Thermosensitive Hydrogels for Enhanced Antitumor Efficacy in Human Breast Xenograft. *Drug Deliv* **2018**, *25* (1), 1495–1503. <https://doi.org/10.1080/10717544.2018.1474971>.
  97. Han, T.-S.; Hur, K.; Choi, B.; Lee, J.-Y.; Byeon, S.-J.; Min, J.; Yu, J.; Cho, J.-K.; Hong, J.; Lee, H.-J.; Kong, S.-H.; Kim, W.-H.; Yanagihara, K.; Song, S.-C.; Yang, H.-K. Improvement of Anti-Cancer Drug Efficacy via Thermosensitive Hydrogel in Peritoneal Carcinomatosis in Gastric Cancer. *Oncotarget* **2017**, *8* (65), 108848–108858. <https://doi.org/10.18632/oncotarget.22312>.
  98. Gong, J.; Wang, L.; Wu, J.; Yuan, Y.; Mu, R. J.; Du, Y.; Wu, C.; Pang, J. The Rheological and Physicochemical Properties of a Novel Thermosensitive Hydrogel Based on Konjac Glucomannan/Gum Tragacanth. *LWT* **2019**, *100*, 271–277. <https://doi.org/10.1016/J.LWT.2018.10.080>.
  99. Xu, G.; Li, B.; Wang, T.; Wan, J.; Zhang, Y.; Huang, J.; Shen, Y. Enhancing the Anti-Ovarian Cancer Activity of Quercetin Using a Self-Assembling Micelle and Thermosensitive Hydrogel Drug Delivery System. **2018**. <https://doi.org/10.1039/c8ra03274b>.
  100. Lv, Q.; Yu, S.; Quan, F.; He, C.; Chen, X. Thermosensitive Polypeptide Hydrogels Co-Loaded with Two Anti-Tumor Agents to Reduce Multi-Drug Resistance and Enhance Local Tumor Treatment. *Adv Ther (Weinh)* **2020**, *3* (3), 1900165. <https://doi.org/10.1002/adtp.201900165>.
  101. Gao, Y.; Ren, F.; Ding, B.; Sun, N.; Liu, X.; Ding, X.; Gao, S. A Thermo-Sensitive PLGA-PEG-PLGA Hydrogel for Sustained Release of Docetaxel. *J Drug Target* **2011**, *19* (7), 516–527. <https://doi.org/10.3109/1061186X.2010.519031>.
  102. Zhao, D.; Hu, C.; Fu, Q.; Lv, H. Combined Chemotherapy for Triple Negative Breast Cancer Treatment by Paclitaxel and Niclosamide Nanocrystals Loaded Thermosensitive Hydrogel. *European Journal of Pharmaceutical Sciences* **2021**, *167*, 105992. <https://doi.org/10.1016/J.EJPS.2021.105992>.
  103. Cho, H.; Gao, J.; Kwon, G. S. PEG- b -PLA Micelles and PLGA- b -PEG- b -PLGA Sol-Gels for Drug Delivery. *Journal of Controlled Release* **2016**, *240*, 191–201. <https://doi.org/10.1016/j.jconrel.2015.12.015>.
  104. Elstad, N. L.; Fowers, K. D. OncoGel (ReGel/Paclitaxel) – Clinical Applications for a Novel Paclitaxel Delivery System. *Adv Drug Deliv Rev* **2009**, *61* (10), 785–794. <https://doi.org/10.1016/j.addr.2009.04.010>.
  105. ClinicalTrials.gov. *Efficacy and Safety of OncoGel™ Added to Chemotherapy and Radiation Before Surgery in Subjects With Esophageal Cancer*. <https://www.clinicaltrials.gov/ct2/show/NCT00573131#:~:text=OncoGel%20is%20a%20new%20experimental%20drug%20delivery%20system,to%206%20weeks%20as%20it%20releases%20the%20paclitaxel> (accessed 2022-06-06).
  106. DeWitt, J. M.; Murthy, S. K.; Ardhanari, R.; DuVall, G. A.; Wallner, G.; Litka, P.; Daugherty, C.; Fowers, K. EUS-Guided Paclitaxel Injection as an Adjunctive Therapy to Systemic Chemotherapy and Concurrent External Beam Radiation before Surgery for Localized or Locoregional Esophageal Cancer: A Multicenter Prospective Randomized Trial. *Gastrointest Endosc* **2017**, *86* (1), 140–149. <https://doi.org/10.1016/j.gie.2016.11.017>.
  107. ClinicalTrials.gov. *A Phase 1/2 Dose Escalation Study of Locally-Administered OncoGel™ in Subjects With Recurrent Glioma*. <https://clinicaltrials.gov/ct2/show/NCT00479765?term=oncogel&cond=Cancer&draw=2&rank=2> (accessed 2022-06-06).
  108. ClinicalTrials.gov. *The OLYMPUS Study - Optimized DeLivery of Mitomycin for Primary UTUC Study (Olympus)*. <https://clinicaltrials.gov/ct2/show/NCT02793128?term=Mitomycin+gel&cond=upper+tract+urothelial+carcinoma&draw=2&rank=2> (accessed 2022-02-06).
  109. Donin, N. M.; Duarte, S.; Lenis, A. T.; Caliliw, R.; Torres, C.; Smithson, A.; Strauss-Ayali, D.; Agmon-Gerstein, Y.; Malchi, N.; Said, J.; Raman, S. S.; Holden, S.; Pantuck, A.; Beldegrun, A. S.; Chamie, K.



- Sustained-Release Formulation of Mitomycin C to the Upper Urinary Tract Using a Thermosensitive Polymer: A Preclinical Study. *Urology* **2017**, *99*, 270–277. <https://doi.org/10.1016/j.urology.2016.09.039>.
110. Kleinmann, N.; Matin, S. F.; Pierorazio, P. M.; Gore, J. L.; Shabsigh, A.; Hu, B.; Chamie, K.; Godoy, G.; Hubosky, S.; Rivera, M.; O'Donnell, M.; Quek, M.; Raman, J. D.; Knoedler, J. J.; Scherr, D.; Stern, J.; Weight, C.; Weizer, A.; Woods, M.; Kaimakliotis, H.; Smith, A. B.; Linehan, J.; Coleman, J.; Humphreys, M. R.; Pak, R.; Lifshitz, D.; Verni, M.; Adibi, M.; Amin, M. B.; Seltzer, E.; Klein, I.; Konorty, M.; Strauss-Ayali, D.; Hakim, G.; Schoenberg, M.; Lerner, S. P. Primary Chemoablation of Low-Grade Upper Tract Urothelial Carcinoma Using UGN-101, a Mitomycin-Containing Reverse Thermal Gel (OLYMPUS): An Open-Label, Single-Arm, Phase 3 Trial. *Lancet Oncol* **2020**, *21* (6), 776–785. [https://doi.org/10.1016/S1470-2045\(20\)30147-9](https://doi.org/10.1016/S1470-2045(20)30147-9).
  111. US Food and Drug Administration. *FDA Approves First Therapy For Treatment Of Low-Grade Upper Tract Urothelial Cancer*.
  112. ClinicalTrials.gov. *Efficacy and Safety of UGN-101 in Recurrent Patients (Retreatment)*. <https://clinicaltrials.gov/ct2/show/NCT04006691?term=Mitomycin+gel&cond=upper+tract+urothelial+carcinoma&draw=2&rank=1> (accessed 2022-06-06).
  113. Chevli, K. K.; Shore, N. D.; Trainer, A.; Smith, A. B.; Saltzstein, D.; Ehrlich, Y.; Raman, J. D.; Friedman, B.; D'Anna, R.; Morris, D.; Hu, B.; Tyson, M.; Sankin, A.; Kates, M.; Linehan, J.; Scherr, D.; Kester, S.; Verni, M.; Chamie, K.; Karsh, L.; Cinman, A.; Meads, A.; Lahiri, S.; Malinowski, M.; Gabai, N.; Raju, S.; Schoenberg, M.; Seltzer, E.; Huang, W. C. Primary Chemoablation of Low-Grade Intermediate-Risk Nonmuscle-Invasive Bladder Cancer Using UGN-102, a Mitomycin-Containing Reverse Thermal Gel (Optima II): A Phase 2b, Open-Label, Single-Arm Trial. *Journal of Urology* **2022**, *207* (1), 61–69. <https://doi.org/10.1097/JU.0000000000002186>.
  114. Stover, A. M.; Basak, R.; Mueller, D.; Lipman, R.; Teal, R.; Hilton, A.; Giannone, K.; Waheed, M.; Smith, A. B. Minimal Patient-Reported Side Effects for a Chemoablative Gel (UGN-102) Used as Frontline Treatment in Adults with Nonmuscle-Invasive Bladder Cancer. *Journal of Urology* **2022**, *208* (3), 580–588. <https://doi.org/10.1097/JU.0000000000002747>.
  115. Luo, S.-D.; Wu, S.-C.; Chen, W.-C.; Wu, C.-N.; Chiu, T.-J.; Yang, Y.-H.; Li, S.-H.; Fang, F.-M.; Huang, T.-L.; Hsiao, C.-C.; Chen, C.-H. Low-Dose Aspirin Confers a Survival Benefit in Patients with Pathological Advanced-Stage Oral Squamous Cell Carcinoma. *Scientific Reports* **2021**, *11*, 17161. <https://doi.org/10.1038/s41598-021-96614-y>.
  116. Hu, L.-P.; Huang, W.; Wang, X.; Xu, C.; Qin, W.-T.; Li, D.; Tian, G.; Li, Q.; Zhou, Y.; Chen, S.; Nie, H.-Z.; Hao, Y.; Song, J.; Zhang, X.-L.; Sundquist, J.; Sundquist, K.; Li, J.; Jiang, S.-H.; Zhang, Z.-G.; Ji, J. Terbinafine Prevents Colorectal Cancer Growth by Inducing DNTP Starvation and Reducing Immune Suppression. *Molecular Therapy* **2022**, *30* (10), 3284–3299. <https://doi.org/10.1016/j.ymthe.2022.06.015>.

**Disclaimer/Publisher's Note:** The statements, opinions and data contained in all publications are solely those of the individual author(s) and contributor(s) and not of MDPI and/or the editor(s). MDPI and/or the editor(s) disclaim responsibility for any injury to people or property resulting from any ideas, methods, instructions or products referred to in the content.

## Appendix A5

**Author Guidelines** (Available at: <http://www.sapj.co.za/index.php/SAPJ/about/submissions>)

**Submitted manuscripts that are not in the correct format and without the required supporting documentation specified in these guidelines will be returned to the author(s) for correction and will delay publication.**

### AUTHORSHIP

Named authors must consent to publication **by signing a covering letter** which should be submitted as a supplementary file. Authorship should be based on substantial contribution to:

- (i) conception, design, analysis and interpretation of data;
- (ii) drafting or critical revision for important intellectual content; and
- (iii) approval of the version to be published. These conditions must all be met (uniform requirements for manuscripts submitted to biomedical journals; refer to [www.icmje.org](http://www.icmje.org)); and
- (iv) exact contribution of each author must be stated and
- (v) a motivation as to why the article should be published in the SAPJ.

### DECLARATION OF CONFLICT OF INTEREST

Authors must declare all sources of support for the research and any association with a product or subject that may constitute a conflict of interest. If there is no conflict of interest to declare please include the following: The authors declare no conflict of interest.

### FUNDING SOURCE

All sources of funding should be declared. Also define the involvement of study sponsors in the study design, collection, analysis and interpretation of data; the writing of the manuscript; the decision to submit the manuscript for publication. If the study sponsors had no such involvement, this should be stated as follows: No funding source to be declared.

### RESEARCH ETHICS COMMITTEE APPROVAL

The submitting author must provide written confirmation of Research Ethics Committee approval for all studies including case reports. The ethics committee as well as the approval number should be included.

### STATISTICAL ANALYSIS

Authors are advised to involve medical statisticians at the protocol stage of their research project: to plan sample size, and the selection of appropriate statistical tests for analysis and presentation.

### PROTECTION OF PATIENT'S RIGHTS TO PRIVACY

Identifying information should not be published in written descriptions, photographs, and pedigrees unless the information is essential for scientific purposes and the patient (or parent or guardian) gives informed written consent for publication. The patient should be shown the manuscript to be published. Refer to [www.icmje.org](http://www.icmje.org).

### ETHNIC CLASSIFICATION

The rationale for analysis based on racio-ethnic-cultural categorisation should be indicated.

### CATEGORIES OF SUBMISSIONS

Shorter items are more likely to be accepted for publication, owing to space constraints and reader preferences.

#### **Original articles**

Original articles on research relevant to the pharmaceutical sciences should not exceed 3 000 words, no more than 30 references, with up to 6 tables or figures. A structured abstract under the following headings, Background, Methods, Results, and Conclusions is a requirement and should not exceed 250 words.

**Scientific letters/short reports**

Short reports should not exceed 1 500 words with a maximum of 10 references. Only one table or illustration is permissible. A structured abstract under the following headings, Background, Methods, Results, and Conclusions, is a requirement and should not exceed 250 words.

**Case reports**

Case reports should not exceed 1 500 words with no more than 10 references. Figures are limited to 2 figures and may include images or photographs. The case report should have three headings: Summary (not exceeding 100 words), Case report (with no introduction) and Discussion. Case reports will be published online only. The summary and the URL will appear in the printed version.

**Editorials**

Opinions, etc. should not exceed 1 000 words and are welcome, but unless invited, will be subjected to the SAPJ peer review process.

**Review articles**

Review articles relevant to pharmaceutical sciences should not exceed 5 000 words, with a maximum of 50 references and no more than 6 tables or figures. A summary of 250 words or less is required.

**Letters to the editor**

Letters to the editor should be 400 words or less with only one image or table.

**Obituaries**

Obituaries should be 900 words or less and should be accompanied by a photograph.

**MANUSCRIPT PREPARATION**

Refer to articles in recent issues for the presentation of headings and subheadings. If in doubt, refer to 'uniform requirements' - [www.icmje.org](http://www.icmje.org). Manuscripts must be provided in **UK English**.

**Qualification, affiliation and contact details**

This information must be provided for ALL authors and must be submitted as a supplementary file. Email addresses of all author must be provided. ORCID number of ALL authors must be provided – if authors do not have ORCID, please register at <https://orcid.org/>

**Abbreviations**

All abbreviations should be spelt out when first used and thereafter used consistently, e.g. 'intravenous (IV)' or 'Department of Health (DoH)'.

**Scientific measurements**

Scientific measurements must be expressed in SI units except blood pressure (mmHg) and haemoglobin (g/dl). Litres is denoted with a lowercase 'l' e.g. 'ml' for millilitres). Units should be preceded by a space (except for %), e.g. '40 kg' and '20 cm' but '50%'. Greater/smaller than signs (> and <) should also be preceded by a space e.g. > 20 years. No spaces should precede ± and °, i.e. '35±6' and '19°C'. **Numbers** should be written as grouped per thousand-units, i.e. 4 000, 22 160... **Quotes** should be placed in single quotation marks: i.e. The respondent stated: '...' Round **brackets** (parentheses) should be used, as opposed to square brackets, which are reserved for denoting concentrations or insertions in direct quotes.

**General formatting**

The manuscript must be in Microsoft Word or RTF document format. Text must be 1,5-spaced, in 12-point Times New Roman font, and contain no unnecessary formatting (such as text in boxes, except for Tables). *The manuscript must be free of track changes.*

**Disclaimers** should follow the Conclusion and it should be in the following order: Acknowledgements, Declaration of interest, Funding declaration, Ethics declaration and ORCID.

**ILLUSTRATIONS AND TABLES**

If tables or illustrations submitted have been published elsewhere, the author(s) should provide consent to republication obtained from the copyright holder.

**Tables** may be embedded in the manuscript file **and** provided as '**supplementary files**'. They must be numbered in Arabic numerals (1,2,3...) and referred to consecutively in the text (e.g. 'Table 1'). Tables should be constructed carefully and simply for intelligible data representation. Unnecessarily complicated tables are strongly discouraged. Tables must be cell-based (i.e. not constructed with text boxes, tabs or enters) and accompanied by a concise title and column headings. Footnotes must be indicated with consecutive use of the following symbols: \* † ‡ § ¶ || then \*\* †† ‡‡ etc.

**Figures** must be numbered in Arabic numerals and referred to in the text e.g. '(Figure 1)'. Figure legends: Figure 1: 'Title...'. All illustrations/figures/graphs must be of **high resolution/quality**: 300 dpi or more is preferable, but images must not be resized to increase resolution. Unformatted and uncompressed images must be attached as '**supplementary files**' upon submission (not embedded in the accompanying manuscript). TIFF and PNG formats are preferable; JPEG and PDF formats are accepted, but authors must be wary of image compression. Illustrations and graphs prepared in Microsoft PowerPoint or Excel must be accompanied by the original workbook.

## REFERENCES

Authors must verify references from the original sources. *Only complete, correctly formatted reference lists will be accepted.* Reference lists may be generated with the use of reference manager software, but the final document must be delinked from the reference database or otherwise generated manually. Citations should be inserted in the text as superscript, e.g. These regulations are endorsed by the World Health Organization,<sup>2</sup> and others.<sup>3,4-6</sup> The superscript reference number should come after the punctuation mark.

All references should be listed at the end of the article in numerical order of appearance in the **Vancouver style** (not alphabetical order). Approved abbreviations of journal titles must be used; see the List of Journals in Index Medicus. Names and initials of all authors should be given; if there are more than six authors, the first three names should be given followed by et al. First and last page, volume and issue numbers should be given. **Wherever possible, references must be accompanied by a digital object identifier (DOI) link and PubMed ID (PMID)/PubMed Central ID (PMCID).** Authors are encouraged to use the DOI lookup service offered by [CrossRef](#). Crossref DOIs should always be displayed as a full URL link in the form <https://doi.org/10.xxxx/xxxxx>

**Journal references:** Price NC, Jacobs NN, Roberts DA, et al. Importance of asking about glaucoma. *Stat Med* 1998;289(1):350-355. [<http://dx.doi.org/10.1000/hjgr.182>] [PMID: 2764753]

**Book references:** Jeffcoate N. Principles of Gynaecology. 4th ed. London: Butterworth, 1975:96-101. *Chapter/section in a book:* Weinstein L, Swartz MN. Pathogenic Properties of Invading Microorganisms. In: Sodeman WA jun, Sodeman WA, eds. Pathologic Physiology: Mechanisms of Disease. Philadelphia: WB Saunders, 1974:457-472.

**Internet references:** World Health Organization. The World Health Report 2002 - Reducing Risks, Promoting Healthy Life. Geneva: World Health Organization, 2002. <http://www.who.int/whr/2002> (accessed 16 January 2010).

**Other references (e.g. reports)** should follow the same format: Author(s). Title. Publisher place: publisher name, year; pages. Cited manuscripts that have been accepted but not yet published can be included as references followed by '(in press)'. Unpublished observations and personal communications in the text must not appear in the reference list. The full name of the source person must be provided for personal communications e.g. '(Prof. Michael Jones, personal communication)'

## COVERING LETTER

A covering letter to the editor is mandatory and must include statements that the manuscript has not been published previously and is not under review elsewhere. It should state details of any prior publication of the research in abstract form or in Congress proceedings. The letter must declare if any of the authors have a conflict of interest and that the requirements for submission, including ethics approval and patient permission for case reports have been fulfilled. A motivation as to why the article should be published in the SAPJ should also be included.

All authors must sign the covering letter.

Please provide the names and email addresses of three possible reviewers for this manuscript.

### **REVIEW PROCESS**

Manuscripts, after vetting by the editorial team, are assigned for peer-review to 3 reviewers, conversant with the particular field of research. The reviewers and the authors are blinded to each other's identity. The turn-around time for review and initial editorial decision notification aims to be within 6 weeks of submission.

### **PROOFS**

A PDF proof of an article may be sent to the corresponding author before publication to resolve remaining queries. At that stage, **only** typographical changes are permitted; the corresponding author is required, having conferred with his/her co-authors, to reply within 2 working days in order for the article to be published in the issue for which it has been scheduled.

### **CHANGES OF ADDRESS**

Please notify the editorial department of any contact detail changes, including email, to facilitate communication.

### **CHARGES**

There is no charge for the publication of manuscripts.

### **COPYRIGHT NOTICE**

The South African Pharmaceutical Journal (SAPJ) reserves copyright of the material published. The work is licensed under a Creative Commons Attribution-Non-Commercial Works 4.0 South Africa License. Material submitted for publication in the SAPJ is accepted provided it has not been published elsewhere. The SAPJ does not hold itself responsible for statements made by the authors.

### **Copyright Notice**

By submitting manuscripts to SAPJ, authors of original articles are assigning copyright to Medpharm Publications (Pty) Ltd. Authors may use their own work after publication without written permission, provided they acknowledge the original source. Individuals and academic institutions may freely copy and distribute articles published in SAPJ for educational and research purposes without obtaining permission.

### **Privacy Statement**

The SAPJ is committed to protecting the privacy of the users of this journal website. The names, personal particulars and email addresses entered in this website will be used only for the stated purposes of this journal and will not be made available to third parties without the user's permission or due process. Users consent to receive communication from the SAPJ for the stated purposes of the journal. Queries with regard to privacy may be directed to [robyn@jesser-point.co.za](mailto:robyn@jesser-point.co.za).

UNIVERSITY of the  
WESTERN CAPE

## Design and characterisation of a Pluronic-F127-based injectable thermoresponsive intratumoural hydrogel

Sandrine Tanga<sup>1</sup>, Marique Aucamp<sup>1</sup>, Poornima Ramburrun<sup>2</sup>

<sup>1</sup>Department of Pharmaceutics, School of Pharmacy, Faculty of Natural Sciences, University of the Western Cape, Bellville, 7535, South Africa

<sup>2</sup>Wits Advanced Drug Delivery Platform Research Unit, Department of Pharmacy and Pharmacology, School of Therapeutic Science, Faculty of Health Sciences, University of Witwatersrand, 7 York Road Parktown, Johannesburg, 2193, South Africa

### Abstract

The intravenous administration of chemotherapeutic agents causes an array of side effects during the treatment course, leading to physical and psychological distress. Additionally, these drugs struggle to permeate deep within the tumorous tissue cells which limits their efficacy. Herein, an intratumoural thermoresponsive hydrogel containing Pluronic™ F127 (PF-127) was designed to improve the targeted delivery of oncology drugs to cancer cells. Natural polymers, chitosan (CH) and *k*-carrageenan (*k*CRG) were employed to enhance the rheological, mechanical and erosion properties of the hydrogel system. The hydrogel maintained a liquid state at 4 °C and transitioned to a gel at 31 °C, with adequate mechanical and erosion properties. The results of this study indicate that CH/*k*CRG/PF-127/LIM shows potential as an injectable thermosensitive hydrogel system for administering drugs within solid tumours.

### Introduction

Chemotherapeutics are effective and widely used against cancer however, their intravenous administration leads to poor permeation and side effects, such as cardiotoxicity, myopathy, nephrotoxicity and immunotoxicity [1]. Several strategies, such as the design of analogues and the use of smart drug delivery systems (DDSs), such as nanoparticles, hydrogels, and liposomes, have been explored to control chemotherapeutic targeting and improve treatment outcomes. Among the smart DDSs used, injectable hydrogels have been widely explored to improve drug targeting in cancer treatment. Hydrogels comprise a 3D polymeric structure which stores drugs within its gel network, allowing for a controlled and slow release. Thermosensitive hydrogels respond to changes in temperature by transitioning from liquid to gel. Thermoresponsive hydrogel delivery systems are advantageous for tumour targeting because they can be modified to maintain therapeutic concentrations of the drug within the tumour site, while providing excellent biocompatibility, degradability, and sustained drug release [2].

However, thermosensitive hydrogels are often associated with weak mechanical properties which limit their ability to remain at the target site without breakage or collapse resulting from biological interference or design defects [2]. The mechanical strength of a hydrogel system is, therefore, of considerable importance to maintain rigidity and structural integrity within the tumour. Pluronic™ F127 (PF-127) is a common thermosensitive polymer frequently employed for its safety and lower critical solution temperature (LCST) at physiological conditions, however, it demonstrates poor mechanical strength when used alone. Therefore, CH and *k*CRG featuring favourable biocompatible properties and mechanical strength were used to improve the mechanical

properties of PF-127. The synergic incorporation of these polymers could improve the *in vivo* stability of thermoresponsive systems, based on their ability to enhance hydrogel mechanical strength in formulations, such as films and wound dressings [3].

To target the issue of poor drug permeation and accumulation in tumours, limonene (LIM), a natural monoterpene, was selected for its high lipophilicity and chemotherapeutic activity in various cancers such as breast, lung, and prostate cancer [4]. Doxorubicin (DOX) was used as a model drug to assess the drug-loading efficiency of the system. The present study investigates the crosslinking of CH, *k*CRG, PF-127 and LIM to obtain an injectable thermoresponsive hydrogel for targeted drug delivery applications. The unique approach of this study is the employment of LIM in the polymer blend to potentially aid DOX diffusion. As such, the formulation could provide sustained drug release and appropriate physicochemical characteristics with improved anticancer activity.

### Materials

DOX was purchased from DB Fine Chemicals (Johannesburg, South Africa). LIM and *k*CRG were purchased from Iffect Chemphar Co., Ltd, Hongkong, P.R. China. Ethanol (96% v/v) was supplied by Laborem (Johannesburg, South Africa). PF-127, CH (medium molecular weight), sodium hydroxide (NaOH), disodium hydrogen phosphate, potassium dihydrogen phosphate and chromatography grade methanol were obtained from Sigma-Aldrich (Johannesburg, South Africa). Analytical grade glacial acetic acid was obtained from Saarchem (Pty) Ltd (Johannesburg, South Africa).

### Methods

#### Preparation of thermosensitive hydrogel

CH and *k*CRG solutions were prepared separately according to a method adapted from Pourjavadi and colleagues [5]. Briefly, 10 mL of CH and *k*CRG solutions of 0.3% w/v were prepared by dissolving 300 mg CH in 1% v/v glacial acetic acid, and 300 mg *k*CRG in deionized water heated to  $60 \pm 2$  °C. After mixing for 10 min at 800 rpm, the two solutions were further diluted to 40 mL each. *k*CRG solution was then transferred dropwise (5 mL/min) to the CH solution while vigorously stirring at 1400 rpm at  $50 \pm 2$  °C. Thereafter, the CH/*k*CRG solution was transferred to a rotary evaporator ( $50 \pm 2$  °C) and left to evaporate until the volume was reduced to approximately 10 mL.

For drug loading, 0.0005% w/v DOX solution prepared in 20% v/v ethanol and 0.1% v/v LIM was subsequently added and mixed into the solution. The CH/*k*CRG solution was mixed into the DOX-LIM solution. Thereafter, the CH/*k*CRG/LIM-DOX solution was transferred to an ice water bath, and 15% w/v PF-127 was added to the solution. The polymer blend was stirred until a homogenous, red-coloured solution was obtained. The pH of the solution was adjusted to approximately 5 using 2 M NaOH. The sample was transferred to a refrigerator at  $4 \pm 2$  °C where it was stored for 24 hrs. The synthesis process is depicted in Figure 1.

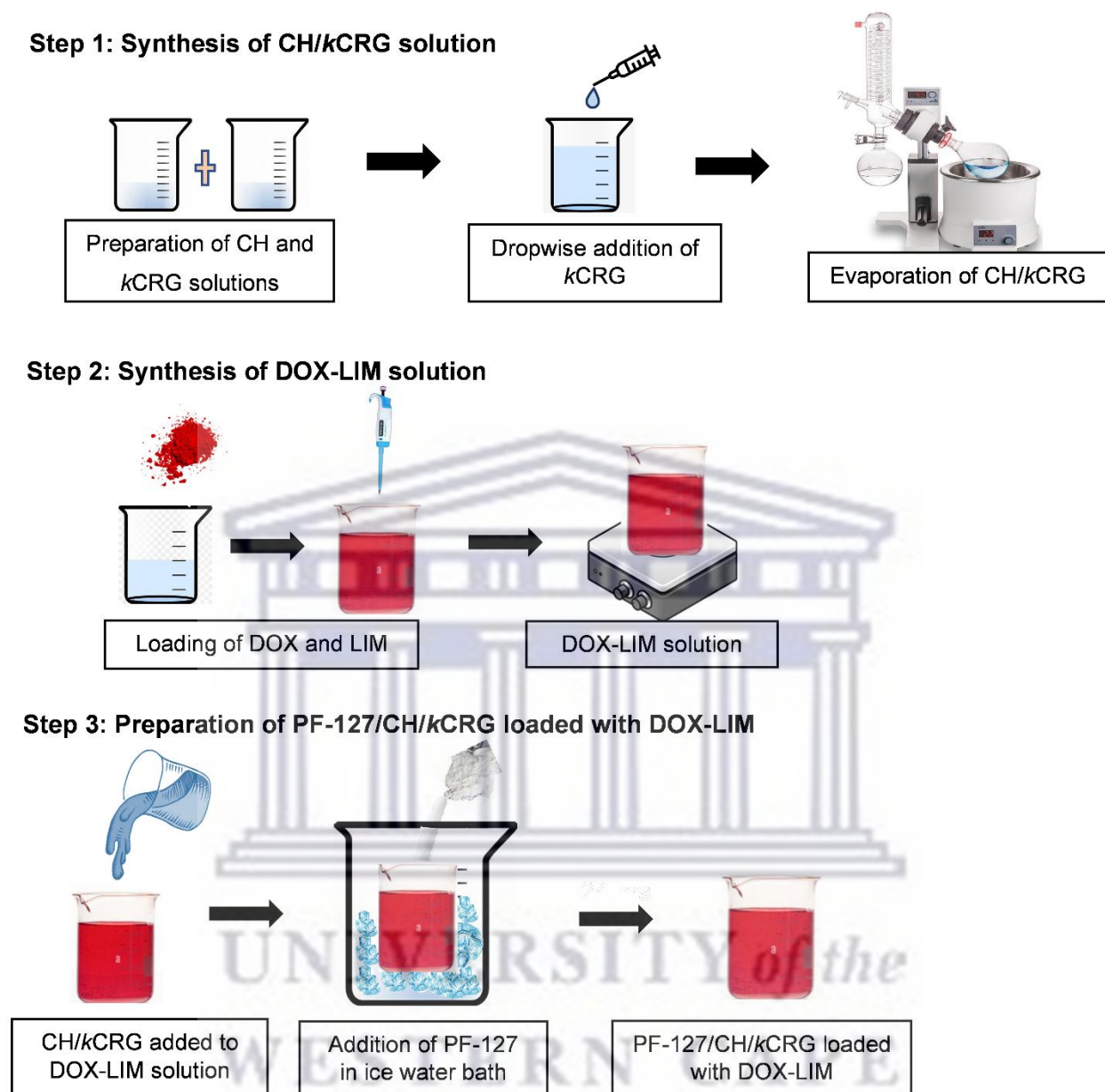


Figure 1: Schematic representing the synthesis of thermoresponsive PF-127/CH/kCRG hydrogel with DOX-LIM.

#### Fourier transform infrared spectroscopy (FTIR)

The molecular transitions and chemical composition of the hydrogel were confirmed using FTIR (Perkin Elmer 400 FTIR) over a wavenumber range of  $4000\text{--}650\text{ cm}^{-1}$  for interactions between polymers and excipients.

#### Thermal analysis

The thermal behaviour of the hydrogels was analysed using thermal gravimetric analysis (TGA) (Perkin Elmer TGA 4000 thermogravimetric analyser, Waltham, USA).



The hydrogel sample was heated at 10 °C/min from 20 - 600 °C with nitrogen gas at a flow rate of 20 mL/min.

### **Rheological analysis**

The hydrogel sample was analysed using an ElastoSens™ Bio<sup>2</sup> rheometer (Rheolution Inc, Montreal, Canada). Hydrogel samples of 5 mL were analysed for storage modulus and loss modulus over a temperature range of 4-40 °C.

### **Compressive strength**

The compression strength of the hydrogel was measured using a Mecmesin mechanical analyser, Poly Test Instruments (Johannesburg, South Africa). The hydrogel sample (5 mL), placed in a size 6 poly top vial maintained in a water bath at 37 ± 2 °C, was compressed under a load of 20 N, speed of 10 mm/min, and displacement of 5 mm.

### **Erosion**

Erosion studies were performed over a period of six weeks. A hydrogel mass of 1 g was left to gel in a poly top vial at 37 ± 2 °C. PBS (1 mL, pH 6.8) was then added to the gel. The sample was maintained at 37 ± 2 °C and 70 ± 2% RH in a humidity chamber (Labdesign Engineering (Pty) Ltd, South Africa). On weekly intervals, the PBS was removed, the swollen hydrogel was weighed and fresh medium was added to the hydrogel.

## **Results and discussion**

### **Synthesis of hydrogel**

The PF-127/CH/*k*CRG hydrogel was successfully prepared and a red solution was obtained (resulting from the colour of DOX). FTIR revealed the presence of pertinent functional groups of DOX, CH, *k*CRG, PF-127 and LIM crosslinking (Figure 2). In the hydrogel formation, the broad peak between 3000-3800 cm<sup>-1</sup> is reflective of the N-H and O-H functional groups in CH, *k*CRG and DOX. The intensity of this peak is significantly increased in the DOX-hydrogel compared to the individual constituents. The increase in intensity is attributed to the electrostatic interaction between the NH<sub>3</sub><sup>+</sup> of CH and OSO<sub>3</sub><sup>-</sup> of *k*CRG chains. A similar interaction is observed at the 1600 cm<sup>-1</sup> peak due to the C-O and N-H groups of CH and *k*CRG. The small peaks between 2900 - 2800 cm<sup>-1</sup> and between 900 - 1100 cm<sup>-1</sup>, represent the characteristic alkane and alkene groups in LIM and PF-127, respectively.

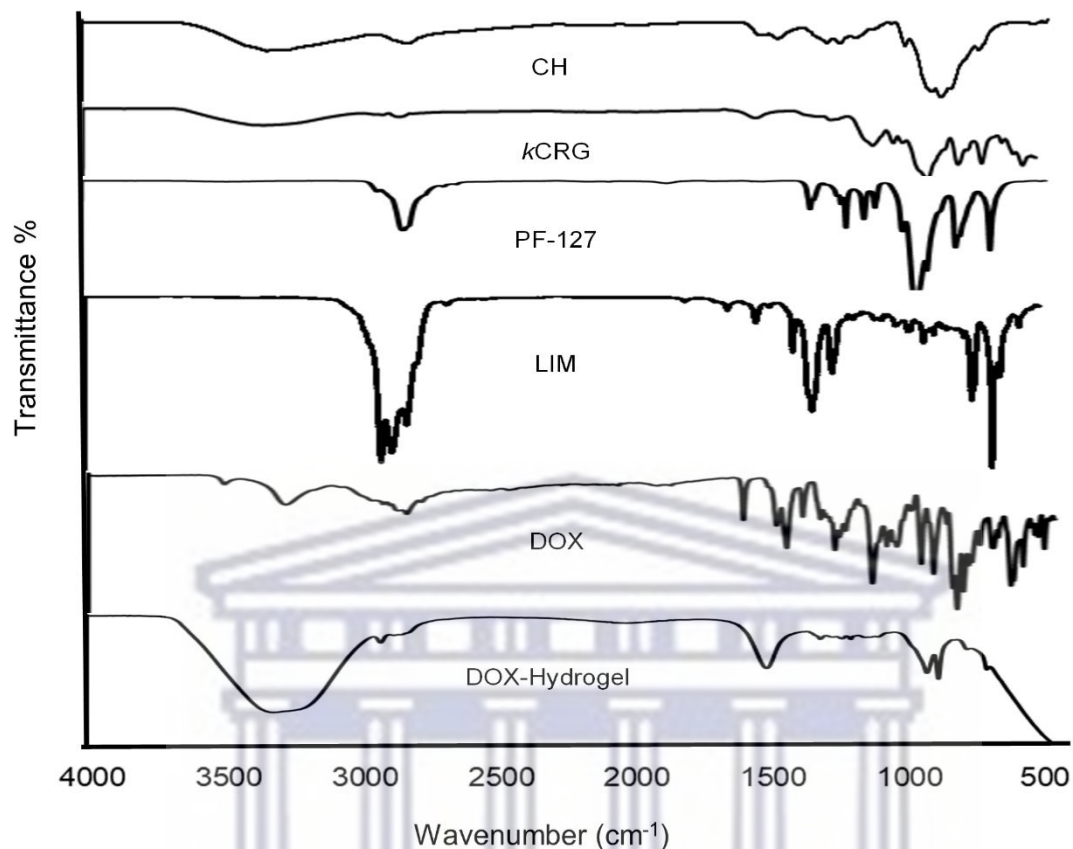


Figure 2: FTIR spectra of hydrogel formulation indicating peak similarities to CH, *k*CRG, PF-127, and LIM.

### Thermal analysis

TGA analysis was performed to assess the thermal stability of the hydrogel formulation (Figure 3). A two-step degradation process was observed from the TGA thermogram, with a mass loss of 20 % in the first step due to the evaporation of water and the volatile LIM from the hydrogel network. At 350 °C, the second step occurred with a mass loss of 30% indicating degradation of the polymers. This degradation at high temperatures indicates the extensive crosslinking of the constituents as revealed by FTIR, and high stability over a wide temperature range.

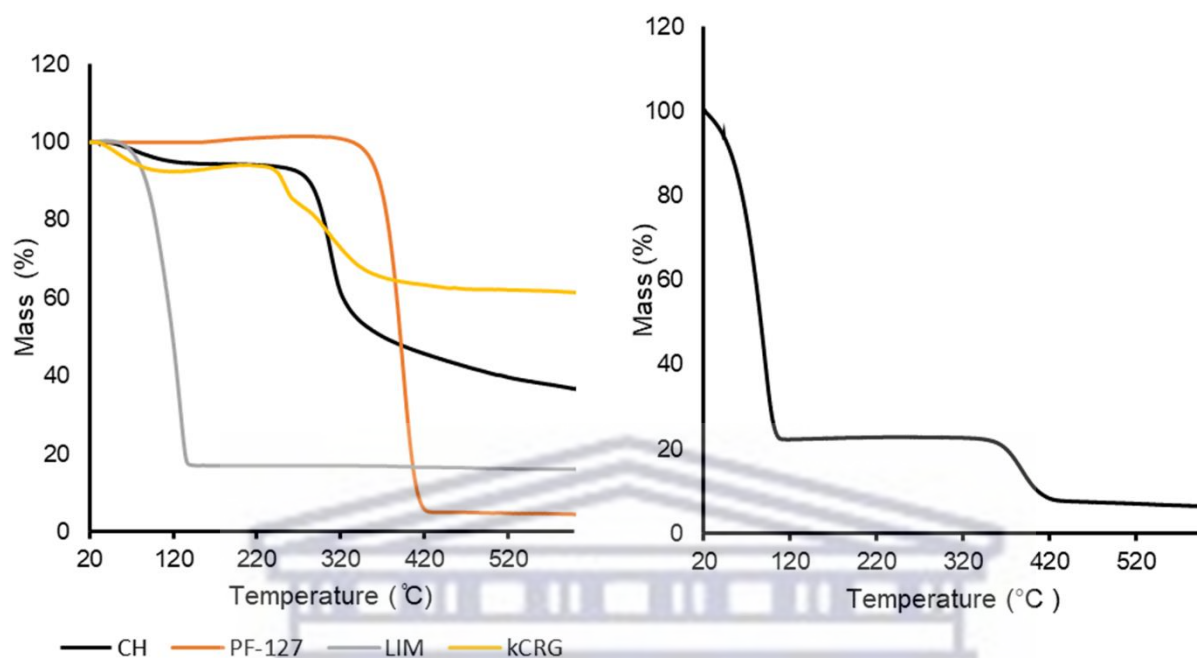


Figure 3: TGA curves of CH, PF-127, kCRG, LIM (left) and hydrogel formulation(right).

### Rheological analysis

Figure 4 shows the rheological behaviour of the hydrogel as temperature increases. Above the LCST (31 °C), PF-127 underwent thermal gelation which increased the storage modulus  $G'$  of the hydrogel network to 1400 Pa at 37 °C, while the loss modulus  $G''$  (310 Pa at 37 °C) slightly increased due to aggregation of the hydrophobic poly(ethylene oxide) chains of PF-127 [4]. The high storage moduli compared to loss moduli with increasing temperature, indicate the elastic nature of the hydrogel. The LCST of 31 °C was reached within 3 min and is favourable for the thermoresponsive design of an injectable formulation, since the system maintains its liquidity at ambient temperature for ease of administration.

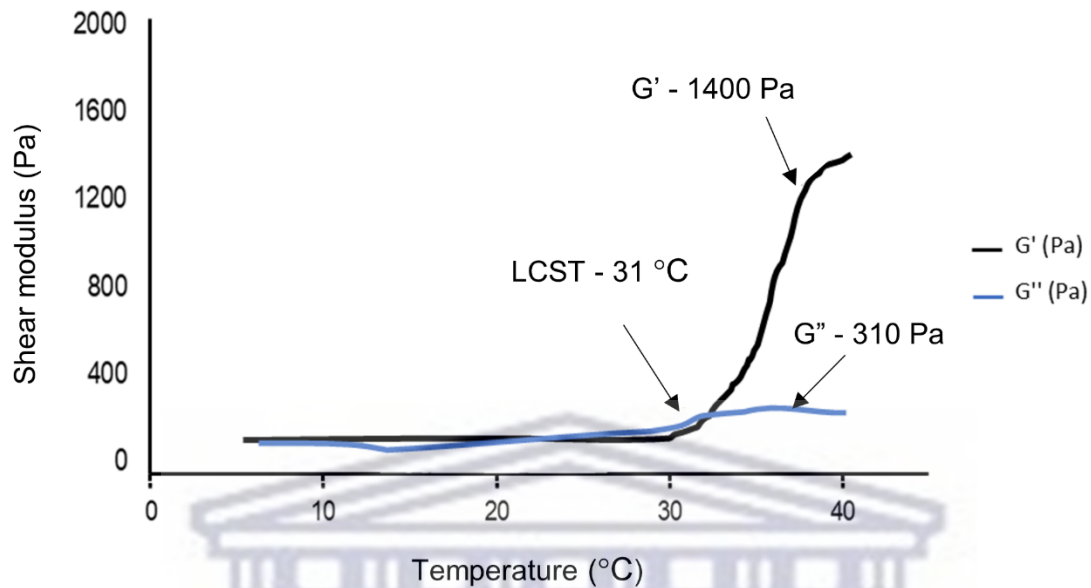


Figure 4: Shear storage ( $G'$ ) and shear loss ( $G''$ ) modulus as a function of temperature (4-40 °C) for PF-127-hydrogel.

### Compressive strength

The compressive strength of a system is instrumental in identifying Young's modulus ( $E$ ), which informs the degree of stiffness of the hydrogel when force is applied lengthwise. As shown in Figure 5,  $E$  was 0.0526, and the highest force, obtained at a distance of 5 mm, was 0.510 N which is within the range of tumorous tissue strength (1000 Pa - 7000 Pa) [6]. The high force can be attributed to the elasticity and energy-storing ability of the hydrogel, as well as the extensive crosslinking between CH and  $k$ CRG which stabilises the polymer network.

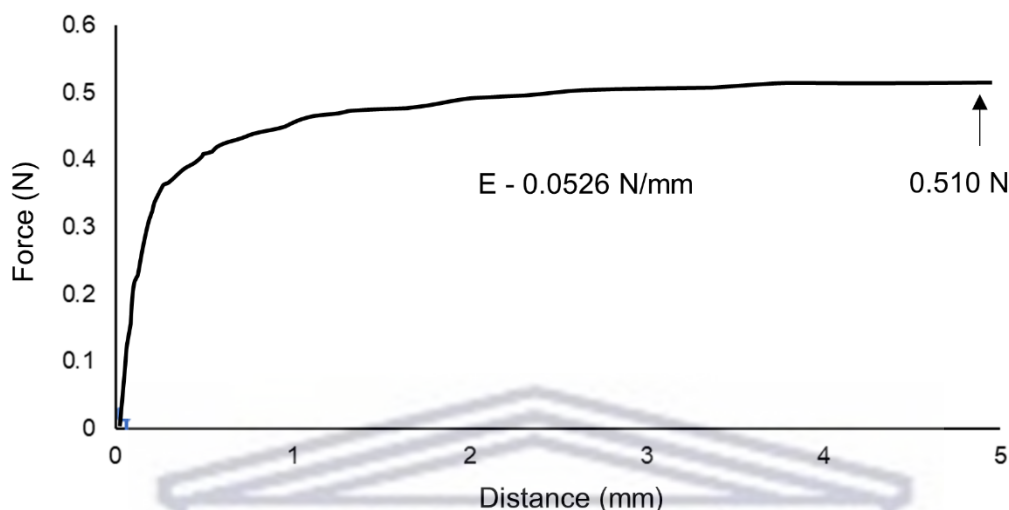


Figure 5: Compression graph indicating the peak force and Young's modulus (E) of PF127-hydrogel (0.3% CH, 0.3% *k*CRG, 15% PF-127, 0.1% LIM) at 37 °C.

### Erosion

For sustained DOX release, the hydrogel should gradually degrade over time. The thermosensitive hydrogel eroded very slowly in the first week (2.26% mass loss) due to the physical crosslinking of CH and *k*CRG which enhanced mechanical strength and reduced water penetration into the hydrogel network. At 5 weeks, the hydrogel underwent 75% erosion, thus, showing capacity for long-term drug release.

### Conclusion

A thermosensitive PF-127-based hydrogel was designed with sol-gel transition at 31 °C within 3 min. Crosslinking of CH, *k*CRG, and PF-127 with LIM was successful, according to FTIR and thermal analysis. The mechanical and rheological profiles show the potential for improved drug accumulation at the tumour site, and the system's erosion of 5 weeks shows potential for long-term drug release. The thermosensitive hydrogel could serve as a promising strategy for site-specific drug delivery to tumours while reducing side effects.

### References

1. Mohammadi, M., Arabi, L. and Alibolandi, M. 2020. Doxorubicin-loaded composite nanogels for cancer treatment. *Journal of Controlled Release*, 328, pp.171-191.
2. Seo, J.W., Shin, S.R., Lee, M.Y., Cha, J.M., Min, K.H., Lee, S.C., Shin, S.Y. and Bae, H. 2021. Injectable hydrogel derived from chitosan with tunable mechanical properties via hybrid-crosslinking system. *Carbohydrate Polymers*, 251, p.117036.
3. Kesharwani, P., Bisht, A., Alexander, A., Dave, V. and Sharma, S., 2021. Biomedical applications of hydrogels in drug delivery system: An update. *Journal of Drug Delivery Science and Technology*, 66, p.102914.

4. Jaafar, A.M. and Thatchinamoorthi, V. 2018. Preparation and Characterisation of Gellan Gum Hydrogel containing Curcumin and Limonene. In *IOP Conference Series: Materials Science and Engineering*. IOP Publishing. Article ID: 10.1088/1757-899X/440/1/012023
5. Larrañeta, E., Stewart, S., Ervine, M., Al-Kasasbeh, R. and Donnelly, R.F. 2018. Hydrogels for hydrophobic drug delivery. Classification, synthesis and applications. *Journal of Functional Biomaterials*, 9(1), p.13.
6. Jain, R.K., Martin, J.D. and Stylianopoulos, T. 2014. The role of mechanical forces in tumor growth and therapy. *Annual Review of Biomedical Engineering*, 16, p.321-346.

